Regulation of inflammation by differential neutrophil migration patterns in zebrafish

Hannah Marie Isles

Department of Biomedical Science

A thesis submitted in partial fulfilment of the requirements for the degree of Doctor of Philosophy

September 2018

Abstract

Current treatments for chronic inflammatory diseases including chronic obstructive pulmonary disease (COPD), acute respiratory distress syndrome (ARDS) and cystic fibrosis (CF) are non-specific and generally ineffective, thus the need to identify novel targets to develop more effective clinical treatments is essential. The excessive tissue damage characteristic of respiratory chronic inflammatory diseases is caused by the inappropriate retention of neutrophils in the lungs, however the underlying mechanisms are not fully understood. The identification of novel neutrophil migration patterns including neutrophil swarming and reverse migration add complexity to the modulation of neutrophil migration and retention within inflamed tissue, the precise molecular mechanisms of which remain to be fully elucidated.

Here I used a zebrafish model of spontaneously resolving inflammation to study the effect of differential neutrophil migration on the outcome of inflammation. I aimed to characterise the neutrophil swarming response and investigate the initiation of swarming by cell death signalling. Furthermore I investigated the hypothesis that the CXCR4/CXCL12 signalling axis generates a neutrophil retention signal at the wound site. Inflammation was induced in larvae by tail-fin transection and differential neutrophil migration patterns were observed using transgenic reporter zebrafish lines. CXCR4/CXCL12 signalling was inhibited using the compound AMD3100 which was administered by injection or incubation.

Here I identified that neutrophil swarming occurs following the migration of neutrophils to the wound site in three distinct phases. I demonstrated that swarms are initiated by 'pioneer' neutrophils and began to investigate cell death in the context of swarm initiation. Zebrafish neutrophils predominantly express the Cxcr4b receptor, whose ligand Cxcl12a is detected at the wound site in injured larvae. Pharmacological inhibition of CXCR4 accelerates inflammation resolution by accelerating neutrophil reverse migration. The findings of this study suggest that CXCR4/CXCL12 signalling may play an important role in neutrophil retention at sites of inflammation, and provides one of the first attempts at characterising the neutrophil swarming response. Furthermore this work has formed the basis for future studies to dissect a role for CXCR4/CXCL12 signalling in inflammation resolution through the modulation of neutrophil swarm resolution.

Acknowledgements

First I would like to thank my wonderful supervisors Steve Renshaw, Phil Elks and Cat Loynes for the continuous guidance, support and advice they have provided throughout my PhD. To Steve for being the wisest person I know, and to Phil for teaching me to take it on the chin. Extra special thanks to Cat for being the best 'boss', role-model, and friend, and for teaching me never to drink a bad glass of wine again.

To all the amazing post-docs and research team in the lab, for teaching me everything I know, letting me steal last minute reagents, smiling whilst eating my terrible baked goods and for providing a friendly, warm and wonderful place to work.

Next to all the students past and present who have provided entertainment, help, joy and coffee breaks, and encouraged the consumption of excessive amounts of cake on an almost-daily basis. Special thanks to Josh, Joey and Kyle, for the films, quizzes and for turning me into the nerd I am today. To Rebecca and Liam for the all gigs, wine and adulting. To Kate and Holly, for being there during the stressful times and being constantly amazing supportive friends who I am so lucky to have met. To Hannah Roddie for all the laughs, gigs, silly times and consistently coming to the pub.

Massive thanks to my family for their continuous love, patience and support, especially to my mum for being at the end of the phone 24/7. Thank you for supporting me in every way and enabling me to have the most amazing 3 years. I hope this thesis may give you all some insight into what on earth I have been doing for the last 3 years, I promise I will come and visit more .

To The National and JK Rowling, for creating Trouble Will Find Me and Harry Potter. Both of which provided the background noise for writing the thesis, both of which I never want to hear again.

To the Leadmill for being the finest establishment in the country.

To Leo for keeping me smiling when I was at my grumpiest, continually providing encouragement, love and support, and reminding of the fun more important things in life.

And finally to my amazing sister Melissa, whose constant support, encouragement and confidence carried me through the hardest parts. Thanks for cooking me veggie sausages and boiled eggs, for sitting with me in the office, for bringing me coffee, for being there doing a jigsaw, for cleaning my room and washing my clothes, for drinking awful wine after a bad week, and for being the best friend in the world. I promise I will clean the kitchen after I've printed my thesis.

List of abbreviations

AA Arachidonic acid

ANOVA Analysis of variance

ARDS Acute respiratory disease syndrome

Cas9 CRISPR associated protein 9

CF Cystic fibrosis

COPD Chronic obstructive pulmonary disease

CRISPR Clustered Regularly Interspaced Short Palindromic Repeats

CRISPRi CRISPR interference

CXCL C-X-C chemokine

CXCR C-X-C chemokine receptor

DAMP Damage associated molecular pattern

DMSO Dimethyl sulfoxide

DNA Deoxyribonucleic acid

dpf Days post-fertilisation

E3 Embryo medium

eGFP Enhanced GFP

fMLP Formyl-Methionyl-Leucyl-Phenylalanine

FPKM Fragments per kilobase of exon per million fragments mapped

FRET Forster resonance energy transfer

G-CSF Granulocyte-colony stimulating factor

GFP Green fluorescent protein

GM-CSF Granulocyte macrophage colony-stimulating factor

GPCR G protein coupled receptor

h Hours

HIF Hypoxia inducible factor

hpf Hours post-fertilisation

hpi Hours post-injury

IL Interleukin

LMP Low melting point

LPS Lipopolysaccharide

LT Leukotriene

LTB4 leukotriene B4

MAPK Mitogen activated protein kinase

mol Moles

MPO Myeloperoxidase (human)

mpx Myeloid-specific peroxidase (zebrafish)

mRNA Messenger RNA

n Number of individual subjects

NADPH Nicotinamide Adenine Dinucleotide Phosphate

NET Neutrophil extracellular trap

NF-KB Nuclear factor-kappa light chain enhancer of activated B cells

ns Not significant

NSAID Non-steroidal anti-inflammatory drug

P Calculated probability value

PAMP Pathogen associated molecular pattern

PBS Phosphate buffered saline

PBT Phosphate buffered saline + Tween

PFA Paraformaldehyde

PG Prostaglandin

PRR Pattern recognition receptor

r Pearson correlation coefficient

RNA Ribonucleic acid

RNAseq RNA-sequencing

ROI Region of interest

ROS Reactive Oxygen Species

SEM Standard error of the mean

temp Temperature

Tg Transgenic

TIIA Tanshinone IIA

TNFα Tumour necrosis factor alpha

TLR Toll like receptor

UAS Upstream activating sequence

vol Volume

WHIM Warts, hypogammaglobulinaemia, infection and myelokathesis

WISH Whole mount *in situ* hybridisation

WHO World Health Organisation

ZFIN Zebrafish Information Network

Contents

List of figures

1 Introduction

1.1 The immune response

The immune system protects the body from threats including bacteria, fungi and viruses by recognising and responding to antigens recognised as non-self. There are two arms of the immune response; the innate and adaptive responses. The innate response exists in all metazoan organisms and provides a rapid response to conserved patterns expressed on pathogens (Barton, 2008) whilst the adaptive response is antigen-specific and has evolved in vertebrates to generate a targeted response to specific pathogens (Cooper and Alder, 2006). The pathways involved in immune cell signalling have been in existence since before the divergence of humans and plants, indicating that between all species there will be some conservation of signalling molecules. Both arms of the immune system are regulated tightly by a range of mediators which ensure that the immune response is activated only when necessary and for the appropriate length of time to prevent a chronic immune response driving host tissue damage.

1.1.1 The innate immune system

The innate immune system is comprised of a system of physical and chemical barriers to infectious agents. The physical barring of pathogens from entry into the host by epithelial surfaces provides the first line of defence against pathogen entry to the host (Guttman and Finlay, 2009). Loss of epithelial cell integrity renders the host susceptible to infection as pathogens can invade where the epithelial layer is broken. A group of cells have evolved to defend the host against pathogens following their breach of the epithelial layer. Specifically, mast cells, phagocytes, dendritic cells and natural killer cells evolved long before the emergence of higher organisms including mice, rats and humans. These innate immune cells elicit a multitude of anti-microbial mechanisms in response to non-self molecular patterns conserved on pathogens as well as damaged cells (Medzhitov and Janeway, 2002). The vertebrate innate immune response plays a crucial role in the recognition of a broad range of pathogen and damage associated molecular patterns (DAMPs and PAMPs) (Mogensen, 2009). The major functions of innate immunity in vertebrates are identification of foreign substances by specialised white blood cells, production of cytokines to recruit immune cells to sites of infection, activation of the complement cascade and activation of the adaptive immune response by antigen presentation. The ability to distinguish self from non-self in order to mount an effective response is one of the most basic functions of the innate immune system.

1.1.2   The adaptive immune system

The adaptive immune system exists in vertebrates and is comprised of a system of highly specialised humoral and cell-mediated defence mechanisms which function to provide long-term defence against specific pathogens. The adaptive response occurs over a longer period of time than the innate response and is essential for removing microbes through recognition of antigens which are not recognised by innate immune cells (Clark and Kupper, 2005). The major functions of the adaptive immune response include recognition of non-self molecules through antigen presentation, generation of a tailored immune response to target specific pathogens or infected cells, and the development of immunological memory. The immune memory acquired following an adaptive response to specific pathogens provides the host with long-lasting defence against previously encountered pathogens which enables an enhanced response following subsequent exposure (McFall-Ngai, 2007). Enhancing the adaptive immune response is the basis for vaccination, recognised as the most effective method of preventing disease (WHO, 2011). Pioneering work by the physician Edward Jenner following his work on cowpox and smallpox began a medical revolution leading to development of the vaccine, stemming from the Latin word 'vacca' for cow (Riedel, 2005).

1.2   The inflammatory response

Inflammation is a multicomponent response initiated following tissue damage induced by trauma, bacteria, heat or toxins (Medzhitov and Horng, 2009). The inflammatory response is triggered by the detection of an inflammatory stimulus by innate immune cell receptors. The activation of the inflammatory response results in the production of mediators which modulate a multitude of physiological processes to regulate local changes to the tissue environment creating a tissue environment which is unfavourable to pathogens. The combined effect of these inflammatory mediators is the substantial increase in blood supply to the inflamed tissue, an increase in capillary permeability and the migration of leukocytes into the inflamed tissue. This results in the classic symptoms of inflammation heat (calor), redness (rubor), pain (dolor), swelling (tumor) and loss of function. A build-up of inflammatory exudate following the extravasation of fluid into the tissue, increases vascular permeability and contributes to the swelling observed in inflamed tissue. Vascular permeability is regulated by inflammatory cytokines such as histamines and bradykinin, released primarily by mast cells following activation by neuropeptides or bacterial products (Claesson-Welsh, 2015, Nathan, 2002a) . Bradykinin is also responsible for stimulation of nerve endings associated with pain at the inflammatory site (Medzhitov, 2010). Other pro-inflammatory cytokines released include TNF-α, IL-1 and Il-6 which regulate the permeability of the vasculature by activating

endothelial cells and leukocytes, promoting the transmigration of blood cells into the tissue (Medzhitov, 2008).

During inflammation, the first innate immune cells to be recruited to inflamed tissue are neutrophils, where they function to prevent pathogens from establishing a foothold in the host tissue and remove any infectious agents. The anti-microbial effects of neutrophils are essential in order to contain infection. Their lack of specificity, however, can lead to tissue damage when their behaviour becomes dysregulated. It is crucial that the inflammatory response successfully resolves following removal of the initiating stimulus to prevent permanent and irreversible host tissue damage. Persistent inflammation and inappropriate behaviour of innate immune cells are associated with the pathogenesis of chronic inflammatory diseases including rheumatoid arthritis and COPD (Serhan, 2007).

1.3   Hypoxia signalling

Under normal or healthy tissue conditions cells are exposed to around 5% oxygen, a requirement for the aerobic metabolism and function of all aerobic organisms (McKeown, 2014). Hypoxia is a shortage in oxygen availability when cells receive less than 2% oxygen, and is observed in states of physiological and pathological stress including altitude, ischemia, cancer, infection and inflammation (Majmundar et al., 2010). A decrease in oxygen availability in hypoxic tissue can be harmful, hence cells must be able to rapidly adapt to the new tissue environment and alter energy expenditure demands to match oxygen supply. The main cellular players which modulate the response to hypoxia are the hypoxia inducible factor (HIF) family of transcription factors, which activate the transcription of a myriad of downstream responsive genes whose promoters contain hypoxia responsive elements (HREs) (Wenger et al., 2005). Many HIF responsive genes are involved in the reprogramming of cellular metabolism and restoration of oxygen supply through the modulation of processes including angiogenesis, secretion of survival factors and cell cycle arrest (Ortiz-Barahona et al., 2010).

1.4   Inflammatory mediators

Following the initiation of inflammation, sentinel cells pre-stationed in the tissue intensify and propagate the inflammatory response (Nathan, 2002b). Cells including mast cells and macrophages release soluble chemical mediators into the tissue to promote local morphological and biochemical changes to the tissue environment, as well as causing systemic effects. The combined effect of these mediators is the recruitment of leukocytes from the blood stream, the first of which is the neutrophil (Barton, 2008).

1.4.1   Chemokines

The chemokines are a family of chemotactic cytokines which control the migration of all immune cells (Griffith et al., 2014). Chemotaxis was first defined as the directional migration of leukocytes along a chemokine gradient (Pfeffer, 1884). Production of chemokines such as c5a, fMLP, LTB_4 and the CXC family of chemokines is induced by infectious stimuli including bacterial LPS, as well as pro-inflammatory cytokines TNFα and IL-1β produced by damaged cells (Furie and Randolph, 1995). The secretion of cytokines and chemokines from cells at sites of injury or infection promote the influx of other innate immune cells.

The chemokine family consists of approximately 50 chemokine ligands which stimulate the recruitment of cells expressing cognate chemokine receptors. Two major chemokine sub-families have been identified based on the position of their first 2 conserved cysteine residues at the N-terminus; the major C-X-C (α chemokines) and the C-C family (β-chemokines) as well as the minor sub-families CX3C   (δ chemokines) and C (γ chemokines) (Ransohoff, 2009). Chemokines elicit their function by binding to their receptors which are members of the G protein coupled receptor family.

1.1.2.1   G protein coupled receptor signalling

The GPCR family is the largest family of receptors in the human genome, which encodes over 800 GPCR genes. GPCRs are 7 transmembrane spanning cell surface receptors coupled to intracellular g-protein partners, which transduce external signals through conformational changes induced by ligand binding. G proteins activate downstream signalling pathways through the recruitment of cellular enzymes and second messengers (Hanlon and Andrew, 2015). Outside-in signalling through GPCRs is summarised in Figure 1.1.

G-proteins are heterotrimeric proteins comprised of Gα, β and γ subunits closely associated with the intracellular face of GPCRs on the plasma membrane. In its inactive state, the Gα-subunit is bound to a Gβγ dimer and guanine diphosphate (GDP), which facilitates its tethering to the plasma membrane. Activation of G proteins is facilitated by guanine nucleotide exchange factors (GEFs) which exchange bound GDP for guanine triphosphate (GTP). GPCRs function as GEFs following ligand induced conformational changes, enabling these receptors to facilitate exchange of GDP for GTP on the Gα subunit and subsequent G protein activation (McCudden et al., 2005). GTP bound Gα-subunits dissociate from their Gβγ subunits, both of which can interact with downstream effector proteins in the membrane to transduce secondary messenger signals. Gα regulates its own activity through intrinsically expressing a guanosine triphosphatase

(GTPase) which hydrolyses GTP back to GDP, subsequently inactivating the Gα subunit. GDP bound Gα subunits re-form an inactive heterotrimer with a Gβγ subunit in the membrane and signalling is terminated. Phosphorylation of the GPCR by GRKs stimulate B-arrestin binding and subsequent internalisation of the receptor.
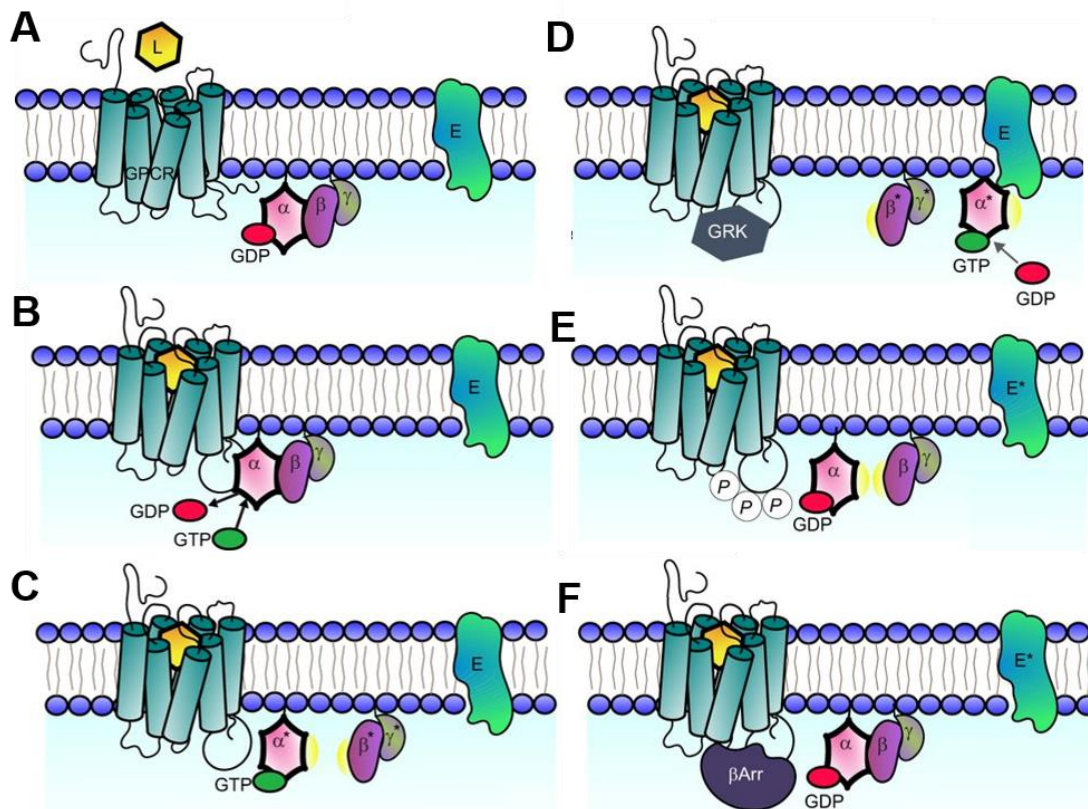
Figure 1.1 : Outside-in signalling through G Protein coupled receptors.

Adapted from Hanlon and Andrew, 2015. (A) In their basal state, GPCRs are 7 transmembrane spanning proteins which are not bound to ligand. (B) Ligand binding induces a conformational change in the GPCR. The GPCR is now able to act as a guanine nucleotide exchange factor (GEF) to facilitate the exchange of GDP for GTP on the Gα subunit of the associated G protein. (C) Activation of the G protein and dissociation of the Gα subunit from the Gβγ subunits. (D) Interaction of G protein subunits with downstream effectors and activation of second messenger signalling 'outside-in signalling'. (E) Hydrolysis of GTP to GDP on Gα subunit promotes the re-association of the G protein and its inactivation. Phosphorylation of the GPCR by GRKs. (F) GPCR phosphorylation stimulates B-arrestin binding and subsequent internalisation of the receptor which is then recycled back to the surface or degraded.

Ligand activated GPCR internalisation is a characteristic feature of GPCR signalling, which regulates cell sensitivity to chemokine gradients through the recycling of cell surface receptors. In the absence of ligand, GPCRs are internalised at a constitutive level followed by degradation or recycling. Upon ligand binding, internalisation of GPCRs is enhanced and trafficking of receptors to and from the membrane occurs at a more rapid rate (Neel et al., 2005). This internalisation of receptors plays a crucial role in cell signalling through negatively regulating the expression level of membrane receptors, thus preventing over-activation of downstream pathways (Sorkin and von Zastrow, 2009).

1.4.2 Lipid mediators

A family of lipid mediators known as the eicosanoids are highly involved in regulating a large number of processes in promoting and resolving inflammation, as well as a multitude of homeostatic processes including vascular homeostasis, platelet aggregation and a protective role in the gut mucosa (Harizi et al., 2008). In the context of inflammation, the biosynthesis of eicosanoids is increased in inflamed tissues by innate immune cells including macrophages and neutrophils which harbour the machinery required to metabolise arachidonic acid bound to the cell membrane. These potent lipid mediators regulate immune processes such as cytokine production, cell migration, proliferation and inflammation resolution (Dennis and Norris, 2015). Dysregulation of eicosanoid production is implicated in many diseases including asthma (Wan and Wu, 2007), cancer (Greene et al., 2011) and rheumatoid arthritis (Korotkova and Jakobsson, 2014).

1.4.2.1 The cyclooxygenase pathway and prostaglandins

Arachidonic acid is released from phospholipid membrane bilayers following the cleavage of membrane phospholipids by the enzyme phospholipase A2. Free arachidonic acid is available for oxidative metabolism by two distinct pathways to produce the eicosanoid families of prostaglandins and thromboxanes, or leukotrienes and lipoxins, through the action of either cyclooxygenase or lipoxygenase enzymes respectively (Dennis and Norris, 2015).

Cyclooxygenase enzymes COX-1 and COX-2 are differentially expressed in tissues (Crofford, 1997). COX-1 is expressed constitutively and is involved in homeostatic processes including vascular haemostasis and gastroprotection from acid produced during digestion (Peskar et al., 2003). COX-2 is induced during inflammation and promotes the formation of pro-inflammatory prostaglandins which are able to exert their effect through mediating autocrine and paracrine signalling loops (Ricciotti and FitzGerald, 2011). There are reports of a COX-3 enzyme which many groups argue is the

target of paracetamol, although its role in eicosanoid production remains controversial (Schwab et al., 2003).

Downstream products of COX activity form prostaglandin precursors, which through a series of intermediate metabolic steps, produce prostaglandins PGD_2, PGE_2, PGF_2 and PGI_2 PGG_2 as well as thromboxane A_2 (Marnett et al., 1999). Prostaglandins can alter vasodilation, platelet aggregation and increasing vascular permeability. TXA2 is responsible for the vasoconstriction, platelet aggregation and bronchoconstriction seen in asthma (Simmons, 2004).

1.4.2.2   The lipoxygenase pathway and leukotrienes

Leukotrienes are another family of lipid mediators produced by the metabolism of arachidonic acid, which have inflammatory functions including leukocyte recruitment, vasodilation and intercellular relay signalling (Lämmermann et al., 2013; Medzhitov, 2008). The leukotriene family can be classified into the cysteinyl leukotrienes LTC_4, LTD_4 and LTE_4, and a second family consisting of LTB_4. The cysteinyl leukotrienes have a profound effect on airway function and play a large role in the pathogenesis of asthma through bronchoconstriction (Ogawa and Calhoun, 2006).

Leukotrienes are synthesised through the metabolism of arachidonic acid by the lipoxygenase enzymes, of which humans have 3. This family of enzymes oxygenate arachidonic acid on different residues, resulting in the formation of different leukotriene isoforms. The lipoxygenases are differentially expressed within different peripheral blood cells resulting in the production of different arachidonic acid metabolites produced by different cell types (Serhan and Sheppard, 1990).

LTB_4 exerts its role in inflammation by acting predominantly on receptors expressed on neutrophils. LTB_4 signalling activates pathways involved in neutrophil chemotaxis and activation, neutrophil-endothelial cell interactions, reactive oxygen species production and degranulation (Sharma and Mohammed, 2006). Recently LTB_4 has been identified as a signal relay molecule which augments neutrophil chemotaxis to formyl peptides (Afonso et al., 2012), and as one of the factors mediating intercellular signal relay during the neutrophil swarming response (Lämmermann et al., 2013).

1.5   Initiation of inflammation

An acute inflammatory response is observed within the first few hours following tissue injury during which time the body orchestrates a complex series of events that function to remove any threat to the host and restore tissue homeostasis. Inflammation can be activated by both exogenous and endogenous stimuli, both of which present different

challenges to the host. Whilst infection of the host by microbes requires the immune system to rapidly remove the pathogen, the inflammatory response must rapidly repair host cells to prevent bacteria from establishing a foothold in the host following their breaching of protective epithelial layers (Newton and Dixit, 2012).

The inflammatory response is triggered by the activation of pattern recognition receptors (PRRs) expressed on tissue resident immune cells including mast cells, macrophages and dendritic cells. These evolutionarily conserved receptors recognise prokaryotic patterns known as pathogen associated molecular patterns (PAMPs) on pathogens including lipopolysaccharide (LPS), bacterial flagellin, lipoteichoic acid and peptidoglycan. Equally PRRs recognise damage associated molecular patterns (DAMPs) secreted in damaged tissues by necrotic cells such as heat shock proteins, β-defensin and HMGB1 (Lotze and Tracey, 2005). This enables the innate immune system to distinguish pathogens and damaged cells from healthy host cells.

PRRs such as toll-like receptors , nod-like receptors and mannose receptors can sense PAMPs and DAMPs (Kumar et al., 2011). Activation of PRRs by PAMPs induces the production of transcription factors, including NF-κB and interferon regulatory factors (IRFs) initiating opsonisation, phagocytosis and pro-inflammatory cytokine production (Barton, 2008). Activation of pattern recognition receptors by DAMPs induces downstream signalling, ultimately driving the expression of pro-inflammatory genes including TNF-α and IL-1. Expression further activates the inflammatory response through cytokine production and immune cell activation (Nathan, 2002b).

Regardless of the initiating stimulus, signalling through PRRs play a crucial role in establishing an inflammatory setting in order to contain the infection and activate the adaptive immune response (Barton, 2008).

1.5.1 Toll like receptors

The toll like receptors are single-pass membrane glycoproteins of the type 1 membrane glycoprotein family which function primarily to detect a broad range of bacterial components. TLRs are found on the outer or endosomal membranes of cells where they function as monomers, homodimers or heterodimers, signalling through which produces a cytokine response (Marie Moresco et al., 2011).

There have been 12 TLRs found to be expressed in mammalian cells, the majority of which are expressed on cells of the innate immune system including macrophages and neutrophils. Of the identified human TLR family members, most have been well characterised. TLR4 was the first receptor to be characterised by Bruce Beutler who

identified that TLR4 could recognise LPS on gram-negative bacteria (Poltorak et al., 1998).

Ligand activation of TLRs ultimately induces the phagocytosis of the foreign pathogen and activation of pro-inflammatory signalling pathways. Depending on the adaptor proteins recruited to the intracellular domain of the TLR, following ligand activation, there is either a myd88 dependent activation of the NF-kB signalling pathway and cytokine release, or activation of the TRIF pathway leading to activation of IRFs and interferon production (Piccinini and Midwood, 2010). Interestingly, some TLR ligands are host-derived, such as the intracellular components of necrotic cells, highlighting the role of these receptors in damage signalling as well as pathogen sensing (Mori et al., 2015),.

1.5.2   Nod Like Receptors

PRRs can also be intracellular, which are useful if the pathogen has been internalised by the cell. The nucleotide oligomerization domain-like (NOD-like) receptors (NLRs) are a family of intracellular PRRs which function in a comparable manner to the TLRs (Franchi et al., 2010). Nod1 and Nod2 recognise peptidoglycan moieties on gram negative and positive bacteria respectively (Franchi et al., 2009). Signalling through some of the NLRs activates NF-kB signalling to enhance expression of pro-inflammatory genes including IL-6, IL-1β and TNFα (Nathan, 2002). Conversely activation of other intracellular NLRs triggers the assembly of a protein complex known as the inflammasome, ultimately resulting in processing of inflammatory mediators such as IL-1β, IL-18 and IL-33 (Medzhitov, 2007).

Mutations in the gene encoding Nod2 are found in a small proportion of individuals with Crohn's disease. These mutations effect the leucine rich region of the receptor, which is proposed to alter recognition of microbial components in the gut as well as over-activating NF-kB in monocytes (Hugot et al., 2001). Mutations in the nucleotide binding domain of Nod2 are associated with Blau syndrome, a rare autosomal dominant disorder characterized by early-onset granulomatous arthritis, uveitis and skin rash (Miceli-Richard et al., 2001), although the mechanisms underlying disease when caused by this mutation are currently not understood.

Regardless of the initiating stimulus, the activation of the immune response ultimately leads to the recruitment of leukocytes from the blood to the site of inflammation, the first of which is the neutrophil.

1.6 The neutrophil

The granulocyte family of white blood cells were discovered following advances in cell-staining techniques which were utilised by scientist Paul Ehrlich in the late nineteenth century (Kay, 2016). Initially, the neutrophil was thought to act as a promoter of infection by interacting with invading bacteria, where the effects were considered detrimental to host tissues. However, in 1893 evolutionary biologist Elie Metchnikoff proved that, following his research using starfish embryos, phagocytes played a key role in the clearance of foreign material and were found to have key roles as antimicrobial molecules during the immune response (Mečnikov, 1892). Developments over the last century have led to the current understanding that the neutrophil plays a crucial role in inflammation and immunity (Kolaczkowska and Kubes, 2013). Neutrophils are the most prevalent of the immune cells in the circulation and play a crucial role in the innate immune response where they are recruited to the site of damage within minutes of trauma (Su and Richmond, 2015). The destructive mechanisms inflicted by neutrophils are immediate and their lack of specificity can be detrimental to tissue resident cells if unregulated. Failure of the immune system to resolve neutrophilic inflammation is damaging to host cells in multiple organ systems (Alessandri et al., 2013).

1.1.3 Neutrophil life cycle

Neutrophil lifespan is regulated by its production during granulopoiesis, storage in bone marrow in mammals, release into the circulation, clearance from the blood and finally, destruction (Summers et al., 2010).

1.6.1.1 Granulopoiesis

The granulocyte family of mature polymorphonuclear neutrophils, basophils, and eosinophils are produced from precursor myeloblasts during a series of maturational steps. Macrophages and neutrophils are produced from the same progenitor cells, with their fate being determined by the expression of myeloid transcription factors in individual niches within the bone marrow. Granulocyte colony stimulating factor (G-CSF) is the principal regulator of granulocyte production from hematopoietic stem cells which in humans occurs in the venous sinuses of bone marrow. G-CSF induces the differentiation of hematopoietic stem cells, such that they commit to the myeloid lineage, and regulates the proliferation of granulocytic precursors (Summers et al., 2010). The crucial role of G-CSF in modulating neutrophil production is demonstrated in humans with dominant negative G-CSF receptor mutations, whereby they suffer from congenital neutropenia characterized by a premature arrest of granulopoiesis (Germeshausen et al., 2008).

1.6.1.2   Neutrophil trafficking from bone marrow

It is estimated that between $5x10^{10}$ and $10x10^{10}$ neutrophils are produced in human bone marrow every day (Summers et al., 2010). In addition to the bone marrow reserve where the majority of neutrophils are found, there exists a marginated pool of neutrophils in the capillary beds of organs including the spleen, liver and lungs. Circulating neutrophil numbers in the blood are tightly regulated by balancing the bone marrow retention, release and clearance from the circulation. Retention signals in this context are generated through the production of ligand by stromal cell populations in the marrow, which signal through G protein coupled receptors to maintain neutrophils in the bone marrow niche. The CXCR4/CXCL12 signalling axis plays a crucial role in modulating the homeostasis of neutrophils, the important role of which is highlighted in patients with Warts, hypogammaglobulinaemia, infection and myelokathesis (WHIM) syndrome. Gain of function WHIM mutations result in increased CXCR4 signalling, the consequence of which is severe neutropenia with increased neutrophil retention in the bone marrow (Kawai and Malech, 2009).

CXCL12 signals through neutrophil cell surface CXCR4 receptors, with the ligand being constitutively produced by stromal cell populations in the bone marrow (Day and Link, 2012). This signalling retains immature neutrophils in the hematopoietic niche under normal physiological conditions. There is growing evidence to suggest that crosstalk between CXCR4/CXCL12 and the VLA-4/VCAM1 signalling axis modulates neutrophil adhesions in the bone marrow. Bone marrow neutrophils express the α4-integrin VLA-4 which binds to its major ligand vascular cell adhesion molecule 1 (VCAM1) expressed on bone marrow stromal cells (Day and Link, 2012). CXCL12 and VCAM1 are co-localised in murine bone marrow and the expression profile of VLA-4 of neutrophils decreases with age, matching that of CXCR4. Furthermore CXCR4 augments VLA-4 adhesion to VCAM-1 *in vitro* and blockade of both CXCR4 and VLA-4 caused synergistic neutrophil egress from bone marrow (Petty et al., 2009).

Loss of functional G-CSF receptors has been shown to cause severe neutropenia in mice and humans (Druhan et al., 2005; Lieschke et al., 1994). G-CSF regulates the release of neutrophils from bone marrow through modulation of the CXCR4/CXCL12 signalling axis. Mature neutrophils express high levels of G-CSF and low levels of CXCR4 (Summers et al., 2010). Administration of G-CSF to mice reduces stromal cell production of CXCL12 (Semerad et al., 2002) and decreases CXCR4 expression on myeloid cells (Kim et al., 2006) resulting in attenuated neutrophil responses to CXCL12 gradients in bone marrow and subsequent release into the circulation.

A combination of G-CSF and CXCR4 antagonists are used therapeutically to release hematopoietic stem cells from bone marrow. As mentioned, G-CSF reduces CXCL12 production by bone marrow stromal cells, but in combination with a CXCR4 antagonist, retention signals are interrupted, resulting in the synergistic release of HSCs from the bone marrow which can be used for transplantation (Broxmeyer et al., 2005).

More recently an antagonistic role of the CXCR2 signalling axis has been implicated in neutrophil release from the bone marrow. Perfusion of the CXCR2 ligand MIP-2 induced the rapid release of neutrophils from rat femoral bone marrow (Deininger et al., 2005). Murine CXCR2$^{-/-}$ neutrophils are retained preferentially over wildtype neutrophils in the bone marrow of chimera mice. This phenotype was not observed in double CXCR2$^{-/-}$ CXCR4$^{-/-}$ neutrophils which were mobilised constitutively, highlighting the dominant role of CXCR4 signalling in neutrophil release and retention (Eash et al., 2010).

It has been proposed that opposing cues from the two signalling axis modulates neutrophil egress from bone marrow in a tug-of-war scenario (Figure 1.2). In this model, endothelial derived chemokines such as CXCL1 and 2 direct neutrophil migration towards the vasculature and drive egress from the bone marrow, whilst osteoblast derived chemokines, such as CXCL12, promote neutrophil retention. In a normal physiological state, the balance of signalling favours neutrophil retention through dominant CXCR4/CXCL12 signalling. The balance is tipped in infection or inflammation by the production of pro-inflammatory cytokine G-CSF which increases CXCL2 expression by endothelial cells and reduces CXCR4/CXLC12 expression, promoting neutrophil egress into the circulation from the bone marrow (Day and Link, 2012).
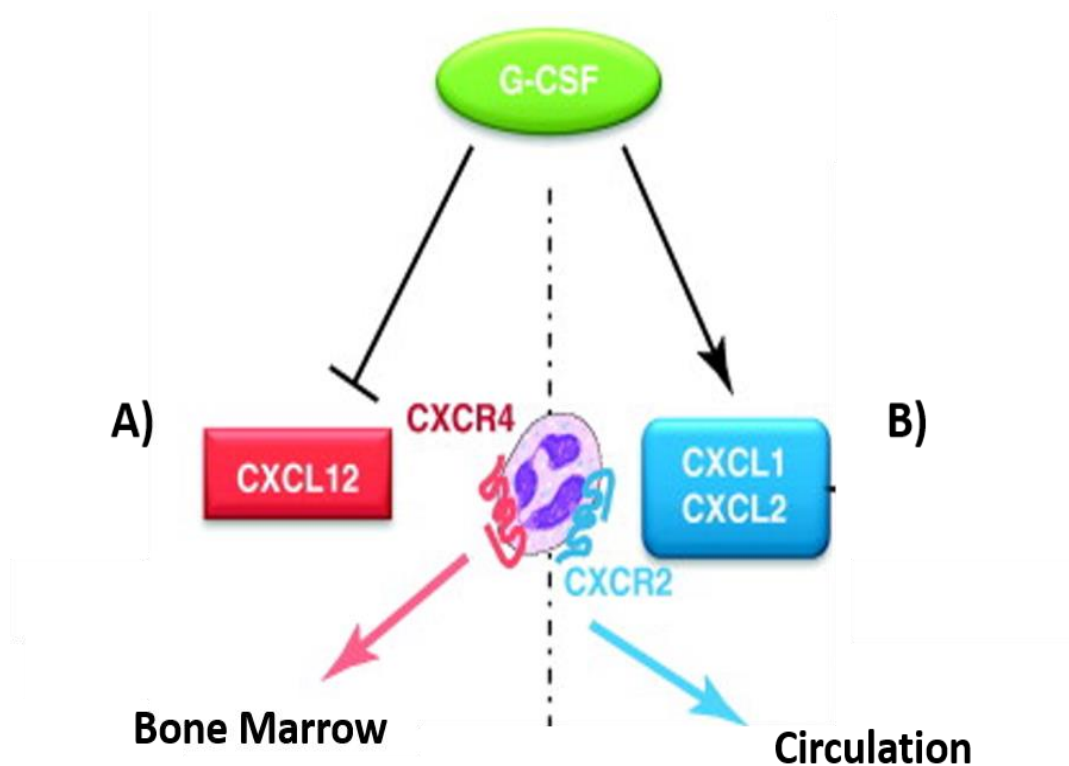
Figure 1.2: Neutrophil release from the bone marrow is regulated by a tug-of-war between CXCR2 and CXCR4 signalling.

Adapted from Sadik et al., 2011. CXCL12 signalling through CXCR4 promotes the retention of neutrophils in the bone marrow (A), whilst CXCR2 signalling through endothelial derived chemokines CXCl1 and 2 promote neutrophil release into the circulation (B). The granulocyte-colony stimulating factor (G-CSF) adjusts the balance of CXCR4 and CXCR2 by reducing CXCL12 production by osteoblasts (A), and increasing the production of CXCL1 and 2 to increase promote egress into the bloodstream (B).

1.6.1.3   Neutrophil homing and clearance

The half-life of circulating neutrophils in humans was traditionally believed to be around 8 hours (Dancey et al., 1976). Deuterium labelling of neutrophils provided evidence ti suggest that under homeostatic conditions circulating neutrophils have a half-life of 5.4 days (Pillay et al., 2010). However, this study was met with much contention due to fundamental problems with the mathematical modelling used to calculate the peripheral blood lifespan of neutrophils and the ability of deuterium to label newly dividing neutrophil precursors, and is thus still a subject of debate (Tofts et al., 2011).

Under basal conditions, mature neutrophils home back to the bone marrow where they undergo apoptosis and are phagocytosed by stromal macrophages (Summers et al., 2010). There is evidence to suggest that the homing behaviour of mature neutrophils is dependent on their upregulated expression of CXCR4 which acts as a homing signal to promote the migration of neutrophils to CXCL12 enriched bone marrow niches, although this process has not been fully defined.

1.1.4   Neutrophil recruitment

In healthy adults, <2% of neutrophils are found in the circulation (Sadik et al., 2011). Those which are circulating do so in an inactive state, causing no harm to host tissue (Wright et al., 2010). During inflammation neutrophils are rapidly recruited to sites of tissue damage or infection in a multi stage series of events. The neutrophil recruitment cascade is modulated by a range of overlapping signals which guide neutrophils to the inflammatory site.

Cellular stress and systemic inflammation promote the egress of neutrophils from the bone marrow through the production of pro-inflammatory mediators such as TNF-α, IL-8, C5a and LTB$_4$, as well as G-CSF and CXCR2 agonists MIP-2 and CXCL1 produced at inflammatory sites (Burdon et al., 2008). Priming of neutrophils prevents their inappropriate degradation and matches neutrophil function to the level of threat.

1.6.1.4   Leukocyte adhesion cascade

Neutrophil recruitment to inflamed tissue is initiated by the activation of endothelial cells lining the lumen of blood vessels by inflammatory mediators such as histamine and cytokines. The process of neutrophil recruitment to inflamed tissue has been extensively studied and occurs via a process known as the leukocyte adhesion cascade. The leukocyte adhesion cascade is a well-defined sequence of events whereby neutrophils form interactions with activated luminal endothelial cells along which they roll, before forming firm adhesions. Tethered neutrophils then transmigrate through the endothelial layer and into the interstitial tissue (Ley et al., 2007).

In healthy blood vessels, neutrophils circulate passively in the centre of the vessel due to laminar flow. During inflammation, blood flow is reduced in post-capillary venules due to changes in haemodynamics. Reduced flow increases the chances of neutrophils coming into contact with the endothelial cells lining the vessel wall (Muller, 2013).

Activated endothelial cells alter their surface expression of adhesion molecules such as P and E selectin on the luminal surface (Lorenzon et al., 1998).The binding of P and E selectin to their glycosylated ligands on the neutrophil surface forms weak interactions such that neutrophils bind tentatively to the endothelium which they slowly move along in a process known as rolling.

Neutrophils roll along the surface of the endothelium in the direction of blood flow where they are primed and activated. Full activation of neutrophils involves priming by pro-inflammatory factors including cytokines, growth factors and bacterial products (Hallett and Lloyds, 1995). Neutrophil priming maximises neutrophil function by activating the NADPH oxidase pathway and promoting appropriate degranulation (Kelly et al., 2007).

Neutrophil activation is mediated by haptotactic gradients of endothelial chemokines which signal via CXCR2, heparin sulphate proteoglycans and duffy antigen receptor for chemokines (DARC). Activated neutrophils increase their expression of cell surface integrins that show higher affinity for their ligands, including immunoglobulin-like cell adhesion molecules (ICAMs) expressed by endothelial cells. Adhered neutrophils then transmigrate through intracellular junctions in the endothelium and into the interstitial tissue (Schenkel et al., 2004).

1.1.5 Neutrophil migration in interstitial tissue

Upon entry into the interstitial tissue, a complex array of chemoattractant signals, including bacterial and tissue derived chemoattractant signals, guide neutrophils through the extracellular matrix towards the source of chemokine production (Sadik et al., 2011). Neutrophils respond to chemoattractant gradients through the activation of cell surface chemoattractant G protein coupled receptors (GPCRs). Signalling through these receptors induces calcium mobilisation from intracellular stores and downstream signalling, resulting in actin polymerisation at the point in the cell where chemokine concentration is highest.

A key signalling axis which modulates the chemotaxis of neutrophils through the interstitial tissue is the CXCR1/2-CXCL8 signalling axis, which activates intracellular signalling pathways to regulate neutrophil motility. CXCR1 and CXCR2 are GPCRs which are activated by CXCL8 and bind to each with different binding affinities (Holmes et al.,

1991; Murphy and Tiffany, 1991). CXCR2 knockout mice have a diminished neutrophil response to viral infection in the lung (Wareing et al., 2007). Genetic and pharmacological inhibition of CXCR2 signalling in zebrafish larvae prevents the recruitment of neutrophils to CXCL8 produced at inflammatory sites following tail-fin transection (de Oliveira et al., 2013).

Chemotaxis of neutrophils requires temporal and spatial regulation of external signals through prioritising competing chemoattractant gradients in order to polarise and migrate in the required direction (Hind et al., 2016). In the interstitium, a range of chemoattractants including CXCL8, LTB_4 and fMLP are derived from host cells and pathogens. The migration of neutrophils towards individual chemokines has been well characterised, however, due to limitations in assays used to study neutrophil chemotaxis towards multiple chemoattractants, less is known about how neutrophils prioritise these competing signals. Hierarchical neutrophil responses have been observed following exposure to competing chemokine gradients such that end point chemoattractants which emerge in the immediate vicinity of an invading pathogen such as fMLP or C5a override the intermediary signals derived from host cells such as CXCL8 and LTB_4 (Kim and Haynes, 2012).

To achieve forward migration, neutrophils polarise by forming a leading edge (pseudopod) at the highest concentration of chemoattractant, and a trailing edge (uropod). At the leading edge the extension of broad lamellipodia or spike-like filopodia form adhesions with the substratum, processes which are controlled by the rearrangement of the actin cytoskeleton (Ridley et al., 2003). The f-actin polymerisation at the leading edge required for neutrophil migration is mediated by the formation of the Arp2/3 complex which redistributes to the region of the neutrophil where the highest concentration of chemoattractant is sensed (Weiner et al., 1999). At the trailing edge, Rac signalling modulates the degradation of adhesion molecules and actin polymerisation allows the back of the cell to contract (Ridley et al., 2003). Upon encountering a chemotactic gradient, neutrophils like many eukaryotic cells polarise by accumulating the lipid PtdIns(3,4,5)P3 (PIP3) to the membrane where the highest concentration gradient is sensed (Servant et al., 2000). Initially it was believed that external chemokine gradients induced the formation of pseudopods to direct the cell towards the highest concentration of chemoattractant. However, more recent findings suggest that pseudopods form independently, and the detection of external gradients promotes the maintenance of existing pseudopods to drive movement in the required direction (Insall, 2010). Cross talk between a multitude of downstream signalling pathways modulates the cytoskeletal rearrangements required for neutrophil migration (Cho et al., 2014).

Two key signalling pathways have been identified in neutrophil migration. The phosphatidylinositol-3-OH kinase (PI3K) phosphatase pathway is activated by tissue-derived chemokines, whilst the p38 mitogen-activated protein kinase (MAPK) pathway is activated by bacterial derived chemokines. In recent years, it has become apparent that neutrophils elicit differential responses to competing chemokine gradients (Kim and Haynes, 2012). Signalling through p38 MAPK is able to over-ride the PI3K signalling pathway, suggesting that bacterial derived chemokines are prioritised by neutrophils (Heit et al., 2002a). The preferential migration of neutrophils to opposing gradients is modulated in part by the phosphatase PTEN which is distributed around the circumference of the neutrophil where it inhibits PI3K signalling at the cell surface (Heit et al., 2008).

Advances in *in vitro* assays used to expose human neutrophils to competing chemokine gradients has identified that neutrophils are activated more rapidly in response to fMLP gradients compared to LTB_4 (Cho et al., 2014). Tracking of human neutrophils *in vitro* in competing gradients suggests a signalling hierarchy exists, whereby neutrophils prioritise end-point chemoattractants such as pathogen derived fMLP over gradients of intermediary endogenous chemokines such as CXCL8, CXCL2 and LTB_4 (Kim and Haynes, 2012). These end target chemoattractants drive neutrophil migration preferentially towards bacterial infection by activating the p38/MAPK pathway rather than the PI3K/AKT pathway, which is activated by intermediary chemoattractants (Heit et al., 2002b). This is modulated by the phosphatase PTEN which is distributed throughout the circumference of the entire neutrophil following exposure to competing end-point chemoattractants. PTEN inhibits PI3K signalling at the leading edge, such that migration is driven via the p38/MAPK pathway towards bacterial derived chemoattractants. The role of PTEN in gradient prioritisation is demonstrated in PTEN-/- neutrophils which are unable to prioritise chemokine gradients (Heit et al., 2008). Whilst the dynamics of neutrophil migration under competing gradients are beginning to be dissected (Cho et al., 2014), the complex integration of chemical signals by neutrophils remains to be fully elucidated.

1.7 Neutrophil function

During inflammation, neutrophils are activated and their longevity increases, such that they are able to function as effective anti-microbial cells to defend the host against infection using multiple mechanisms. These include the phagocytosis of pathogens, production of reactive oxygen species and degranulation, formation of extracellular traps

to capture pathogens outside of the cell and neutrophil swarming (Kolaczkowska and Kubes, 2013).

1.1.6   Phagocytosis

Neutrophils, along with macrophages, are members of the phagocyte family of immune cells which have the ability to recognise and engulf opsonised pathogens. Following recognition by cell surface receptors, actin cytoskeletal rearrangements lead to the formation of a membrane derived vacuole to encompass the receptor ligand complex, which is internalised by and destroyed intracellularly through degradative enzymes. Pathogens opsonised by immunoglobulins are recognised by neutrophil Fc receptors whilst those opsonised by complement are recognised by complement receptors (van Kessel et al., 2014). Binding of TLRs to conserved DAMPs also triggers phagocytosis. Internalised vacuoles or 'phagosomes' undergo a lengthy maturation step in which a potent anti-microbial environment is created through fusion of the phagosome with secretory vesicles and granules, such that the mature phagosome contains the machinery to destroy and degrade its internal cargo (Lee et al., 2003).

1.1.7   Degranulation

The cytoplasm of a neutrophil contains a host of granules containing cytotoxic substances critical for neutrophil function as anti-microbial cells. Cytotoxic substances are delivered to the phagosome to assist intracellular pathogen killing, or to the cell surface where they are expelled into the tissue to degrade extracellular matrix components or facilitate extracellular killing (Häger et al., 2010). Of all the anti-microbial effects of neutrophils, degranulation is the process which must be most tightly regulated as the release of toxic granule components into the tissue is damaging to the host (Faurschou and Borregaard, 2003).

Neutrophils have three types of cytoplasmic granules which differ in internal composition, propensity for mobilisation and time of formation (Häger et al., 2010). Initial classification of neutrophil granules was based on their myeloperoxidase (MPO) content. Azurophilic (primary) granules stain positive for MPO whilst specific (secondary) and gelatinase (tertiary) do not (Borregaard and Cowland, 1997). Classification of granules is flexible as neutrophil granule formation is a continuum whereby primary granules develop and share granule components with tertiary granules (Borregaard and Cowland, 1997). Primary granules are formed during the early stages of granulopoiesis and contain enzymes for digestive and bactericidal functions including MPO, α-defensins, cathepsin G and proteinase-3 (Falloon and Gallin, 1986). Secondary and tertiary granules are

formed later in neutrophil development and are characterised by the presence of lactoferrin and gelatinase respectively.

The physiological role of neutrophil granules is demonstrated in patients with neutrophil-specific granule deficiency, a rare congenital disorder characterised by increased susceptibility to pyogenic infection and persistent infections by s*taphylococcus aureus* and *Pseudomonas aeruginosa* (Gallin et al., 1982*).

1.1.8   ROS production

Reactive oxygen species are produced in neutrophils via a respiratory burst. Following the phagocytosis of pathogens, neutrophils undergo a burst of oxygen consumption, the majority of which is converted to highly reactive oxygen species (Klebanoff, 2005). The NADPH oxidase complex is assembled in phagosomes where it catalyses the reactions resulting in the formation of hydrogen peroxide, the superoxide anion and subsequent downstream reactive oxygen species inside the phagosome (Dahlgren and Karlsson, 1999). Inside the phagosome, the activity of myeloperoxidase released following the degranulation of primary granules catalyses the formation of the potent anti-microbial substance hypochlorous acid from hydrogen peroxide and chloride (Klebanoff, 2005).

NADPH oxidase can also be recruited to the plasma membrane where it assembles and catalyses the production of reactive oxygen species which are released by neutrophils into the tissue to destroy extracellular pathogens, however ROS release into tissue is responsible for the tissue-damaging properties of neutrophils (El-Benna et al., 2008). Inactivation of the NADPH oxidase complex by anti-inflammatory signalling molecules limits the production of ROS and avoids extensive host tissue damage.

The crucial role of NADPH oxidase in controlling infection is demonstrated in patients with chronic granulomatous disease (CGD) who suffer from recurrent infections due to mutations in their NADPH oxidase gene (Volpp et al., 1988).

1.1.9   NET formation

A more recently identified neutrophil defence mechanism is the formation and release of extracellular traps to capture and destroy pathogens extracellularly. Neutrophil extracellular traps are web-like chromatin structures embedded with granule proteins released by activated neutrophils. NETs were first visualised *in vitro* using electron microscopy, where it was identified that activated but not naïve neutrophils made prominent extracellular structures following stimulation by interleukin-8 (IL-8), phorbol myristate acetate (PMA), or lipopolysaccharide (LPS) as well as gram positive or gram negative bacteria (Brinkmann et al., 2004). Since the identification of extracellular traps

in neutrophils, it has been identified that other cell types including eosinophils (Yousefi et al., 2008), macrophages (Chow et al., 2010) and mast cells (von Kockritz-Blickwede et al., 2008) are capable of extracellular trap formation.

NETs are composed of a backbone of nuclear chromatin and histones, embedded with antimicrobial proteins capable of killing a wide range of microbes. These include neutrophil elastase, cathepsin G, proteinases, defensins, lactoferrin and (MPO) (Remijsen *et al.*, 2011). The release of NETs by neutrophils *in vitro* occurs within 2-4 hours following activation (Fuchs et al., 2007). *In vitro* NETs can be degraded by DNAses, and some pathogens have evolved strategies to evade capture by NETs through the production of DNAses (Beiter et al., 2006) or modifications to cell wall structures (Wartha et al., 2007).

The antimicrobial activity of extracellular traps has been demonstrated in many settings, however the extent with which NETs contribute to pathogen killing is a topic of controversy. Interestingly, there exists evidence of extracellular trap formation being detrimental to the host through the induction of autoimmune responses, for example, in systemic lupus erythematosus and rheumatoid arthritis (Zhong et al., 2007).

In some circumstances NETs can form in the context of cell death (Fuchs et al., 2007). The process of extracellular trap release has been termed ETosis, or NETosis for neutrophils specifically, after the identification that in some contexts, extracellular trap release from neutrophils is accompanied by the programmed cell death of the neutrophil (Wartha and Henriques-Normark, 2008). It is currently understood that when NET formation occurs in the context of cell death, this cell death programme is distinct from apoptosis and necrosis, and occurs independently of caspases and certain kinases such as RIP-1 (Remijsen *et al.*, 2011). NETosis begins with the activation of surface receptors and the adhesion of the neutrophil to the substratum (Figure 1.3A-B). This is followed by decondensation of nuclear chromatin and disintegration of nuclear and granular membranes. In the cytoplasm, granular membranes are disrupted, allowing the leakage of granule components including MPO and neutrophil elastase into the cytoplasm (Figure 1.3C). This also facilitates the release of the chromatin leaking from the nucleus into the tissues (Fuchs et al., 2007). The neutrophil then rounds up and the plasma membrane ruptures, expelling the nuclear material embedded with granule proteins into the extracellular space (Figure 1.3D) (Brinkmann and Zychlinsky, 2012).
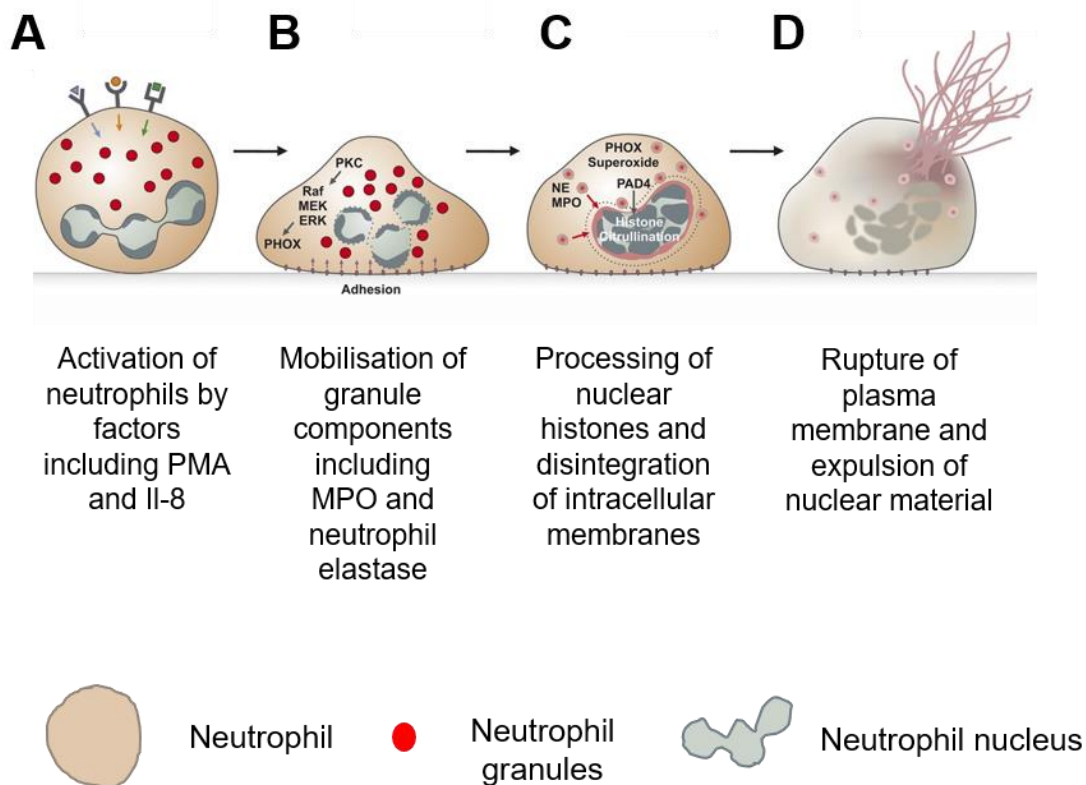
Figure 1.3: Neutrophil extracellular trap formation during NETosis.

Adapted from Brinkmann and Zychlinsky 2012. (A) Neutrophil activation leads to morphological changes. (B) Neutrophils flatten and adhere to the substratum and granule components are released. (C) Nuclear chromatin decondenses, the nucleus loses its lobules and the intracellular membranes disintegrate causing nuclear contents to mix with the cytoplasm. (D) Rupture of the plasma membrane causes expulsion of the nuclear material embedded with granule components.

Whilst some of the cellular processes which modulate NETosis have been dissected, many aspects still remain unresolved (Goldmann and Medina, 2012). The current understanding is that NETosis is mediated by histone citrullination, superoxide production and autophagy in neutrophils where apoptotic machinery is inhibited (Remijsen *et al.*, 2011). The crucial role of ROS production by NADPH oxidase in NETosis is demonstrated in patients with Chronic Granulomatous Disease, who have impaired NET production (Fuchs et al., 2007). There is evidence to suggest that ROS production blocks the apoptotic pathway in neutrophils as some reactive oxygen species inhibit caspases (Fadeel et al., 1998; Hampton et al., 2002). Downstream of NADPH oxidase and superoxide generation, a role for MPO in extracellular trap formation has also been identified as neutrophils from MPO deficient donors have a reduced capacity to form extracellular traps (Metzler et al., 2011).

Histone citrullination at arginine residues by the enzyme peptidylarginine deiminase (PAD4) drives nuclear decondensation. ROS production by NADPH oxidase in activated neutrophlis activates PAD4. Inhibition of PAD4 in HL-60 cells reduces histone hypercitrullination and NET formation (Wang et al., 2009). Furthermore, neutrophils in PAD4 deficient mice are unable to form NETs (Li et al., 2010).

An essential role of autophagy in NETosis is emerging, as recent evidence identified that pharmacological inhibition of autophagy prevents the intracellular chromatin decondensation essential for NET formation and NETosis (Remijsen *et al.*, 2011). How autophagy synergizes with ROS production to regulate chromatin decondensation remains unclear, although it has been suggested that Ca^{2+} leakage from disrupted ER membranes may promote PAD4 activity and histone citrullination (Remijsen *et al.*, 2011).

Conversely, evidence from initial NET studies suggests that in some contexts extracellular traps are released by viable neutrophils, as no cytosolic proteins were found in NETS and most cells excluded vital dyes. These NETs were induced rapidly following stimulation with neutrophil survival factors such as IL-8 and LPS (Brinkmann et al., 2004). More recent investigations have identified that the source of chromatin from NETs released by viable cells is from mitochondria rather than the nucleus. This type of viable NET production was induced by GM-CSF followed by TLR4 or C5a receptor stimulation, and like NETosis, was dependent on ROS production (Yousefi et al., 2008).

It is suggested that NET production by viable or dying cells should be considered as two separate entities. The reasons why only some neutrophils produce NETs is currently not understood, although it is likely that tissue context, neutrophil age and the heterogeneity of neutrophils could all contribute (Remijsen *et al.*, 2011).

1.8   Neutrophil swarming

Recent advances in *in vivo* imaging of neutrophil dynamics within interstitial tissues have identified that neutrophils coordinate their behaviour to arrange themselves into clusters. The dynamics of this clustering behaviour has been compared to the swarming behaviour seen in insects and birds, and has therefore been termed neutrophil swarming (Lämmermann et al., 2013).

Neutrophil swarms are the result of migration patterns coordinated through relay signalling between neutrophils through the production of self-generated chemoattractant gradients. Thus far the lipid leukotriene B_4 has been identified as one such relay signal, which is sensed by neutrophils over long range through auto-signalling (Lämmermann et al., 2013).

It has been proposed that swarm formation is a host-protective mechanism with an important role in limiting the extent of microbial infections (Chtanova et al., 2008) (Lämmermann, 2015). On the other hand neutrophil swarming comes at the cost of host tissue integrity, as large dense clusters of activated neutrophils can inevitably lead to tissue damage (Kreisel et al., 2010). Neutrophil swarming at intravascular lesions of Candida albicans has been linked to capillaritis with pulmonary haemorrhage. Clustering is absent in mice lacking the LTB_4 receptor and capillaritis is attenuated following inhibition of LTB_4 signalling, highlighting that dysregulation of neutrophil swarming can be detrimental to the host (Lee et al., 2018).   Regardless of their precise role it is clear that neutrophil swarming has a crucial role in regulating the balance between host protection and tissue destruction. Understanding the molecular controls of these novel neutrophil migratory behaviours may provide further insight into the drivers of neutrophil mediated tissue damage associated with chronic inflammatory diseases.

Although there are relatively few studies describing the modulation of neutrophil swarming due to its recent discovery, it is clear that neutrophil swarming is a highly regulated process coordinated by chemokines, lipids and integrins (Lämmermann et al., 2013). Intravital imaging studies have revealed that neutrophil clustering at inflammatory sites occurs following multi-step attraction cascades whose precise sequence varies depending on the precise tissue context (Lämmermann, 2015).

Evidence from studies in the ear dermis of mice suggest that neutrophil swarming is a 5-step cascade of events (Lämmermann et al., 2013). Thus far a series of sequential events has been proposed to describe the formation of neutrophil swarms, although confirmation of these stages in other systems is important (Kienle and Lämmermann, 2016). Initial recruitment of scouting neutrophils proximal to the wound site is observed rapidly following the introduction of an inflammatory stimulus and is modulated through the release of chemoattractant molecules from damaged cells and pathogens at the wound site. This first phase of chemotaxis is followed by a substantial neutrophil response whereby the vast numbers of highly directed neutrophils from sites distal to the wound site are recruited. These neutrophils migrate with increased directionality and speed, and coordinate themselves within the tissue environment to form large dense neutrophil clusters (Lämmermann et al., 2013). Initial amplification of neutrophil recruitment correlates with the appearance of a propidium iodide positive lesion at the wound site, suggesting a role for cell death in early signal propagation.

This is followed by paracrine signalling between neutrophils through the release of the lipid LTB_4 which amplifies recruitment signals over long range distances, resulting in a large influx of highly directed neutrophil migration followed by accumulation and cluster formation. The scouting and amplification stages are followed by an aggregation phase in which integrin receptors maintain cluster structure and integrity whilst neutrophils remodel the extracellular matrix surrounding the swarm to form a tight collagen-free wound seal, followed by swarm resolution which correlates with macrophage appearance around the outside of the clusters. These stages are summarised in figure 1.4.

A Stage 1
Swarm initiation
through tissue injury

B Stage 2
Swarm amplification
through cell death

C Stage 3
Swarm amplification
through relay signals

D Stage 4
Swarm aggregation
and tissue remodelling

E Stage 5
Swarm resolution
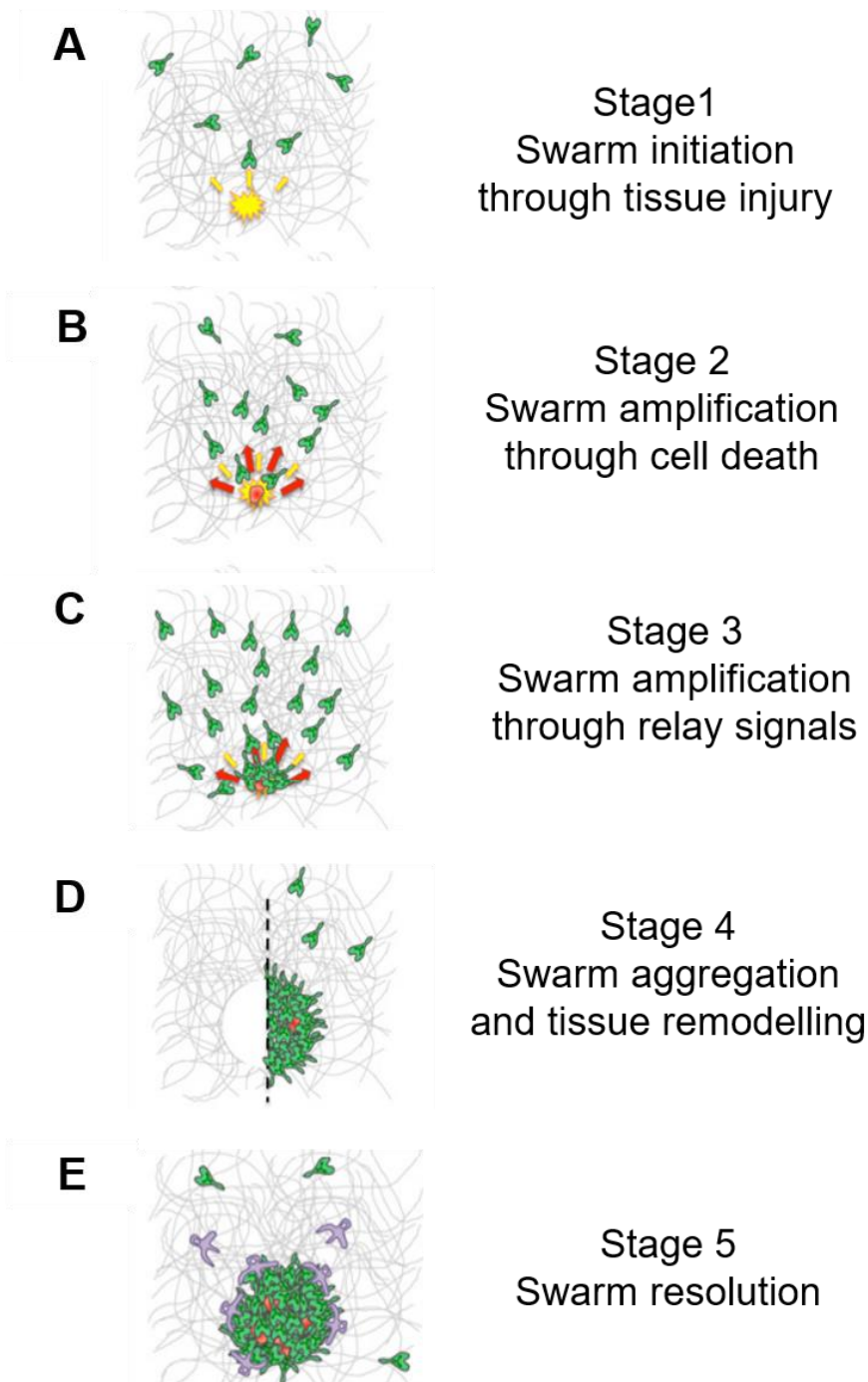
Figure 1.4: Proposed 5- stage model of the neutrophil swarming response

Adapted from Lammermann et al., 2015. (A) Neutrophils proximal to sites of local tissue damage sense short range chemotactic signals which induce their recruitment. (B) The death of dew dying neutrophils releases a first wave of amplification signals. (C) Clustering neutrophils secrete LTB_4 which acts as a relay signal to amplify recruitment signals to neutrophils over long distances. (D) Aggregating neutrophils displace collagen fibers and clusters persist to form a tight wound seal dependent on LTB_4, CXCR2 ligands, FPR2 ligands and integrins. (E) Macrophages appear around the outside of neutrophil clusters which coincide with swarm dissipation.

The current understanding is that neutrophil swarming is dependent on the tissue context in the inflamed tissue. The coordinated behaviour of neutrophils required for swarm formation occurs following the optimal combination of guidance factors from tissue lesions, and release of chemoattractant molecules from bystander cells and dying cells at the wound site (Kienle and Lämmermann, 2016). *In vitro* microfluidic studies have identified that human neutrophil swarming can be induced on a chip by zymosan beads, and that induction of swarming is dependent on the size of and distance between the beads, highlighting the role of gradient sensing and tissue context in regulating neutrophil migratory behaviours (Reátegui et al., 2017).

The key regulators of neutrophil swarming identified thus far, are cell death signalling which plays a role in swarm initiation, relay signalling through the release of LTB_4 and the role of integrin receptors to maintain cluster structure and integrity (Lämmermann, 2015).

1.1.10 Swarm initiation by cell death signalling

The recent identification of neutrophil swarming behaviour means that few studies have been able to dissect the molecular cues which govern this process, largely due to limitations in experimental systems required to understand the complexities of the swarming response.

Cell death signalling has been implicated in the initiation of neutrophil swarming to focal tissue damage in mice. The death of a few neutrophils in the inflamed tissue environment was enough to induce the chemotactic transition, leading to highly directed neutrophil migration characteristic of the swarming response. The appearance of propidium iodide positive lesions at the wound site correlates with the influx of highly directed neutrophil migration leading to swarm formation, suggesting a role for non-programmed cell death in swarm initiation (Lämmermann et al., 2013).

Necrosis is a form of uncontrolled cell death which occurs through autolysis and release of cellular components into the extracellular tissue. Different in almost every respect to programmed cell death, necrosis is the outcome of the direct effect of extreme stresses including heat, mechanical stress, nutrient deprivation or osmotic shock to the cell. The sequence of events leading to necrotic cell death include the swelling of the cytoplasm followed by the rupture of the plasma membrane and organelle breakdown. The liberation of factors from these dead cells into the tissue alerts cells of the immune system, initiating a local inflammatory response which often results in collateral tissue damage. Unlike apoptotic cells which are usually cleared rapidly by phagocytosis,

necrotic cells are removed incompletely through macropinocytosis, leaving much of their cellular debris behind (Golstein and Kroemer, 2007).

The precise chemotactic factors secreted by dying cells are currently unknown. A role for cell death signalling by NAD+ released by dying cells has been proposed. NAD+ is catabolised to cyclic ADP-ribose (cADPR) by neutrophils, where it has a role as a second messenger to mobilise calcium from intracellular stores (Lee, 1997). Inhibition of cADPR in neutrophils impairs the characteristic amplification of neutrophil recruitment seen in wildtype neutrophil swarming response (Ng et al., 2011). The role of NAD+ in swarm initiation has been investigated in mice, although currently no single receptor which utilises cADPR for calcium mobilisation has been implicated in modulating neutrophil recruitment amplification (Lämmermann et al., 2013).

1.8.1 Swarm amplification by relay signalling

The precise mechanisms governing swarm amplification are still being elucidated, however there now exists clear evidence that neutrophils modulate this phenomenon through intercellular relay signal communication. In particular, the role of LTB_4 as a signal relay molecule between neutrophils has been defined. GPCR signalling is essential in swarm amplification, as genetic depletion of the $G\text{-}\alpha_{i2}$ subunit in neutrophils, impaired the late recruitment of neutrophils during swarm amplification (Lämmermann et al., 2013). The role of many GPCRs in modulating swarm formation was investigated, however only neutrophils lacking the LTB_4 receptor have been shown to exhibit impaired neutrophil swarming responses. Neutrophils lacking the high affinity receptor for leukotriene B_4, BLT-1, showed no defect in their ability to recruit to focal tissue damage during the early phases of recruitment. However during the second phase of signal amplification these BLT-1 deficient neutrophil did not exhibit the bi-phasic response to focal damage seen in wildtype neutrophils, and recruitment of neutrophils from distal sites was impaired (Lämmermann et al., 2013). In this model neutrophils are a major source of LTB_4 essential in auto-signalling during swarm amplification.

1.8.2 Swarm aggregation and integrin signalling

In terms of the outcome of neutrophil swarming, neutrophil swarms in mice and human neutrophils can be transient or persistent. Transient swarms have been observed at sites of infection, where pathogens and dead cells are randomly distributed. These swarms persist for less time than the swarms observed at sites of focal tissue damage, where regions of dead cells are concentrated within a stable swarm centre (Lämmermann et al., 2013)..

The migration of individual neutrophils once inside clusters is drastically reduced and neutrophils begin to aggregate on top of one another. The tight association of swarming neutrophils is mediated by neutrophil-derived chemokines, lipids and other sources of chemokines. Movement in the clusters at this stage is dependent on $G\alpha_{i2}$ signalling, as neutrophils depleted of this subunit were excluded from clusters during the aggregation phase whilst control neutrophils continued to aggregate. More specifically a role for the β2 integrin family has been identified in regulating the homotypic adhesions in neutrophil clusters (Lämmermann et al., 2013). During swarming, as well as producing large amounts of LTB_4, human neutrophils produce lipoxin A_4, resolvin E_3, and prostaglandins D_2 and E_2 (Reátegui et al., 2017). A role for lipoxin A_4 produced by neutrophil swarms during the aggregation phase has been identified in modulating swarm size *in vitro*, suggesting a role for pro-resolving lipid mediators in swarm modulation at its later stages (Reátegui et al., 2017).

The formation of substantial neutrophil aggregates results in the remodelling of tissues in the swarm environment. The extracellular matrix underlying the neutrophil swarm is remodelled by factors released by the aggregating neutrophils. Evidence suggests that neutrophil-induced proteolysis is driven by factors such as neutrophil elastase induced by LTB_4 (Lämmermann et al., 2013). It has been proposed that cluster maintenance is modulated by signalling through multiple GPCRs to promote neutrophil adhesions and persistent clustering (Lämmermann, 2015).

1.8.3   Swarm resolution

The mechanisms which result in the cessation of neutrophil clustering are unknown, although one possible explanation is that neutrophil-derived signals responsible for maintaining neutrophils in stable aggregates are overridden by other competing attractant signals within the inflammatory environment (Lämmermann, 2015). Potential modulation could be the antagonism of LTB_4 signalling in neutrophils to prevent additional neutrophils from joining the cluster, or activation of receptors involved in inflammation resolution to drive the dissipation of swarms (Lämmermann, 2015). Profiling of cytokine and chemokines released by human neutrophils during swarming *in vitro* has identified that pro-resolving lipid mediators such as lipoxin A4, resolvin E3 and prostaglandins D2 and E2 are produced during the swarming response. A specific role for lipoxins A4 in modulating swarm stop signals has been identified, as neutrophils pre-treated with lipoxins A4 prior to swarming assays form substantially smaller neutrophil clusters (Reátegui et al., 2017).

The mechanisms which govern the persistence of swarming remain to be elucidated. *In vitro* human neutrophil assays are being used to profile the mediators released from swarming neutrophils compared to non-swarming neutrophils, and thus far 45 have been identified, which may play a role in the start and stop signals required for the swarming response (Reátegui et al., 2017).

1.8.4   Physiological roles of neutrophil swarming

The precise physiological role for swarming is not known, although arguments are currently being made for both host-protective and host-damaging outcomes. It has been suggested that, like all aspects of neutrophilic inflammation, swarming is a double-edged sword, the role of which is important in preventing bacteria from establishing a foothold in the host (Reátegui et al., 2017). The role of swarming as a host-protective mechanism has been demonstrated in zebrafish where neutrophil clustering at sites of microbial infection has been observed (Chtanova et al., 2008). On the other hand, neutrophil swarming comes at the cost of host tissue integrity, as large dense clusters of activated neutrophils can inevitably lead to tissue damage (Kreisel et al., 2010).

Regardless of the dynamics of neutrophil recruitment to, and behaviour in, the interstitial tissue, having completed their role as anti-inflammatory foot soldiers, neutrophils must be removed from the inflammatory site to enable the restoration of tissue homeostasis.

1.9   Inflammation resolution

During inflammation, neutrophil survival factors produced by the local inflammatory environment modulate the longevity of neutrophils to ensure they successfully perform their anti-microbial roles at sites of infection and tissue damage. Survival factors are both host- and pathogen-derived signals, including GM-CSF, G-CSF, IL-2, IFNγ, IL-1β and TNF-α (Geering et al., 2013).

Following the neutralisation of an inflammatory stimulus, a series of coordinated processes must occur to promote the restoration of tissue integrity. For tissue homeostasis to be restored, neutrophil recruitment from the blood must cease, the production of pro-inflammatory factors must be inhibited, and extravasated neutrophils at the inflammatory site must be removed (Ortega-Gómez et al., 2013). These processes are mediated by chemokine depletion at the wound site, as well as neutrophil and macrophage derived mechanisms such as neutrophil apoptosis, uptake of apoptotic bodies by macrophages and macrophage class switching (Ortega-Gómez et al., 2013). Depletion of chemokine production at inflammatory sites abrogates further neutrophil recruitment. The local chemokine concentration sensed by neutrophils is reduced by the

catabolism of chemokines through their proteolysis, or through chemokine sequestration by neutrophil decoy receptors (Ortega-Gómez et al., 2013).

Having performed their role at the inflammatory site, neutrophils may undergo apoptosis and are removed from the tissue by macrophages. Apoptotic neutrophils release factors such as annexin A1 and lactoferrin, which directly inhibit neutrophil recruitment to promote the restoration of tissue homeostasis (Bournazou et al., 2008; Dalli et al., 2008). Apoptotic neutrophils are also thought to express 'find me' and 'eat me' signals which promote their clearance by scavenger phagocytes (Ravichandran, 2010). The uptake of apoptotic bodies by macrophages in a process known as efferocytosis triggers their class switching from a pro-inflammatory M1 phenotype to an anti-inflammatory M2 phenotype. M2 polarised macrophages have a distinct transcriptomic profile, with genes involved in antigen processing and presentation, T and B cell recruitment and inflammatory cell clearance being upregulated (Stables et al., 2011). They also produce anti-inflammatory cytokines such as TGF-β, IL10, and prostaglandin E2 (PGE$_2$) (Fadok et al., 1998).

1.9.1 Neutrophil apoptosis

Apoptosis is the process by which cells perform programmed suicide by activating intracellular pathways, resulting in the collapse of the cytoskeleton, defragmentation of nuclear DNA and cell shrinkage - all key characteristic of apoptotic cells (Hengartner, 2000). Apoptosis can be activated by external and internal factors which ultimately result in the activation of a caspase cascade, degrading cellular organelles in a tightly controlled manner.

The caspase family of proteases mediate the biochemical modifications orchestrated in cells during apoptosis. The caspases are a highly conserved family of proteins which are synthesised in cells as precursor procaspases lacking protease activity. Constitutive production of inactive caspases allows cells to rapidly activate their apoptotic machinery following a death stimulus. The inactive caspases gain function through a cascade of proteolytic cleavage events which ultimately results in the degradation of cellular organelles. The initiator caspases (typically caspases 8, 9 and 10) exist early in the proteolytic cascade, where they exert their protease activity to activate downstream effector caspases through cleavage from pro caspases to active caspases (Witko-Sarsat et al., 2011). Once activated, the effector caspases (caspase 3, 6 and 7) are able to cleave key functional proteins following their activation, resulting in the characteristic morphological changes seen in apoptotic cells. (McIlwain et al., 2013). Neutrophil

apoptosis occurs via either the extrinsic or intrinsic apoptosis pathways which are activated by different stimuli.

1.9.1.1   The extrinsic apoptosis pathway

The extrinsic apoptotic pathway involves the induction of caspase mediated cell death through the activation of cell death receptors by other cells. Extracellular ligands including TNF and FAS ligand bind to their receptors, TNF related apoptosis-inducing receptor (TNFR) and FAS receptor, respectively. Following the activation of these death receptors, conformational changes result in the activation of intracellular associated receptor death domains and the recruitment of proteins including effector procaspases 8 and 10 to form a complex known as the death-inducing signalling complex (DISC). The clustering of these proteins in the DISC results in the activation of procaspases 8 and 10 to trigger the proteolytic caspase, resulting in the activation of effector caspases to drive the degradation of cellular organelles (Cohen, 1997; Renshaw et al., 2003).

1.9.1.2   The Intrinsic apoptosis pathway

The intrinsic or mitochondrial apoptotic pathway is activated in response to intracellular stresses including DNA damage, growth factor withdrawal and oncogenic stress. The intrinsic pathway is characterised by the release of pro-apoptotic agents into the cytoplasm following mitochondrial permeabilisation, where they trigger the assembly of the apoptosome. Intrinsic apoptosis is regulated by the BCL-2 family of pro and anti-apoptotic proteins. The release of pro-apoptotic agents from the mitochondria is dependent on the formation of membrane pores or channels through the aggregation of pro-apoptotic BCL-2 proteins Bax and Bak. The channel forming activity of these constitutively expressed proteins is repressed in healthy cells by anti-apoptotic BCL-2 proteins which bind to and sequester their activity, preventing the cell from triggering the apoptotic machinery. Cellular stressors drive the expression of a second family of pro-apoptotic BCL-2 proteins including Bim, Bid, Puma, Noxa and Bad. These proteins bind to and sequester the activity of the anti-apoptotic BCL-2 proteins, resulting in the restoration of the channel forming functions of Bak and Bax to drive the cell down the apoptosis pathway through the release of pro-apoptotic agents, including cytochrome c, apoptotic-protease activating factor-1 (APAF-1) and second mitochondria-derived activator of caspases (SMAC) into the cytoplasm (KILE, 2009).

1.9.2   Neutrophil reverse migration

Human neutrophils are now recognised to have alternative fates in addition to apoptosis following their role at inflammatory sites. Reverse migration is the term used to describe the retrograde migration of neutrophils away from an inflammatory site. Encompassed within this term are the migratory behaviours of neutrophils ranging from those which

have completely reversed their polarity, to those making a U-turn (Nourshargh et al., 2016).

Neutrophil reverse migration was first identified in a zebrafish model of tail fin injury, where neutrophil motility away from injured tissue was reported (Mathias et al., 2006). There now exists strong evidence for reverse migration which has now been observed *in vivo* in many models including mice (Wang et al., 2017; Woodfin et al., 2011), human neutrophils (Buckley et al., 2006) and zebrafish embryos (Elks et al., 2011; Mathias et al., 2006).

1.9.2.1 Modes of reverse migration

For a neutrophil to migrate from an inflammatory site, there are multiple environmental cues to integrate and barriers for neutrophils to breach, hence neutrophil reverse migration has several modes. The first stage of reverse migration involves the movement of neutrophils from inflammatory sites in the tissue, through the surrounding interstitial tissue. The dispersal of neutrophils into the interstitial tissue has been proposed to be a mechanism by which the inflammatory burden is dissipated (Nourshargh et al., 2016). To re-enter the circulation following movement through the tissue, neutrophils must breach the pericyte layer separating the interstitium and the vascular lumen. Once in the sub-capillary space between the pericytes and the lumen, neutrophils must finally migrate back through the endothelial layer, a process termed reverse transendothelial migration (rTEM).

Evidence for all modes of reverse migration is building, however currently there is uncertainty with regards to the mechanisms which govern all modes of reverse migration, and whether these modes share common mechanisms. Of the work carried out to dissect the molecular control of reverse migration, mechanisms governing reverse luminal crawling and reverse transendothelial migration are being elucidated, and there exists evidence to suggest signalling pathways which control reverse interstitial migration.

1.9.2.2 Reverse transendothelial migration

Reverse transendothelial migration is likely to be modulated by multiple mechanisms. The endothelial junction protein JAM-C has been implicated in reverse transendothelial migration, evidence from human and murine models suggests that neutrophils exhibit significant rTEM when JAM-C function is diminished (Woodfin et al., 2011). Redistribution of JAM-C from endothelial cell junctions has been reported in some acute inflammatory conditions, as well as through cleavage by neutrophil elastase. It has been proposed from these studies that JAM-C modulates the barrier function of endothelial cells such that

expression of JAM-C maintains endothelial cells in a polarised manner, resulting in a one-way gate to allow migration of neutrophils from the lumen into the tissue. The current hypothesis is that removal of endothelial JAM-C from endothelial junctions alters their junctional integrity and therefore barrier function, enabling rTEM**.** The mechanisms mediating luminal-to-abluminal migration through JAM-C during neutrophil recruitment are not fully understood, but have been speculated about (Nourshargh et al., 2016).

Another scenario has been proposed to explain reverse transendothelial migration, in which neutrophils in the sub-endothelial capillaries between the lumen and pericytes migrate back through the endothelium. It has been proposed that in this scenario neutrophils migrate back into the lumen due to diminished chemokine gradients to provide guidance signals to promote migration, for example during inflammation resolution. Conversely, rTEM could be a result of impaired integration of environmental cues due to receptor or downstream signalling desensitisation following prolonged exposure to gradients, for example in prolonged or excessive inflammation (Nourshargh et al., 2016).

1.9.2.3   Reverse interstitial migration

Reverse interstitial migration describes the retrograde movement of neutrophils through the interstitium away from the inflammatory site. Two competing hypotheses are currently being dissected to explain this phenomenon. The first, is that neutrophils respond to both chemotactic or chemorepulsive gradients, and reverse interstitial migration occurs due to fugetactic gradients repelling neutrophils from inflammatory sites (Powell et al., 2017; Tauzin et al., 2014). The second is that neutrophils become desensitised to chemotactic gradients through modulation of surface receptors or signalling pathways, and revert back to their default patrolling behaviours during reverse interstitial migration (Holmes et al., 2012). Evidence currently exists to support both hypotheses, and it is possible that the high redundancy of the immune system would allow for both of these methods of modulation to occur synergistically to drive inflammation resolution.

Evidence from zebrafish studies implicate a role for macrophage-produced reactive oxygen species (ROS) signalling in driving neutrophil reverse migration via a contact-dependent mechanism. Macrophage recruitment to inflammatory sites is important in driving inflammation resolution through the action of redox-SFK (Src family kinase), although neutrophils reverse migration still occurs in the absence of macrophage contact, suggesting a role for other factors in driving this process (Tauzin et al., 2014).

A specific role for the CXCR2/CXCL8 signalling axis has been identified in zebrafish larvae, where reverse migration is impaired in Cxcr2 and Cxcl8 deficient neutrophils. Evidence from this study suggests that macrophages or other cells at the wound site produce pro-resolving factors, such as Cxcl8, which drive reverse migration. Macrophages at the wound site were unable to drive reverse migration as previously reported (Tauzin et al., 2014) in the absence of CXCR2/CXCL8 signalling (Powell et al., 2017).

The precise action by which CXCR2/CXCL8 signalling drives reverse migration is not fully understood. It is suggested that rather than acting to directly repel neutrophils, exposure to Cxcl8 alters neutrophil chemokinesis. *In vitro* findings identified that priming of neutrophils by pre-exposure of neutrophils to CXCL8 impairs their migration along CXCL8 gradients, promoting their random motility in both directions along the gradient (Powell et al., 2017). These findings support the hypothesis that neutrophils at inflammatory sites switch from active migration by chemotaxis, to a random migration mode, a theory based on the mathematical modelling of neutrophil reverse migration in zebrafish (Holmes et al., 2012).

1.9.3   Retention signalling hypothesis

Neutrophils experience a range of extracellular signals at the inflammatory site which allows them to coordinate their behaviour. There is a growing body of evidence to suggest that a subset of these signals may be responsible for the retention of neutrophils at sites of inflammation through the provision of spatiotemporal guidance cues, which tell neutrophils where the wound site is.

Hypoxia inducible factor (HIF) signalling has been identified as a master regulator of neutrophil reverse interstitial migration in zebrafish. Activation of HIF signalling at inflammatory sites is a well characterised process which in primary human neutrophils, mice, and zebrafish is shown to result in the prolonged survival and activity of neutrophils (Walmsley et al., 2005). In zebrafish larvae, stabilisation of HIF-1α using both pharmacological and genetic approaches delays the resolution of inflammation induced by tail-fin transection, by reducing both neutrophil apoptosis and reverse migration (Elks et al., 2011). This study indicates that downstream targets of HIF signalling retain neutrophils at inflammatory sites.

Recent findings in zebrafish demonstrate that reverse migration can be targeted therapeutically to accelerate the resolution of inflammation. The compound Tanshinone IIA, derived from a Chinese medicinal herb, is able to accelerate both neutrophil

apoptosis and reverse migration to drive inflammation resolution in zebrafish. The pro-resolving effects of Tanshinone IIA were able to override the pro-inflammatory signalling generated through HIF1a stabilisation to drive reverse migration even in a model of chronic inflammation.

Mathematical analysis of neutrophil positions in zebrafish larvae was performed to identify cell migration dynamics in the context of neutrophil reverse migration (Holmes et al., 2012). Dynamic modelling was performed based on simulations which estimated whether neutrophil movement away from wound sites best fit a mathematical model whereby neutrophils randomly redistribute into the tissue, or a model in which neutrophils are actively driven away by fugetactic gradients. Evidence from this study suggests that neutrophil reverse migration is the stochastic redistribution of neutrophils into the surrounding tissue, rather than their active migration away from the wound site (Holmes et al., 2012). These data suggest that neutrophils lose their responsiveness to local chemotactic gradients over and redistribute into the tissue (Holmes et al., 2012).

Taken together the evidence from these studies suggests that a downstream target of HIF-1α which can be targeted therapeutically generates a neutrophil retention signal. We hypothesise that desensitisation of neutrophils to 'retention signals' causes their removal from inflammatory sites by reverse migration. Retention signals could overlap with neutrophil survival signals which modulate prolong neutrophil lifespan at sites of inflammation.

Hypothetically, generation of a neutrophil retention signal at the wound site requires two parts. The first being the detection of a gradient at the wound site by neutrophils, which tells them where the wound site is, and the second is the tuneable sensitivity of neutrophils to these gradients, allowing them to become desensitised. A retention signal could be achieved by an upregulation of ligand produced at the wound site, an upregulation of receptors on the neutrophil surface to increase neutrophil sensitivity to a ligand gradient, or a combination of the two. Equally, desensitisation of the neutrophil to a retention signal could arise from a decrease in ligand production at the wound site, a decrease in receptor expression on the cell surface, a decrease in ligand availability through the expression of decoy receptors, or a combination of all three.

Intracellular signalling in response to extracellular ligand occurs following ligand binding to GPCRs which induces a conformational change in the receptor and G protein activation. Cellular desensitisation to extracellular ligand through receptor internalisation is a characteristic feature of signalling through G protein coupled receptors. The chemokine receptors are a family of GPCRs of many of which are

expressed on the surface of neutrophils (Futosi et al., 2013). The role of many of these GPCRs in inflammation have been well characterised (Su and Richmond, 2015; Wareing et al., 2007).

Therapeutically targeting neutrophil reverse migration would be a successful way to drive inflammation resolution to treat chronic inflammatory diseases. It is possible that reverse migration plays a larger role in inflammation resolution than apoptosis or draining of neutrophils to lymph nodes. By targeting neutrophil reverse migration, initial recruitment to the inflammatory site would not be effected so the host remains protected against infection, and reverse migrated neutrophils would behave like tissue resident neutrophils without causing damage to other tissues.

Further work to elucidate the mechanisms underlying the reverse migration is required to fully understand the complex array of signalling which drives the movement of neutrophils away from inflammatory sites. During this project I will investigate the hypothesis that neutrophils are desensitised to retention signals generated through G protein coupled receptor signalling through ligand mediated receptor internalisation, and that this causes their reverse migration into the surrounding tissue (summarised in Figure 1.5).
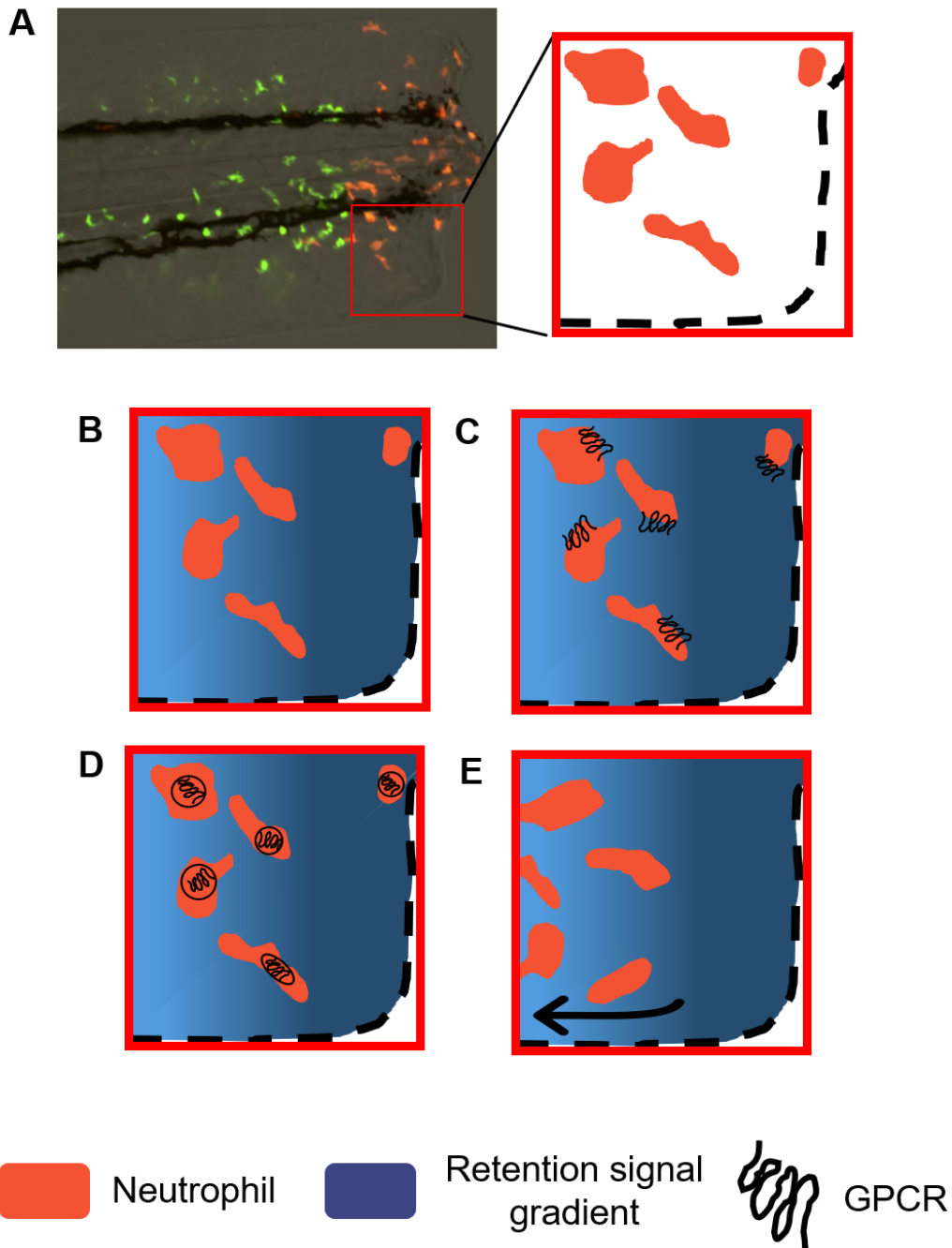
Figure 1.5 Retention signalling hypothesis.

(A) Image of photoconverted neutrophils at the wound site in a 3dpf zebrafish larvae to provide context to the hypothesis. (B) Neutrophils integrate numerous signals to choreograph their movement within complex 3D structures, which in zebrafish occurs by the presentation of directional cues in soluble form or haptotactic gradients. We propose that a subset of these gradients acts as a retention signal to tell neutrophils where the wound site is. (C) Neutrophils sense retention signals in the form of chemokines through GPCRs which retain them at the wound site during inflammation. (D) A characteristic feature of GPCR signalling is ligand mediated receptor internalisation. We hypothesise that neutrophils become desensitised to retention signals through receptor internalisation. (E) Decreased receptors on the neutrophil surface leads to decreased retention signalling, and the migration of neutrophils into the surrounding tissues.

50

1.10 The zebrafish

The zebrafish (*Danio rerio*) has emerged as an excellent model to study many vertebrate processes and is used widely as a model in labs throughout the world (Henry et al., 2013). The ease with which zebrafish can be genetically and pharmacologically manipulated along with their optical transparency, small size and fast generation time make zebrafish a powerful model system for the study of many developmental processes. Molecular biologist Dr. George Streisinger produced the first zebrafish clone in the 1970's which was originally used by the developmental biology community for *in vivo e*arly vertebrae development (Streisinger et al., 1981). Today, the zebrafish is recognised as a model organism for studies across multiple fields including behavioural genetics (Norton and Bally-Cuif, 2010), organogenesis, (Thisse and Zon, 2002) and infection and immunity (Trede et al., 2004).

1.10.1 Transgenic zebrafish lines to study inflammation

To study immune cell behaviour during inflammation in vertebrates, the zebrafish circumvents limitations associated with imaging of murine tissues. There is high homology of multiple cells of the innate immune system, which is competent from the early stages of development, between the zebrafish and mammals (Loynes et al., 2010). This combined with the 4 week period in which the immune system of the larvae is entirely reliant on the innate immune response, makes the zebrafish an apt model to study inflammation (de Oliveira et al., 2013). Furthermore, the external fertilisation of larvae and ease with which genetic manipulations can be introduced into the genome mean that genes of interest can be easily manipulated to investigate their function.

There are 450 million years of divergence between zebrafish and humans, yet there exists a remarkable degree of conservation between the two immune systems (Kumar and Hedges, 1998). The pathways governing hematopoiesis are highly conserved, and a large number of the transcription factors which modulate hematopoiesis in mammals have orthologues in zebrafish (Davidson and Zon, 2004). Like other vertebrates, zebrafish have primitive and definitive waves of hematopoiesis (de Jong and Zon, 2005). Primitive hematopoiesis occurs in the intermediate cell mass (ICM) and the anterior lateral mesoderm (ALM), where the production of erythrocytes occurs in the ICM and myeloid cells in the ALM (Lieschke et al., 2002). The definitive wave begins in the aorta-gonad-mesonephros at around 2dpf. During definitive hematopoiesis, self-renewing pluriopotent HSCs are produced. After colonization and maturation steps during larval development, these blood cells colonize the adult kidney marrow, which is the zebrafish equivalent of human bone marrow (Chen and Zon, 2009).

Unlike other invertebrate models used to study inflammation and immune disease such as *Caenorhabditis elegans* and *Drosophila melanogaster*, zebrafish possess an adaptive immune system (Lieschke and Currie, 2007). Along with their adaptive humoral and cellular immune responses, the zebrafish innate immune system shares similarities with that of mammals with immune cells including macrophages and neutrophils, as well as TLRs, complement factors and homologues to mammalian cytokines including TNFa and IL1b (Lieschke and Currie, 2007).

Zebrafish neutrophils share characteristic morphological features of human neutrophils such as segmented nuclei and cytoplasmic granules. Like other teleosts, zebrafish possess two types of granulocyte. One population of neutrophil granulocytes or heterophils have a multilobulated segmented nucleus which comprised more than 95% of circulating granulocytes, and a smaller population of eosinophil granulocytes with a peripheral nonsegmented nucleus (Lieschke et al., 2001). Functionally zebrafish neutrophils are analogous to human neutrophils, being recruited to sites of injury and infection where they produce reactive oxygen species, degranulate and phagocytose pathogens (Lieschke *et al.*, 2001). Primitive neutrophilic granulocytes are detected in the circulation in zebrafish larvae by 48hpf whilst eosinophilic granulocytes aren't detected until 5dpf (Lieschke *et al.*, 2001).

Zebrafish heterophil granulocytes are morphologically similar to human neutrophils, with segmented nuclei and cytoplasmic granules. A zebrafish specific myeloperoxidase homologue is expressed specifically in neutrophils, and is detected at around 18hpf in the posterior intermediate cell mass. From 24hpf mpx positive cells can be detected within the vasculature and then become visible throughout the whole embryo, enabling the visualisation and study of neutrophils from early stages of development (Bennett et al., 2001).

Understanding of the pathophysiology of the immune system has been accelerated by the development of transgenic zebrafish models which are today used by many research groups (Henry et al., 2013). Perhaps the most attractive feature of the zebrafish is their optical transparency during early stages of development, which enables the visualisation of fluorescently labelled cell populations *in vivo* in real time (Renshaw et al., 2006).

Identification of the zebrafish myeloperoxidase promoter which drives gene expression in all neutrophils enabled the development of a stable transgenic line using BAC recombineering to drive the expression of GFP in neutrophils specifically (Renshaw et al., 2006). This novel transgenic line has been used by many groups to observe the neutrophilic inflammatory response to tissue injury and infection and has provided

advances in the understanding of many aspects of neutrophil biology (Dalli et al., 2008; Elks et al., 2011; Robertson et al., 2014).

Limitations of this transgenic line are that individual neutrophil populations cannot be distinguished during the recruitment and resolution phases of inflammation. To overcome these limitations, transgenic lines expressing photoactivatable fluorophores such as dendra2 or kaede, under neutrophil specific promoters *lyz* or *mpx* have been developed (Elks et al., 2011; Mathias et al., 2006). The photoconvertible properties of the fluorescent protein kaede enable neutrophils recruited to inflammatory sites to be converted from green to red fluorescence following excitation by UV light. This enables the tracking of the red population of cells which have visited the inflammatory site, to be tracked during the resolution of inflammation and is susceptible to pharmacological and genetic manipulations. These transgenic lines have provided an invaluable tool to study the behaviour of neutrophils following their activity at inflammatory sites (Ellett et al., 2015; Holmes et al., 2012).

Injury to the tail-fin of zebrafish larvae initiates an acute neutrophilic inflammatory response which resolves with similar kinetics to that of mammals (Renshaw and Loynes, 2006). Reverse migration in zebrafish is quantifiable using a photoconversion system in which neutrophils driving the photoswitchable protein kaede can be converted from green to red fluorescence at the wound site using UV light (Elks et al., 2011; Robertson et al., 2014). Photoconverted cells which have been to the wound site can then be tracked during the inflammation resolution phase, providing a read out of neutrophil reverse migration.

The function of zebrafish gene products can be investigated using chemical compounds through incubation in zebrafish water or injected directly into their blood circulation. Neutrophil apoptosis and reverse migration can be manipulated in zebrafish larvae using chemical compounds to accelerate or delay these processes (Elks et al., 2011; Robertson et al., 2014). Future studies using these tools will enable the elucidation of the mechanisms which govern the migratory behaviours of neutrophils during the inflammatory response.

1.10.2 Disadvantages of the zebrafish model

As with every model organism, there are disadvantages to using the zebrafish model. Zebrafish are evolutionarily more distant from humans than mammalian models including mice and rats, hence findings from zebrafish studies likely need to be replicated in mammalian systems before translating to human therapies. Zebrafish are ectothermic,

meaning their circadian clock and physiological response to temperature changes differs to mammals (Lahiri et al., 2005)

The zebrafish genome underwent a duplication event following the divergence of teleosts and mammals, consequently zebrafish are polypoid for many of their genes (Taylor et al., 2003). This feature of zebrafish genetics often hinders the generation of knockout strains, as approaches to disrupt one gene copy may not disrupt the second copy. Furthermore a high degree of genetic diversity has been observed between individual zebrafish genomes, even within fish of the same strain (Guryev et al., 2006).

There currently exist a limited number of cross-reacting antibodies for use in zebrafish, meaning that it is difficult to study protein expression (Staudt et al., 2015). To circumvent this, whole *mount in situ hybridisation* is an approach used to study the expression pattern of the mRNA for proteins of interest. Despite these disadvantages, the zebrafish is used widely in the scientific community to model human disease.

1.10.3 Zebrafish mutagenesis

The zebrafish is highly amenable to genetic manipulation, where forward and reverse genetic approaches have been used to understand gene function in biology (Lawson and Wolfe, 2011). Targeted mutations can be introduced into the zebrafish genome using approaches such as zinc-finger nucleases (Meng et al., 2008), TILLING (Moens et al., 2008) and TALENs (Sander et al., 2011). Morpholino-modified antisense oligonucleotides or injection of mRNA can be used to study the function of candidate genes transiently before committing to generate a stable mutant zebrafish line (Nasevicius and Ekker, 2000). The current gold standard for genetic approaches to gene is CRISPR.

1.10.3.1 CRISPR/Cas9

Advances in genome editing technology such as CRISPR (clustered regularly interspaced short palandromic repeats)/ Cas9 technology have resulted in the ability to genetically manipulate genes of interest rapidly and with ease (Cong et al., 2013). The streptococcus pyogenes type II CRISPR/Cas9 system is an adaptive immune mechanism by which s.pyogenes can respond to and remove foreign genetic material (Mojica et al., 2005). Immunity to bacteriophage or plasmid infection in s.pyogenes is provided by the CRISPR loci which contains many protospacer sequences of DNA with specificity to viral or plasmid DNA between palindromic DNA repeats (Bolotin et al., 2005). These protospacer sequences are transcribed and specificity is achieved by trans-activating cRNAs (tracr RNAs) which cleave the RNA to create crRNAs of approximately 20 base pairs in length. These crRNAs guide the Cas9 nuclease to the foreign DNA where it is able to introduce a double stranded break, providing sequence specific immunity against bacteriophage

DNA (Marraffini, 2016). The CRISPR/Cas9 system is able to introduce mutations into the genome through exploiting cellular DNA repair machinery mechanisms. Double stranded breaks are repaired by cellular machinery including homology directed repair, or non-homologous end joining (NHEJ).

Homologous recombination integrates exogenous repair templates into the genome to repair the double stranded break. This machinery can be exploited by providing new DNA sequences to be inserted into the genome, however the occurrence of this DNA repair machinery is rare and hence integration of the sequences is relatively inefficient (Gratz et al., 2014). Improvements to this system, for example by inhibiting the NHEJ machinery to drive homologous recombination, hold promise for the future of gene therapy (Zhang et al., 2017). NHEJ is the most common double stranded break repair process, however it is error prone and often results in DNA insertions or deletions (InDels) at the DNA break site. If the InDel results in a loss of function mutation including in-frame insertions, deletions or frame shift to introduce a premature stop codon, the function of the gene is altered (Su et al., 2016). This system has been adapted for use in organisms including mammalian cells, yeast, mice and zebrafish. By combining the spacer and tracer RNAs into one synthetic guide RNA, any genomic locus can be targeted by directing the Cas9 to any 20 base pair sequence directly upstream of a protospacer adjacent motif (PAM) sequence (Ran et al., 2013).

1.10.3.2 CRISPR interference

Modifications of the Cas9 nuclease through mutating its two nuclease domains HNH and RuvC have expanded the gene editing capabilities of the CRISPR/Cas9 system (Qi et al., 2013). A catalytically dead version of Cas9 'dCas9' which has no nuclease activity has been developed which is able to sterically block gene transcription through preventing transcription elongation (Larson et al., 2013). Synthetic guide RNAs are used to target the dCas9 to the genomic region of interest, where it interferes with the binding of key transcription factors to prevent transcription (Qi et al., 2013). Furthermore, modified versions of dCas9 containing transcriptional activators such as VP64, or repressors such as KRAB, can be used to activate or repress transcription more successfully (Dominguez et al., 2015). Repurposing of the Cas9 in this way has created a method of RNA-guided transcriptional regulation without altering the genome. This approach to knock down genes has potential for cell specific expression of the dCas9 to create cell-specific gene repression, as well as inducible dCas9 to control the time at which genes are repressed. The dCas9 has been shown to inhibit transcription successfully in bacteria, however repression in mammalian cells was only modest, hence the development of modified dCas9 fused to transcriptional repressors such as the Krüppel-associated box (KRAB)

(Gilbert et al., 2013). CRISPRi offers simplified approach for rapid and reversible genetic manipulation which holds huge promise for the future.

Currently both CRISPR/Cas9 and CRISPRi technologies are used widely in the zebrafish community to target genes of interest using guide RNAs to interrupt gene function at specific loci. The development of CRISPR interference technology means that targeted gene knockdown in specific lineages is now possible. Transgenic zebrafish lines driving a dead cas9 under cell-specific promoters will be used in future to achieve a transient silencing of gene expression in cells of interest.

1.11   Thesis aims

Neutrophil persistence at inflammatory sites is a major contributor to the pathogenesis of chronic inflammatory disease. The current therapies available to treat inflammatory disease do not target the neutrophilic component of these diseases, and this is perhaps why they are not effective in curing the diseases. Novel neutrophil behaviours including neutrophil reverse migration and neutrophil swarming have been identified in the last decade, which when understood more comprehensively, will open up a new range of therapeutic targets to accelerate the removal of neutrophils from inflammatory sites to treat the neutrophilic component of inflammatory disease.

I hypothesised that by using the zebrafish to study both neutrophil swarming and reverse migration, I could identify novel pathways involved in the inappropriate retention of neutrophils at inflammatory sites. The aims of this thesis are:

-        To define and characterise the neutrophil swarming response in zebrafish

-        To investigate the initiation of neutrophil swarming in order to identify key signalling pathways which amplify neutrophil recruitment to wound sites

-        To investigate the role of the CXCR4/CXCL12 signalling axis in modulating neutrophil removal from the wound site

2 Materials and methods

2.1 Reagents

All reagents and chemicals were purchased from Sigma Aldrich (Poole, UK) unless stated otherwise.

2.2 Zebrafish husbandry

All zebrafish were raised in the Bateson Centre at the University of Sheffield in UK Home Office approved aquaria and maintained following standard protocols (Nüsslein-Volhard and Dahm, 2002). Tanks were kept at 28°C with a continuous re-circulating water supply and a daily light cycle of 14 hours of light and 10 hours of dark. Zebrafish > 13 days post fertilisation (dpf) were given a diet of live artemia which was provided twice daily, whilst zebrafish >5dpf were fed Tetra A-Z powdered fish food.

To acquire zebrafish embryos, mating set up (described below) was carried in out in the evening before the light cycle changed, and embryos were collected the following morning. 'Marbling' adult tanks was commonly used to acquire embryos and was performed by placing a small tank of marbles into adult tanks containing between 10 and 40 fish. Adults lay eggs into the marbles which sit on top of a grid to allow embryos to filter through for collection. Alternatively, two adult fish of different genders were placed into a small mating tank separated by a divider which was removed when the light cycle changed in the morning, and embryos were filtered by a plastic grid into the space below for collection. Embryos at the same stage of development were then sorted into petri dishes, with 50-60 embryos per dish, in approximately 30mls of E3 media and kept in an incubator at a temperature of 28°c.

To sacrifice embryos at the end of an experiment or because they were approaching 5.2 dpf, embryos were anaesthetised using 0.017% 3-amino benzoic acid ethyl ester, or 'tricaine' and immersed in bleach.

All procedures were performed on embryos less than 5.2 dpf which were therefore outside of the Animals (Scientific Procedures) Act, to standards set by the UK Home Office.

2.3 Zebrafish anaesthesia

In all experiments tricaine was used as an anaesthetic prior to experimental work. Larvae were anesthetised by immersion in 0.168 mg/mL tricaine in E3. For imaging, larvae were maintained in 0.168mg/mL tricaine in LMP agarose until the end of experiment. Where

required, larval recovery was completed through replacing medium with fresh E3 which did not contain tricaine.

2.3.1 Tail-fin transection

To induce an inflammatory response, zebrafish larvae at 2 or 3dpf were anaesthetised in 0.017% tricaine (3-amino benzoic acid ethyl ester) in E3 media and visualised under a dissecting microscope. Unless stated otherwise tail-fins were transected consistently using a scalpel blade (5mm depth, WPI) by slicing in the pigment gap at 3dpf and ensuring the circulatory loop isn't damaged (Figure 2.1). When injuring larvae at 2dpf when the pigment gap was not developed, extra care was taken to transect the circulatory loop consistently proximal to the circulatory loop without damaging it. Following tail-fin transection larvae were placed in fresh E3 medium and left to recover at 28°c.

Figure 2.1: Tail fin transection of zebrafish larvae

Image to illustrate the region where tail fin transection of zebrafish larvae was performed at 3dpf to initiate an inflammatory response.

2.3.2 Non-standard methods of tail-fin transection

Where illustrated in figure legends, alternate methods were used to induce an inflammatory response. Figure 2.2 illustrates the injury severity types. A mild inflammatory response is induced by slicing the caudal tail-fin in the dorsal to ventral section to nick the tissue without damaging the notochord or circulation (A). A mild inflammatory response can also be induced by at the end of the caudal tail-fin without transecting the notochord or circulation (B). A severe inflammatory response is induced by cutting the whole length of the tissue at the end of the caudal tail-fin and transecting both the notochord and circulatory loop (C).
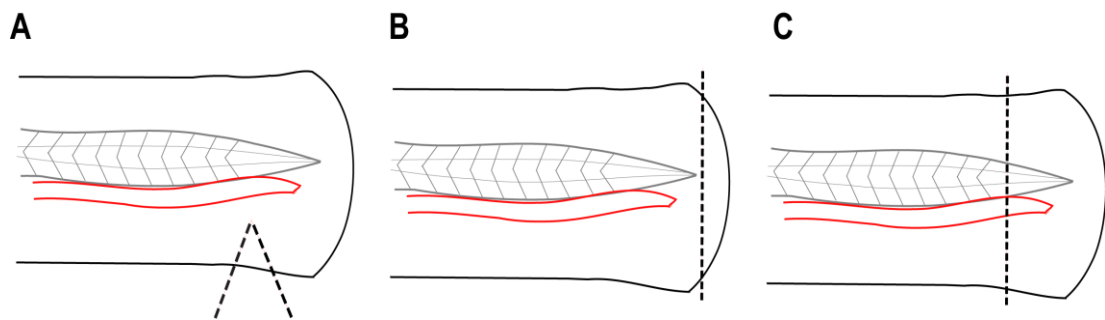
Figure 2.2: Non-standard methods of tail fin transection

An inflammatory response of varying severity can be induced by performing tail fin transections at different parts of the tail tin.

2.3.3 Microinjection of embryos

For injection of RNA or DNA embryos at the one cell stage, adults were placed in pair mating tanks and dividers removed at 8am to coincide with aquarium light cycles. Embryos were collected 20 minutes later and positioned against a glass cover slip inside a petri dish (Menzel-Gläser, Germany). Injections were performed using non-filament glass capillary needles (Kwik-Fil^{TM} Borosilicate Glass Capillaries, World Precision Instruments (WPI), Herts, UK) pulled using a Flaming Brown micropipette puller (Sutter Instrument Co., Novato, USA). RNA and DNA were prepared in sterile Eppendorf tubes and phenol red was added to allow for visualisation of injections. A graticule was used to measure 0.5nl droplet sizes to allow for consistency of injections. Injections were performed under a dissecting microscope attached to a microinjection rig (WPI). For DNA injections, the needle was aimed at the developing cell (Figure 2.3A). For RNA injections the needle was aimed at any point in the embryo including the yolk to enable faster injections (Figure 2.3B). Following microinjection embryos were transferred to clean E3 media and left to recover at 28°c.

2.3.4 Microinjection of larvae

For microinjection of compounds into the duct of cuvier, 2dpf larvae were anaesthetised and placed onto plates consisting of agarose dissolved in E3. Larvae were positioned using a fine hair taped into the end of a pipette tip, which allowed for gentle manipulation without causing damage to larvae. Injections were performed as described for microinjection of embryos, however the needle was aimed at the circulatory loop in the duct of cuvier. 1nl of compound was injected into the duct of cuvier and phenol red was added to compounds to visualise successful injections as it can be seen to circulate in the blood stream over the yolk sac. Following microinjection larvae were transferred to clean E3 media and left to recover at 28°c.
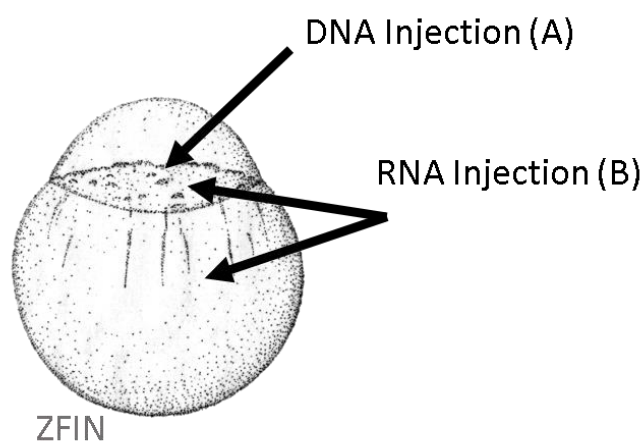
Figure 2.3: Microinjection of DNA and RNA into embryos at the one cell stage

Image of a zebrafish embryo at the one cell stage adapted from ZFIN. DNA injections were aimed at the developing cell to increase the chance of integration into the genome (A). RNA injections were aimed at any point in the yolk and cell (B).

2.3.5 Equation to determine dose of compounds for microinjection

To work out the dilution factor for stock solutions of compounds, an equation to determine the concentration of compound required in a 1nl injection to reach a desired body concentration in larvae was used by considering the total body volume of larvae (Figure 2.4).

$$\frac{Injection\ volume\ (nl)}{Larvae\ body\ volume\ (nl)} \quad \times \quad \begin{matrix} Concentration \\ in\ tube \end{matrix} \quad = \quad \begin{matrix} Final\ concentration \\ in\ larvae \end{matrix}$$

$$\frac{1nl}{370nl} \quad \times \quad \begin{matrix} Concentration \\ in\ tube \end{matrix} \quad = \quad \begin{matrix} Final\ concentration \\ in\ larvae \end{matrix}$$

Figure 2.4: Equation used to work out injection concentrations

When determining the dilution factors of stock solutions for injection into larvae, the above equation was used to work out the concentration required in tube to achieve desired final concentration in the body volume of larvae at 2dpf.

2.3.6   Compound incubation

Chemical compounds were dissolved in DMSO unless otherwise indicated. For compound treatment by incubation larvae were incubated in 6 or 24 well plates (SLS), containing no more than 12 larvae in 400µl of E3 for 24 well plates, or 20 larvae in 1900µl E3 for 6 well plates. Compounds were prepared in Eppendorf tubes suspended in 100µl E3 media which was added to wells to give a total volume of 500µl or 2000µl for 24 and 6 well plates respectively. For reverse migration assays AMD3100 was added directly to a 1% LMP agarose solution at 38°c to reduce the time between compound administration and imaging.

2.3.7   Mounting of larvae for microscopy

Prior to imaging, larvae were anaesthetised in tricaine and transferred to a mounting dish. For high power microscopy mounting dishes consisted of a 0.1mm cover slip (#0, SLS) placed into a circular receptacle secured using high vacuum grease (Dow Corning, Seneffe, Belgium) and for lower power imaging a 4x4 chamber mounting dish was used. Excess E3 was removed from larvae once placed in the mounting dish and covered in a low melting point (LMP) agarose (Sigma Aldrich) dissolved in clear E3 containing 4.2% tricaine. Unless stated otherwise LMP agarose solutions were made up to 1%. When necessary, appropriate volumes of compounds were also dissolved into the agarose solution for time lapse imaging. For long periods of imaging, a solution of clear E3 with 4.2% tricaine was added on top of the solidified agarose solution to prevent dehydration of larvae.

2.4 Neutrophil behavioural assays

2.4.1 Neutrophil recruitment assays

To observe the effect of compounds on the recruitment of neutrophils to the wound site, compounds were administered to larvae at 2 or 3dpf for 1 hour prior to injury. For administration to larvae at 2dpf, embryos were dechorionated and compounds were injected into the duct of Cuvier. For administration to larvae at 3dpf, compounds were dissolved in E3 media for 1 hour prior to injury which were left to recover in fresh medium containing the same dose of compounds. For injection assays larvae were injected and left to recover in E3 for 1 hour prior to injury. Neutrophils recruited to the wound site were counted at times indicated in figure legends.

2.4.2 Inflammation resolution assays

To study the resolution of inflammation, neutrophils were counted at the wound site at intervals during the resolution phase from 8-24 hours post injury in 2 or 3dpf *mpx:GFP* larvae as indicated in figure legends. Larvae were dechorionated (for 2dpf) and anaesthetised prior to injury by tail-fin transection and left to recover at 28°c in fresh E3 media. Larvae were screened for good neutrophil recruitment (around 20 neutrophils at the wound site) at 3-4hpi. Compounds were administered to larvae through injection into the duct of Cuvier in 2dpf larvae, or by incubation in the E3 media for 3dpf larvae at times indicated in figure legends. Neutrophils at the wound site were counted at 6hpi at the peak of recruitment to confirm that compound treatment did not alter the recruitment of neutrophils before counting during the resolution of inflammation.

2.4.3 Percentage resolution calculation

To determine the percentage resolution of larvae, neutrophils were counted at the peak of recruitment at 6hpi, and at time points during the resolution phase indicated in figure legends. The equation illustrated in Figure 2.5was used to calculate the percentage resolution.

$$\frac{\begin{array}{c}\textit{Neutrophil counts at}\\\textit{peak recruitment (6hpi)}\end{array} - \begin{array}{c}\textit{Neutrophil counts at}\\\textit{resolution time point}\end{array}}{\begin{array}{c}\textit{Neutrophil counts at}\\\textit{peak recruitment (6hpi)}\end{array}} \times \; 100$$

Figure 2.5: Equation for calculating % resolution of inflammation

2.4.4 Analysis of total body neutrophil count

Whole body neutrophil counts were measured in larvae at time points indicated in figures. Larvae were mounted in 1% agarose with tricaine and a single slice image was taken using a 4x NA objective lens on an Eclipse TE2000 U inverted compound fluorescence microscope (Nikon UK Ltd., Kingston upon Thames, UK). A GFP-filter was used at excitation of 488nm. Two images were taken per larvae, one of the head region and one of the tail region. Neutrophils were counted manually from both images and combined to give a total body neutrophil count.

2.4.5 Reverse migration assay

Reverse migration assays were performed using larvae expressing the photoconvertible protein kaede under the neutrophil specific mpx promoter; *Tg(mpx:GAL4;UAS:Kaede)i222* line (referred to as *mpx:kaede* thus forth). At 2 or 3dpf as specified in figure legends, larvae were anaesthetised and injured by tail-fin transection and left to recover at 28°c. Larvae were screened for good neutrophil recruitment at 3.5hpi. AMD3100 was administered at 4hpi by injection into the duct of Cuvier of 2dpf, or by incubation in LMP agarose at 5hpi in 3dpf larvae. Photoconverstion of kaede labelled neutrophils at the wound site was performed using an UltraVIEWPhotoKinesis^{TM} device (Perkin Elmer and Analytical Sciences) on an UltraVIEWVoX spinning disc confocal laser imaging system (Perkin Elmer).

The photokinesis device was calibrated using a coverslip covered in photobleachable substrate (Stabilo Boss^{TM}, Berks UK). Photoconverstion was perfomed using a 405nm laser at 40% using 120 cycles, 250 pk cyles and 100ms as previously published (Elks et al., 2011). Following calibration a region of interest was drawn at the wound site between the edge of the circulatory loop and encapsulating the entirety of the wound edge. Successful photoconversion was detected through loss of emission detected following excitation at 488nm, and gain of emission following 561nm excitation. Larvae were then transferred to an Eclipse TE2000-U inverted compound fluorescence microscope with 10x NA objective lense to acquire images using an andor zyla 5 camera (Nikon). Time lapse imaging of neutrophil reverse migration was performed for 5 hours using 2.5 minute intervals using GFP and mCherry filters with 488 and 561 nm excitation respectively.

For analysis of reverse migration, NIS elements software was used to compress z-slices into maximum intensity projections. A region of interest was drawn around the region away from the wound site, as illustrated in figure 2.6. For quantification of neutrophils moving away from the wound site, a threshold was applied to detect mCherry neutrophils from background noise and NIS elements software calculated the number of objects detected in the ROI at each time point, providing a read out of reverse migration.
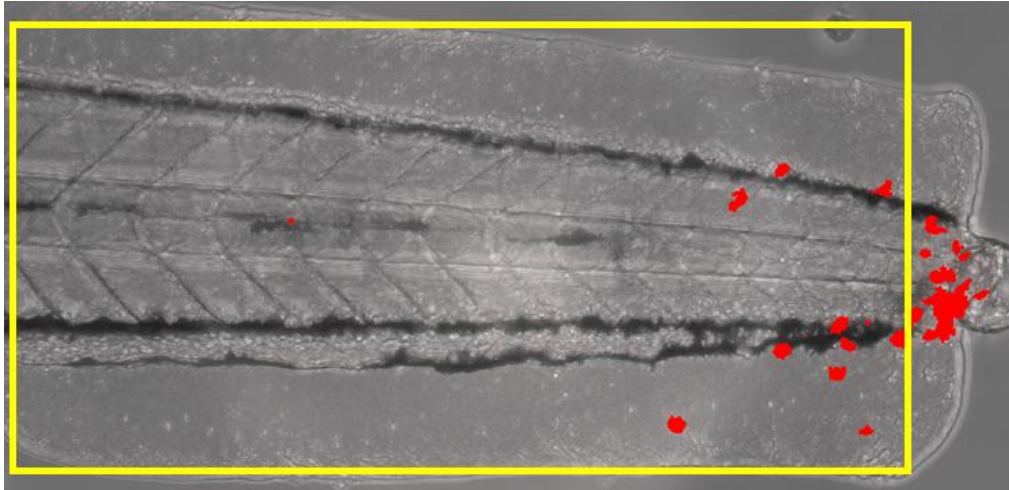
Figure 2.6 Quantification of neutrophil reverse migration

Neutrophil reverse migration was quantified using *mpx:kaede* larvae. Photoconverted neutrophils were quantified as they migrated away from the wound site using an automated assay to detect objects within a region of interest (yellow).

2.4.6 Fixation of larvae

Larvae were fixed prior to whole mount *in situ* hybridisation. Larvae were anaesthetised in tricaine at time points indicated in the figure legends. No more than 20 larvae were transferred to 1ml Eppendorf tubes and excess liquid was removed without damaging larvae. 1ml of paraformaldehyde (PFA) at 4°c was added to Eppendorf tubes for the fixation step. Larvae were stored at -20°c for at least 24 hours prior to use.

2.4.7 Whole mount *in situ* hybridisation

WISH was performed to examine the spatial expression of CXCL12a mRNA at the wound site in injured larvae. After 24 hours in PFA, fixed nacre larvae were transferred through a methanol series increasing in concentration and stored in 100% methanol at -20°c until use.

Larvae were rehydrated by transferring them through a reverse methanol series containing increasing concentrations of phosphate buffered saline plus tween 20 (Sigma-Aldrich) (PBT). Larvae were digested in proteinase K (Thermo Fisher) at 10μg/ml for 40 minutes and washed in PBT. Digested larvae were then fixed in 4% PFA at room temperature for 20 minutes followed by another PBT wash.

Pre-hybridisation buffer (PreHyb) was heated to 70°c in a water bath and larvae were incubated in PreHyb for 3 hours at 70°c. Probe-hybridisation buffer was heated to 70°c and PreHyb was replaced with ProbeHyb in which larvae were incubated overnight at 70°c. Buffers and wash solutions were prepared as described (Chitramuthu and Bennett, 2013).

The ProbeHyb was gradually removed by a series of washes containing decreasing concentrations of ProbeHyb and increasing concentrations of a HybWash:2x SSC solution at 70°c. Larvae were then washed in a 2x SSC solution at 70°c before being transferred through a reverse series of 2x SSC containing decreasing concentrations of 2x SSC and increasing concentrations of PBT. Finally larvae were washed in a PBT solution.

Following the wash stages a larvae were gently rocked in a blocking solution for 2 hours at room temperature. An anti-DIG-AP antibody (Roche, UK) was incubated in the blocking solution at a dilution of 1:5000 overnight at 4°c with gentle rocking.

The antibody was removed the next day and larvae were washed in PBT at room temperature followed by a series of washing in staining wash. Larvae were then transferred to a 24 well plate for incubation in staining solution until staining developed. The 24 well plate was wrapped in tin foil. Staining was terminated using 1mM EDTA and larvae were washed in PBT. Larvae were fixed in 4% PFA at room temperature for 20 minutes and then transferred through a methanol series to be stored in 100% methanol until imaging.

For imaging larvae were transferred through a reverse methanol series containing increasing concentrations of glycerol. Imaging was performed by placing larvae in an 80% glycerol solution onto a glass cover slip (SLS) and adjusting their position gently using a human hair. Imaging was performed using a fluorescent dissecting microscope with a Leica DFC310 camera and NIS elements software (Version 4.3).

2.4.8   Propidium iodide staining of larvae

To study the plasma membrane integrity of neutrophils, 3dpf *mpx:GFP* larvae were incubated in propidium iodide (1µg/ml) unless otherwise stated for 30 minutes prior to tail-fin transection. Larvae were mounted in a 1% agarose containing 1µg/ml PI immediately following injury. Images of the wound site were taken using a 20x objective on an UltraVIEWVoX spinning disc confocal laser imaging system (Perkin Elmer) using GFP and mCherry specific excitation filters.

2.5   Microcscopy

2.5.1   Timelapse imaging of neutrophil recruitment

For neutrophil swarming experiments, 3dpf *mpx*:GFP larvae were mounted in a 1% low melting point agarose solution (Sigma-Aldrich) containing 4.2% tricaine for imaging immediately after tail transection. Agarose was covered with 500µl of a clear E3 solution containing 4.2% tricaine to prevent dehydration. Time lapse imaging was performed from 0.5-5 hours post injury with acquisition every 30 seconds using an Eclipse TE2000-U

fluorescence microscope with a 1394 ORCA-ERA camera (Hamamatsu Photonics Inc). 10 z-planes were captured per larvae over a focal range of 100µm using a GFP specific filter with excitation at 488nm. Maximum intensity projections were generated by NIS elements to visualise all 10 z-planes.

2.5.2 Imaging of the caudal hematopoietic tissue in *mpx*:GFP larvae

3dpf mpx:GFP embryos were mounted in a 1% low melting point agarose solution (Sigma-Aldrich) containing 4.2% tricaine. A single time point was captured using an 10x objective on an Eclipse TE2000-U fluorescence microscope with a 1394 ORCA-ERA camera (Hamamatsu Photonics Inc). 10 z-planes were captured per larvae over a focal range of 100µm using a GFP specific filter with excitation at 488nm. Maximum intensity projections were generated by NIS elements to visualise all 10 z-planes.

2.5.3 Application of binary layers to time courses

Binary layers were used to detect neutrophils in time lapses during their recruitment to the wound site. NIS elements software is able to accurately detect individual objects, using a combination of thresholding based on fluorescence intensity, circularity and size. These features can be refined by cleaning and smoothing binary layers, as well as turning on the object separation function which enables the software to separate touching objects. Binary layers were added to time courses by applying a threshold based on fluorescence intensity of neutrophils to exclude background noise. The accuracy of binary layers was improved by smoothing, cleaning and separating objects. A size restriction was applied where necessary to exclude small and large objects which did not correspond to individual neutrophils.

2.5.4 Automated assay to detect object area

To detect neutrophil swarms at a wound site, the object size measurement feature on NIS Elements software was used. To measure the area of neutrophils in the time courses a binary layer was applied and accuracy was confirmed by checking multiple time points in the time courses. Binary layers were smoothed and cleaned, however object separation and size restrictions were not applied for this assay to ensure large objects were included in the binary layer. The measurements feature on NIS Elements (Version 4.3) was used to calculate the area of every object detected in each time frame. A region of interest was drawn at the wound site and the area of objects detected in this area was calculated.

2.5.5 Tracking of neutrophils during recruitment to wound sites

Tracking of GFP labelled cells was performed using NIS Elements (Version 4.3) with an additional NIS elements tracking module. A binary layer was added to time courses as previously described.

Binary layers were tracked based on algorithms generated by NIS elements software. A probability ellipse is calculated by the software following the input of information based on the movement of neutrophils. Parameters such as neutrophil speed, motion, fluorescence intensity and distance travelled were used to generate accurate neutrophil tracks. Post-tracking modifications were performed to remove short or inaccurate tracks, as well as to join gaps between tracks.

Object features including position, heading, speed, displacement, area and circularity index are recorded by the tracking software to provide numbers parameters to study neutrophil migration.

2.5.6 Fluoresence resonance energy transfer (FRET) imaging

To visualise apoptotic events in the context of neutrophil swarming, 3dpf *Tg(mpx:FRET)sh237* were injured and mounted in a 1% agarose with tricaine solution. Agarose was covered with 500μl of a clear E3 solution containing 4.2% tricaine to prevent dehydration. FRET imaging was performed from 30 minutes post injury using a 20x objective lens on an UltraVIEWVoX spinning disc confocal laser imaging system (Perkin Elmer) with acquisition every 2 minutes. 10 z-planes were captured per larvae over a focal range of 100μ using the following filters: a donor CFP channel (440nm for excitation, 485nm for detection), an acceptor YFP channel (514nm for excitation and 587nm for detection), and a FRET channel (440nm for excitation and 587nm for detection). An Ultraview dichroic mirror passes 405,440,515,640 was used to increase imaging speed using these filter blocks.

Volocity™ software was used to calculate normalised FRET values (NFRET). To compensate for the bleed through of the CFP and YFP fluorophores into the FRET channel, FRET bleed through constants were calculated. Control samples containing HeLa cells transfected with CFP alone or YFP alone were imaged using the same settings used for data acquisition of the *mpx:FRET* zebrafish reporter line. ROIs were drawn around a population of cells in the frame and Volocity™ software calculated FRET bleed through values as the mean intensity of the recipient channel (FRET) divided by the mean intensity of the source (CFP or YFP).

These FRET constants were then used by Volocity™ to calculate a normalised FRET value to generate a FRET value which reflects only the emission of acceptor YFP following excitation from the donor CFP considering the FRET bleed through and the background fluorescence emissions from each channel. Neutrophil apoptosis was observed by overlaying the YFP and NFRET channels.

2.5.7 Ratiometric Imaging of HyPer

To measure hydrogen peroxide concentration in neutrophils, fluorescence imaging of neutrophils expressing HyPer were acquired using an UltraVIEWVoX spinning disc confocal laser imaging system (Perkin Elmer). Fluorescence for HyPer$_{420}$ was acquired using an excitation wavelength of 440nm and emission was detected at 587nm. Fluorescence for HyPer$_{500}$ was acquired using an excitation wavelength of 514nm and emission was detected at 587nm as previously described for zebrafish (Niethammer et al., 2009a). 10 z-planes were captured per larvae over a focal range of 100μm. Data was collected for both channels on each z-plane before moving through the focal range to reduce the time between HyPer$_{420}$ and HyPer$_{500}$ excitation as recommended (Pase et al., 2012).

Velocity^{TM} software was used to calculate HyPer ratios. Images were thresholded and backgrounds were subtracted. The ratio channel was generated by dividing HyPer$_{500}$ by HyPer$_{420}$ (Hyper$_{500}$/HyPer$_{420}$). A rainbow LUT was applied to the HyPer ratio channel with an R minimum of 0 and an R maximum of 3.

2.5.8 Confocal imaging of red and green fluorescence

For imaging the *lyz*:histone2a.mCherry transgenic line, Cxcr4b.GFPx *lyz*:mCherry reporter line and *mpx*:GFP larvae for propidium iodide experiments, confocal imaging of red and green fluorophores was performed. Larvae were mounted in a 1% low melting point agarose solution (Sigma-Aldrich) containing 4.2% tricaine for imaging immediately after tail transection. Agarose was covered with 500μl of a clear E3 solution containing 4.2% tricaine to prevent dehydration. Propidium iodide was added to agarose at a final concentration of 1μg/ml where described in figure legend. Imaging was performed from 30 minutes post injury using a 10, 20x or 40x objective as described in figure legends on an UltraVIEWVoX spinning disc confocal laser imaging system (Perkin Elmer). Fluorescence for GFP was acquired using an excitation wavelength of 488nm and emission was detected at 510nm. Fluorescence for mCherry or propidium iodide was acquired using an excitation wavelength of 525nm and emission was detected at 640nm.

2.6 Molecular Biology

2.6.1 Whole mount *in situ* hybridisation (WISH) probe synthesis

WISH antisense RNA probe for *cxcl12a* was synthesised from linearised plasmid DNA obtained from a plasmid vector containing the zebrafish *cxcl12a* coding sequence, provided as a kind gift from Dr. Anne Robertson (University of Sheffield). RNA was transcribed using an SP6 RNA digoxigen labelling kit (Roche). 1μg of linearised DNA was

incubated in a final volume of 20µl containing transcription reagents described in table 2.1 for 2 hours at 37^{oc}.

Reagent	Volume (µl)
Linearised DNA	0.937
Transcription buffer	2
NTP-DIG-RNA labelling mix	2
RNAse inhibitor	1
SP6 Polymerase	1
dH20	13

Table 1: List of reagents used for transcription reactions

Following the transcription reaction, the DNA template was removed by adding 4µl DNAse for 20 minutes at 37^{oc}. Lithium chloride was used for RNA precipitation. 1 µl EDTA (0.5M, ph8) was added with 2.5 µl LiCl (4M) and 75 µl 100% ethanol, which was stored at -80^{oc} for 30 minutes followed by a centrifugation step at 14000rpm in 4^{oc} for 30 minutes. Supernatent was removed and the pellet was resuspended in 75 µl 70% ethanol. Resuspended RNA was centrifuged for a further 10 minutes at 14000rpm in 4^{oc} centrifuge, supernatant was removed and pellet was air dried for 5 minutes before being resuspended in 20 µl sterile water. 1 µl was loaded into a 1% agarose gel and gel electrophoresis was performed to confirm the presence of RNA. 80 µl formamide was added to RNA following confirmation of its presence and stored at -80^{oc}.

2.6.2   Transformation

Plasmid DNA was transformed using Top10 competent cells (Invitrogen, Paisley, UK). 1µl of plasmid indicated was added to 25µl of Top10 cells, mixed and incubated on ice to permeabilise cells for 30 minutes. Permeabilised cells were heat shocked for 45 seconds at 45^{oc} and placed back on ice for 10 minutes. 150µl SOC media (Invitrogen) was then incubated with cells for a 1 hour vigorous shaking period of 200rpm at 37^{oc}. Cells were plated on dry antibiotic selection plates specific to the antibiotic resistance cassette in the plasmid and cultured at 37^{oc} overnight. Selection plates were made using autoclaved LB agar and 50µg/ml of the relevant antibiotic.

2.6.3 DNA purification

Following transformation, single colonies were selected from plates and grown over night by shaking rigorously at 37°c in 50µl autoclaved LB broth containing 50µg/ml of the relevant antibiotic.

A HiSpeed Plasmid Midi Kit (QIAGEN, Manchester, UK) was used to purify DNA followed by an additional purification step using a MinElute PCR Purification Kit (QIAGEN) as described by the manufacturers' instructions. The DNA concentration was determined by Nanodrop™ spectrophotometer (Thermo Scientific, Hemel Hempstead, UK).

2.7 Analysis of RNA expression in zebrafish neutrophils

Cxcr4 and Cxcl12 expression was analysed using RNA sequencing data shared with our group by our collaborator Anne-Marie Meijer (accession code: GSE78954). Briefly, RNA sequencing of FACS-sorted neutrophils was performed to detect expression of genes by neutrophils in zebrafish larvae at 5dpf, as described (Rougeot et al., 2014). From this data the fpkm values for both isoforms of *cxcr4* and *cxcl12* in neutrophils was extracted.

2.8 Development of transgenic lines

Plasmid DNA containing the construct was injected with *Tol2* mRNA into *mpx*:GAL4 larvae at the one cell stage. At 3dpf, F0 larvae with visible expression of the construct of interest in the caudal hematopoietic tissue were selected for raising to adulthood. Founders were identified by outcrossing these F0 larvae to wildtype larvae and seeing positive expression in the CHT in offspring of these crosses. A founder was identified and outcrossed to a wildtype adult fish and offspring of this pairing were raised to produce a heterozygous population of F1 fish. For the *Tg(mpx:GAL4)i222;Tg(UAS:cxcr4b.GFP)sh503* line, experiments were performed on the offspring of these F1 larvae by incrossing or outcrossing. For experiments using the *Tg(lyz:mcherry.histone2a,)sh503* experiments were performed on the offspring of F1 larvae by incrossing.

2.9 Software

1- Graph pad Prism software (version 7.03) was used for all data entry as well as statistical analysis, as described in individual figure legends.

2- NIS elements (version 4.3) was used where described for analysis and visualisation of experiments performed using the Nikon wide field microscope.

3- Volocity™ software (version 6.3) was used where described to analyse experiments performed using the UltraVIEW VoX spinning disk confocal microscope (Perkin Elmer, Cambridge, UK).

2.10 Statistical analysis

GraphPad Prism® software was used for all statistical analysis. For comparisons between 2 groups an unpaired two-tailed t-test was used. Where comparisons were made between 2 groups from the same paired data, a paired t-test was used. For 2 or more comparisons a one-way anova was used with Dunnett's or Bonferroni's correction. For reverse migration assays linear regression analysis was used to compare the difference between slopes.

3 Pioneer neutrophils initiate the swarming response to tissue injury in zebrafish larvae

3.1 Introduction and aims

As the most abundant of the circulating immune cells, neutrophils are one of the body's first line of defence against infection. Neutrophils are recruited to an inflammatory site within minutes of trauma where their major role is to eliminate pathogens using anti-microbial functions including phagocytosis of pathogens, generation of the oxidative burst, degranulation and formation of extracellular traps (Wright et al., 2010). The non-specific microbicidal effects of the neutrophil, whilst preventing pathogens from establishing a niche within the host, are detrimental to host tissues when their activity becomes unregulated (Headland and Norling, 2015).

Neutrophil recruitment to inflammatory sites has been extensively studied and the highly regulated cascade of events leading to the extravasation of neutrophils through vascular endothelial cells into the inflamed tissue has been well defined (Ley et al., 2007)(Kelly et al., 2007). It is currently understood that following egress from the blood stream, neutrophils are guided by a range of chemoattractant molecules released from pathogens or damaged cells at the inflammatory site, although the precise signalling pathways involved in coordinating neutrophil dynamics beyond the vasculature are not fully understood.

Recent advances in intravital imaging of the inflammatory response have provided a new prospective on neutrophil responses within inflamed tissue (Lämmermann et al., 2013; Wang et al., 2017). Neutrophils are able to coordinate their migration within inflamed tissue such that following highly coordinated chemotaxis, neutrophils accumulate in clusters at inflammatory sites. This newly identified directed migration or 'neutrophil swarming' is reminiscent of the swarming behaviours observed in insects and birds (Lämmermann, 2015).

The molecular controllers of the swarming response at the single-cell and whole population levels are currently being dissected (Reátegui et al., 2017). It is clear that neutrophil tissue navigation and clustering at injury sites follow multistep attraction cascades, whose exact molecular sequence and outcome is dependent on tissue context.

Neutrophil swarming is now recognised as an important process during the neutrophilic inflammatory response. Whilst the precise physiological role for neutrophil swarming at inflammatory sites is not fully understood, arguments are currently being made for both host-protective and host-damaging outcomes (Kienle and Lämmermann, 2016).

The development of high resolution imaging of mouse tissue have allowed the mechanisms governing the swarming response at its later stages to begin to be dissected (Lämmermann et al., 2013). However, little is known about the early initiation of the swarming response where our current understanding is based on preliminary or unpublished findings (Lämmermann, 2015).

In order to gain further insight into the neutrophil swarming response, high resolution *in vivo* imaging is required alongside genetically tractable models to dissect the mechanisms of this phenomenon at a single-cell stage. Zebrafish larvae provide an excellent model to study the behaviour of neutrophils at sites of injury or infection due to their thin tissue depth and optical transparency which allows the tracking of neutrophil behaviour *in vivo* in real time in high resolution (Renshaw and Loynes, 2006). The zebrafish is a model which can be used to overcome the limitations associated with *in vivo* imaging in mice as well as providing a truly physiological model to study the endogenous neutrophil swarming response.

The aims of this chapter are to characterise the neutrophil swarming response to tissue injury in zebrafish larvae and investigate the initiation stages of neutrophil swarming on a single-cell level.

3.2 Neutrophil swarming is observed in response to tail-fin transection in zebrafish larvae

No reports currently exist to describe neutrophil swarming in response to tail-fin transection in zebrafish larvae, although swarming has been observed at sites of infection. I hypothesised that neutrophil swarming could be observed at the wound site during the recruitment phase of inflammation in zebrafish larvae.

To determine the dynamics of the inflammatory response following tail-fin transection, the number of neutrophils present at the wound site were counted at regular intervals during the first 24 hours following injury (Figure 3.1). Recruitment of neutrophils was observed for the first 6 hours post injury, followed by a resolution phase which began from 8 hours post injury when the number of neutrophils at the wound began to decrease until returning to almost base line levels by 24 hours post injury. From these experiments I determined that the dynamics of neutrophil recruitment to tail-fin injury could be studied within the first 6 hours following injury.

To investigate the migratory behaviours of neutrophils during recruitment to wound sites in zebrafish larvae, tail-fin transection of 3dpf *mpx:*GFP larvae was performed

followed by time lapse imaging from 30 minutes post injury for 5 hours, as described in methods.

Neutrophil recruitment to the tail-fin was observed during the first 5 hours following tail-fin transection. Neutrophil aggregates were observed which were reminiscent of those seen in mice. In larvae where aggregates were observed, the recruitment of the first neutrophils to the wound site was followed by the highly directed migration of a population of neutrophils which, instead of scouting the wound site, organised themselves to form a cluster (Figure 3.2). I hypothesised that the aggregates I observed in zebrafish tissue could be examples of neutrophil swarming, so I set out to characterise this process in zebrafish larvae.
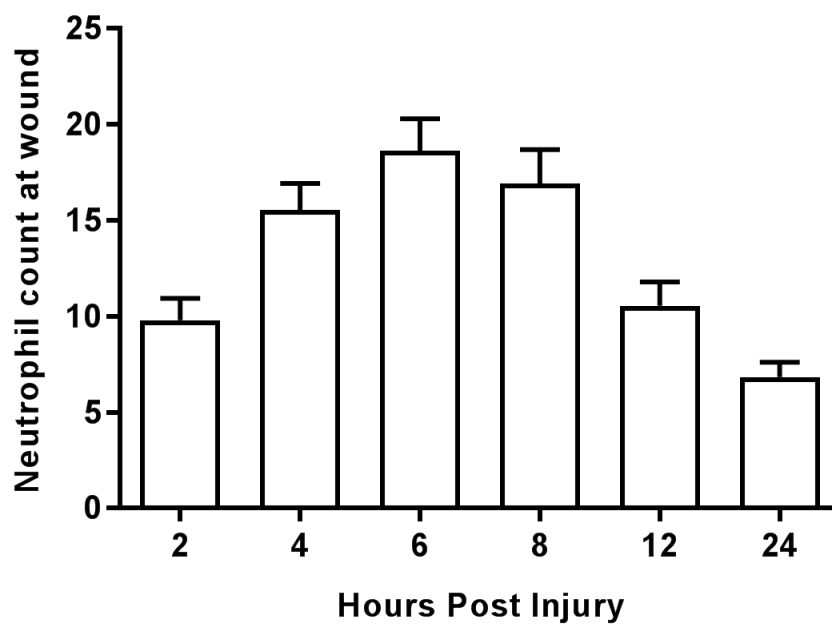
Figure 3.1: Dynamics of the neutrophilic response to tissue injury

Tail fin transection was performed on 3dpf mpx:GFP larvae. The number of neutrophils at the site of injury were counted at 2, 4, 6, 8, 12 and 24 hours post injury. Neutrophil recruitment to the wound site was observed for up to 6 hours following injury. Inflammation resolution was observed from 8-24 hours post injury when the number of neutrophils at the wound site decreased over time (Data are shown as mean +/- sem, n= 53 larvae from 3 experimental repeats).

3.3 An unbiased assay to detect neutrophil swarming

Before characterising any of the behaviours leading to neutrophil swarm formation at the wound site, I developed an unbiased assay to detect swarms within a population of larvae. This is important as there currently exists no definition of neutrophil swarming, something which is required for consistency between studies. The area of aggregating neutrophils is visibly larger than the area of individual neutrophils at the wound site, so I hypothesised that overlapping neutrophils such as those in the clusters would be detected as one large object. I developed an assay using the application of binary layers to the images which enabled the detection of all objects at the wound site in every time point during the imaging period.

The area of neutrophils at the wound site was measured automatically in every point from time courses taken following tail-fin transection of 3dpf *mpx*:GFP larvae as described in methods. The area of the majority of neutrophils detected at the wound site was consistently clustered around the 100µm^2 mark. In larvae where aggregates were seen at the wound site, the presence of an outlier object with an area exceeding 1000µm^2 was observed in the data (Figure 3.3A). This larger outlier was not seen in larvae where aggregates were not observed (Figure 3.3B). Of the positive hits from this assay where the area of an outlier population with an area closer to 1000µm^2 was observed, 100% of the data corresponded to a neutrophil cluster.

From these experiments I determined that neutrophil aggregates could be detected within a population of larvae by measuring the area of objects detected at the wound site. This unbiased assay provides a robust method to identify neutrophil clusters within a population of zebrafish larvae to ensure consistency when selecting larvae to study swarming.
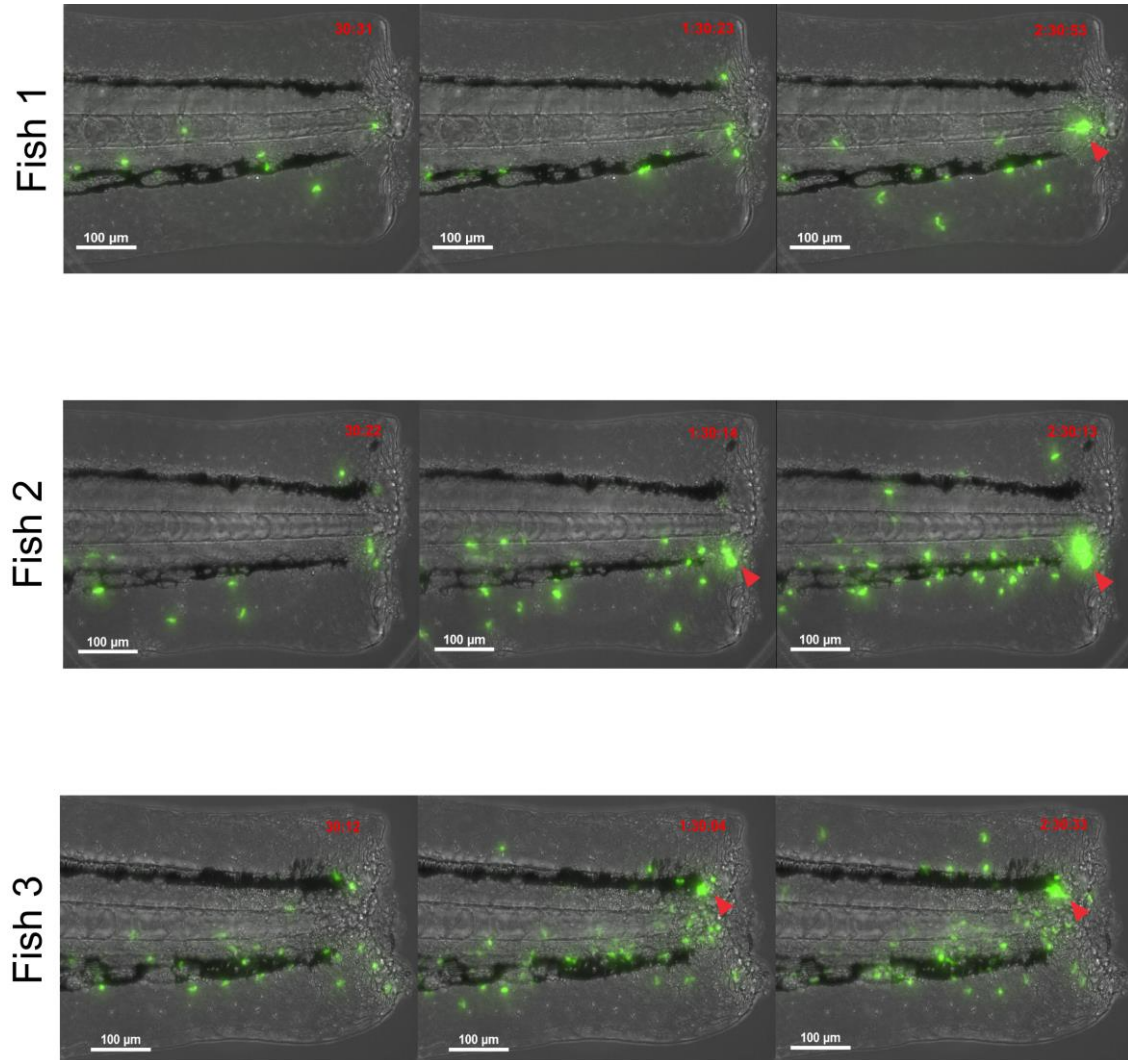
Figure 3.2: Neutrophil clusters are observed at the wound site

Tail fin transection of 3dpf mpx:GFP larvae was performed followed by time lapse imaging from 30 minutes post injury for 5 hours. Figure shows neutrophil cluster formation at the wound site (red arrows) at time points indicated during the recruitment of neutrophils to the wound site in 3 representative larvae. Time stamps shown in red (hh:mm:ss) are relative to the start of imaging at 30 minutes post injury.
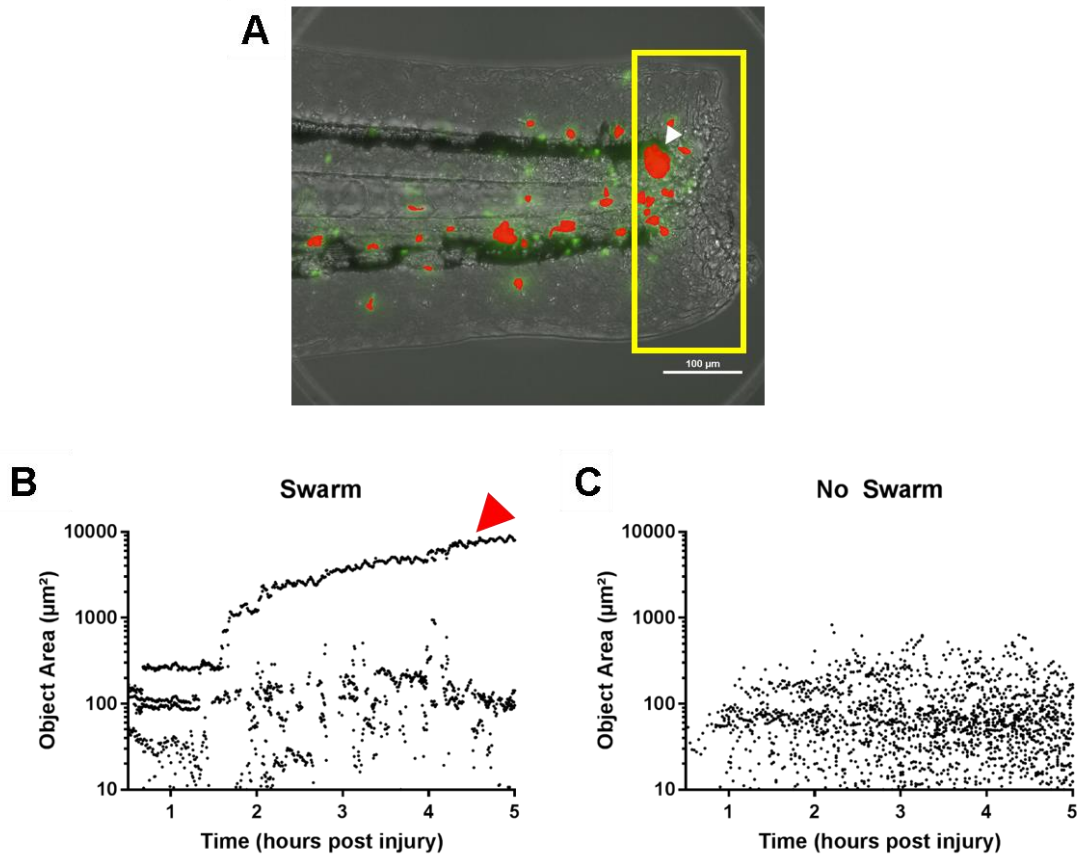
Figure 3.3: An automated assay to detect neutrophil clusters at the wound site

Time lapse imaging of neutrophil recruitment was performed on 3dpf *mpx*:GFP larvae following tail fin transection from 30 minutes post injury for 5 hours. A binary layer was applied to each time course and the binary area of individual objects detected in an ROI drawn at the wound site was measured for each time point where swarms were detected as one large object (white arrow, A). Figure shows representative examples of binary object detection in larvae with a swarm at the wound site where objects with an area of up to 10000 μm^2 were detected (red arrow, B) and larvae with no swarms at the wound site where binary objects detected had an area of less than 1000 μm^2(B).

3.4 Multiple neutrophil swarms can form at the wound site and neutrophils can move between competing swarms

Interestingly during these initial observations the formation of multiple neutrophil aggregates at the wound site in larvae was seen. The outcome of neutrophil recruitment to and organisation at the wound site in larvae varied between larvae, where the formation of up to 3 individual neutrophil clusters at the wound site was observed (Figure 3.4A-D). It was apparent that the most common phenotype observed was either no swarming behaviour or one individual swarm at the wound site, either of these phenotypes were observed in 38% of larvae. Multiple swarms were seen at the wound site less frequently, with 2 swarms being detected in 21%, and 3 swarms being detected in 3% of larvae (Figure 3.4E).

Neutrophils have been observed to move between competing swarms in mice (Lämmermann, 2015). Where multiple swarms were observed at the wound site in zebrafish larvae, the movement of neutrophils between competing clusters was observed whereby a pioneer neutrophil initiated a first neutrophil swarm, which dissipated following the migration of neutrophils to a second pioneer neutrophil in close tissue proximity (Figure 3.5). These observations provide evidence that the neutrophil clustering observed in the zebrafish model shares characteristics with that seen in mice.

3.5 Neutrophil swarming occurs in response to a range of inflammatory stimuli

In mice one of the factors proposed to modulate the swarming response is the size of the initiating tissue damage (Kienle and Lämmermann, 2016). To determine whether neutrophil swarming occurred in response to a range of tissue injuries of a varying degree of severity, I changed the size of the inflammatory insult administered to larvae. Tail-fin transection of different severity was performed on 3dpf *mpx*:GFP larvae as described in methods. Neutrophil swarms were detected at the wound using the automated assay to detect large objects (Figure 3.6), indicating that neutrophil swarming can be seen regardless of the size of the inflammatory stimulus.
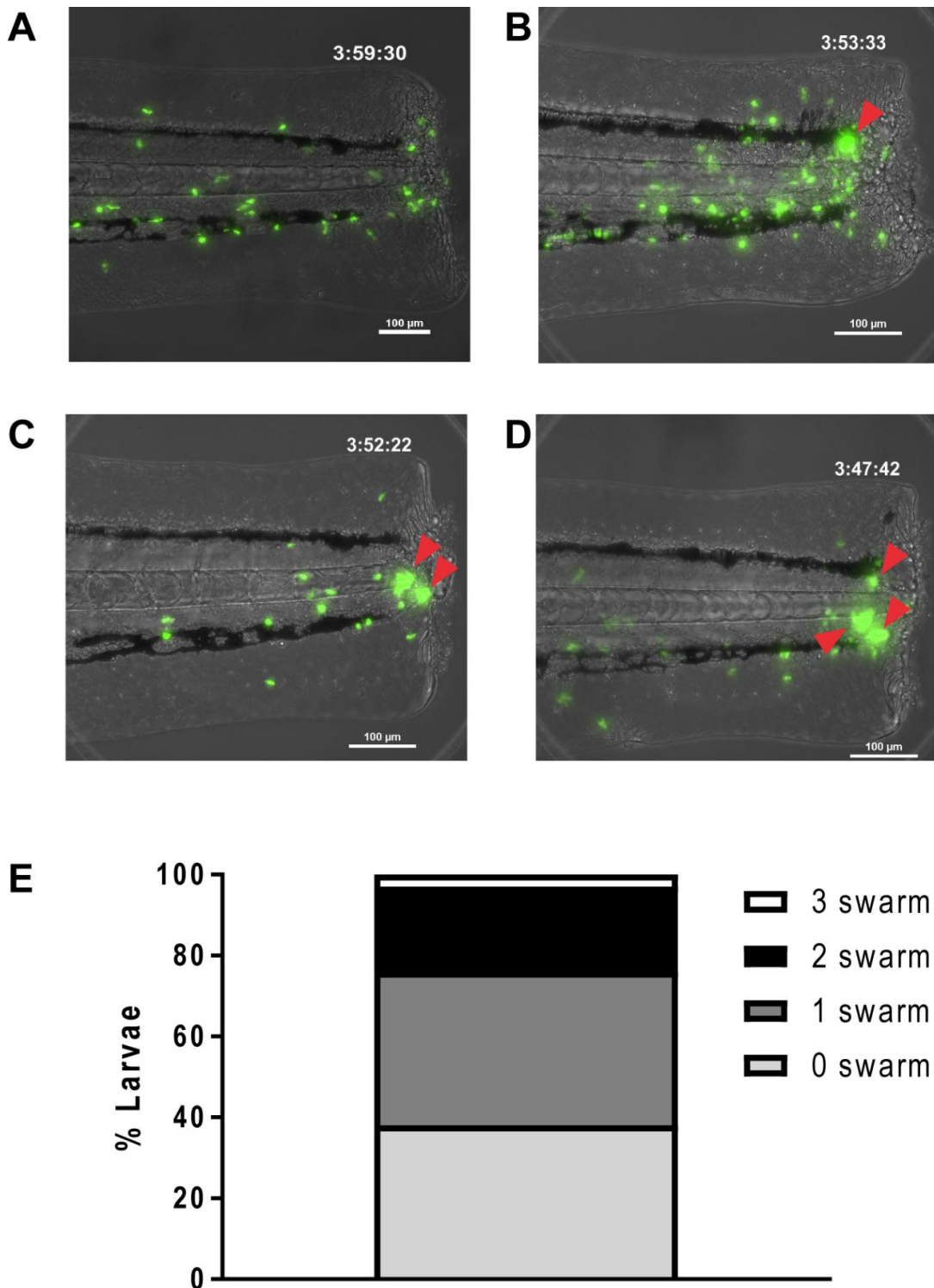
Figure 3.4: Multiple neutrophils swarms can form at the wound site

Time courses of neutrophil recruitment to tail fin transection in 3dpf *mpx*:GFP larvae were studied within the first 5.5 hours following injury. Neutrophil migration and swarming dynamics at the wound site varied between larvae where no swarms (A), 1 swarm (B), 2 swarms (C) and up to 3 swarms (D) were observed. The frequency with which these phenotypes were observed was quantified (E) (*n=29 larvae from 7 experimental repeats).* Time stamps shown in white (hh:mm:ss) are relative to the start of imaging at 30 minutes post injury.
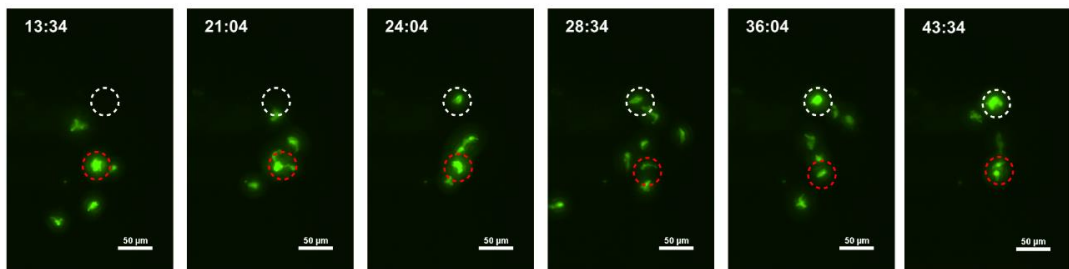
Figure 3.5: Neutrophils migrate between competing swarms

Neutrophil migratory behaviour at the wound site was studied using time courses taken following injury of 3dpf *mpx*:GFP larvae. In some instances where neutrophil swarming behaviour was observed at the wound site, the migration of neutrophils from an initial cluster (red circle) towards a second pioneer neutrophil in close proximity (white circle) was observed. Figure shows representative example of the migration of neutrophils between two swarms. Time stamps shown in white (mm:ss) are relative to the start of imaging at 30 minutes post injury.
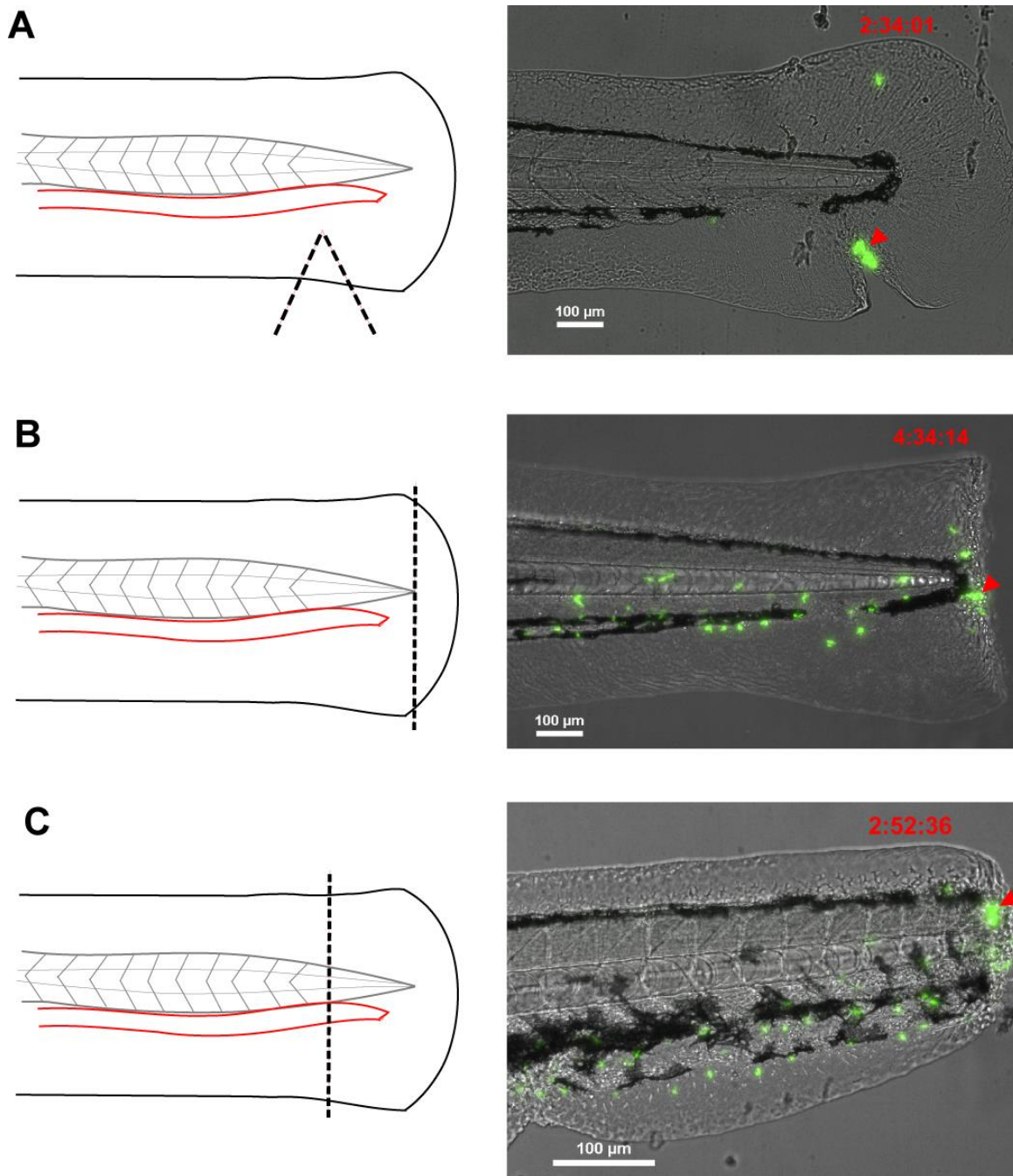
Figure 3.6: Neutrophil swarms form following a range of inflammatory stimuli

Tail fin transection of varying severity was performed on 3dpf *mpx*:GFP larvae followed by time lapse imaging from 30 minutes post injury for 5 hours. Neutrophil swarms were observed (red arrow) at the wound site following a minor nick of the ventral side of the tail fin (A), a linear wound dissecting the tissue at the end of the caudal tail fin (B) and a severe linear wound dissecting the notochord and circulatory loop at the caudal tail fin (C). Time stamps shown in red (hh:mm:ss) are relative to the start of imaging at 30 minutes post

3.6 Dynamics of neutrophil swarming in zebrafish larvae

In mice, neutrophils close to the wound site respond to the tissue insult within minutes. This is followed by a substantial chemotactic response by neutrophils distal to the wound site which exhibit highly directed migration to the wound where they aggregate with early pioneer neutrophils to form substantial neutrophil clusters (Lämmermann, 2015).

After observing the formation of large neutrophil clusters at the wound site in zebrafish larvae in response to a range of inflammatory stimuli, I next sought to characterise the dynamics of the swarming response to determine the similarities and differences of endogenous zebrafish neutrophil swarming.

Although there was variation from fish-to-fish in timing, all swarms formed following this same sequence of events, with kinetics similar to those observed in swarming neutrophils in mice models. This sequence of events can be divided into three distinct phases consisting of neutrophil scouting, swarm initiation and swarm aggregation (Figure 3.7). The neutrophil scouting phase was observed in larvae regardless of swarming behaviour at the wound whereas the initiation and aggregation phases were specific to larvae where swarm formation occurred.

3.6.1 Phase 1: Scouting

Within minutes following tail-fin transection, the recruitment of neutrophils proximal to the wound site began in all larvae (Figure 3.8, Movie 3.1-3.3). This initial 'scouting' phase was observed in all larvae regardless of whether a swarm formed at the wound site and was reminiscent of the scouting phase reported in mice following the release of chemoattractant by damaged tissue (Lämmermann et al., 2013).

3.6.2 Phase 2: Initiation

Traditionally it was believed that neutrophil migration to inflammatory sites was governed by signalling through pattern recognition receptors in response to damaged cells and pathogens at the wound site (Kolaczkowska and Kubes, 2013). The identification of neutrophil swarming and the ability of neutrophils to modulate their own recruitment through intracellular relay signalling has changed the way neutrophil recruitment is perceived. It is currently unknown why neutrophils swarm at inflammatory sites in some contexts and not others, although it is clear that a specific tissue context is required (Lämmermann, 2015).

I hypothesised that in larvae where swarms form at the wound site, a sub population of neutrophils were able to respond to additional chemoattractant cues which induce highly directed migration leading to neutrophil clustering at the wound site.
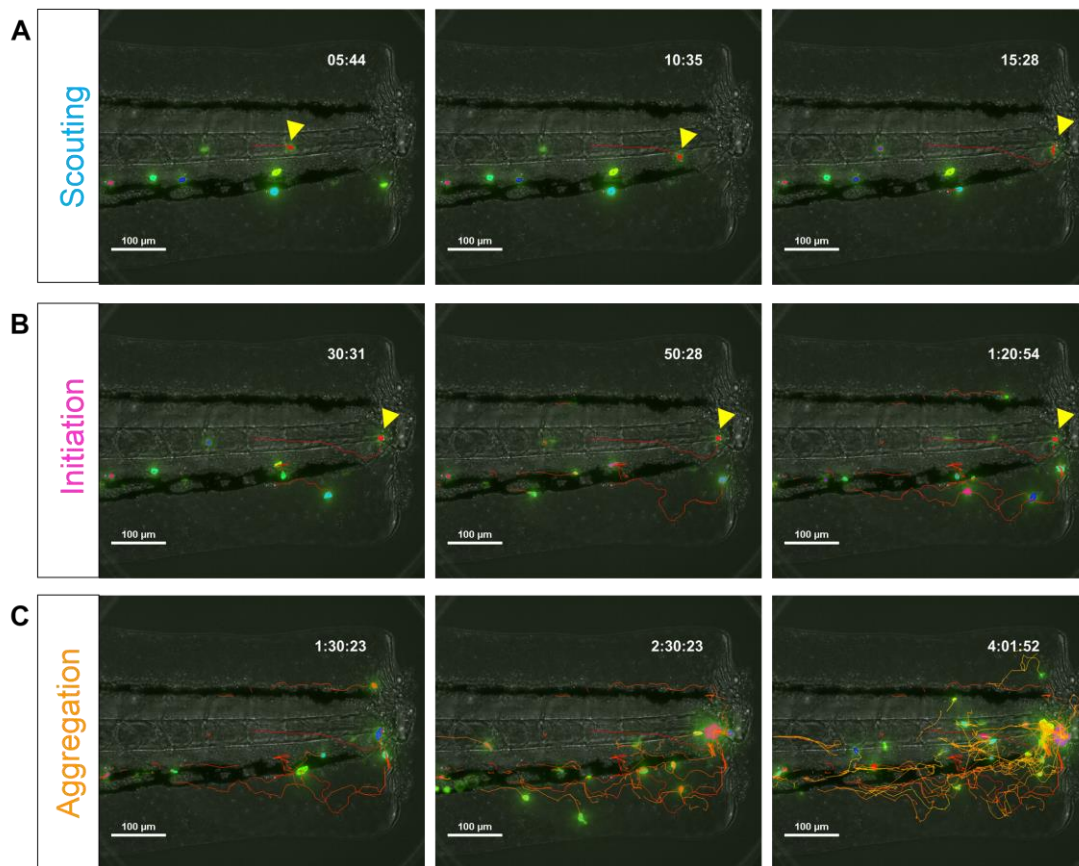
Figure 3.7: Dynamics of neutrophil swarming in zebrafish

Tail fin transection was performed on 3dpf *mpx*:GFP larvae followed by time lapse imaging of neutrophil recruitment to the wound site from 30 minutes post injury for 5 hours. Time courses where neutrophil swarming was observed at the wound site were selected and neutrophils were tracked during their recruitment to the wound. Figure shows the dynamics of neutrophil swarm formation in one representative example larvae. Neutrophil tracks are colour coded by time with red tracks corresponding to early recruited neutrophils and yellow tracks corresponding to neutrophils migrating later. The recruitment of neutrophils proximal to the wound site or 'scouting phase' was observed within minutes following tail fin transection (A). This is followed by a swarm 'initiation' phase in which one swarm-initiating neutrophil becomes chemotactic to other neutrophils at the wound site (B). The directed migration of neutrophils towards this chemotactic neutrophil is then observed during the 'aggregation' phase (C) .Time stamps shown in white (hh:mm:ss) are relative to the start of imaging at 30 minutes post injury.
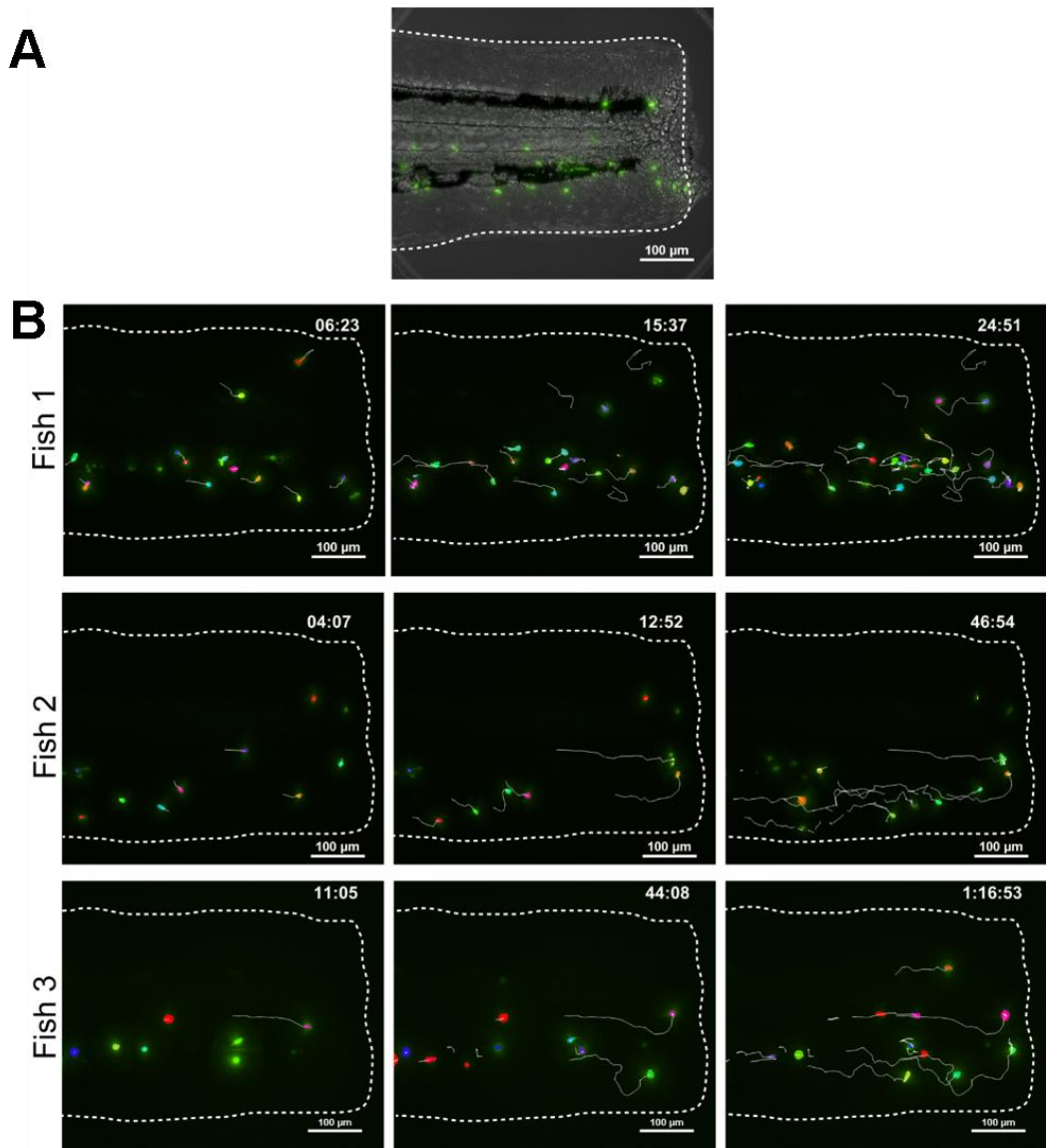
Figure 3.8: Neutrophil scouting occurs within minutes following tail fin transection

Time courses of neutrophil recruitment to tail fin transection in 3dpf *mpx*:GFP larvae were selected for study based on the observation of neutrophil swarming behaviour at the wound site. The region of the tail fin where imaging was performed is illustrated (A). Within minutes following tail fin transection the recruitment of neutrophils proximal to the wound site was observed. Figure shows the neutrophil tracks from 3 representative larvae (B). Time stamps shown in white (hh:mm:ss) are relative to the start of imaging at 30 minutes post injury

To investigate this hypothesis the timecourses in which neutrophil aggregates were identified in larvae were studied. The frames immediately preceding swarm formation could be visualised in high resolution and the initiation of endogenous neutrophil swarming could be seen *in vivo* in real time. The most striking feature of swarm initiation was that the focal point of neutrophil migration was an individual round and immotile neutrophil; a pioneer (Figure 3.9, Movie 3.4-3.6).

To study the recruitment of neutrophils to this immotile neutrophil, time courses were tracked in reverse, such that the migration of the swarm-initiating neutrophils to the wound site could be observed. Following the recruitment of the first neutrophils to the wound site during the scouting phase, a phenotypic change was observed in the swarm-initiating neutrophil, and subsequently the directed migration of neutrophils towards this neutrophil to form a cluster was observed (Figure 3.10-3.12, Movie 3.7-3.9). Swarm initiating neutrophils are referred to as pioneer neutrophils in the literature, so I have used this term to describe the neutrophil which initiates a swarm in zebrafish larvae.

The time period from the change in phenotype of the pioneer neutrophil at the wound site, until it is joined by the first migrating neutrophil to form a neutrophil cluster has been termed the 'initiation' phase. During the initiation phase it would appear that pioneer neutrophils release a chemical which provides an additional chemotactic cue for neutrophils, resulting in a change in polarisation of a population of neutrophils which subsequently migrate to form a neutrophil swarm, rather than traditional patrolling of the wound site. I propose that the phenotypic change in pioneer neutrophils at the wound is induced by a specific tissue context. This could be a physical or mechanical barrier, alteration in chemical concentration/chemotactic cues, or the presence of a dead cells or pathogens.

The phenotypic change in pioneer neutrophils can be illustrated by tracking the pioneer neutrophil during its recruitment to, and duration at, the wound site prior to swarm formation. Behavioural and morphological parameters such as neutrophil speed and circularity index were measured initially as proof of principle to illustrate the loss of motility and rounded morphology observed in pioneer neutrophils. Pioneer neutrophils were tracked during the scouting and initiation phases, during which time a striking change in pioneer neutrophil speed (Figure 3.13 A,C and E) and circularity index was observed (Figure 3.13 B, D and F). These data confirm the existence of a neutrophil phenotype switch at the wound site.
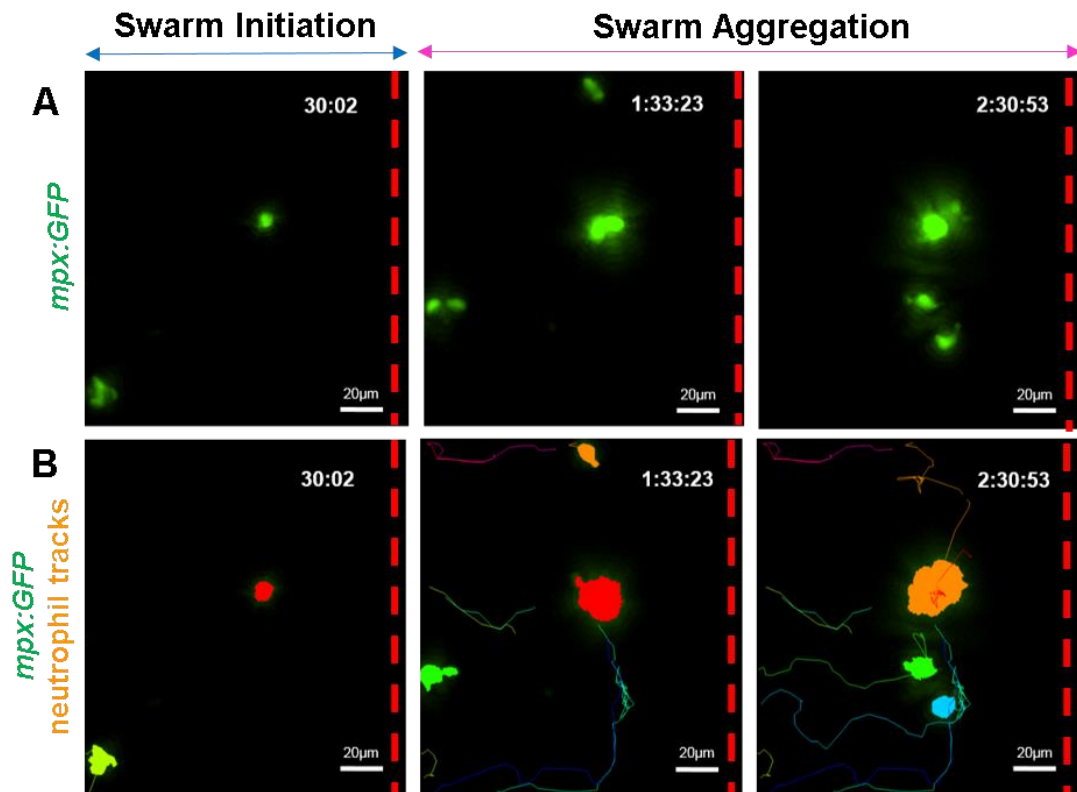
Figure 3.9: Neutrophils direct their migration towards a pioneer neutrophil to initiate the swarming response

Neutrophil swarms were identified in time courses of neutrophil recruitment to tail fin transection in 3dpf *mpx*:GFP larvae during the first 5 hours following injury. Neutrophils were tracked during the initiation and aggregation phases. Figure shows a representative example of the presence of one swarm-initiating pioneer neutrophil at the wound site which was the focal point of directed neutrophil migration leading to swarm formation (A). Tracking of neutrophils illustrates the directed migration towards the pioneer neutrophil (B). Red dashed line represents wound edge. Time stamps shown in white (hh:mm:ss) are relative to the start of imaging at 30 minutes post injury.
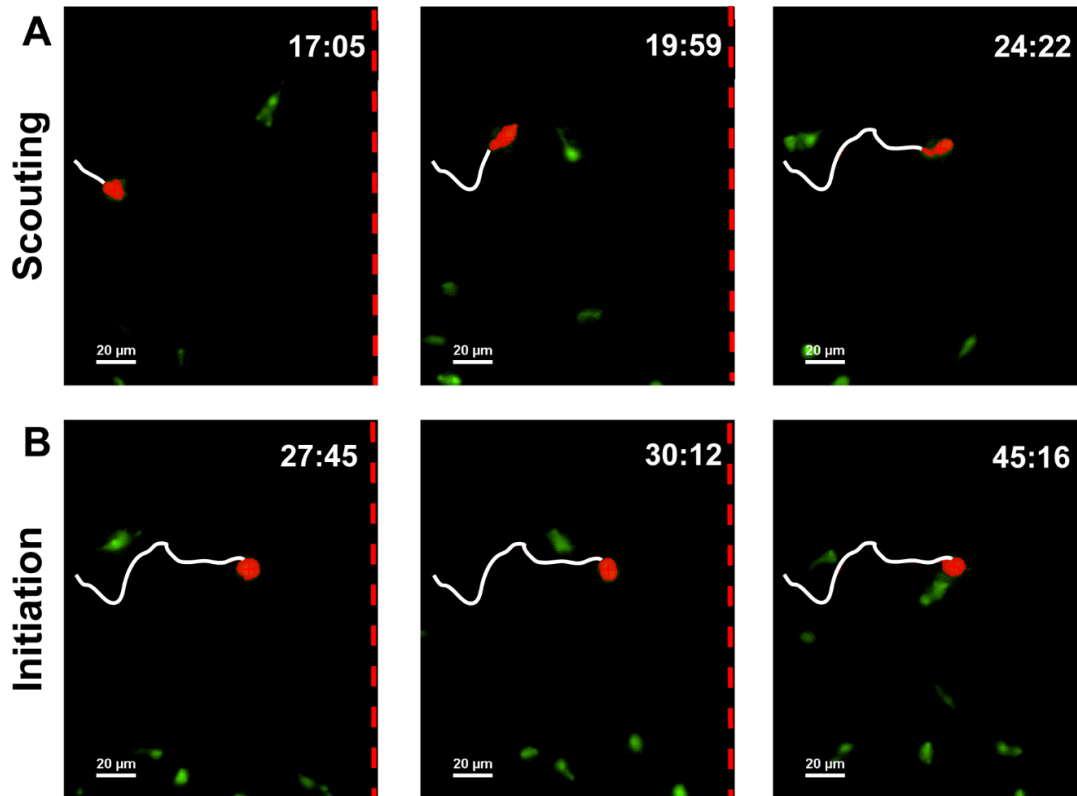
Figure 3.10: Pioneer neutrophils change phenotype at the wound site (example 1)

The migration of swarm-initiating pioneer neutrophils was studied in time courses taken of neutrophil migration to tail fin transection in 3dpf *mpx*:GFP larvae. Pioneer neutrophils highlighted in red were tracked until the frame preceding the aggregation phase of swarming. Figure shows one example of pioneer neutrophil tracks (white) during migration to the wound site in the scouting phase (A). Pioneer neutrophil tracks become stationary with a rounded morphology during the initiation phase (B). Dashed red line represents the wound edge. Time stamps shown in white (mm:ss) are relative to the start of imaging at 30 minutes post injury.
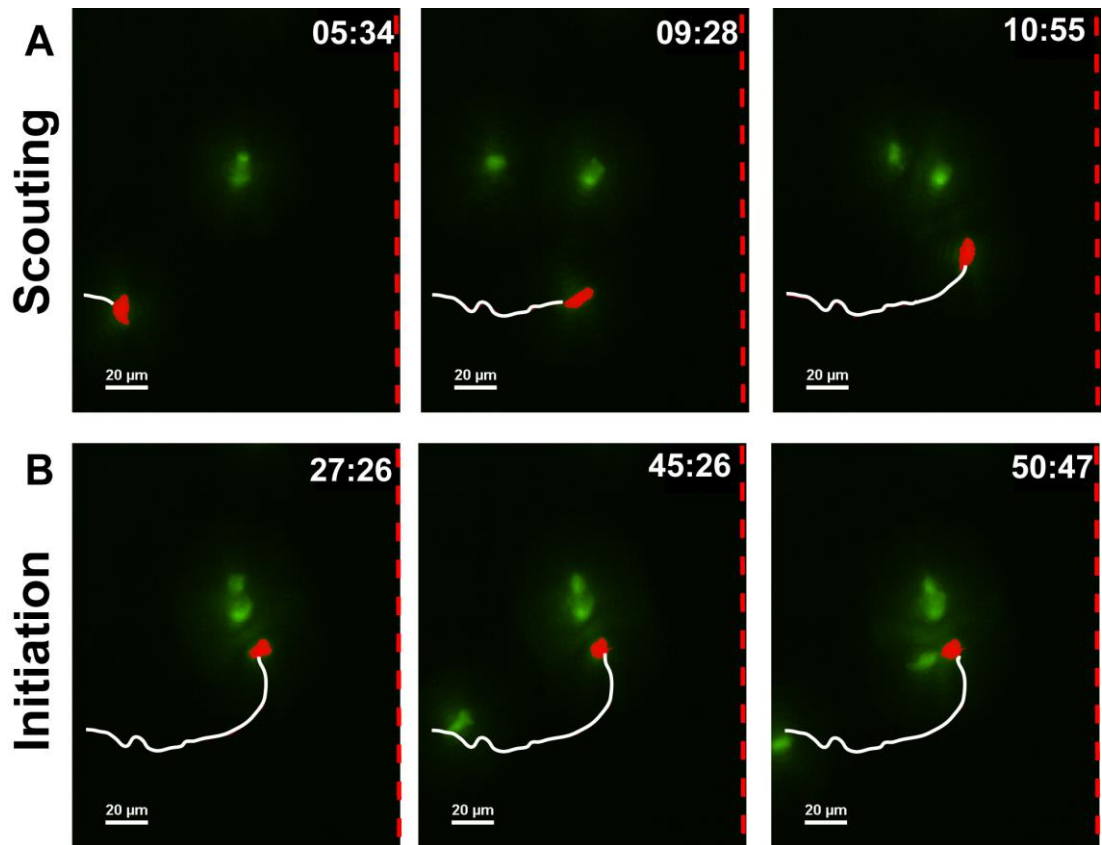
Figure 3.11: Pioneer neutrophils change phenotype at the wound (example 2)

The migration of swarm-initiating pioneer neutrophils was studied in time courses taken of neutrophil migration to tail fin transection in 3dpf *mpx*:GFP larvae. Pioneer neutrophils highlighted in red were tracked until the frame preceding the aggregation phase of swarming. Figure shows one example of pioneer neutrophil tracks (white) during migration to the wound site in the scouting phase (A). Pioneer neutrophil tracks become stationary with a rounded morphology during the initiation phase (B). Dashed red line represents the wound edge. Time stamps shown in white (mm:ss) are relative to the start of imaging at 30 minutes post injury.
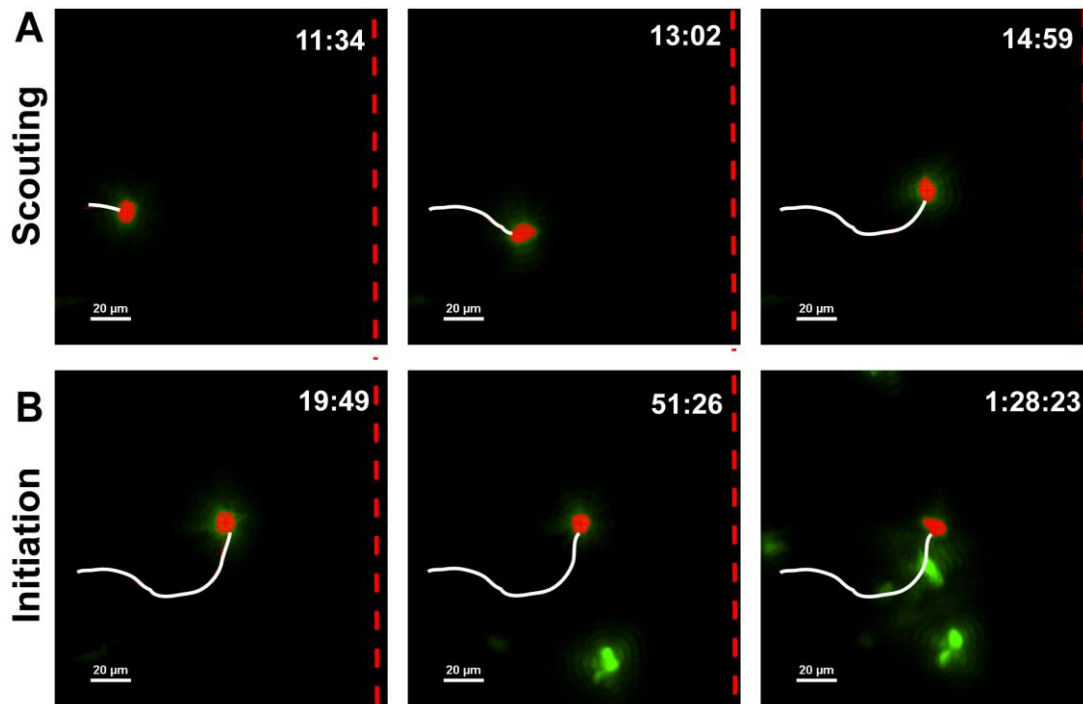
Figure 3.12: Pioneer neutrophils change phenotype at the wound site (example 3)

The migration of swarm-initiating pioneer neutrophils was studied in time courses taken of neutrophil migration to tail fin transection in 3dpf *mpx*:GFP larvae. Pioneer neutrophils highlighted in red were tracked until the frame preceding the aggregation phase of swarming. Figure shows one example of pioneer neutrophil tracks (white) during migration to the wound site in the scouting phase (A). Pioneer neutrophil tracks become stationary with a rounded morphology during the initiation phase (B). Dashed red line represents the wound edge. Time stamps shown in white (hh:mm:ss) are relative to the start of imaging at 30 minutes post injury.

90
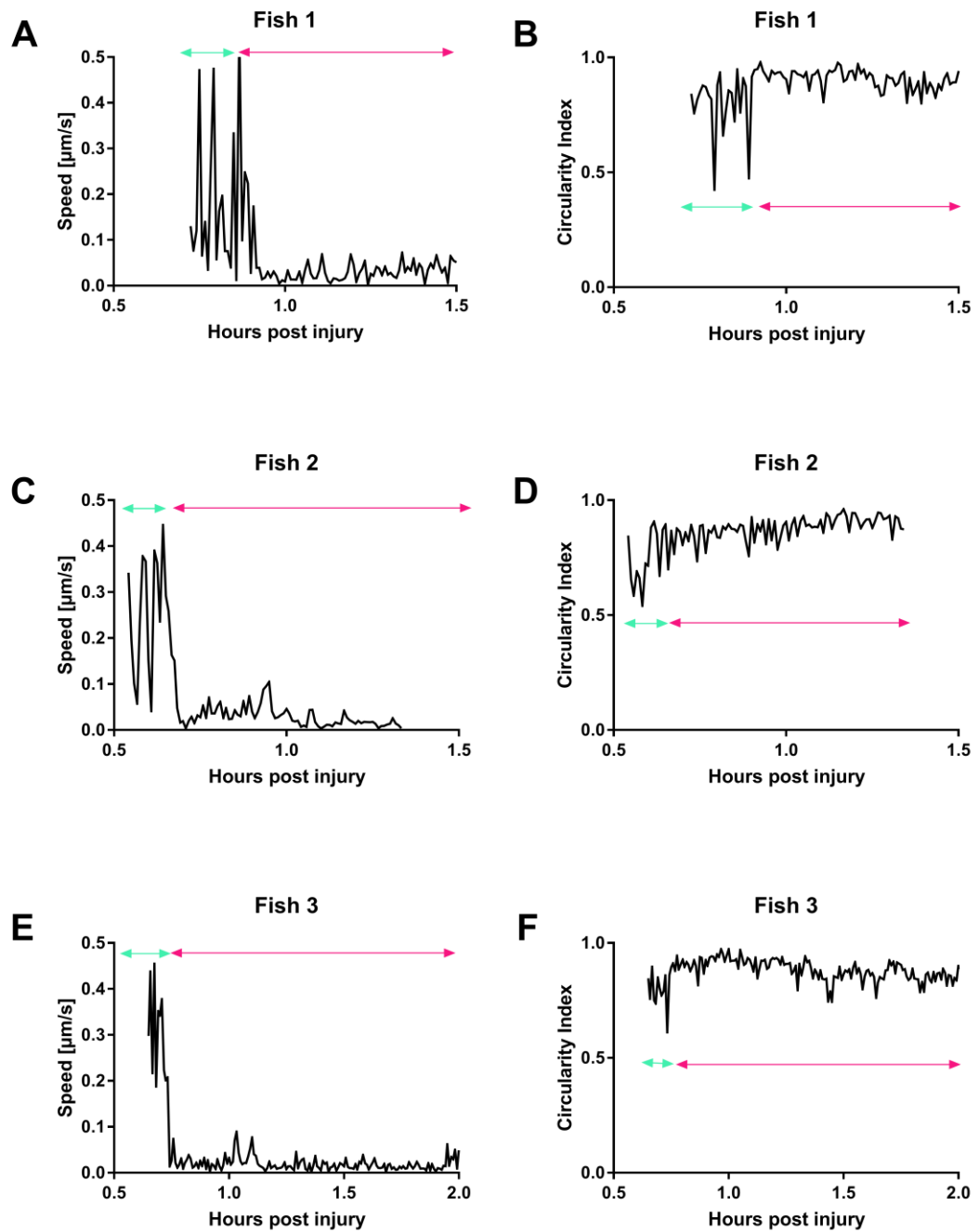
Figure 3.13: Pioneer neutrophils change phenotype at the wound site; proof of principle

The phenotypic changes observed in pioneer neutrophil behaviour at the wound site were confirmed by measuring the speed of neutrophil migration and the circularity index in the frames preceding neutrophil swarm formation. Figure shows the pioneer neutrophil track speed (A, C, E) and circularity index (B, D, F) from three representative larvae. A clear change in speed and circularity index is observed between the scouting phase (cyan arrows) and the initiation phase (magenta arrows).

3.6.3 Pioneer neutrophils undergo a morphological change at the wound site which is not seen in non-pioneer neutrophils

After confirming that pioneer neutrophils changed their phenotype at the wound site throughout time, I next aimed to fully characterise the migratory behaviours of pioneer neutrophils and non-pioneer neutrophils during the scouting and initiation phases.

Neutrophils were selected for tracking if they were equi-distant from or closer to the wound site than the pioneer neutrophil to ensure that selected neutrophils were migrating within a similar tissue-context during the time period measured. Neutrophil tracking was performed during the scouting and initiation phase on five time courses taken from four experimental repeats as described in methods, and pioneer neutrophil tracks were separated from non-pioneer tracks. Parameters which illustrate the migratory behaviour of neutrophils such as speed, displacement (linear distance between the start and end of the neutrophil track) and meandering index were used to study neutrophil migration during swarm initiation. The meandering index is calculated by dividing the displacement of each cell by the length of the path it has travelled, and provides a read out of how directly a cell has moved. A meandering index of 1 indicates movement in a direct line. A representative example of tracking during the scouting and initiation phases is illustrated in figure 3.14, where tracks extracted from the scouting phase are highlighted in cyan, and tracks taken from the initiation phase are highlighted in magenta**.**

3.6.4 Pioneer neutrophils migrate differently to non-pioneer neutrophils during the initiation phase

I aimed to compare the migratory behaviour of pioneer neutrophils to that of non-pioneer neutrophils during the initiation phase. I hypothesised that during initiation, the migratory behaviours of pioneer neutrophils would be different to that of non-pioneer neutrophils.

The speed, displacement and meandering index was measured from pioneer and non-pioneer neutrophil tracks extracted from the initiation phase. Circularity index was also measured as a parameter to describe the roundness of the neutrophils where a value of 1 is completely round. These data demonstrate that pioneer neutrophil speed and displacement was significantly lower than non-pioneer neutrophils (Figure 3.15 A and B), whilst there was no difference in meandering index (Figure 3.15C). Furthermore the circularity index of pioneer neutrophils is significantly higher than non-pioneer neutrophils at the wound site (Figure 3.15D).

These data confirm the observation that pioneer neutrophils adopt a non-motile, rounded morphology at the wound site during the swarm initiation phase.
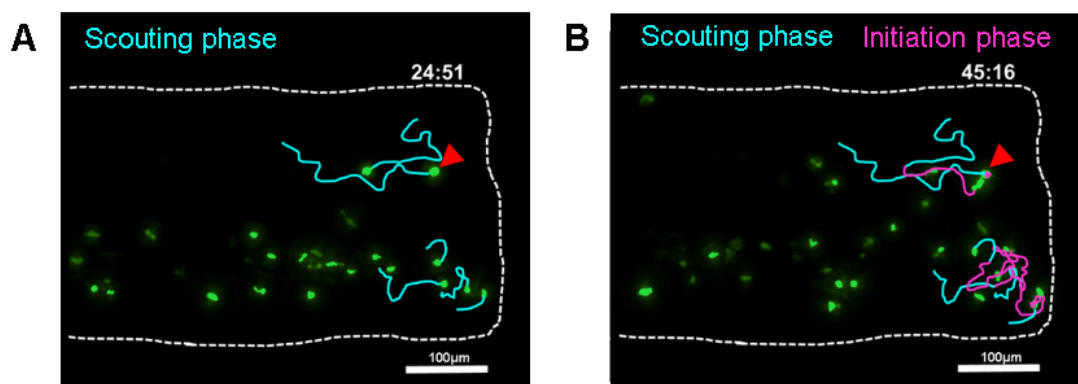
Figure 3.14: Tracking neutrophil migration during the scouting and swarm initiation phases

Tail fin transection was performed on 3dpf *mpx*:GFP larvae followed by time lapse imaging of neutrophil recruitment to the wound site from 30 minutes post injury for 5 hours. Time courses in which pioneer neutrophil recruitment to the wound site was observed prior to swarm formation were selected for analysis. Tracking of pioneer neutrophils and non-pioneer neutrophils equi-distant from or closer-to the wound site was performed during the scouting (A) and initiation (B) phases. Figure shows a representative example of the neutrophils tracked in one larvae during the scouting phase (blue) and the initiation phase (pink). Time stamps shown in white (mm:ss) are relative to the start of imaging at 30 minutes post injury.
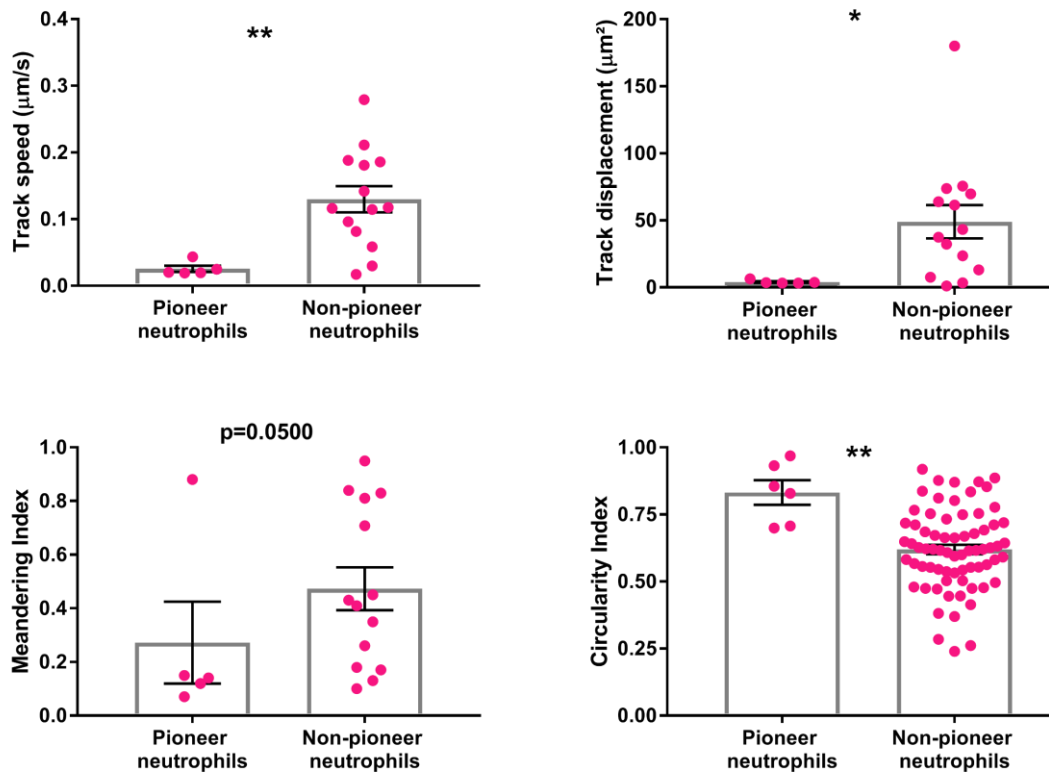
Figure 3.15: Migratory behaviours of pioneer neutrophils are different to non-pioneer neutrophils during the swarm initiation phase

Neutrophils proximal to the wound site were tracked in time courses of neutrophil recruitment to wound sites in 3dpf *mpx*:GFP larvae. Neutrophil migration was measured during the swarm initiation phase using track speed, track displacement and meandering index. Circularity index was used to measure neutrophil circularity. Dots represent individual neutrophils, where experiments were performed on five larvae. Pioneer neutrophils had significantly lower speeds (A) and displacement (B) compared to non-pioneer neutrophils, whilst meandering index was not statistically different (C). The circularity index of pioneer neutrophils was significantly higher than non-pioneer neutrophils during swarm initiation (D). (Data are shown as mean +/- sem. *Unpaired t-test, n=5 *p<0.05 **p<0.01).*

3.6.5 Neutrophil migratory behaviour during the scouting phase is the same between pioneer and non-pioneer neutrophils

There currently exists evidence of heterogeneous neutrophil populations which have distinct functions during inflammatory and pathologic conditions. It is currently unclear if these are neutrophil sub-populations or whether local tissue cues alter the activation or polarisation state of these neutrophils (Deniset and Kubes, 2018).

I hypothesised that if pioneer neutrophils were a sub-population with a distinct pre-programmed, their migratory behaviour may be different to non-pioneer neutrophils during their scouting to the wound site.

To investigate this hypothesis, pioneer and non-pioneer neutrophil tracks were extracted from the scouting phase data and the speed, displacement and meandering index was recorded. These data demonstrate that pioneer neutrophils recruit towards the wound site at the same speed as non-pioneer neutrophils (Figure 3.16A). The displacement of pioneer neutrophils was significantly higher in pioneer neutrophils than non-pioneer neutrophils, indicating that during these experiments, pioneer neutrophils have migrated a larger distance to the wound site (Figure 3.16B). The meandering index was not significantly different between pioneer and non-pioneer neutrophils (Figure 3.16C).

Together these data suggest that pioneer and non-pioneer neutrophils migrate with similar kinetics to the wound site. The increased displacement observed in pioneer neutrophils reflects the selection of neutrophils closer to or equal-distance from the wound site for comparisons in these experiments.

3.6.6 Migratory behavioural changes between the scouting and initiation phases are observed in pioneer neutrophils but not non-pioneer neutrophils

I next aimed to investigate the behavioural change in pioneer neutrophils between the scouting and initiation phase. I hypothesised that the phenotypic switch I have previously reported could be detected by comparing migratory behaviours between the two phases. As proof of concept I have previously shown that by tracking the speed and circularity index of the pioneer neutrophil throughout the scouting and initiation phase, a clear phenotypic change can be observed (Figure 3.13).

I compared the pioneer neutrophil tracks taken from the scouting phase to those taken from the initiation phase. As anticipated I found that the migratory behaviours of pioneer neutrophils was significantly different in the initiation phase, which is highlighted by the significant reduction in speed, displacement and meandering index observed between the scouting and initiation phases (Figure 3.17A-C).
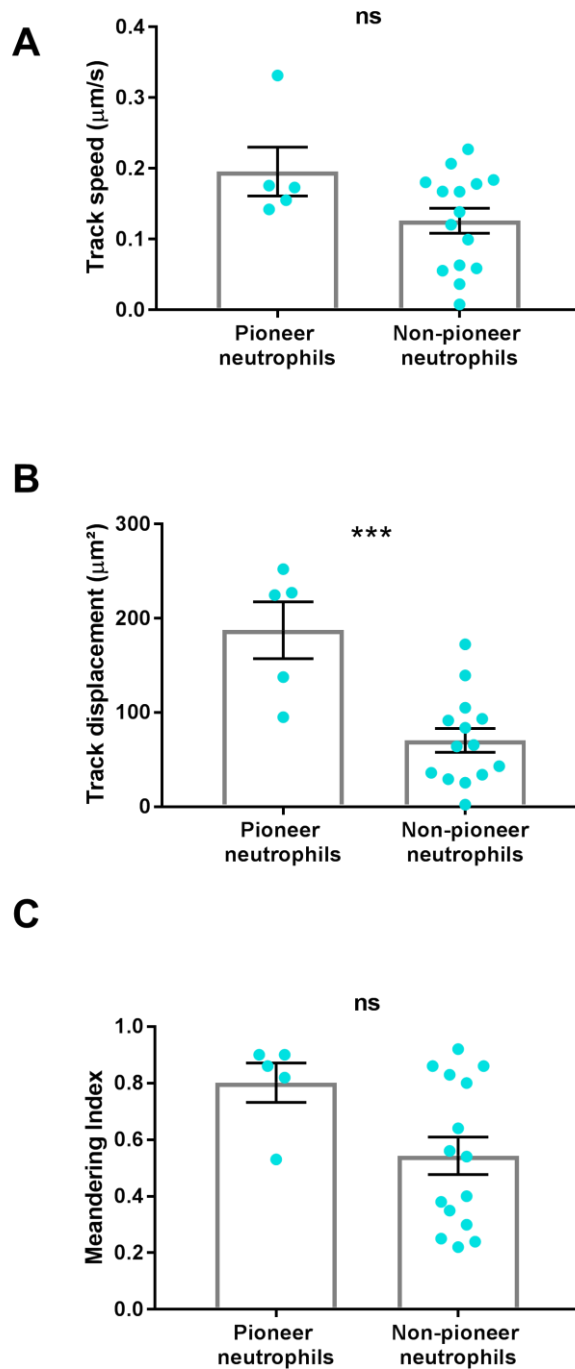
Figure 3.16: Migratory behaviour during the scouting phase is not different between pioneer and non-pioneer neutrophils

Neutrophils proximal to the wound site were tracked in time courses of neutrophil recruitment to wound sites in 3dpf *mpx*:GFP larvae. Neutrophil migration was measured during the scouting phase using track speed, track displacement and meandering index. Dots represent individual neutrophils, where experiments were performed on five larvae. There was no difference in the speed of migration to the wound site between pioneer and non-pioneer neutrophils (A). Pioneer neutrophil displacement was significantly higher than non-pioneer neutrophils (B) whilst there was no difference observed in meandering index (C). (Data are shown as mean +/- sem. *Unpaired t-test, n=5 ***p<0.001).*
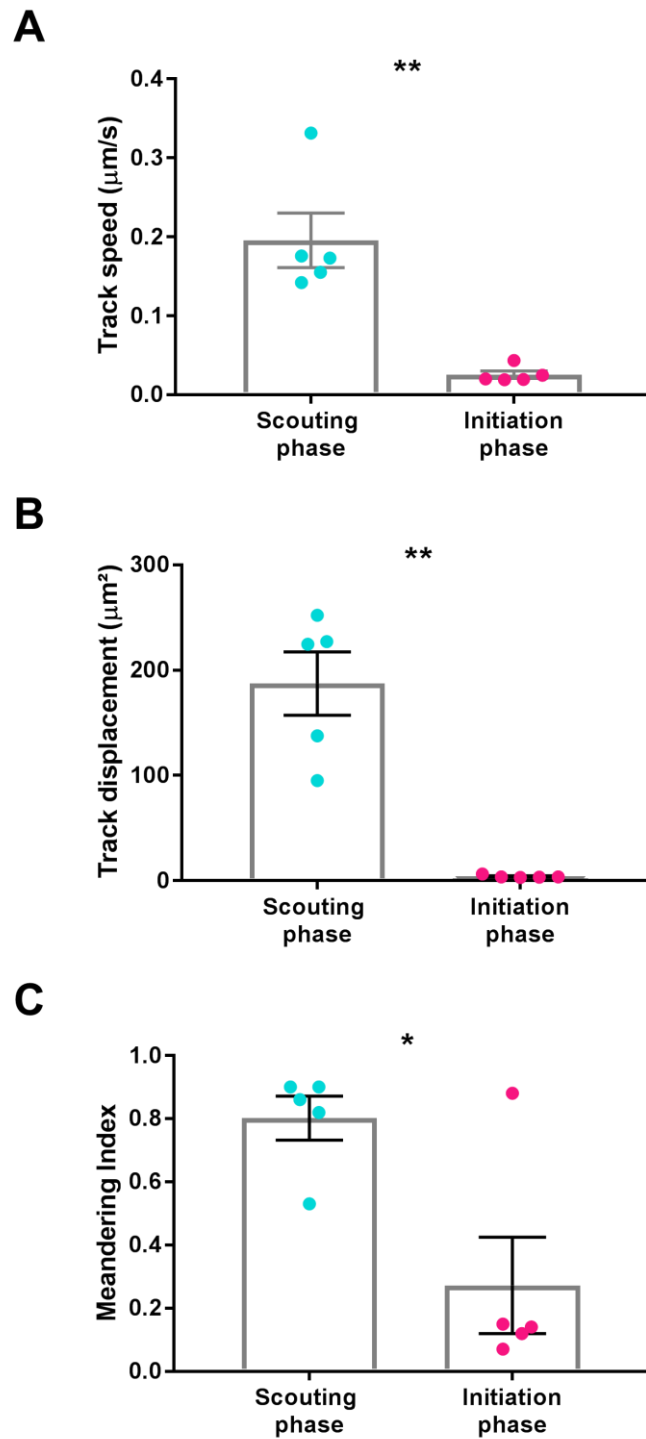
Figure 3.17: Migratory behaviour of pioneer neutrophils is reduced during the swarm initiation phase

Pioneer neutrophils were tracked in time courses of neutrophil recruitment to wound sites in 3dpf *mpx*:GFP larvae. Pioneer neutrophil migration was measured during the scouting and initiation phase using track speed, track displacement and meandering index. Dots represent individual neutrophils, where experiments were performed on five larvae. A significant reduction in pioneer neutrophil speed (A), displacement (B) and meandering index (C) was observed during the swarm initiation phase. (Data are shown as mean +/- sem. *Paired t-test, n=5 *p<0.05 **p<0.01)*

Finally, to determine whether the phenotypic change observed was specific to swarm-initiating pioneer neutrophils, I also studied the tracks of neutrophils which did not start swarms during the scouting and initiation phases from the same 5 larvae.

The migratory behaviours of non-pioneer neutrophils did not differ between the scouting and initiation phases, which is demonstrated by the non-significant difference observed when measuring the neutrophil speed, displacement and meandering index (Figure 3.18A-C)

Together these data suggest that the migratory behaviours of pioneer neutrophils during the scouting phase are the same. Interestingly pioneer neutrophils arrive at the wound site and, unlike other neutrophils, undergo a phenotypic switch in behaviour which is specific to these swarm initiating neutrophils. This highlights that the tissue microenvironment at the wound site potentially induces the behavioural change of pioneer neutrophils.
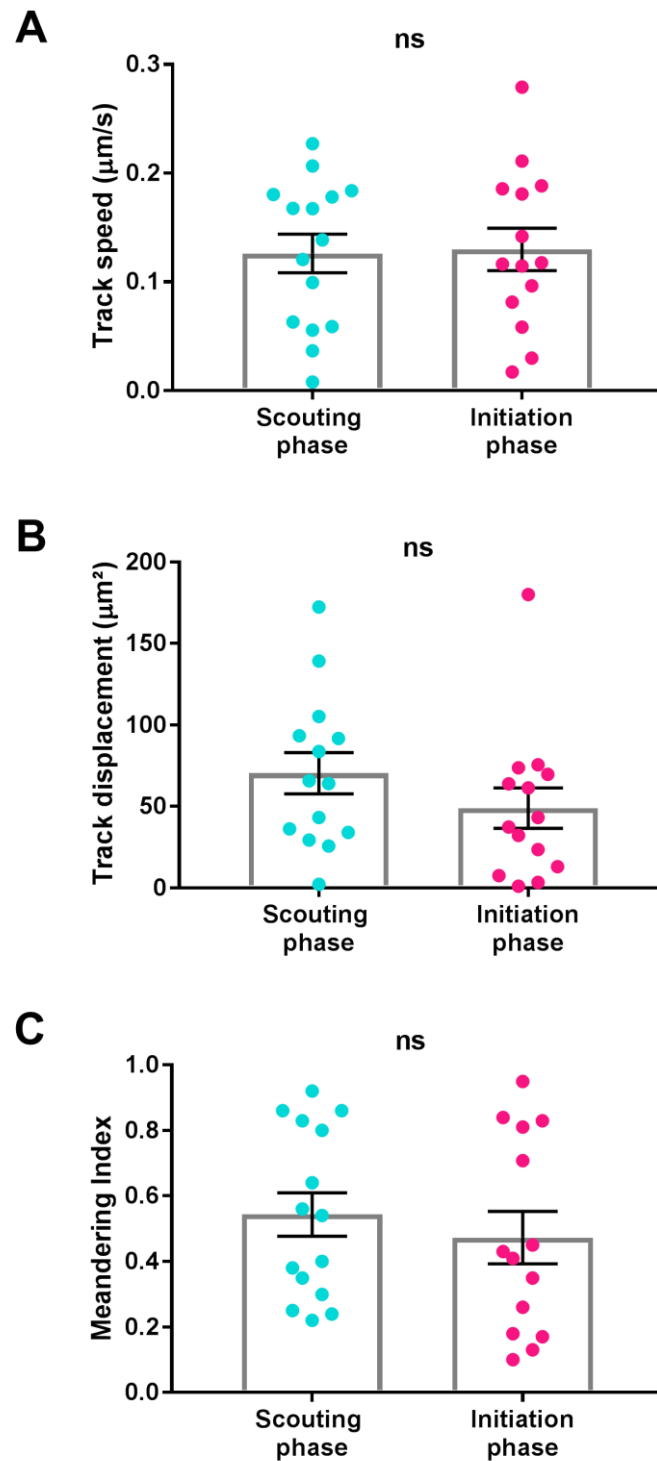
Figure 3.18: Migratory behaviours of non-pioneer neutrophils are unchanged during the scouting and initiation phases

Non-pioneer neutrophils were tracked in time courses of neutrophil recruitment to wound sites in 3dpf *mpx*:GFP larvae. Non-pioneer neutrophil migration was measured during the scouting and initiation phase using track speed, track displacement and meandering index. Dots represent individual neutrophils, where experiments were performed on five larvae. There was no significant difference observed in neutrophil track speeds (A), displacement (B) and meandering index (C) between the scouting and initiation phases. (Data are shown as mean +/- sem. *Paired t-test, n=5).*

3.6.7 Phase 3: Swarm aggregation

The third stage of swarm formation observed in zebrafish larvae was the coordinated migration of a population of neutrophils at the wound site to form neutrophil clusters. Following the phenotypic switch of the pioneer neutrophil during the initiation phase, the directed migration of neutrophils towards the pioneer was observed, resulting in cluster formation at the wound site (Figure 3.19, Movie 3.10-3.12). During the aggregation phase, 2 swarm phenotypes were observed. Large neutrophil swarms were observed which, following initiation continued to grow in size, persisting at the wound site for up to 6 hours post injury (Figure 3.20). A second type of swarm was observed which, following the recruitment of neutrophils to the pioneer, persisted transiently before dissipating and re-forming, often multiple times throughout the time courses (Figure 3.21).

From the time courses recorded for 5 hours following tail-fin transection of 3dpf *mpx*:GFP larvae, persistent swarms were identified using the automated assay previously described, in 6/14, and a further swarm was identified visually in one larva such that 7/14 larvae had a persistent swarm at the wound site. The automated object area assay was not sensitive enough to detect smaller transient swarms, which were instead identified visually by observing the directed migration of neutrophils to form small clusters at the wound site. From these experiments transient swarming was observed in 2/14 larvae (Figure 3.22).

Neutrophil swarming is a dynamic process which requires high speed imaging at regular intervals to observe. Time lapse imaging limits the number of larvae which can be used per experiment due to photo toxicity from lasers and the time taken to image each larva, resulting in low n numbers from each experiment. To overcome these limitations I next aimed to determine whether neutrophil swarming could be observed at the tail-fin in larvae at a static time point without time lapse imaging. 3dpf *mpx:*GFP larvae were injured as described in methods and neutrophil swarms were detected at 3hpi using a stereo microscope with a GFP emission filter. Neutrophil swarms were identified by the presence of an obvious neutrophil cluster at the wound site (Figure 3.23A) which were not detected in larvae with no swarms (Figure 3.23B). From these experiments, neutrophil swarms at the wound site were detected at 3hpi in just 16% of larvae (Figure 3.23C). As the nature of neutrophil swarming is dynamic, I was unable to identify smaller transient swarms using this assay. These data indicate that whilst many more larvae can be used per experiment using this assay, neutrophil swarming is detected in far fewer larvae, suggesting that this is not an effective method to study this process.
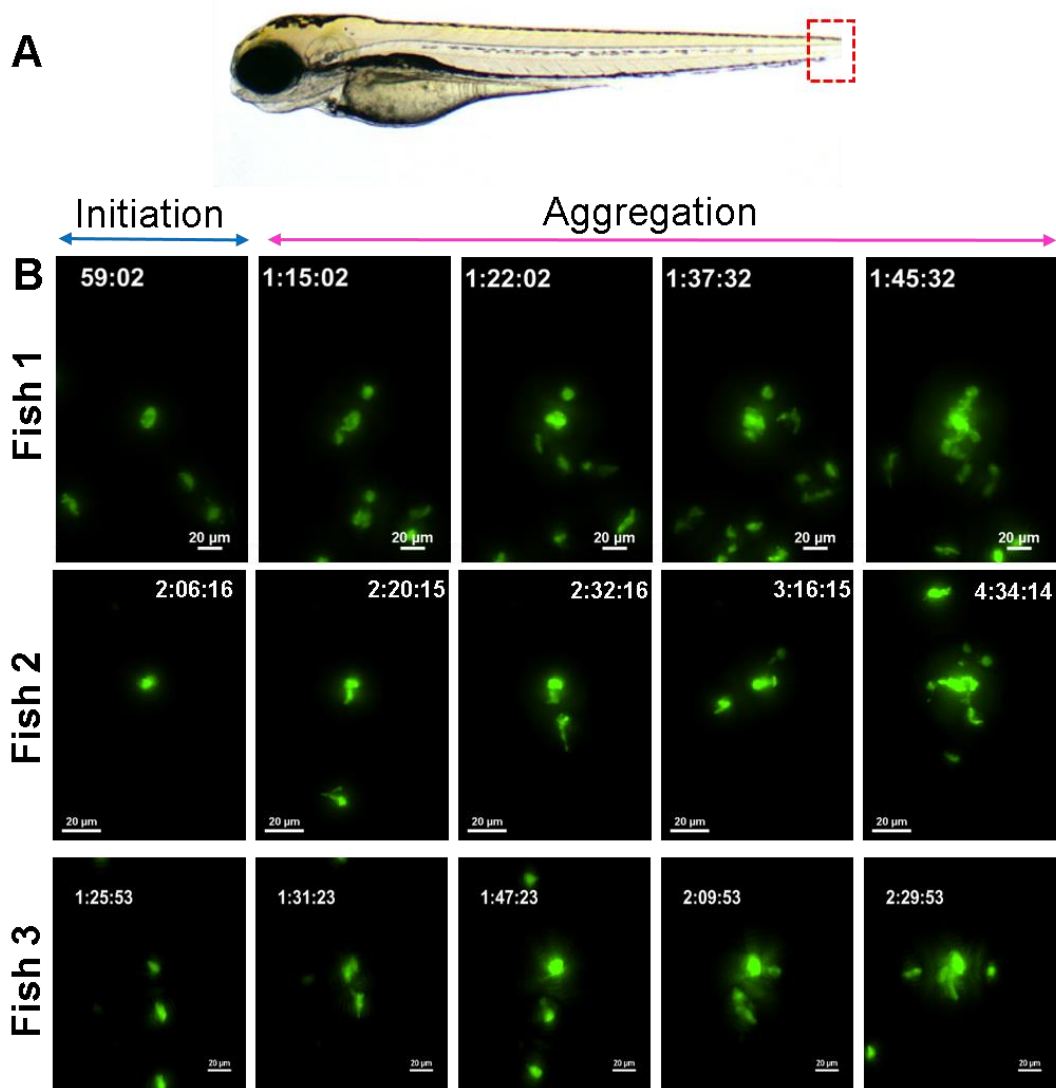
Figure 3.19: The neutrophil swarm aggregation phase

Time course imaging was performed on 3dpf *mpx*:GFP larvae following tail fin transection from 30 minutes post injury for 5 hours. Following the initiation of the swarming response by pioneer neutrophils, phases of directed migration of neutrophils were observed for the remainder of the time courses, resulting in the formation of large neutrophil aggregates at the wound site. Region of imaging is highlighted in (A). Figures shows the aggregation of neutrophils to form swarms around a pioneer neutrophil after the initiation phase in three representative larvae (B). Time stamps shown in white (mm:ss) are relative to the start of imaging at 30 minutes post injury.
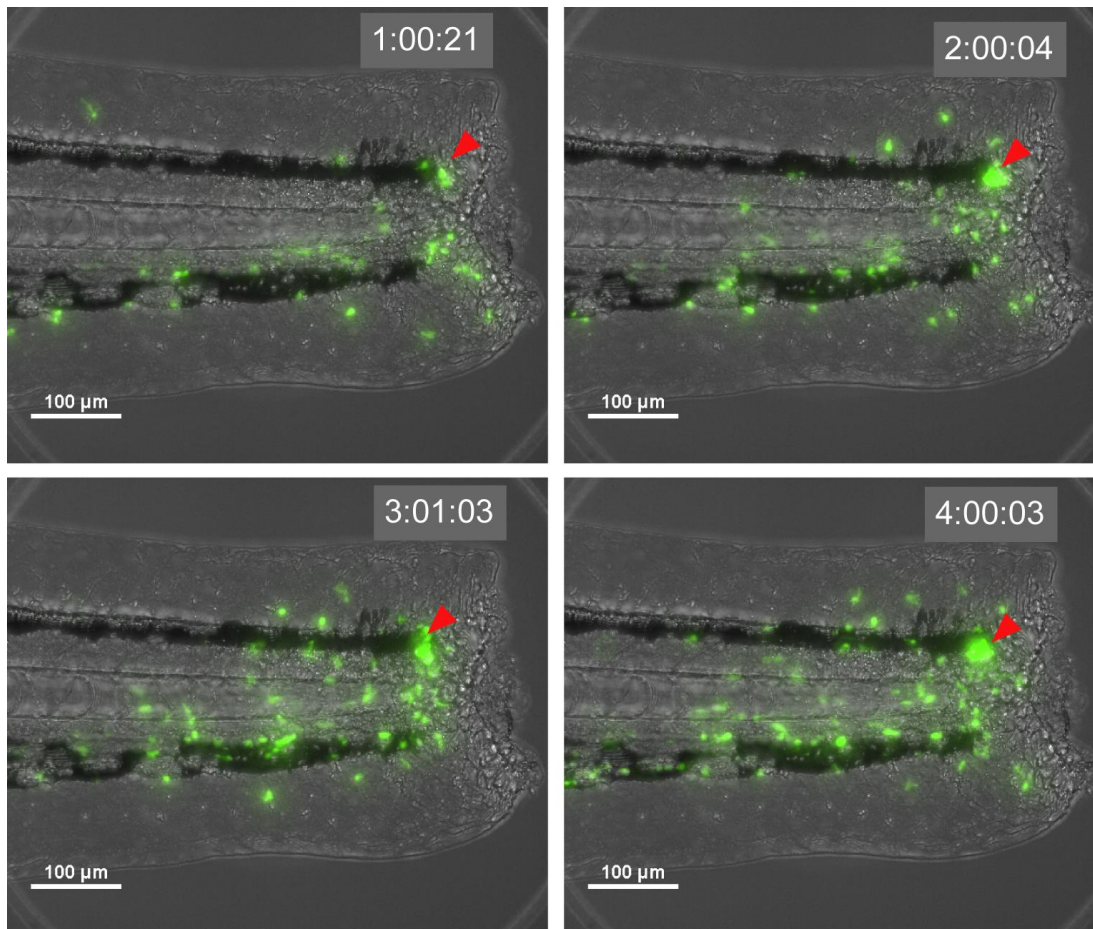
Figure 3.20: Neutrophil swarms can be persistent during the aggregation phase

Neutrophil swarming was observed during the aggregation phase in time courses recorded of neutrophil recruitment to tail fin transection in *mpx*:GFP larvae at 3dpf. A phenotype of neutrophil swarming whereby neutrophils continued to aggregate in clusters at the wound site throughout the duration of the time courses was observed. Figure shows a representative example of a persistent neutrophil swarm at the wound site during neutrophil recruitment. Time stamps shown in white (hh:mm:ss) are relative to the start of imaging at 30 minutes post injury.
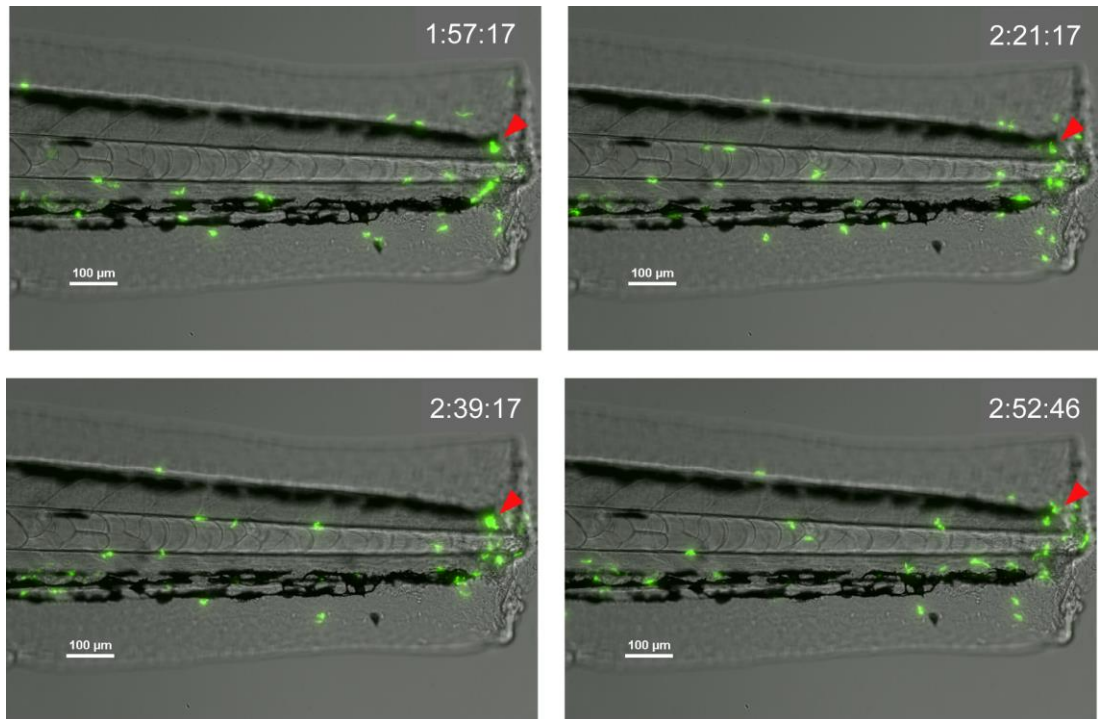
Figure 3.21: Neutrophil swarms can be transient during the aggregation phase

Neutrophil swarming was observed during the aggregation phase in time courses recorded of neutrophil recruitment to tail fin transection in *mpx*:GFP larvae at 3dpf. A phenotype of neutrophil swarming was observed whereby neutrophils formed a cluster around a pioneer neutrophil, which resolved and re-formed multiple times throughout the time course. Figure shows a representative example of a transient neutrophil swarm (red arrow) in which neutrophils aggregate and resolve around a pioneer neutrophil. Time stamps shown in white (hh:mm:ss) are relative to the start of imaging at 30 minutes post injury.
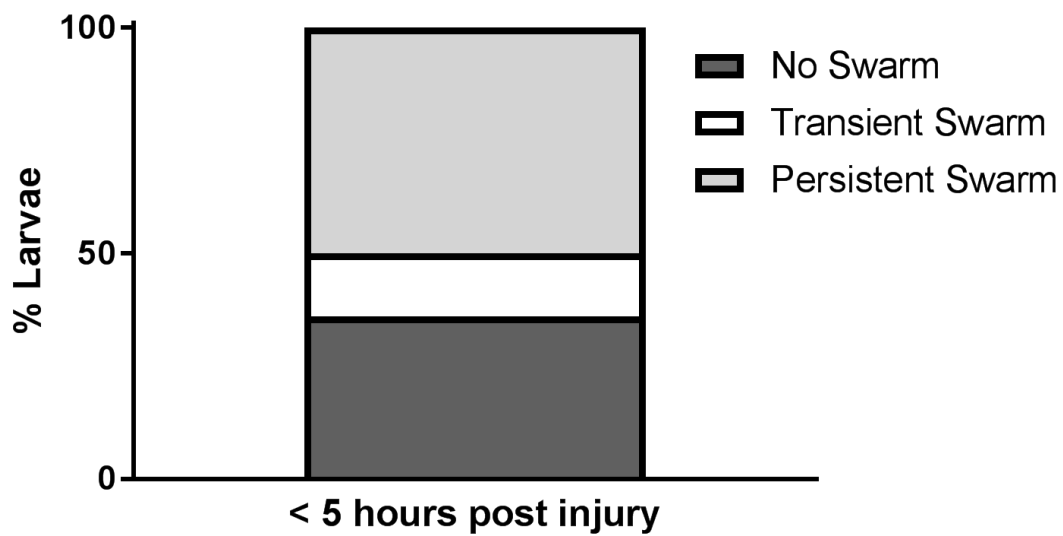
Figure 3.22: Exploring the frequency of persistent and transient swarming

Time courses were studied of neutrophil recruitment to injury sites in 3dpf *mpx*:GFP larvae. Larvae with clusters at the wound site were identified and of these clusters 50% were persistent and 14% were transient. Larvae with no neutrophil swarming events were observed in 36% of time courses. (*n=14 larvae from 5 experimental repeats*).
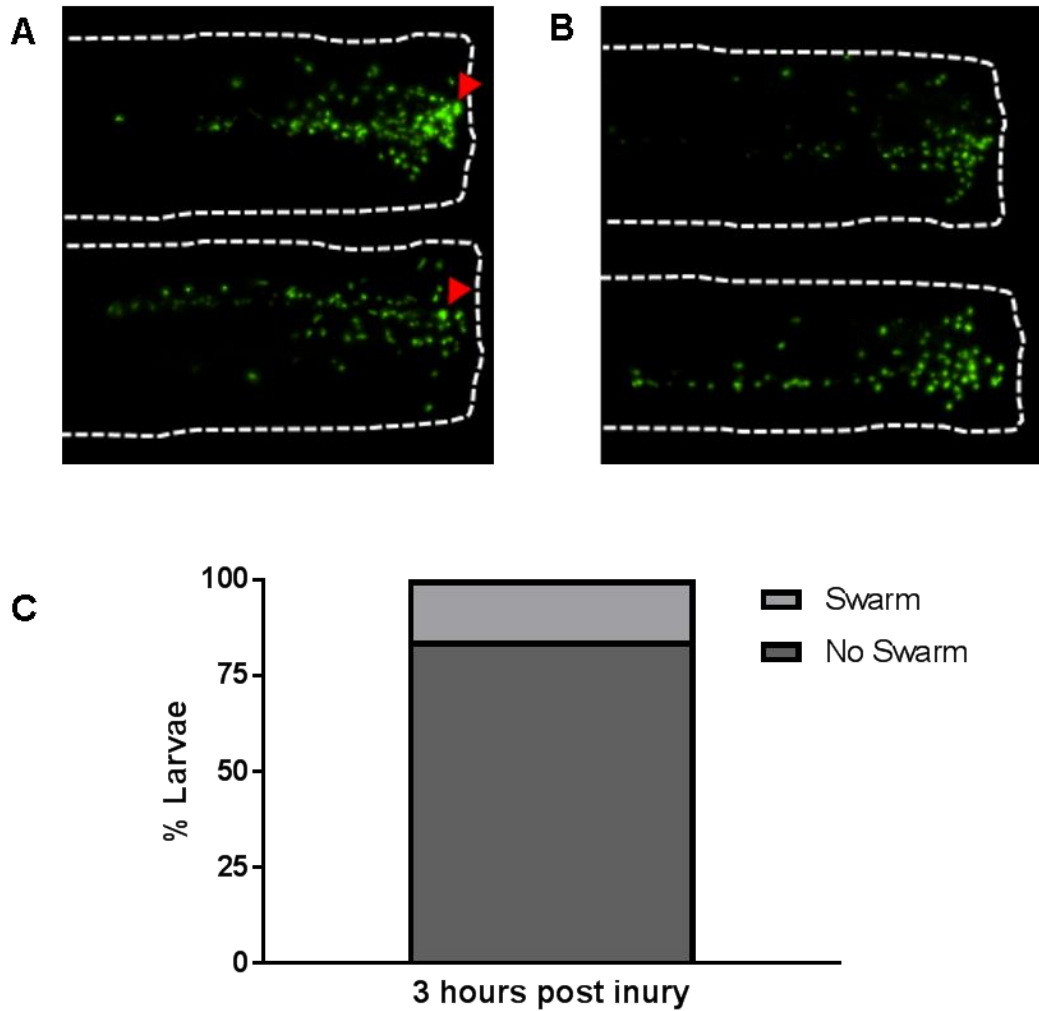
Figure 3.23: Observing neutrophil swarming at a static time point

Tail fin transection was performed on 3dpf *mpx*:GFP larvae and neutrophil recruitment to the wound site was observed at 3hpi. Neutrophli swarming was identified by the presence of obvious neutrophil clusters at the wound site (red arrows, A) which were not present in larvae where swarming wasn't observed at 3hpi (B). The number of larvae with obvious clusters at the wound site was quantified (C). 16% of larvae had neutrophil swarms at the wound site, whilst 84% did not. (*n=293 larvae from 3 experimental repeats*).

3.7 Quantification of aggregation phase phenotype

Parameters used to quantify neutrophil swarming *in vitro* include swarm area and neutrophil counts in the swarm. To quantify the swarming phenotypes observed during the aggregation phase, the number of neutrophils recruited to swarms were counted at hourly intervals for the first 5 hours following tail-fin transection in individual larvae with swarms (Figure 3.24A and C respectively). From these experiments I found that the average number of neutrophils recruited to persistent swarms continued to increase until reaching their peak at the end of the time course at 5hpi (Figure 3.24B), whilst the average number of neutrophils recruited to transient swarms peaked earlier at 2hpi (Figure 3.24D). The average number of neutrophils recruited to persistent swarms at their peak (at 5hpi) was higher than the average number of neutrophils recruited to transient swarms at their peak recruitment (at 2hpi), although this difference was not significant (unpaired t-test with Welch's correction, p=0.076) (Figure 3.25E).

These findings are recapitulated when measuring the area of neutrophil swarms at hourly intervals in individual larvae with persistent and transient swarms (Figure 3.25A and C respectively). The average area of persistent neutrophil swarms was highest at 4hpi, after which point a small but not significant decrease was observed at 5hpi, suggesting that these swarms remain stable at least until the end of the time course when they begin to decrease in size (Figure 3.25B). The average area of transient neutrophil swarms peaked at 2 hours post injury and continued to decrease and completely dissipate by the end of the time course (Figure 3.25D). The average area of persistent swarms at their peak size was significantly higher than that of transient swarms (Figure 3.25E), further demonstrating that persistent swarms are larger than transient swarms.

These data demonstrate that persistent neutrophil swarms are larger than transient swarms as highlighted by their larger area and higher number of recruited neutrophils. From these experiments I found that differences in neutrophil swarming phenotypes during the aggregation phase can be quantified by measuring parameters such as swarm area and neutrophil counts, which may be useful for future studies of neutrophil swarming.
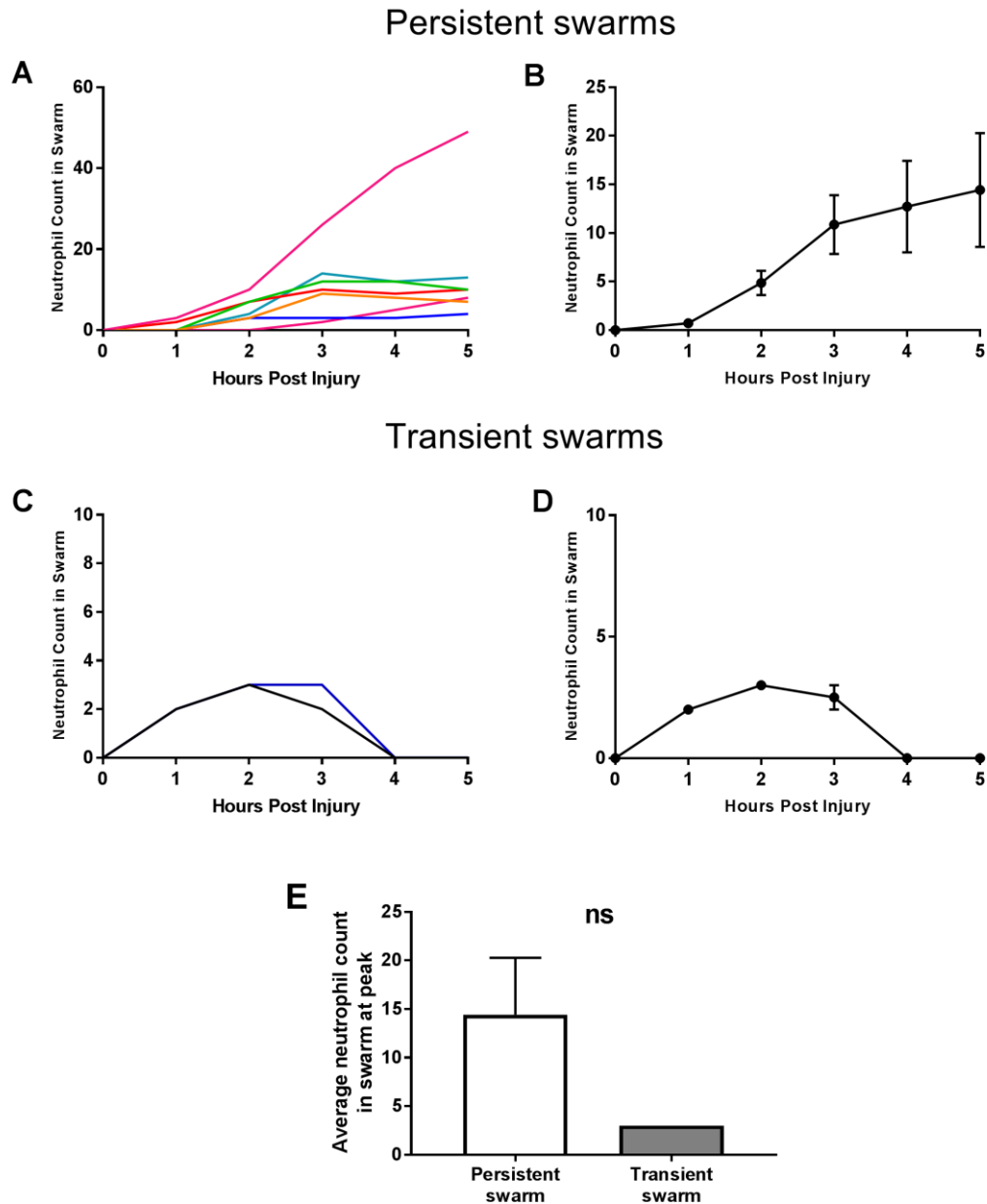
Figure 3.24: Evaluation of neutrophil counts in persistent and transient swarms

Time course imaging was performed on 3dpf *mpx*:GFP larvae following tail fin transection from 30 minutes post injury for 5 hours and those with persistent and transient neutrophil swarms at the wound site were selected for analysis. Neutrophils were counted manually in individual swarms at hourly intervals in persistent and transient swarms (A,C). Neutrophil counts were pooled for persistent and transient swarms (B-D). The maximum number of neutrophils recruited to persistent and transient swarms was compared. There was no significant difference in the maximum number of neutrophils recruited to persistent or transient swarms peak (E). (Data are shown as mean +/- sem. *n= 7 persistent and 2 transient swarms from 5 experimental repeats)*
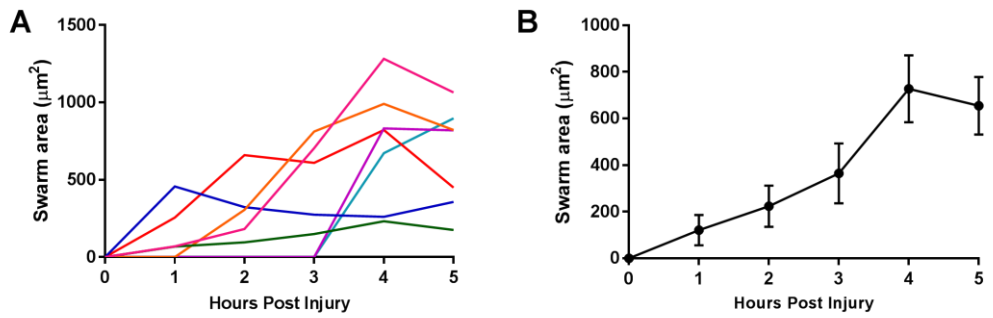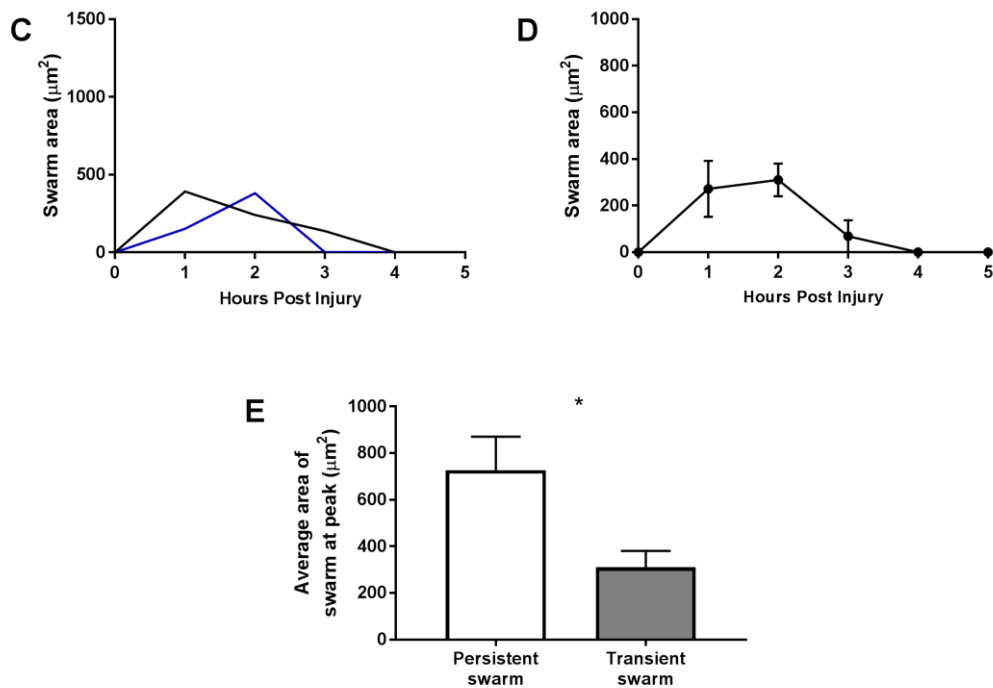
Figure 3.25: Evaluation of neutrophil swarm area in persistent and transient swarms

Time course imaging was performed on 3dpf *mpx*:GFP larvae following tail fin transection from 30 minutes post injury for 5 hours and those with persistent and transient neutrophil swarms at the wound site were selected for analysis. The area of individual neutrophil swarms was measured at hourly intervals throughout the time courses in persistent and transient swarms (A,C). Swarm area was pooled for persistent and transient swarm phenotypes (B,D). The maximum area of neutrophil swarms compared between persistent and transient swarms, identifying that persistent swarms had significantly larger area than transient swarms. (Data are shown as mean +/- sem. *n= 7 persistent and 2 transient swarms from 5 experimental repeats. Unpaired t-test *P<0.01)*

3.8 Investigating the spatio-temporal dynamics of the swarming response

After identifying three phases of migration leading to neutrophil swarming, I next characterised the temporal component of these phases to provide insight into the time point when the swarming response takes place, as well as to determine the fish-to-fish variation in these phases.

Persistent swarms were selected from time courses recorded for 5 hours following tail-fin transection of 3dpf *mpx*:GFP larvae, and the time frame in which the initiation and aggregation phases began was recorded. To recap, the scouting phase was the initial recruitment of neutrophils to the wound site, the initiation phase was defined as the first time frame in which a phenotypic change was observed in the pioneer neutrophil, and the aggregation phase was defined as the time frame in which the first neutrophil is recruited to the pioneer. Neutrophil scouting was observed from the start of the time course at 0.5 hours post injury, although it is likely that this begins within minutes of the tail-fin transection. In these experiments the initiation phase began within 1hpi in the majority of larvae, although interestingly in a minority of larvae the initiation phase began much later at around 4 hours post injury, indicating that later onset neutrophil swarming is also observed. The aggregation phase began within 2hpi in most larvae, however again there was a later onset population of swarms which began between 2.5-4.5hpi (Figure 3.26A).

The duration of each phase of swarm formation was also recorded to determine the average time of each phase. From these experiments, the mean duration of the scouting, initiation and aggregation phases was 88.18+/- 23.63 minutes, 36.45+/- 7.40 minutes, and 183+/- 25.52 minutes respectively (Figure 3.26B). To determine the entire duration of the aggregation phase longer time lapses are required as swarms were still aggregating at the end of the time courses.

These data show that on average the scouting phase occurs during the first one hour following tail-fin transection. The initiation phase is the shortest of the three phases and usually occurs for around half an hour. Swarm formation usually begins within 180 minutes post injury and persists at least until 5.5 hours post injury.

From these initial observations I have identified three distinct and consistent stages of the neutrophil swarming response in zebrafish, as well as two phenotypes of neutrophil swarming.
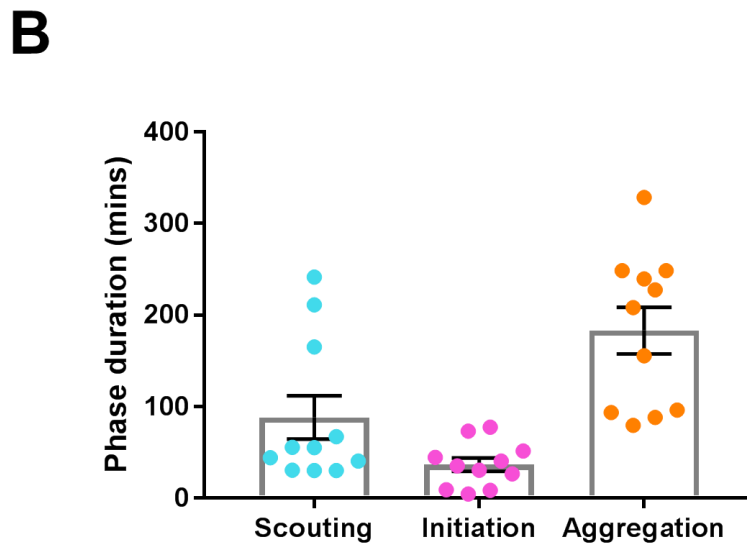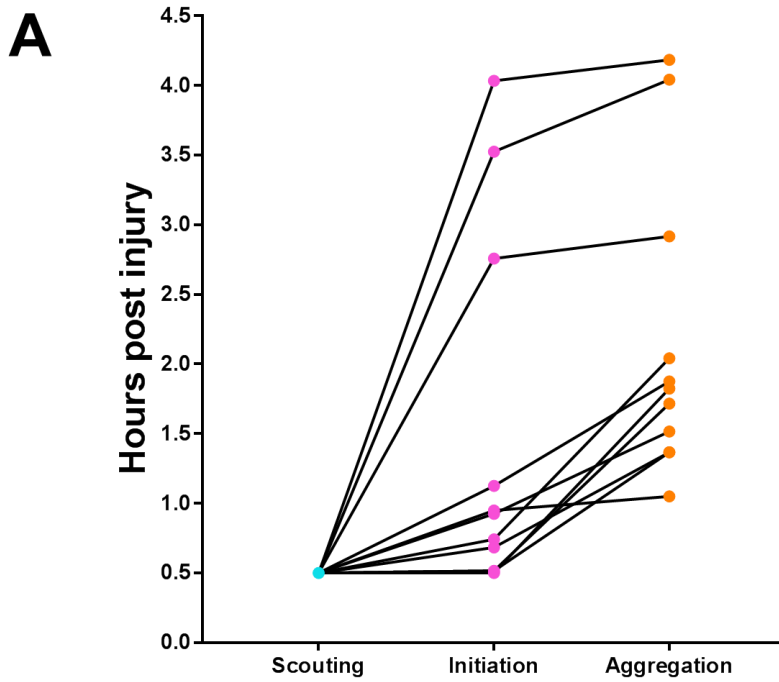
Figure 3.26: Characterisation of the temporal component of neutrophil swarming

Time course imaging was performed on 3dpf *mpx*:GFP larvae following tail fin transection from 30 minutes post injury for 5 hours. The time in which the initiation and aggregation phases of neutrophil swarming began was recorded (A). The scouting phase begins within minutes following tail fin transection and is observed by time course imaging from 30 minutes post injury. The initiation phase of the majority of swarms begins approximately 1 hour post injury and the aggregation phase usually begins between 1 and 2 hours post injury. The duration of the scouting, initiation and aggregation phases was also measured (B). (Data are shown as mean +/- sem. *n=11 swarms from 5 experimental repeats*).

I propose that the zebrafish could provide an excellent model to study the initiation phase of swarming due to the ability to observe pioneer neutrophils throughout the entirety of their recruitment to the wound site and initiation of swarms.

3.8.1   Pioneer neutrophils change morphology within 60μm of the wound edge

I next investigated the hypothesis that the phenotype change in pioneer neutrophils was tissue context dependent. To do this I selected persistent swarms from time courses recorded for 5hpi following tail-fin transection of 3dpf mpx:GFP larvae. I hypothesised that if tissue context was important for inducing the pioneer neutrophil phenotype switch, there would be consistency in the position at the wound site where the phenotypic switch took place.

The position at the wound site where pioneer neutrophils undergo their phenotypic switch was measured in order to gain insight into the tissue context required for swarm initiation. Time lapse sequences were studied from six experimental repeats and 15 swarms were detected from 11 larvae (multiple swarms were detected in some larvae). The x and y position of pioneer neutrophils relative to the edge of the tail-fin and the ventral edge of larvae was recorded in the frame preceding the aggregation phase. To provide approximate spatial information regarding the position of swarms at the wound site, these data were superimposed on top of a representative tail-fin region as indicated by green circles superimposed (Figure 3.27A). By looking at the x position of pioneer neutrophils relative to the wound edge, I identified that all pioneer neutrophils initiated swarms within 60μm from the wound edge, with the average distance being 42.8+/-6.287μm (Figure 3.27B). The small standard deviation of points around the mean illustrates that neutrophil swarm formation at the wound site is consistently within 38-50μm from the wound edge. When looking at the y position of pioneer neutrophils relative to the ventral edge of larvae, I found that swarms did not form within 132μm of the ventral edge of the larvae, and no swarms were detected above 362.5μm from the ventral edge (Figure 3.27C). These data demonstrate that on average swarms do not form within 132 μm of the ventral edge, and 82.5μm from the dorsal edge. The average position of swarm formation in the y dimension was 260.8+/-72.98μm. The large standard deviation of points from the mean identifies that the distribution of neutrophils in the y dimension at the wound site is large, I therefore concluded that neutrophil swarms form anywhere within an approximately 300μm range in the centre of the fish in the y direction.

Together these data demonstrate that the x position of swarm formation is highly conserved between larvae whilst the y position is variable, suggesting that the perhaps a tissue context exists within 60μm of the wound edge which induces a pioneer neutrophil phenotype switch.
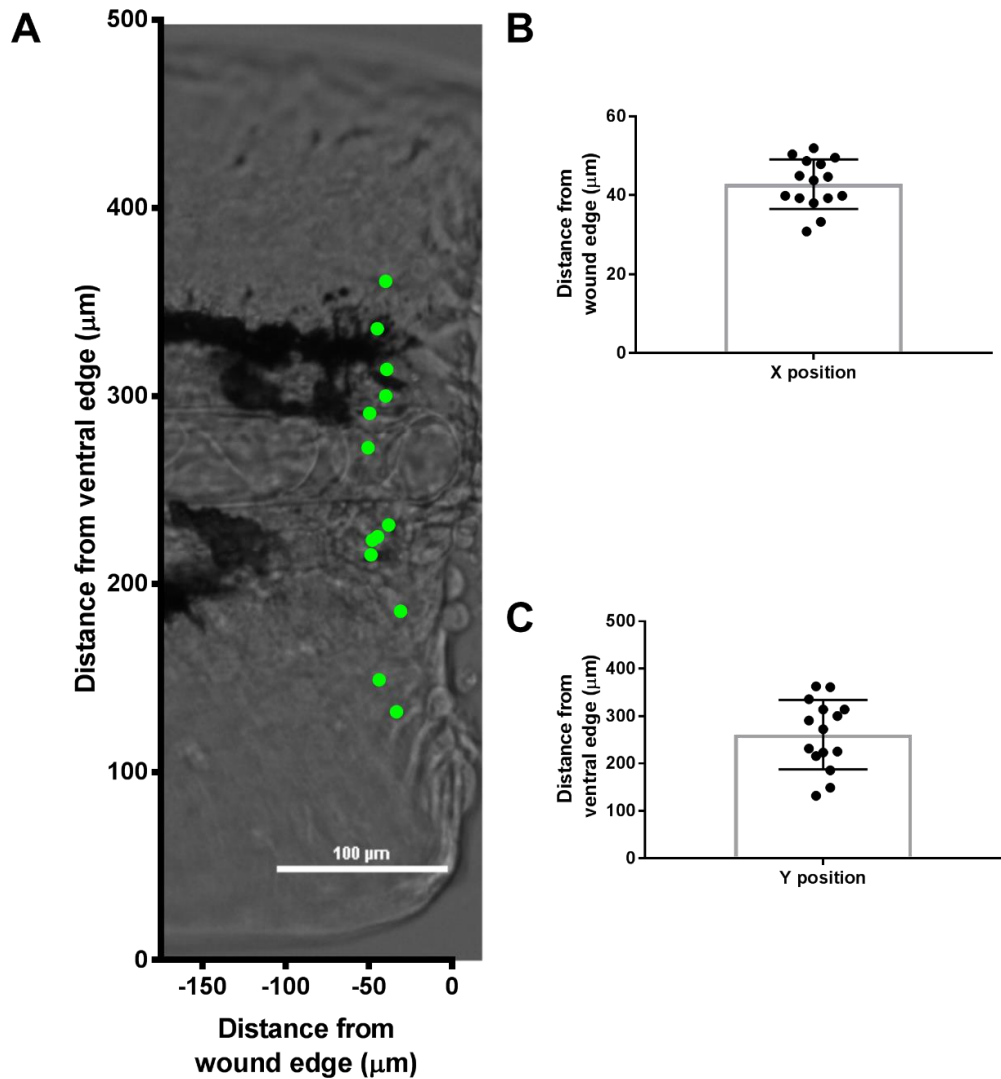
Figure 3.27: Investigating the position of swarm formation at the wound site

3dpf *mpx*:GFP larvae with persistent neutrophil swarms at the wound site following time lapse imaging were selected for analysis. The x and y coordinate of the position where pioneer neutrophils initiated swarm formation relative to the wound edge and the ventral fin edge was recorded. Green spots represent position of individual swarm formation (A). The x position of neutrophil swarm formation was within a 30μm niche within 60μm from the wound (B). The y position of swarm formation was within a 400μm niche in the centre of the wound edge, with no swarms being observed within 100μm of the dorsal or ventral edges of the larvae (C). (Data are shown as mean +/- sd. n=15 neutrophils from 5 experimental repeats).

3.9 A zebrafish reporter line to investigate hydrogen peroxide concentration in pioneer neutrophils

The proximity to the wound edge in which pioneer neutrophils adopt their change in morphology as well as the consistency between larvae suggests that these neutrophils encounter a tissue environment which initiates their change in phenotype. Following activation of the inflammatory response leukocytes are recruited from large distances within minutes. In zebrafish this is modulated in part by the release of reactive oxygen species such as hydrogen peroxide by cells at the wound margin. This hydrogen peroxide gradient diffuses up to 200μm into the tail-fin epithelium, peaking in concentration at around 20 minutes post injury and persisting for over 99 minutes post injury (Niethammer et al., 2009a). Hydrogen peroxide induces programmed cell death in eosinophils (Reis et al., 2015) as well as programmed and necrotic cell death in human retinal pigment epithelial cell lines (Kim et al., 2003) and is therefore a candidate to investigate swarm induction.

I hypothesised that high levels of hydrogen peroxide at the wound site may induce the pioneer cell death resulting in the morphological changes observed in pioneer neutrophils and cell death signalling to induce neutrophil swarming. To investigate this hypothesis I used a genetically encoded biosensor expressed specifically in neutrophils under the lyz promoter.

HyPer consists of a circularly permuted YFP (cpYFP) conjugated to the bacterial hydrogen peroxide sensitive OxyR transcription factor. OxyR undergoes a conformational change following cysteine oxidation by hydrogen peroxide, such that the spectral emission properties of the cpYFP are altered. At higher concentrations of hydrogen peroxide, emission of the cpYFP increases following excitation at 500nm, and a decrease in emission is observed when excited at 420nm. Generating a HyPer ratio signal (YFP_{500}/YFP_{420}) provides a spatiotemporal read-out of hydrogen peroxide concentration in individual neutrophils at the wound site.

3.10 Exogenous hydrogen peroxide increases HyPer ratio

The *Tg(lyz:HyPer)sh274* reporter line was made in collaboration by Katherine Henry and Graham Lieschke using gateway cloning (Renshaw lab unpublished). I first aimed to confirm that this reporter line accurately provides a read out of hydrogen peroxide concentration in neutrophils. I hypothesised that following the addition of exogenous H_2O_2, the OxyR domain of HyPer would detect an increase in H_2O_2 in the neutrophils and subsequently the HyPer ratio would increase.

To validate the function of the HyPer reporter line, 3dpf *lyz*:HyPer larvae were mounted in a 1% agarose solution and ratiometric imaging was performed as described in methods, focusing on the CHT region of larvae using a 40x lens (Figure 3.28A). Exogenous hydrogen peroxide was poured on to the top of the agarose and allowed to diffuse into the agarose for 5 minutes when imaging was performed again (Figure 3.28B). A YFP_{500}/YFP_{420} ratio channel was generated and a rainbow lookup table was applied to the pre and post H_2O_2 images as described in methods. ROIs were drawn around individual neutrophils in the CHT and the mean intensity of the ratio channel was recorded. Although this experiment was only performed once, the HyPer ratio of neutrophils in the CHT increased following the addition of exogenous H_2O_2 (Figure 3.29C), demonstrating that the reporter is able to successfully provide a read out of H_2O_2 concentration in neutrophils.

Due to time constraints preliminary experiments were performed to determine whether neutrophil swarming could be observed in *lyz*:HyPer larave before investigating hydrogen peroxide production in pioneer neutrophils. 3dpf *lyz*:HyPer larvae were injured by tail-fin transection as described in methods. HyPer imaging was performed from 30 minutes post injury for 4 hours. A ratio channel was generated by dividing the $HyPer_{500}$ channel by the $HyPer_{420}$ channel as described in methods. From the first experimental repeat neutrophil swarming was observed in one larvae. The pioneer neutrophil could be visualised within the first few frames of the time course (red arrow, Figure 3.29). This demonstrates that pioneer neutrophils can be visualised prior to swarm formation and that hydrogen peroxide production can be measured in these neutrophils. This tool is now ready for the evaluation of H_2O_2 concentration in neutrophils and its relationship to pioneer neutrophil function.
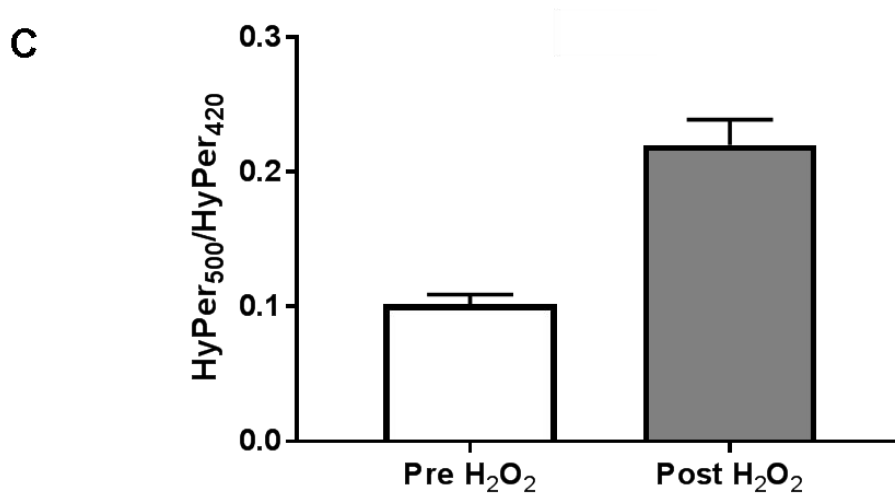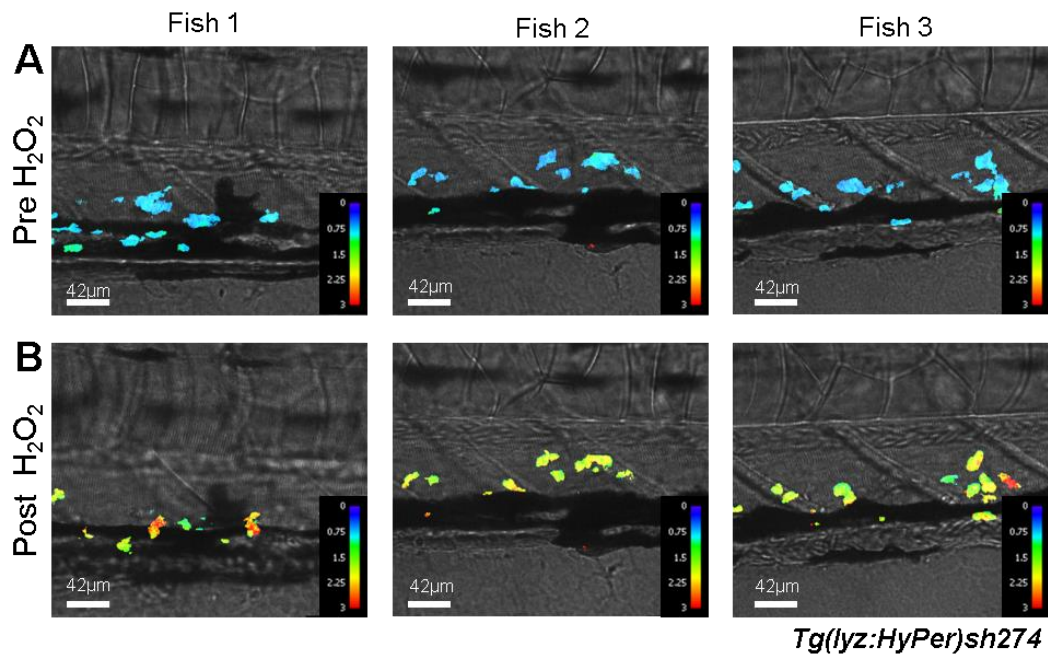
Figure 3.28: Exogenous hydrogen peroxide increases HyPer ratio

Ratiometric imaging of the CHT region of 3dpf *lyz*:HyPer larvae was performed and a ratio channel was generated (A). Exogenous hydrogen peroxide was administered to larvae by incubation and left to diffuse for 5 minutes. Ratiometric imaging of the same region of the CHT was performed post hydrogen peroxide addition (B). The HyPer ratio was calculated for individual neutrophils in the CHT, which increased following exogenous hydrogen peroxide administration (C). (Data are shown as mean +/- sem. *n=19 neutrophils from 3 larvae from 1 experimental repeat*).
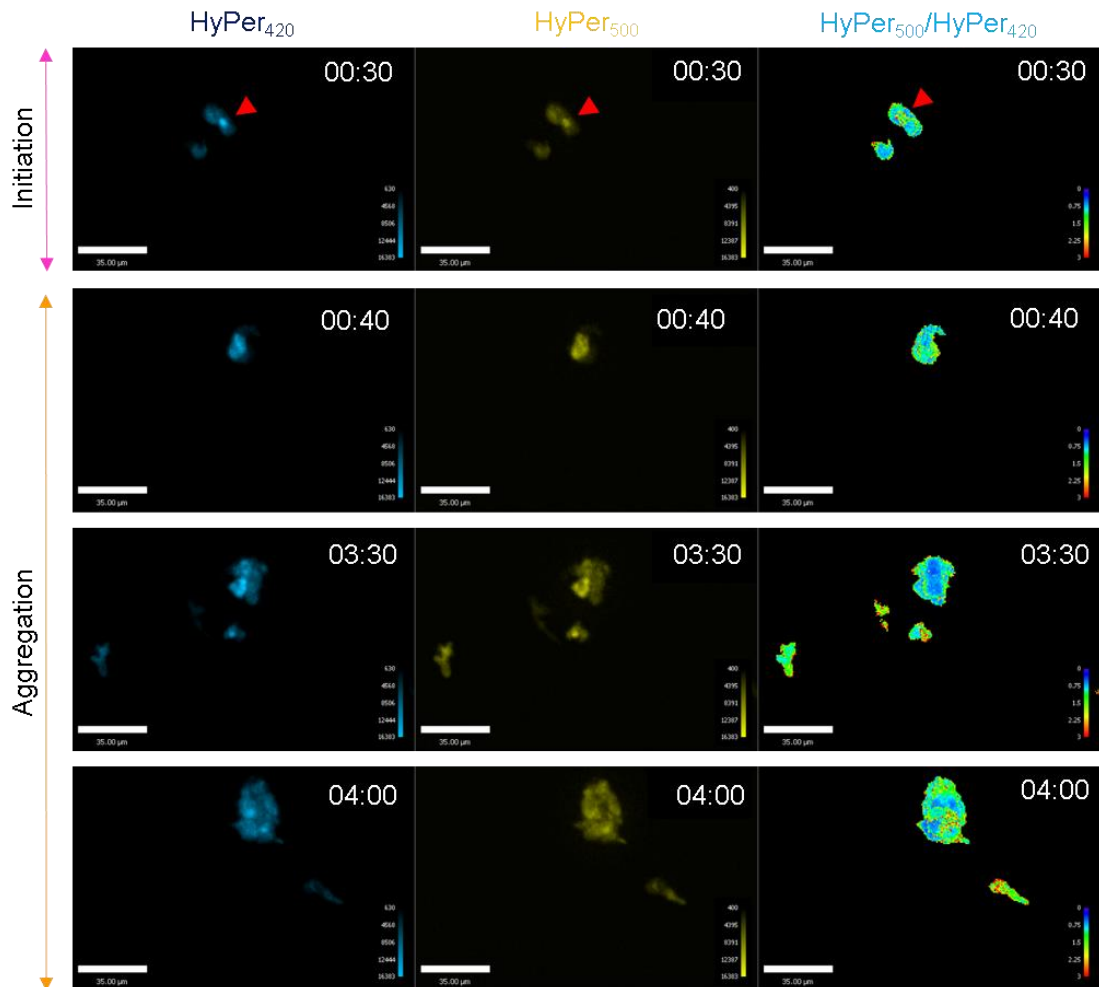
Figure 3.29: Pioneer neutrophil hydrogen peroxide concentration can be measured during swarm initiation

3dpf *lyz*:HyPer larvae were injured ratiometric imaging was performed from 30 minutes post injury for 4 hours and a HyPer ratio channel was generated for each time point. Figure shows a representative example of a pioneer neutrophil which can be studied during the initiation phase to determine hydrogen peroxide concentration prior to swarm formation (red arrow).

3.11 Investigating pioneer cell death as a mechanism for neutrophil swarm initiation

The early stages of neutrophil swarm initiation are not fully understood largely due to limitations in *in vivo* imaging and challenges in measuring intracellular molecular signalling. Currently the accepted paradigm is that cell death signalling by propidium iodide positive pioneer neutrophils initiates the first amplification stage of neutrophil swarming (Kienle and Lämmermann, 2016; Lämmermann, 2015; Lämmermann et al., 2013; Reátegui et al., 2017). The appearance of propidium iodide positive neutrophils correlates with the accelerated recruitment of neutrophils to form a swarm in mice, suggesting that cell death by necrosis is important in swarm initiation (Lämmermann et al., 2013).

Cell death presents with macroscopic morphological alterations which historically were employed to classify cell death into 3 different forms. Type 1 cell death or apoptosis is characterised by cytoplasmic shrinkage, chromatin condensation, nuclear fragmentation, and plasma membrane blebbing. Type 2 cell death or autophagy is characterised by extensive cytoplasmic vacuolization. Type 3 cell death or necrosis does not present the morphological features observed in type 1 and 2. The outcome of type 1 and 2 cell death is phagocytic uptake and lysosomal degradation whilst the cell corpses following necrosis are deposited into the tissue without evidence of phagocytic removal (Galluzzi et al., 2007). Since 2005 the Nomenclature Committee on Cell Death (NCDD) have frequently updated the classification of cell death modalities based on a mixture of genetic, pharmacological, biochemical and functional features of cell death, rather than morphological features, to ensure more accurate detection of cell death (Galluzzi et al., 2018). It is important to employ multiple, methodologically unrelated assays to quantify dying and dead cells, where guidelines exist to quantify and interpret cell death-related parameters (Galluzzi et al., 2009).

The rounded morphology and loss of motility I have observed in swarm initiating pioneer neutrophils suggests that cell death may be an initiating factor of swarm formation in the zebrafish model. I therefore hypothesised that a tissue context encountered by pioneer neutrophils at the wound site induced their death, and that cell death signals causes the initiation of swarm formation. This section of work aims to use available tools to dissect the behaviour of pioneer neutrophils during the initiation phase of swarm formation in zebrafish larvae.

3.12 Pioneer neutrophils do not become propidium iodide positive during swarm initiation

I hypothesised that pioneer neutrophils become necrotic prior to swarm formation in zebrafish larvae. To test this hypothesis I used the DNA intercalating agent propidium iodide. Propidium iodide labels intracellular RNA or DNA by intercalating between the bases and as a cell impermeable compound, it can only access the DNA and RNA in the nucleus if the plasma membrane is compromised.

3.12.1 Determining a dose of propidium iodide for live imaging

Propidium iodide (PI) has been used to label nucleotides in fixed zebrafish tissues but no reports of live imaging currently exist (Okuthe, 2013; Zampolla et al., 2008). Live imaging of plant tissues incubated with PI has been performed for short time periods (Jones et al., 2016).

To determine an appropriate dose of PI which was able to label nucleotides in zebrafish larvae without toxicity, a dose-response assay was performed using three concentrations of propidium iodide. 3dpf *mpx*:GFP larvae were pre-incubated with PI at concentrations of 1, 5 and 50 µg/ml for 30 minutes followed by tail-fin transection. Whole body images of larvae were taken at 6hpi to observe any obvious features of toxicity. Larvae incubated in 1 µg/ml PI showed no visible signs of toxicity whilst those incubated in 5 and 50µg/ml showed clear signs of toxicity as indicated by the appearance of propidium iodide positive lesions in the brain as well as dark regions of tissue (Figure 3.30). From these observations I was able to determine that doses of PI above 5 µg/ml were toxic to larvae following a 6 hour incubation so I decided to use a dose of 1µg/ml PI for live imaging.
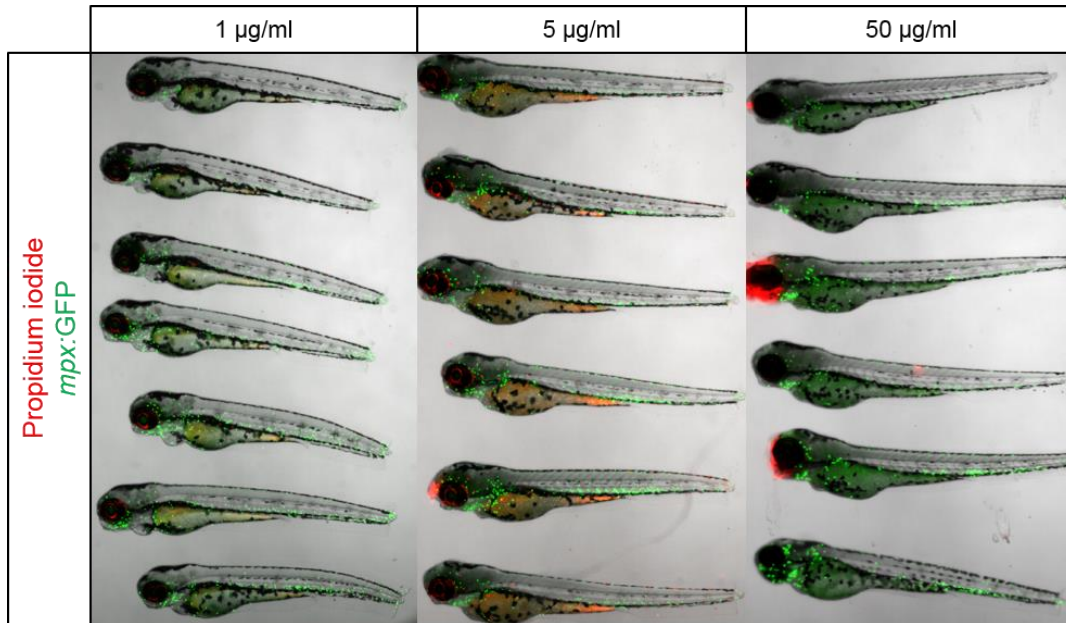
Figure 3.30: Determining a non-toxic dose of propidium iodide for live imaging

3dpf *mpx*:GFP larvae were pre-incubated in propidium iodide at concentrations of 1, 5 and 50 µg/ml for 30 minutes prior to tail fin transection. Whole body images were taken of larvae following a 6 hour incubation in propidium iodide following tail fin transection. Larvae incubated in doses of 5 and 50 µg/ml showed obvious signs of toxicity as indicated by propidium iodide positive lesions present in the brain. This toxicity was not seen in larvae incubated in propidium iodide at 1 µg/ml.

I next observed the ability of propidium iodide at a non-toxic dose to label cells at the wound site following tail-fin transection. 3dpf *mpx:*GFP larvae were pre incubated in propidium iodide (1 µg/ml) before tail-fin transection and images were taken at 30 minutes post injury as described in methods. From these initial experiments a population of cells at the wound site stained positive for PI (Figure 3.31A). This is demonstrated by measuring the intensity through a line drawn at the wound site (Figure 3.31B), suggesting that propidium iodide is able to intercalate into the DNA of a population of cells at the wound edge which have lost their plasma membrane integrity.

After determining a non-toxic dose of propidium iodide which was able to label a population of cells at the wound edge, I next aimed to observe the viability of pioneer neutrophils during the initiation phase.

3dpf m*px:GFP* larvae were pre-incubated in 1µg/ml PI for 20 minutes prior to injury. Larvae were mounted in a 1% agarose solution containing 1µg/ml PI and time lapse imaging was performed from 30 minutes following injury for 4 hours. Larvae with neutrophil swarms at the wound site were selected for further analysis. Single slice image analysis of the pioneer neutrophil in the initiation phase in the frame prior aggregation determined that there was no colocalisation of propidium iodide and GFP signal from the pioneer, indicating that the pioneer is not PI positive prior to swarm formation (Figure 3.32A-B). Single slice analysis of neutrophil swarms during the aggregation phase was also performed and no colocalisation was observed between GFP and propidium iodide (Figure 3.32C).

These data illustrate that pioneer neutrophils have intact plasma membranes during the initiation phase of neutrophil swarming, suggesting that primary or secondary necrosis does not, contrary to reports in the literature, initiate neutrophil swarming.
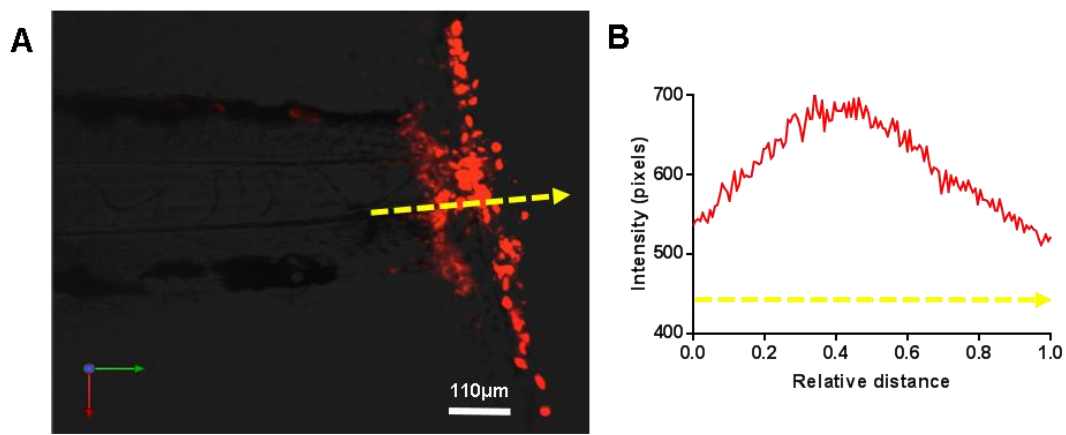
Figure 3.31: Propidium iodide labels a population of cells at the wound site

3dpf *mpx*:GFP larvae were pre-incubated in propidium iodide at 1 µg/ml for 30 minutes prior to tail fin transection. Images were taken of the wound site at 30 minutes post injury. Figure shows a representative example of the population of cells labelled with propidium iodide observed at the wound edge (A). The red fluorescence intensity through a line was measured to demonstrate the intensity of propidium iodide through a line at the wound edge (B).
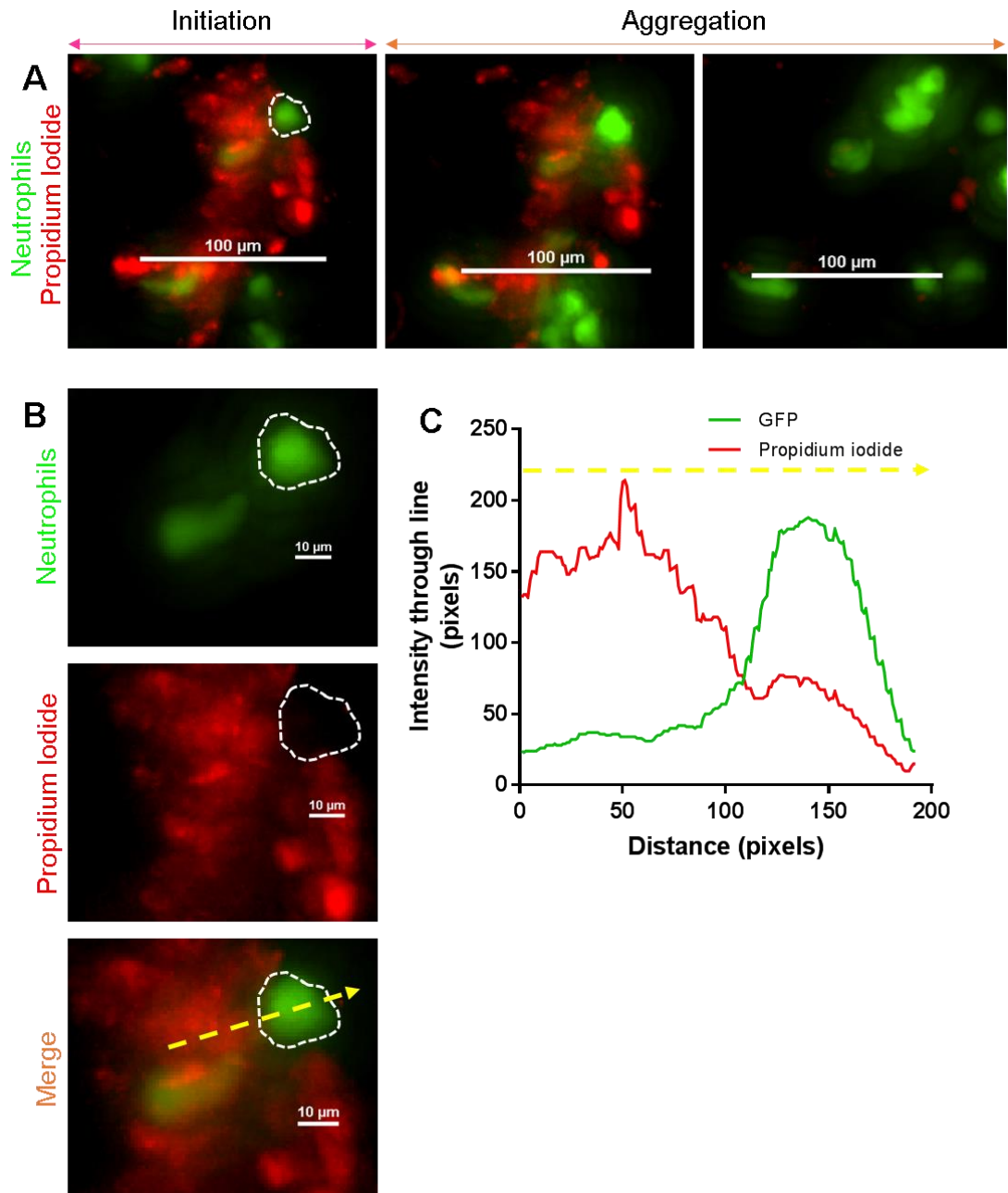
Figure 3.32: Pioneer neutrophils are not propidium iodide positive prior to swarm formation

3dpf *mpx*:GFP larvae were pre-incubated in propidium iodide (PI) at 1 μg/ml for 30 minutes prior to tail fin transection. Time lapse imaging was performed from 30 minutes post injury for 4 hours and larvae with neutrophil swarms at the wound site were identified. Pioneer neutrophil is highlighted by white ROI during the initiation phase. (A). Fluorescence signals from GFP and PI in pioneer neutrophils (white ROI) were analysed on single z-planes to determine any overlap between fluorescence (B). An intensity line profile was measured through pioneer neutrophils in the frame prior to swarm aggregation (yellow line, B). There was no overlap in intensity from the PI signal (red) and the GFP pioneer neutrophil signal (green) (C). Figure shows representative example from 4 experimental repeats.

3.13 Pioneer neutrophils are not undergoing caspase-3 mediated apoptosis prior to swarming

After determining that in zebrafish larvae, pioneer neutrophils are not propidium iodide positive, I next aimed to investigate other modes of cell death which could initiate swarming through cell death signalling. The rounded morphology of pioneer neutrophils observed on average for half an hour suggests that pioneer neutrophils could be undergoing a programmed cell death. Caspase-3 mediated neutrophil apoptosis can be observed using our *Tg(mpx:FRET)sh237* zebrafish line (Robertson et al., 2016). This zebrafish line expresses a genetically encoded FRET biosensor consisting of a caspase-3 cleavable DEVD sequence flanked by a CFP YFP pair, under the neutrophil specific *mpx* promoter. Förster resonance energy transfer (FRET) is a distance-dependent transfer of energy from an excited donor fluorophore to a neighbouring acceptor fluorophore. Emission from the acceptor fluorophore can be detected following excitation of the donor fluorophore, only when the pair are within the Förster radius (Förster, 1965). The proximity of the CFP and YFP when flanking an intact DEVD sequence is within the Förster radius such that FRET occurs following excitation of the donor CFP fluorophore. Cleavage of the DEVD sequence by caspase-3 during apoptosis results in the proximity of the CFP YFP pair falling outside of the Förster radius, and a subsequent loss of FRET, providing a read out of caspase-3 mediated apoptosis in neutrophils. Of the numerous methods of performing FRET, a sensitised emission of acceptor FRET (NFRET) method was used to detect apoptosis in neutrophils (Xia and Liu, 2001).

To observe neutrophil apoptosis in the context of pioneer cells initiating swarming, 3dpf *mpx:FRET* larvae were injured and FRET imaging was performed as described in methods. Normalised FRET (NFRET) values were calculated for each time point to account for bleed through and fluorophore cross talk as described in methods.

Following the data acquisition period and generation of an NFRET channel, larvae with neutrophil swarms at the wound site were selected from the population for further investigation. Pioneer neutrophils were identified and visualised during the scouting and initiation phases. During these experiments, an NFRET signal was detected in all pioneer neutrophils during both the scouting and initiation phases (Figure 3.33). Conversely, neutrophils which lost their NFRET signal did not initiate swarm formation at least in the observed time window (Figure 3.34).

Together these observations demonstrate that pioneer neutrophils are not undergoing caspase-3 dependent apoptosis prior to swarm initiation.
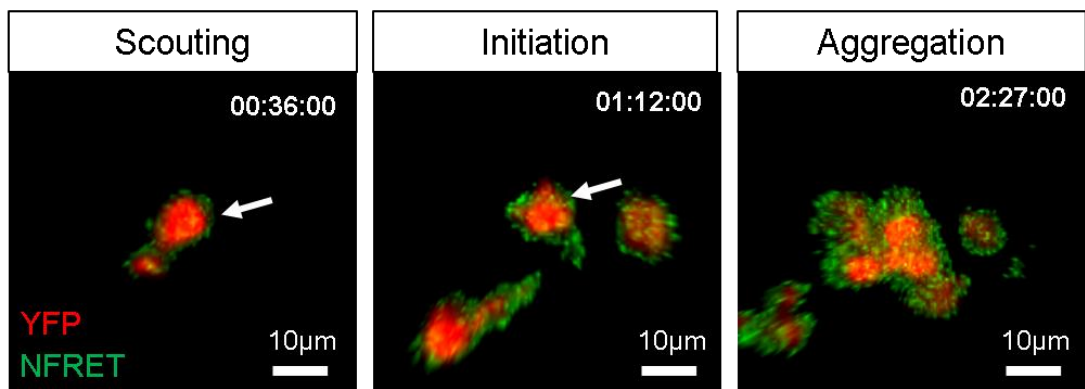
Figure 3.33: Pioneer neutrophils are not undergoing caspase-3 mediated apoptosis

3dpf *mpx:FRET* larvae were injured and time lapse imaging was performed from 30 minutes post injury for 5 hours. Time courses containing neutrophil swarms were selected for analysis and a normalised FRET (NFRET) channel was created for every time point. Figure shows a representative example of a pioneer neutrophil during the scouting and initiation phases (white arrow) with its NFRET signal intact. This was observed in 100% of neutrophil swarm initiation events. Figure shows representative image of 4 pioneer neutrophils from 4 experimental repeats.
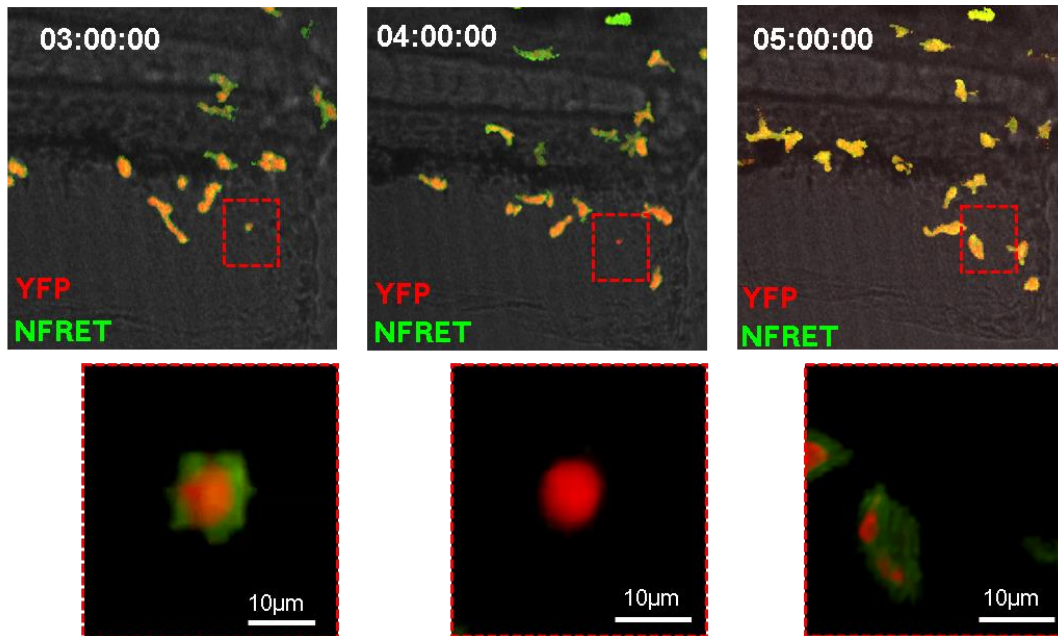
Figure 3.34: Neutrophils which lose their NFRET signal do not initiate swarming

3dpf *mpx:FRET* larvae were injured and time lapse imaging was performed from 30 minutes post injury for 5 hours. Time courses containing neutrophil swarms were selected for analysis and a normalised FRET (NFRET) channel was created for every time point. Figure shows a representative example of a neutrophil at the wound site losing its NFRET signal at 4hpi. No directed migration to this neutrophil was observed following loss of NFRET, at least in the time period observed Figure shows representative image of 4 pioneer neutrophils from 4 experimental repeats.

3.14 A neutrophil specific histone2a reporter to visualise neutrophil extracellular trap formation

Recently neutrophil extracellular trap formation has been implicated in neutrophil swarming in response to aluminium hydroxide injection (Stephen et al., 2017). I hypothesised that cell death by NETosis could provide the chemoattractant signals required to initiate neutrophil swarming. *In vivo* imaging of NETs has not been performed extensively, so to test this hypothesis I generated a reporter of NETosis.

To observe extracellular trap formation by neutrophils, I have generated a transgenic line expressing an mCherry tagged histone 2a construct (made by Dr. Katherine Henry using gateway cloning) under the neutrophil specific lyz promoter. The construct was prepared by transformation from plasmid DNA followed by DNA purification steps as described in methods, prior to injection into larvae. I injected the construct into the *mpx:GFP* background and raised larvae to adulthood from the F2 generation to produce a stable line in a neutrophil reporter background as described in methods.

The stable line is currently growing up for experiments on the F2 generation in the future. Preliminary observations of larvae from the F1 generation were performed. 3dpf *lyz*:histone2a.mCherry larvae from the F1 generation were imaged in the CHT region as described in methods. The histone2a.mCherry transgene was found within neutrophils in the CHT of larvae, (Figure 3.35). Tail-fin transection of 3dpf F1 *lyz*:histone2a.mCherry larvae was performed and recruitment of double labelled neutrophils to the tail-fin was observed in all larvae imaged (Figure 3.36, Movie 3.13**).** These initial observations suggest that the *Tg(lyz:histone2a.mCherry)* line will be useful for visualising NETosis *in vivo* in real time, where the histone localisation in pioneer neutrophils will be studied during the initiation phase of the swarming response.
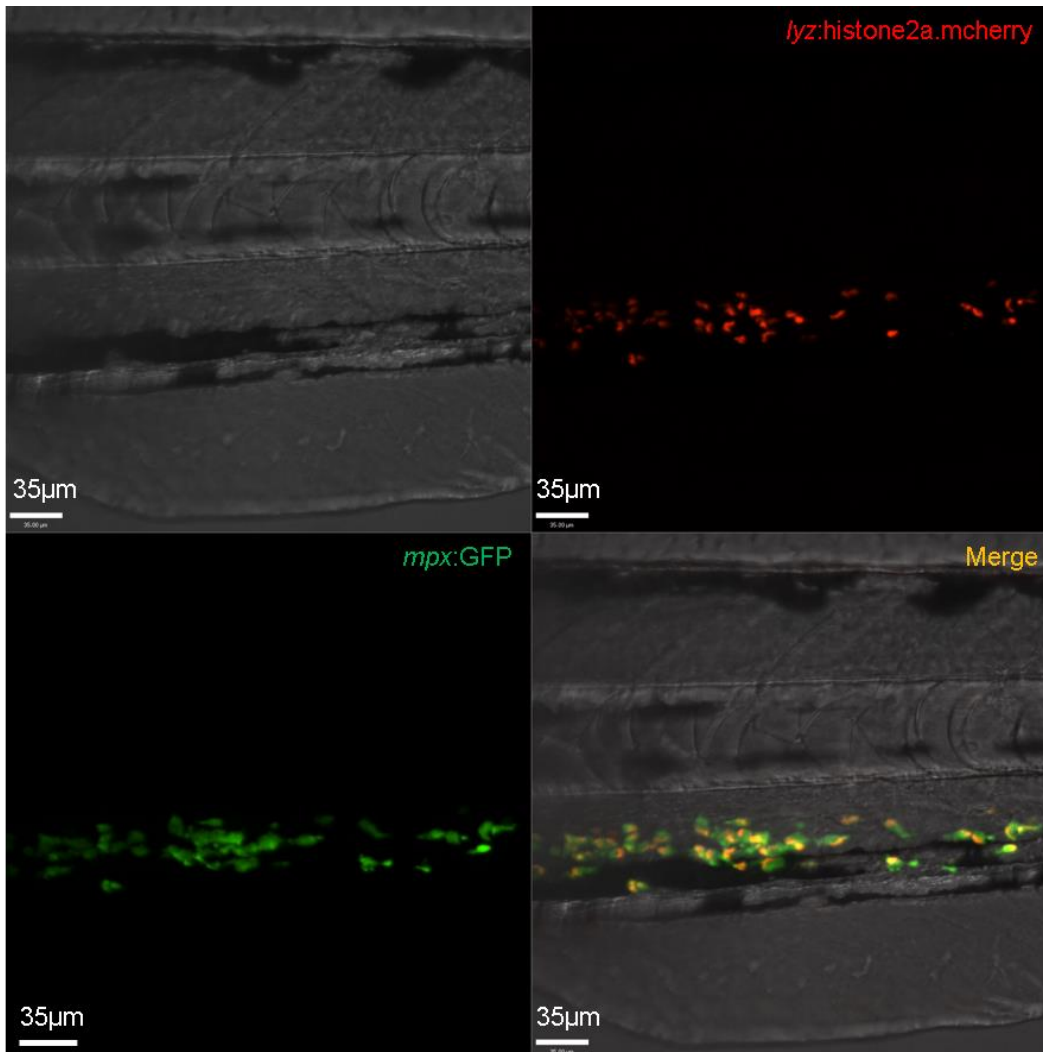
Figure 3.35: A histone2a.mCherry constructs labels the nucleus of neutrophils

A histone2a.mcherry construct was injected into *mpx*:GFP embryos at the 1 cell stage. Larvae were screened for double positive expression of both transgenes in the CHT at 3dpf. F0 larvae were grown to adulthood and founders which transmitted the transgene to their gametes were identified by the presence of offspring with double labelling in the CHT. These F1 offspring are being raised to adulthood. Figure shows a representative image taken of the CHT region in 3dpf larvae from the F1 generation. F1 larvae have the nucleus of their neutrophils labelled with mCherry.
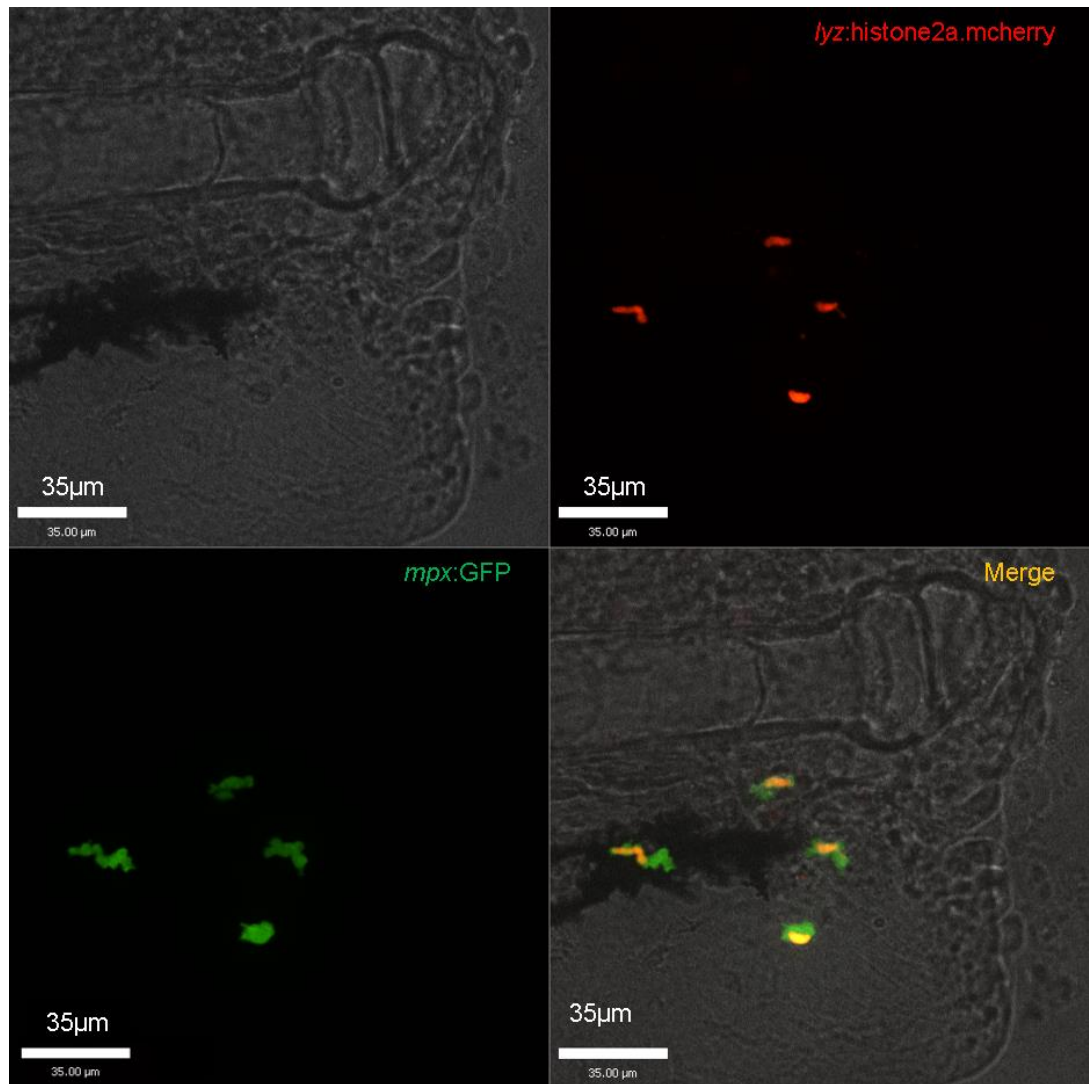
Figure 3.36: Histone.mCherry labelled neutrophls recruit to inflammatory sites

A histone2a.mcherry construct was injected into *mpx*:GFP embryos at the 1 cell stage. Larvae were screened for double positive expression of both transgenes in the CHT at 3dpf. F0 larvae were grown to adulthood and founders which transmitted the transgene to their gametes were identified by the presence of offspring with double labelling in the CHT. These F1 offspring are being raised to adulthood. Preliminary investigations were performed on F1 offspring, which were injured at 3dpf. Neutrophil recruitment to the wound site was observed at 2hpi in all larvae (*n=4 larvae from one experimental repeat*).

3.15 Conclusions and chapter discussion

In this chapter I have described a novel neutrophil behaviour which has not been previously reported in response to tissue injury in zebrafish. By studying the migratory behaviours of neutrophils at sites of inflammation, I have characterised the neutrophil swarming response. Here, I demonstrate that neutrophil swarming in zebrafish shares characteristic features with the swarming response reported in human and murine neutrophils. I have identified that neutrophil swarming in zebrafish is initiated by an individual 'pioneer' neutrophil which exhibits non-characteristic behaviour at the wound site. My work has begun to dissect the cell death signalling mechanisms previously reported to initiate the swarming response. I have identified that, contrary to evidence in murine models, neutrophil swarming in zebrafish is not initiated by propidium iodide positive cells. I have investigated alternative cell death pathways which could be involved in neutrophil swarm initiation and have collaboratively generated a new tool to visualise NETosis *in vivo* in real-time. I have provided the first evidence of neutrophil swarming in an endogenous and physiologically relevant model, where neutrophils are attracted to chemoattractants released at the wound site but migrate towards additional chemoattractants to form swarms at the wound site. Most notably the zebrafish provides a new and exciting platform to study the initiation of the swarming response which thus far has proved challenging to observe in other models.

3.15.1 Neutrophil swarming is observed at the wound site in zebrafish larvae

The swarming response has been studied in only a handful of reports thus far. Early reports of neutrophil cluster formation identified a multi-phase response leading to the aggregation of neutrophils at sites of infection (Chtanova et al., 2008; Peters et al., 2008), focal tissue injury (Lämmermann et al., 2013), and *in vitro* around zymosan coated beads (Reátegui et al., 2017). These studies identify that neutrophil swarming is a recognised phenomenon which is conserved between species. Neutrophil swarming can be studied using many systems and models, however more physiologically relevant models are required to characterise all aspects of this novel neutrophil behaviour.

The zebrafish immune system shares many features with the mammalian immune system, and the response of neutrophils to tissue injury induced by tail-fin transection of larvae has similar kinetics to that reported in mammalian inflammatory response (Renshaw and Loynes, 2006). Analysis of neutrophil number at the wound site has been used as an assay to study inflammation by many research groups and accurately provides a read-out of the neutrophilic component of the inflammatory response to tissue injury (de Oliveira et al., 2013; Renshaw and Loynes, 2006; Tauzin et al., 2014). This inflammatory response can be manipulated pharmacologically and genetically to dissect the mechanisms governing neutrophil migration to and removal from the wound site (Elks et al., 2011; Powell et al., 2017; Robertson et al., 2014). Tail-fin wounding of zebrafish larvae using scalpel blades has been used as a method to induce an inflammatory response by many research groups within the zebrafish community (de Oliveira et al., 2013; Elks et al., 2011; Renshaw and Loynes, 2006). Performing a time course to quantify the neutrophilic inflammatory response to tail-fin transection identified that the response induced in my assays is consistent to published reports from our group (Renshaw and Loynes, 2006). These data demonstrate that, in keeping with published reports, neutrophil recruitment can be studied within the first 6 hours following tail-fin transection in zebrafish larvae.

Neutrophil swarming, in response to non-sterile tissue injury, has not been reported in zebrafish larvae. This study provides the first evidence of endogenous neutrophil aggregates at the wound site during the recruitment phase, which were reminiscent of those reported at site of focal tissue damage and infection in mice and zebrafish (Chtanova et al., 2008; Lämmermann et al., 2013). Caution was taken before referring to this behaviour as neutrophil swarming, since there currently exist no guidelines to accurately define neutrophil swarms. Neutrophil swarms are currently recognised by the field as the formation of large neutrophil aggregates which form following stages of highly directed neutrophil recruitment.

3.15.2 Characterisation of the neutrophil swarming response in zebrafish larvae

Initial attempts to characterise neutrophil swarming using quantifiable parameters identified that swarming is an incredibly dynamic process which varies between larvae. I developed an assay based on a feature common to all swarms. I was able to identify larvae where neutrophil swarming behaviour occurred at the wound site from time courses, based on the area of neutrophils detected at the wound site. This work provides a non-biased read out of neutrophil swarming at the wound site and could be used in future experiments as a robust method to detect swarming behaviour within a population of larvae.

3.15.2.1 Multiple swarms can form at the wound site and neutrophils migrate between competing swarms

Due to the limited number of studies of neutrophil swarming, there currently exists no evidence to describe the number of neutrophil swarms which can form at an injury site. The experiments performed in this chapter identify that, whilst swarming is not seen in all larvae, in those where it does occur, swarms can be observed in multiple regions of the tail-fin at one time. My data provides insight into the migratory behaviours of neutrophils which participate in individual swarms in specific tissue contexts within one wound site, and illustrates that the tissue context required to initiate a swarm can occur at multiple locations in one tail-fin.

There currently exists no primary *in vivo* evidence of neutrophils migrating between competing neutrophil swarms, however it is suggested that this is a commonly observed phenomenon based on unpublished findings (Lämmermann, 2015). *In vitro* human neutrophils migrate between competing swarms when they occur within close enough proximity (Reátegui et al., 2017). The observation that neutrophils migrate between competing swarms at the tail-fin region in zebrafish larvae provides the first primary *in vivo* evidence that neutrophils migrate between competing gradients generated by neutrophil swarms. This is interesting because it illustrates that these neutrophils are able to detect and prioritise additional gradients from a new source. I propose that for this to happen the signalling pathways which maintain neutrophils in their initial clusters must become interrupted. This could be due to cell desensitisation by chemokine receptor downregulation, a reduction in the production of the attractants maintaining neutrophils in clusters, or downregulation of integrin receptor expression. On the contrary neutrophil migration between swarms could occur as a result of random neutrophil migration. These observations also suggest that the swarming response I observed in zebrafish shared features of that observed in mice. The conservation of

these neutrophil migratory behaviours between different species and models suggests a degree of conservation across species and evolution.

3.15.2.2 Swarms form at different tail-fin injuries

This size of the initial tissue damage is proposed to be a factor which shapes the neutrophil swarming response although this has not been experimentally confirmed (Kienle and Lämmermann, 2016). I demonstrated using a variety of tail-fin transection methods, that neutrophil swarms form at all inflammatory sites regardless of the initiating stimulus. Unfortunately, due to time constraints I did not manage to quantify the frequency with which neutrophil swarms were observed in response to these different tissue injuries. This would be interesting to do in future to determine whether the size of the inflammatory stimulus contributes to the frequency with which swarms are observed within a population, or the phenotype of the swarming response.

3.15.2.3 Dynamics of neutrophil swarming in zebrafish larvae

The studies that have addressed the sequential stages of neutrophil swarming at sites of sterile tissue injury have identified a common multistep attraction cascade. First is the initial chemotaxis of neutrophils close to the damage (scouting), followed by the amplified chemotaxis of neutrophils distal to the wound site (amplification), leading to neutrophil clustering (stabilisation) (Ng et al., 2011). More recently, this has been adapted to the five-stage model currently accepted in the field, which describes the initiation of swarming through, 1st tissue injury, and $2^{nd.}$ signal amplification by cell death. This is followed by a 3rd stage of amplification through intercellular LTB_4 relay signalling between neutrophils. The remodelling of tissue underlying the aggregating swarm occurs during the 4th phase, and the 5th stage describes swarm resolution (Lämmermann et al., 2013). These sequential phases describe neutrophil swarming in intravenous/ intradermal neutrophil transfer models, however these assays circumvent the recruitment of endogenous neutrophils from the circulation and do not demonstrate the neutrophil swarming response in a truly physiological setting. Endogenous neutrophil recruitment to swarms has been observed in mice, however the precise phases of this response have not been described (Ng et al., 2011). Further studies are required to study the sequential phases of the endogenous neutrophil swarming response in more physiological settings. By imaging neutrophil recruitment to tail-fin transection in zebrafish larvae I identified the migration of endogenous neutrophils to the wound site resulting, in some cases, in the formation of neutrophil clusters.

Neutrophil migration to the wound site occurred in distinct stages, which appear to be comparable in some respects to the phases described in mouse models (Ng et al., 2011). I observed the initial recruitment of few neutrophils from the hematopoietic niche which

I termed the scouting phase, based on the migration of a few neutrophils proximal to the wound site which switch from random motility to chemotactic movement towards the wound within minutes (Lämmermann, 2015; Ng et al., 2011). The initiation of swarms by pioneer neutrophils is a novel finding which is perhaps similar in function to the first wave of amplification by cell death reported in the mouse model (Lämmermann, 2015). During this stage the migratory behaviours of the neutrophil population as a whole may not change, but the behaviour of the swarm initiating pioneer neutrophil is markedly altered at the wound site. I propose that the initiation stage is a key component of the swarming response and the zebrafish is a good model to study this stage because it can be visualised in its entirety in high resolution. I next observed the migration of neutrophils to form neutrophil clusters which I termed the aggregation phase, due to the presence of aggregating neutrophils and the similarities of this phase to the aggregation phase reported in mice. The aggregation phase in zebrafish encapsulates the amplified recruitment of neutrophils to the wound site as well as their aggregation in clusters. These stages are summarised in Figure 3.37, where I have speculated on the potential signals which could modulate neutrophil migration at different stages of the swarm response.
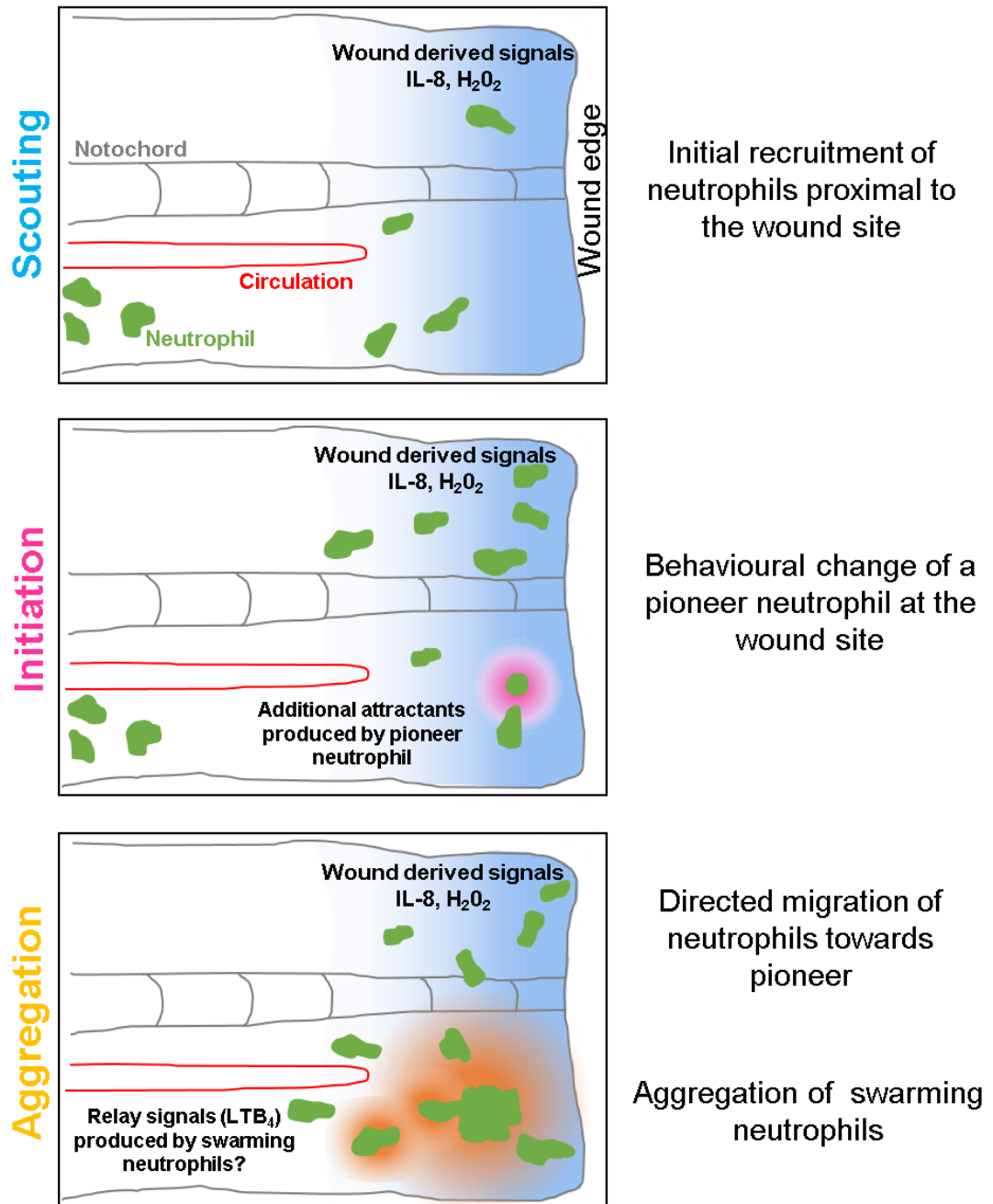
Figure 3.37 Graphical schematic of the neutrophil swarming response in zebrafish

Proposed schematic of the swarming response based on the migratory behaviours of neutrophils observed in response to tail fin transection. Following tail fin transection neutrophils proximal to the wound site migrate towards wound-derived chemoattractants. Swarms are initiated by 'pioneer' neutrophils which change behaviour at the wound site. These pioneer neutrophils release additional gradients which attract neutrophils, resulting in the directed migration of a population of neutrophils to the pioneer neutrophil. These neutrophils aggregate at the wound site where further recruitment of neutrophils to the swarm is then observed.

In the zebrafish, it is not clear whether these stages can be distinguished as I have thus far not identified measurable parameters. In mice the amplification phase is distinguished by a second 'wave' of neutrophil migration which can be clearly identified when looking at the neutrophil tracks (Lämmermann et al., 2013). Tracking of the migration of the whole population of neutrophils in the tail-fin may be useful to determine whether a similar migratory signature could be identified within the aggregation phase. In terms of the molecular signals which govern neutrophil swarming in zebrafish, I have not yet investigated the role of LTB_4 in relay signaling during the aggregation phase. The limitations of studying the endogenous neutrophil swarming response mean that inhibition of signaling molecules involved in the early recruitment of neutrophils is not possible using this model. Attempts during this study to inhibit the LTB4 receptors were performed (data not shown), however the global effect of LTB4 inhibition using BLT1 and 2 inhibitors was the reduction in neutrophil recruitment to the wound site in general, such that the scouting phase was affected and the initiation and aggregation phases could not be studied. This problem is circumvented in the mouse model where neutrophils are directly injected into the ear pinna of mice, such that neutrophil extravasation and early recruitment are bypassed. In future the role for LTB_4 relay signaling in modulating the swarming response in zebrafish should be investigated. Administration of BLT1 and BLT2 inhibitors to larvae where a swarming response has already been established should be performed, and using the assays to quantify swarm phenotype or tracking of the whole neutrophil population in the tail-fin, determine if inhibition of LTB4 signaling could affect the aggregation phase.

I propose that if I had visualised neutrophil swarming during the resolution phase of inflammation, swarm resolution could be studied. This would be interesting to for future experiments to elucidate some of the mechanisms which govern neutrophil stability in clusters, some of which have been suggested based on *in vitro* findings (Reátegui et al., 2017). CRISPRi technology would be useful to dissect some of the mechanisms of swarm resolution by knocking out receptors of interest specifically in neutrophils.

I took advantage of the resolution available when imaging neutrophil recruitment to tail-fin injury, to track the behaviour of swarm-initiating-pioneer-neutrophils and compare their behaviour to neutrophils migrating within the same tissue microenvironment during the same period. These data demonstrate that swarm-initiating pioneer neutrophils at the wound site have reduced motility and a rounded morphology compared to the neutrophils which do not initiate swarms. I confirmed that this was a phenotype specific to swarm initiating neutrophils, which migrate to the wound site with similar behaviour to non-pioneer neutrophils. The limitations of these experiments are

the low number of pioneer neutrophils observed which make statistical analysis challenging. I propose that the difference in pioneer neutrophil migratory behaviours is striking, such that the few examples I have are statistically significant.

I performed power calculations for each set of tracking experiments to determine if the data I generated has statistical power (summarised in table 3.1).

For experiments in figure 3.18 where the difference between neutrophil behaviours is very small, the number of repeats required to see a significant difference is not biologically plausible. I therefore propose that the difference is small and not different. For figure 3.16 I propose that my experiments are underpowered and that it will be worth repeating these experiments up get n numbers to around 15, which would be enough for 80% confidence. For experiments in figures 3.17 where the difference is large, an n of 5 is enough to be 90% confident for speed and displacement, although to see significance in meandering index I could repeat the experiment a few more times. I conclude that repeating the experiments so that I have 10 pioneer neutrophils would enable to me to be 90% confident whilst being plausible in terms of repeating experiments.

Experiment	Parameters	N number	
		80% confidence	90% confidence
Figure 3.15	Meandering index	36	49
	Speed	17	23
	Displacement	7	10
	Circularity index	9	12
Figure 3.16	Meandering index	12	16
	Speed	15	20
	Displacement	155	212
Figure 3.17	Meandering index	6	9
	Speed	3	4
	Displacement	2	3
Figure 3.18	Meandering index	271	371
	Speed	54	73
	Displacement	77	105

Table 3.1 Power calculations for tracking experiments. The equation n= 2 x k x (d^2/sd^2) where n= number of experiments, d= difference and sd= standard deviation was used to calculate the number of repeats required to be 80% (k=7.9) or 90% (k=10.8) confident.

Together my work investigating the dynamics of neutrophil swarming in the zebrafish model has identified that swarming occurs in a multi-step cascade which is similar in parts to that described in other models. I have identified that the zebrafish can be used as a model to study the early initiation of neutrophil swarming, which has thus far not been possible due to limitations in the mouse models used to study swarming. This is promising for determining the factors which govern neutrophil swarm initiation using the zebrafish model.

3.15.2.4 How often do neutrophils swarm at the wound site?

The most recent review of neutrophil swarming: "Neutrophil swarming: an essential process of the tissue response" implies that the swarming response is an essential requisite of the neutrophil response to tissue injury (Kienle and Lämmermann, 2016). I propose that making this claim based on few studies of the swarming response in models with severe limitations is a good example of 'the problem of extrapolation in basic research' (Baetu, 2016). It is assumed from the published studies that neutrophil swarms are observed in 100% of tissue injuries or infections, although the data do not exist to confirm otherwise. The models used to study the swarming response share a common feature: the inflammatory stimuli (focal tissue damage, zymosan bead, pathogen for example) generates chemotactic gradients from a focal point. Chemoattractants released from these focal points diverge outwards from a common centre, producing a gradient which diffuses outwards radially from the source. In these models the secondary gradients produced by neutrophils diffuse with the same spatial dynamics as primary gradients released at the inflammatory source. Perhaps, in these models, the release of a combination of gradients from the same focal centre may promote the formation of neutrophil swarms. Whilst there are some physiological settings in which chemotactic gradients would diverge from a focal point (insect bite, pathogenic infection) the need to study swarming in a model where neutrophils encounter chemotactic gradients from multiple sources is required. The experiments I performed have provided the first study into the frequency with which endogenous neutrophil swarming is observed at a linear wound where chemotactic gradients diffuse into the tissue along the length of the entire wound edge. Interestingly, neutrophil swarms were only observed in a proportion of larvae. I propose that the swarming response is only observed in a proportion of larvae due to the competing gradients released along the linear wound edge. These assays are not performed in sterile conditions so the intrusion of pathogens into the tissue at the wound site is also a possibility, where pathogen derived chemoattractant gradients could induce the swarming response. Perhaps the

precise tissue context required for neutrophils to swarm depends on spatial distribution of the complex array of primary and secondary chemotactic gradients produced at the wound site. Here, I provide evidence that endogenous neutrophil swarming in a physiological setting is only observed in a population of larvae, suggesting that contrary to current claims, the neutrophil swarming response is a dispensable component of the inflammatory response.

3.15.2.5 Quantification of swarm phenotypes

Large dense neutrophil clusters consisting of hundreds to thousands of neutrophils have been observed at a site of focal tissue injury (Lämmermann et al., 2013), whilst smaller clusters persisting for less time have been reported at sites of pathogenic infection (Chtanova et al., 2008; Lämmermann et al., 2013; Peters et al., 2008). It is proposed based on these observations that large persistent neutrophil swarms form at sites of tissue damage whereas smaller more transient neutrophil swarms form in response to diffuse pathogens distributed in tissues (Kienle and Lämmermann, 2016). Arguably, it is difficult from the evidence provided to determine whether this is correct. The differences in experimental settings and models these swarm phenotypes have been observed in mean that this hypothesis has not been tested under experimentally controlled conditions. Whilst this is the case, the hypothesis that transient swarms form at sites of diffuse pathogens in tissues and persistent swarms form at sites of large tissue damage is sensible. My experiments provide examples of both persistent and transient swarming phenotypes using the same experimental conditions. Whilst I observed both persistent and swarm phenotypes during my experiments, the frequency with which transient swarms occurred was incredibly low, suggesting that perhaps sites of injury are more likely to induce persisting neutrophil swarms. The experiments in this study were not performed under sterile conditions, so I propose that the transient swarms observed at the wound site could be induced by pathogens which have infiltrated the tissue, whilst persistent swarms could be induced by local host generated gradients at the wound site, in keeping with the suggestions from the literature. Further studies to increase the number of larvae imaged and the number of transient swarms observed would be useful to gain more insight into the frequency with which the two phenotypes occurred within a larger population. I propose that the zebrafish could be a tractable model to study neutrophil swarming in a dual model of injury and infection to investigate the swarm phenotypes observed in response to infection and tissue injury in the same experimental conditions (Ellett et al., 2015).

Assays to measure the area of neutrophil swarms and the number of neutrophils in a swarm have been used as measurable parameters to study swarm phenotype (Ng et al.,

2011; Reátegui et al., 2017). I propose that the zebrafish may provide an excellent tool to elucidate the mechanisms governing the aggregation and resolution of swarms in future. These studies require an assay to quantify swarming phenotype during the aggregation phase, so I attempted to measure the parameters measured *in vitro* in the zebrafish model. The phenotype of the swarms observed in my experiments were comparable to those reported *in vitro* (Reátegui et al., 2017). These assays provide some of the first examples of methods to measure the endogenous swarming response *in vivo*. In terms of future work, I propose that of these methods to quantify swarm phenotypes, swarm area could be an accurate assay for use in experiments to study factors which may regulate the aggregation and resolution phases of swarming.

3.15.2.6 Investigating the spatio-temporal dynamics of the swarming response

The spatio-temporal dynamics of neutrophil swarming in mouse models are not representative of a physiological swarming response, as these assays circumvent the initial recruitment of endogenous neutrophils from the blood stream (Lämmermann et al., 2013). I investigated the temporal component of neutrophil swarming to determine how long following tissue injury the swarming response occurs, providing one of the first reports of the temporal dynamics of swarming *in vivo*. My data show that swarming is variable in timings between larvae, although the majority of swarms form within the first 2 hours following injury. These findings suggest that the tissue context required to induce swarms in the majority of cases occurs relatively rapidly following injury. From these experiments I proposed that tissue factors released at the beginning of the inflammatory response were responsible for initiating swarms. The identification that neutrophils could initiate a swarm later on in the inflammatory response provides evidence that the tissue context required for swarming can occur later in the inflammatory response. In future I would like to study the aggregation phase to determine how long neutrophil swarms persist for at the wound site, something which was not possible to do from the experiments reported in this chapter due to the length of the time courses.

Evidence from the literature as well as my own findings suggest that tissue context is a factor which determines whether neutrophils swarm at inflammatory sites (Kienle and Lämmermann, 2016). I sought to determine whether there was a common tissue location in which pioneer neutrophils underwent their phenotypic switch prior to the aggregation of neutrophils. My data demonstrates that neutrophil swarming is initiated within a small region close to the wound edge, providing evidence to suggest that the tissue environment within this region at the wound edge provides the context needed for swarm initiation. This is the first data to illustrate the spatial aspect of endogenous neutrophil swarming in relation to the wound edge and provides the first description of

the position where neutrophil swarms form. Together these investigations provide spatio-temporal information about the swarming response and suggest that a tissue context within 50μm of the wound edge, which is generated within 2 hours following injury, is important in swarm initiation. Based on this spatio-temporal evidence, I propose pioneer neutrophils encounter an unfavourable environment at the wound site which induces a cell death programme. Cell death signalling could then amplify the recruitment of the first neutrophils to form a swarm followed by the rapid influx of many more neutrophils.

The recruitment of immune cells to inflammatory sites in zebrafish is modulated by the establishment of a variety of signal gradients by cells at the wound site (Medzhitov, 2008). Following tail-fin transection in zebrafish larvae a hydrogen peroxide gradient is produced by epithelial cells at the wound site within minutes following injury. This gradient diffuses up to 200μm into the tail-fin epithelium, peaking in concentration at around 20 minutes post injury and persisting for over 99 minutes post injury (Niethammer et al., 2009a). Hydrogen peroxide induces programmed cell death in eosinophils (Reis et al., 2015) as well as programmed and necrotic cell death in human retinal pigment epithelial cell lines (Kim et al., 2003).

Ratiometric imaging is used to measure H_2O_2 concentration at the wound edge using a genetically encoded biosensor, HyPer (Niethammer et al., 2009). Our group developed a transgenic zebrafish line using gateway cloning to drive HyPer under the *lyz* promoter, such that the expression was constrained to neutrophils (Renshaw group, unpublished). HyPer eliminates some of the issues associated with using chemically synthesised sensitive fluorescent dyes to measure hydrogen peroxide production (Pase et al., 2012). Using ratiometric imaging to measure H_2O_2 concentration provides an internally controlled parameter which is normalised to artefacts such as uneven protein concentrations in the cell, tissue thickness and cell movement. I demonstrated that the HyPer reporter line detected changes in hydrogen peroxide concentration. Due to time constraints, these experiments were performed only once as proof-of-principle, so in future I would like to repeat these experiments to generate sufficient data to perform statistical analysis. It would also be important to negatively control this experiment by inhibiting hydrogen peroxide production to determine if the HyPer ratio could also be reduced. The enzyme dual oxidase (duox) enzyme catalyses hydrogen peroxide production in zebrafish, so it would be interesting to repeat these experiments alongside a chemical inhibitor of duox, such as DPI (Niethammer et al., 2009b). Additional control experiments to determine that changes in HyPer ratio are attributed only to fluctuations in H_2O_2 concentration and not variation in light intensity from the source to the camera,

or induced by microscopy, will also be performed as recommended (Pase et al., 2012). I performed preliminary tail-fin transection experiments where I observed neutrophil swarms at the wound site, and generated a protocol for ratiometric imaging of HyPer in neutrophils. The next step is to visualise the recruitment of pioneer and non-pioneer neutrophils in *lyz*:HyPer larvae.

Hydrogen peroxide readily diffuses in tissues and can cross cell membranes, meaning that HyPer senses both intracellular production of H_2O_2 as well as extracellular H_2O_2 which has diffused into the neutrophil. This may make the source of hydrogen peroxide detected by HyPer difficult to determine. Perhaps it would be useful to combine data using the *lyz*:HyPer reporter with experiments using ubiquitously expressed HyPer (Niethammer et al., 2009b) to observe the tissue scale gradient of hydrogen peroxide at the precise location at the wound site where pioneer neutrophils change their morphology. In future these experiments using HyPer will provide valuable insight into the role of hydrogen peroxide concentration in swarm initiation.

3.16 Investigating cell death in the context of swarm initiation

The functional dissection of the early signals which modulate early recruitment of neutrophils is technically challenging in mice models. Following tissue injury in the ear dermis of mice, neutrophils close to the injury site migrate towards chemotactic factors released at the wound site. The death of a few neutrophils at the damage site in mice correlates with the second wave of neutrophil recruitment, although other tissue events cannot be ruled out (Lämmermann et al., 2013). Based on this evidence, I hypothesised that pioneer neutrophils would become propidium iodide positive at the wound site prior to swarm formation.

3.16.1 Pioneer neutrophils are not propidium iodide positive

There are no reports, to the author's knowledge, where propidium iodide has been used *in vivo* for periods of live imaging. I developed a method for *in vivo* imaging of propidium iodide in zebrafish larvae, which is useful for the zebrafish research community. I determined an appropriate dose to use for time lapse imaging of zebrafish based on the concentration used for imaging of fixed tissue in zebrafish larvae (Okuthe, 2013). This dose labelled cells at the wound edge without inducing signs of toxicity after a 6 hours incubation. Based on the extensive work I performed observing neutrophil recruitment to the tail-fin in zebrafish larvae, recruitment to the wound site appeared to be reduced in larvae following propidium iodide incubation, although I did not confirm this observation experimentally. Consequently, I observed relatively few neutrophil swarms during these assays. Of the neutrophil swarms which I did observe, 100% of pioneer

neutrophils were not labelled with propidium iodide. I confirmed that propidium iodide was able to label cells in the tail-fin, as cells deeper into the tail-fin tissue were positively labelled with propidium iodide. In future it would be useful to repeat these assays using a second cell-viability stain such as SYTO probes which may be more appropriate for live imaging of zebrafish larvae (Wlodkowic et al., 2009).

This striking observation is potentially exciting as it challenges the current hypothesis that propidium iodide positive pioneer neutrophils induce the first amplification stage of the swarming response (Lämmermann et al., 2013). Further work to confirm these findings in other systems is required. It cannot be ruled out that neutrophil swarms in zebrafish are initiated by different tissue factors than those in mice, although I propose that the limitations associated with the mouse models of swarming mean that swarm initiation is not fully understood in any context. Perhaps the advantages of the zebrafish model could provide a novel insight into swarm initiation and identify the precise mechanisms which govern neutrophil swarming.

3.16.2 Pioneer neutrophils are not undergoing caspase-3 mediated apoptosis

The morphological changes of pioneer neutrophils prior to neutrophil swarming suggest that a programmed cell death mechanism initiates the neutrophil swarming response. Apoptotic cells release soluble "find me" signals which attract phagocytes to the site of cell death within a tissue (Gregory, 2009). I hypothesised that caspase-3 mediated apoptosis could contribute to the morphological features observed in pioneer neutrophils, and the release of soluble mediators by these cells could provide the cell death signals which are proposed to initiate the swarming response.

I utilised the tools available to study programmed cell death in zebrafish larvae. A transgenic zebrafish reporter to study caspase-3 mediated apoptosis has been developed for use in *in vivo* imaging of neutrophil apoptosis during the inflammatory response (Robertson et al., 2016). There are important factors to consider when using fluorescent proteins for FRET studies. The use of FRET pairs with spectrally overlapping properties has drawbacks including the reciprocal excitation of both donor and acceptor fluorophores by the excitation wavelength of the other fluorophore, as well as the bleed-through of fluorescence emission between channels. There are multiple methods to obtain a true FRET signal. The NFRET method of FRET calculates a normalised FRET value by considering the contribution of fluorophore background and bleed through in FRET channel emission, as well as reciprocal cross talk of the fluorophores and local concentration of the fluorophore (Xia and Liu, 2001). Imaging of a HeLa cells transfected with CFP or YFP alone enabled the calculation of FRET constants which contributed to

the NFRET value to correct for bleed through and cross talk of the overlapping fluorophores. From my experiments it was clear that pioneer neutrophils did not lose their NFRET signal at any point prior to swarm aggregation. Furthermore, apoptotic neutrophils observed during these experiments did not initiate neutrophil swarming. Pioneer neutrophils may become apoptotic during the aggregation phase, however once neutrophils have begun to aggregate it is not possible to observe individual neutrophils within the swarm. The limitations associated with the imaging speed of larvae in these experiments due to the acquisition of all channels required for FRET, result in the imaging of only a handful of larvae per experimental repeat. Again, this results in a low number of neutrophil swarms observed per experimental repeat which means that I have only a few examples of pioneer neutrophils. In future I will repeat these experiments to increase the number of examples, as well as perhaps developing a quantitative assay to measure FRET signal in pioneer vs non-pioneer neutrophils during the swarm initiation phase. I would ideally like to confirm these observations using a second method. It is important to employ multiple, methodologically unrelated assays to quantify dying and dead cells, so in future I would like to confirm my observations using an Annexin V transgenic reporter line which has been used for live imaging of apoptotic cells in zebrafish (van Ham et al., 2010).

3.17 Future work and conclusions

This study provides one of the first examples of the swarming response of endogenous neutrophils in a physiological setting. The study of neutrophil migration at the wound site in zebrafish larvae has provided valuable insight into the characteristic features of the endogenous neutrophil swarming response. Perhaps the most important observation was that the signal amplification reported to initiate the swarming response originates from one individual 'pioneer' neutrophil. I identified that the zebrafish is a tractable model to study pioneer neutrophils in the context of swarm initiation and began investigations into the cell death signalling which could initiate the swarming response. Investigations into pioneer neutrophil behaviour from this study have thus far not identified a mechanism of cell death which induces neutrophil swarming. The assays performed during this study suggest that pioneer neutrophils are not propidium iodide positive, and still have intact caspase-3 prior to swarm formation. This to some extent rules out caspase-3 mediated apoptosis and primary or secondary necrosis as initiators of swarming, although it would be useful to confirm these findings using further unrelated assays. I will continue to investigate cell death as a mechanism of swarm induction. I have in collaboration with others, developed a transgenic zebrafish reporter line to study extracellular trap formation in neutrophils, to begin to address the

hypothesis that pioneer cell death by NETosis induces neutrophil swarm formation. This is exciting as live imaging of neutrophil ETosis has not been reported to date, so this is a promising tool which can be used by the zebrafish community to understand NET formation *in vivo* in the context of tissue injury or infection. In future the role of cell death subroutines including pyroptosis, necroptosis, autophagy and senescence should be investigated, the tools for which are currently being developed by our group.

4 Elucidating the mechanisms governing neutrophil reverse migration

4.1 Introduction and aims

Chronic inflammation plays a role in many of the leading causes of death worldwide ("WHO | The top 10 causes of death," 2017). Of these diseases, the unregulated behaviour of neutrophils is a major contributor to disease pathogenesis (Wright et al., 2010). However there currently exists no therapies to target the neutrophilic component of chronic inflammatory diseases.

Neutrophils are removed from inflammatory sites by caspase-dependent neutrophil apoptosis followed by efferocytosis by macrophages. Through extensive studies, methods to both accelerate and delay apoptosis have been identified (Fox et al., 2010; Renshaw and Loynes, 2006). More recently reverse migration has been identified in multiple models as a mechanism by which neutrophils redistribute into the tissue surrounding the inflammatory site, a process which is thought to disperse the inflammatory burden to promote tissue healing (Nourshargh et al., 2016). Further understanding of the mechanisms which modulate neutrophil reverse migration may identify novel targets to treat chronic inflammatory diseases.

This work in this chapter is focussed on understanding the mechanisms which modulate neutrophil reverse migration using the zebrafish as a model to study neutrophil removal form wound sites. During this chapter I will investigate the hypothesis that neutrophil retention signals generated through G protein coupled receptor signalling are responsible for retaining neutrophils at inflammatory sites, and that desensitisation of neutrophils to these retention signals results in their reverse migration. Of the GPCRs receptors expressed on the surface of neutrophils, I will investigate the candidate receptor CXCR4 and its ligand CXCL12 and the role of this signalling axis in modulating neutrophil retention at wound sites.

The CXCR4 receptor (also known as LESTR/fusin/ cd184) and its ligand CXCL12 (also known as stromal derived factor SDF-1 or pre B cell stimulating factor/ PBSF) were first identified through the discovery that CXCR4 was a co-receptor for entry of X4 trophic strains of HIV entry into T-cells (Deng et al., 1996). CXCR4 is expressed developmentally in a broad range of cells of the immune and central nervous system, and mediates the migration of leukocytes and haematopoietic progenitors in response to its ligand, CXCL12 (Zou et al., 1998).

CXCL12 is a small cytokine belonging to the α-chemokine family, which mediates the migration of cells expressing high levels of CXCR4 including hematopoietic progenitors in bone marrow, B cells and primordial germ cells (PGCs). Signalling through the CXCR4/CXCL12 axis therefore regulates the function of many processes including stem cell trafficking (Aiuti et al., 1997), B-cell development and compartmentalisation (Nie et al., 2004) and primordial germ cell migration (Doitsidou et al., 2002). CXCL12 also binds to the CXCR7 receptor, which lacks the intracellular DRYLAIV motif essential for G protein binding and activation of downstream pathways. CXCR7 is thought to be a scavenger receptor which functions to sequester CXCL12, reducing its availability outside of the cell for binding to CXCR4 (McGinn et al., 2013).

There exists growing evidence to support a role for CXCR4/CXCL12 in neutrophil retention signalling. A specific role for the CXCR4/CXCL12 signalling axis in neutrophil retention at wounds has recently been suggested in zebrafish (Paredes-Zúñiga et al., 2017). Expression of the chemokine CXCL12 provides a retention signal to neutrophils in the bone marrow through activation of its receptor CXCR4 (Suratt et al., 2004). Furthermore, CXCR4 and CXCL12 are known HIF targets and their promoters contain HIF responsive elements (Schioppa et al., 2003; Wang et al., 2008).

In terms of chronic inflammation, tissue infiltrated neutrophils from patients with chronic inflammatory lung diseases and rheumatoid arthritis have increased CXCR4 surface expression (Hartl et al., 2008). Neutrophil surface expression of CXCR4 is increased after extravasation into injured lungs in mice (Yamada et al., 2011) and in human tissue samples, where pulmonary CXCL12 expression increases during acute lung injury (Petty et al., 2007). Additionally, the inhibition of CXCL12 using blocking antibodies prevented the accumulation of neutrophils in the lung during the late stages of this LPS induced lung injury (Yamada et al., 2011).

Gain of function CXCR4 mutations are found in patients with WHIM syndrome, who present with neutropenia and increased susceptibility to infections (Kawai and Malech, 2009). CXCR4 is highly expressed on neutrophils, which are inappropriately retained in the bone marrow because of the gain of function mutation in WHIM syndrome. Similarly, CXCR4 knockout mice show a marked increase in neutrophil release from the bone marrow (Gilchrist et al., 2015). Likewise, CXCR4 antagonist AMD3100 is used to mobilise stem cells from the bone marrow in humans (Broxmeyer et al., 2005). Together these findings highlight the role of signalling through the CXCR4/CXCL12 axis in neutrophil retention in mammalian and non-mammalian systems.

The CXCR4/CXCL12 signalling axis is one of the best characterised of all chemokine signalling in the zebrafish. Following the identification of this signalling axis in directing the migration of the posterior lateral line in zebrafish larvae, extensive work has found many roles for CXCR4/CXCL12 in regulating the migration of cells including neural cells (Gilmour et al., 2004), endodermal progenitors (Nair and Schilling, 2008) and neutrophils (Walters et al., 2010).

Zebrafish have two paralogues for CXCR4 and CXCL12 following a genome duplication event in teleost evolution. Mapping of the Cxcr4 genes in zebrafish demonstrates that Cxcr4 is expressed in most cell lineages known to express Cxcr4 in mammals. The developmental roles of Cxcr4 seem to be divided between the two isoforms of the gene, and expression of *cxcr4a* and *cxcr4b* in most cell lineages is mutually exclusive (Chong et al., 2001). Cxcr4a predominantly binds Cxcl12b, whilst Cxcr4b predominantly binds Cxcl12a. Cxcl12a is produced in regions including the head, pronephric duct and CHT of zebrafish larvae at 2dpf, which are regions of neutrophil development or accumulation (Walters et al., 2010). CXCR4b is broadly expressed on immune cells such as neutrophils and macrophages, but also cells including mesodermal cells and motor neurons in the zebrafish (Chong et al., 2001). More recently the a role for the CXCR7 scavenger receptor in modulating cell responsiveness to CXCL12 gradients has been identified (Donà et al., 2013), suggesting that monogamous signalling of CXCL12 through the CXCR4 receptor is an oversimplified model that needs to be revisited (Sánchez-Martín et al., 2013).

AMD3100 is a non-peptide bicyclam which is able to specifically antagonize the CXCR4 receptor at three main interaction residues located around the main ligand binding pocket of CXCR4 in transmembrane domains IV, VI and VII. Binding of AMD3100 competitively inhibits binding of CXCL12 and prevents subsequent downstream signalling (Fricker et al., 2006). AMD3100 is also an allosteric agonist of the low-affinity CXCR7 receptor (Kalatskaya et al., 2009). AMD3100 is used in combination with G-CSF as a mobiliser of stem cells from bone marrow into the blood through its ability to inhibit the CXCR4/CXCL12 signal which retains haematopoietic stem cells in the bone marrow (Liles et al., 2003). AMD3100 is administered to humans and mice via intravenous injection (Liles et al., 2003), and to zebrafish larvae through incubation of the compound at concentrations ranging from 10-30μM in the E3 medium of larvae (Tamplin et al., 2015).

During this chapter I will determine whether the molecular components required to generate a retention signal are present at inflammatory sites in zebrafish larvae, and specifically in neutrophils. I will investigate the inhibition of CXCR4 using the antagonist AMD3100. I aim to inhibit the CXCR4 receptor using chemical manipulation to study its

function in the context of neutrophil recruitment to inflammatory sites. Finally, I will use assays to study the effect of CXCR4 inhibition on driving inflammation resolution and more specifically neutrophil reverse migration.

4.2 Cxcr4b and Cxcl12a are strong candidates for retention signalling

4.2.1 CXCR4 and CXCL12 are conserved between humans and zebrafish

Protein sequence alignment was performed to determine the similarity between human and zebrafish genes. Protein sequences were extracted from the ncbi database and clustal omega was used to align the sequences of the human genes with zebrafish homologues for both CXCR4 and CXCL12 (Figure 4.1a and 4.2a respectively). Interestingly this protein sequence alignment has been recently published by another group (Tulotta et al., 2016). The percentage identity between human and both zebrafish homologue protein sequences for CXCR4 and CXCL12 was determined, as well as the percentage identity between the two zebrafish homologues (Figure 4.1b and Figure 4.2b).

4.2.2 Neutrophil expression of Cxcl12 *and* Cxcr4

To determine which of the CXCR4 homologues are expressed by neutrophils, RNA sequencing data from neutrophils extracted from wildtype larvae at 5dpf, provided kindly by our collaborator Anne-Marie Meijer, was studied. The fragments per kilobase of transcript per million mapped reads (fpkm) values for both Cxcr4 and Cxcl12 isoforms were extracted from the dataset to determine the expression level of both isoforms in zebrafish neutrophils. From this data it was apparent that *cxcr4b* is the predominantly expressed isoform in neutrophils, as the fpkm value for *cxcr4b* was over 100-fold higher than the fpkm value for *cxcr4a* (Figure 4.3). The expression of both Cxcl12 isoforms was relatively similar, however fpkm values were much lower than that of Cxcr4b (Figure 4.4).

These data demonstrate that CXCR4 and CXCL12 are highly conserved between humans and zebrafish, and that zebrafish neutrophils predominantly express the *cxcr4b* isoform. I therefore decided to study the Cxcr4b receptor and its ligand Cxcl12a throughout the inflammatory response in zebrafish.

```
A  hCXCR4    MEGISSIPLPLLQIYTSDNYTEEMGSGDYDS-MKEPCFREENANFNKIFLPTIYSIIFLT 59
   zCXCR4a   MAYYEHI---VFEDDLSADNSSEFGSGDIGANFEVPCDVEVSHDFQRIFLPTVYGIIFVL 57
   zCXCR4b   MEFY---------DSIILDNSSDSGSGDYD--GEELCDLSVSNDFQKIFLPTVYGIIFVL 49
             *             : :.: **** .   :  *   . . :*::*****:*.***:

   hCXCR4    GIVGNGLVILVMGYQKKLRSMTDKYRLHLSVADLLFVITLPFWAVDAVANWYFGNFLCKA 119
   zCXCR4a   GLIGNGLVVLVMGCQKKSRTMTDKYRLHLSVADLLFVLTLPFWAVDAAKDWYFGGFMCVA 117
   zCXCR4b   GIIGNGLVVLVMGFQKKSKNMTDKYRLHLSIADLLFVLTLPFWAVDAVSGWHFGGFLCVT 109
             *::*****:**** *** :.**********:*****:********. .*:**.*:* :

   hCXCR4    VHVIYTVNLYSSVLILAFISLDRYLAIVHATNSQRPRKLLAEKVVYVGVWIPALLLTIPD 179
   zCXCR4a   VHMIYTVNLYSSVLILAFISLDRYLAVVRATNSQGPRKLLANRIIYVGVWLPAALLTVPD 177
   zCXCR4b   VNMIYTLNLYSSVLILAFISLDRYLAVVRATNSQNLRKLLAGRVIYIGVWLPATFFTIPD 169
             *::***:*****************:*:***** ***** :::*:***:** ::*:**

   hCXCR4    FIFANVSEADDRYICDRFYPND---LWVVVFQFQHIMVGLILPGIVILSCYCIIISKLSH 236
   zCXCR4a   LVFAKAESSAIRTFCERIYPQDSFVTWVVAFRFQHILVGFVLPGLVILICYCIIISKLSR 237
   zCXCR4b   LVFAKIHNSSMGTICELTYPQEANVIWKAVFRFQHIIIGFLLPGLIILTCYCIIISKLSK 229
             ::**: .:   :*: **::   * ..*:****::*::***:** **********:

   hCXCR4    SKG--HQKRKALKTTVILILAFFACWLPYYIGISIDSFILLEIIKQGCEFENTVHKWISI 294
   zCXCR4a   GSKGT-QKRKALKTTVVLIVCFFVCWLPYCGGILLDTLMMLEVIPHSCELEQGLQKWIFV 296
   zCXCR4b   NSKGQTLKRKALKTTVILILCFFICWLPYCAGILVDALTMLNVISHSCFLEQGLEKWIFF 289
             ..    *********:**:.** *****  ** :*:: :*::* :.* :*: :.*** .

   hCXCR4    TEALAFFHCCLNPILYAFLGAKFKTSAQHALTSVSRGSSLKILSKGKRGGHSSVSTESES 354
   zCXCR4a   TEALAYFHCCLNPILYAFLGVKFKKSARSALS-PSRGSSLKFLSK-KRTGMSSVSTESES 354
   zCXCR4b   TEALAYFHCCLNPILYAFLGVRFSKSARNALS-ISSRSSHKMLTK-KRGPISSVSTESES 347
             *****:*************.:*..**: **:  *  ** *:*:* **    *********

   hCXCR4    SSFHSS 360
   zCXCR4a   SSFHSS 360
   zCXCR4b   SSALTS 353
             **  :*
```

B

	hCXCR4-zCXCR4a	hCXCR4-zCXCR4b	zCXCR4a-zCXCR4b
% Identity	66.67%	62.07%	74.15%

Figure 4.1: Protein sequence alignment of human and zebrafish CXCR4

Protein sequences were extracted from the Ensembl database. Human CXCR4 was aligned to the zebrafish homologs using Clustal Omega software (A). Asterisks (*) represent fully conserved residues; colons (:) represent strong similarity between residues, and periods (.) indicate weak similarity between residues. The percentage identify between human (h) and zebrafish (z) CXCR4a and b homologs was calculated (B), as well as the percentage identity between zebrafish homologues.

A

```
hCXCL12    MNAKVVVVLVLVLT--ALCLSDGKPVSLSYRCPCRFFESHVARANVKHLKILNTPNCALQ    58
zCXCL12a   MDLKVIVVVALMAVAIHAPISNAKPISLVERCWCRSTVNTVPQRSIRELKFLHTPNCPFQ    60
zCXCL12b   MDSKVVALVALLMLAFWSPETDAKPISLVERCWCRSTLNTVPQRSIREIKFLHTPSCPFQ    60
           *: **:.::.*:        ::.**:**  ** **   . * : .::.:*:*:**.* :*

hCXCL12    IVARLKNNNRQVCIDPKLKWIQEYLEKALNK---------    89
zCXCL12a   VIAKLKN-NKEVCINPETKWLQQYLKNAINKMKKAQQQQV    99
zCXCL12b   VIAKLKN-NREVCINPKTKWLQQYLKNALNKIKKKRSE--    97
           ::*:*** *::***:*: **:*:**::*:**
```

B

	hCXCL12-zCXCL12a	hCXCL12-zCXCL12b	zCXCL12a-zCXCL12b
% Identity	46.59%	46.59%	75.26%

Figure 4.2: Protein sequence alignment of human and zebrafish CXCL12

Protein sequences were extracted from the Ensembl database. Human CXCL12 was aligned to the zebrafish homologs using Clustal Omega software (A). Asterisks (*) represent fully conserved residues; colons (:) represent strong similarity between residues, and periods (.) indicate weak similarity between residues. The percentage identify between human (h) and zebrafish (z) CXCL12a and b homologs was calculated (B), as well as the percentage identity between zebrafish homologues.
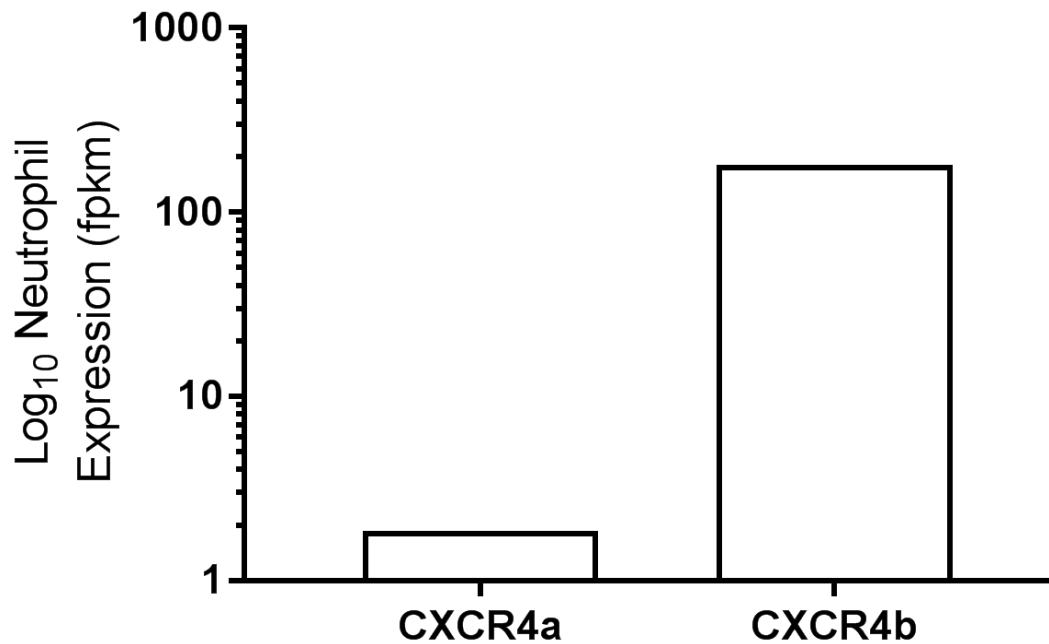
Figure 4.3: Expression of *cxcr4* in zebrafish neutrophils during early development

RNA sequencing of wildtype zebrafish neutrophils at 5 days post fertilisation was performed by a collaborator. Relative expression of transcript in fragments per kilobase of transcript per million mapped reads (fpkm) for both cxcr4a and cxcr4b was extracted from the database of genes provided from 3 independent repeats. Expression of cxcr4b was high, and is the predominantly expressed of the two CXCR4 genes in zebrafish neutrophils.
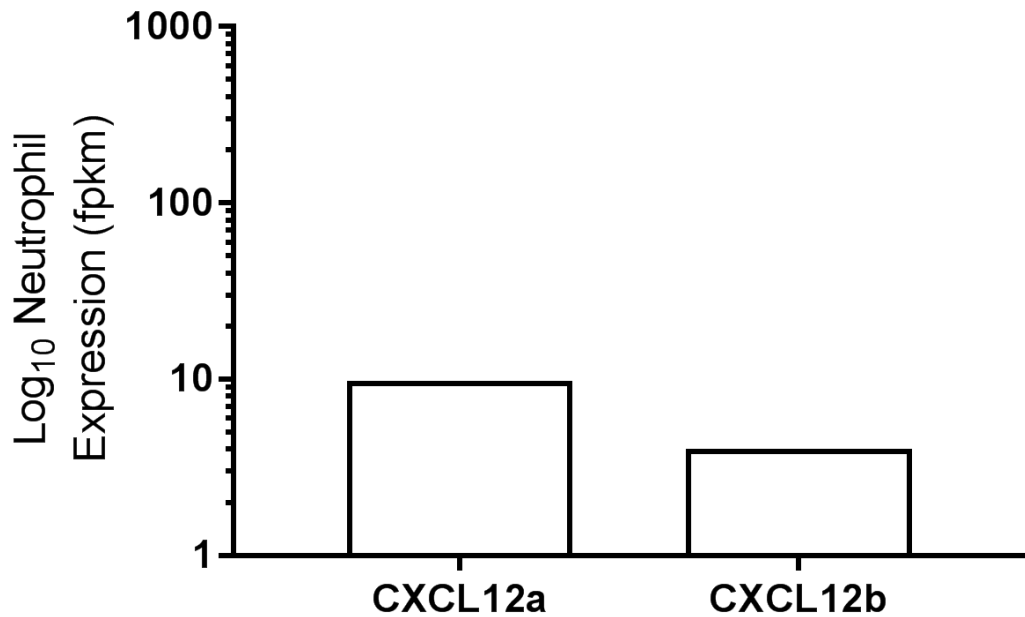
Figure 4.4 Expression of *cxcl12* in zebrafish neutrophils during early development

RNA sequencing of wildtype zebrafish neutrophils at 5 days post fertilisation was performed by a collaborator. Relative expression of transcript in fragments per kilobase of transcript per million mapped reads (fpkm) for both cxcl12a and cxcl12b was extracted from the database of genes provided from 3 independent repeats. Expression of both genes is low in neutrophils.

4.2.3   Cxcl12a is expressed at the wound site in zebrafish larvae

I hypothesised that in order for Cxcl12a to generate a neutrophil retention signal, Cxcl12a must be expressed at the wound site to signal through the Cxcr4b receptor on neutrophils. To assess the expression of the chemokine Cxcl12a in zebrafish larvae, a combination of zebrafish reporter lines and whole mount *in situ* hybridisation (WISH) was used.

A *cxcl12*a reporter zebrafish line *Tg(cxcl12a:eGFP)sh479* was generated at the University of Sheffield by Dr. Robert Wilkinson using a short promoter region (Lund et al., 2014). This line was leant to me on a collaborative basis and will be referred to as *cxcl12a*:GFP thus fourth. To determine the expression profile of *cxcl12a* at 3dpf in the transgenic reporter larvae, imaging of uninjured 3dpf *cxcl12a:*GFP larvae was performed as described in methods. Expression of the *cxcl12a*:GFP transgene was seen in anatomical locations reported in the literature at similar developmental stages such as the disk-shaped somite external cells along the horizontal myoseptum (Svetic et al., 2007), head region (Astin et al., 2014) and lateral mesoderm (Torregroza et al., 2012) (Figure 4.5a). Imaging of these larvae at higher power identified that *cxcl12a* is highly expressed by many cells in the tail-fin of uninjured larvae (Figure 4.5b and c).

To investigate the expression of *cxcl12a* at the wound site *in vivo* in real time, tail-fin transection of 3dpf *cxcl12a*:GFP larvae was performed as described in methods. Imaging of the tail-fin region of these larvae was performed at 6hpi. Representative images of injured larvae at 40x magnification in five representative larvae (Figure 4.6a) alongside age matched uninjured control larvae (Figure 4.6b) demonstrate that there is no detectable increase in fluorescence in injured larvae compared to controls. The high levels of *cxcl12a* expression by cells in the tail-fin make it difficult to determine whether *cxcl12a* expression at the wound site is generated in response to tail-fin injury or whether the expression observed is constitutive.

I therefore could not make any conclusions about the up-regulation of Cxcl12a at the wound site from these experiments.

4.2.4   The *cxcl12a*:GFP transgene is not expressed by neutrophils in detectable levels

I next investigated the production of Cxcl12a by neutrophils at the wound site. Neutrophils are able to generate gradients to modulate their recruitment to wound sites so I hypothesised that neutrophils might produce Cxcl12a at the wound site.

To investigate this hypothesis, I out crossed the *cxcl12a*:GFP reporter line to our *Tg(lyz:mCherry)sh260* neutrophil reporter line. Offspring from this outcross were

selected for double positive expression of both transgenes and tail-fins were transected. Imaging of neutrophils at the wound site was performed at 5hpi as described in methods.

Figure 4.7a shows a maximum intensity projection of *lyz*:mCherry neutrophils at the wound site at 4hpi at 40x magnification. I observed expression of both transgenes in single z-slices to determine if there was any level of colocalisation of mCherry with GFP signal. Figure 4.7b shows a representative example of a single slice of the *lyz*:mCherry x *CXCL12*:GFP larvae after observing expression in at least 30 larvae from 3 experimental repeats. Yellow outline highlights the area in which neutrophils are located, showing that there is no GFP expression where neutrophils are found. Line profiles were drawn through the centre of three neutrophils at the wound site in three fish taken from three experimental repeats, from which colocalisation of mCherry and GFP was seen in zero neutrophils. Figure 4.7c shows a representative example of the intensity measured through a line drawn through the centre of neutrophils corresponding to neutrophils 1, 2 and 3. This data demonstrated that no GFP expression was observed to colocalise with mCherry.

From these experiments I can conclude that neutrophils do not express *cxcl12a* at the wound site in detectable levels at this stage of development.
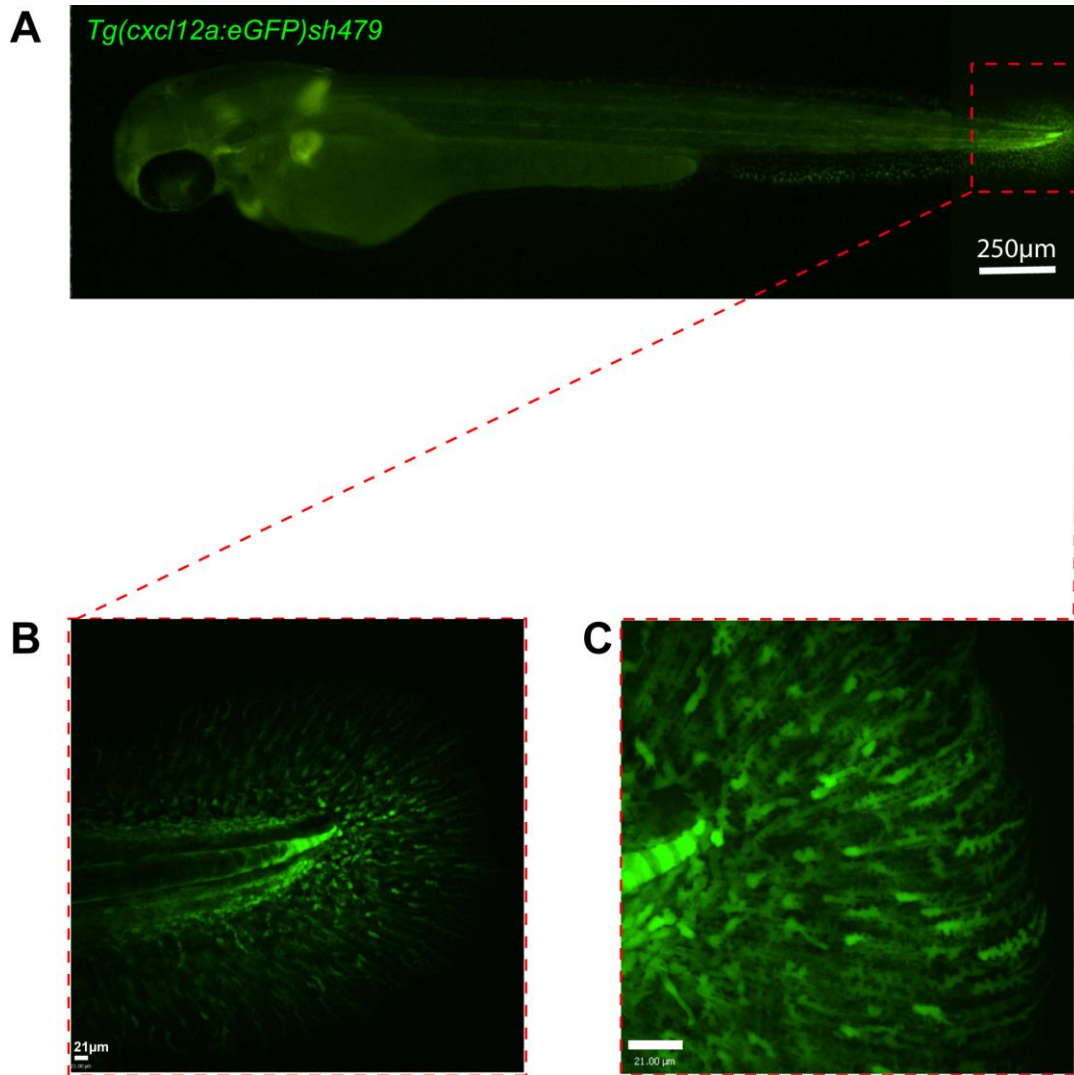
Figure 4.5: Expression profile of Cxcl12a in a transgenic reporter line

A Cxcl12a reporter line was made by a collaborator using a short promoter region to drive the expression of eGFP under the Cxcl12a promoter. Expression of the transgene was observed in 3dpf *Tg(cxcl12a:GFP)sh479* larvae at 2x (A), 20x (B) and 40x (C) magnification. Expression can be seen in the brain, skin and most notably at the end of the notochord protrusion the caudal tail fin.
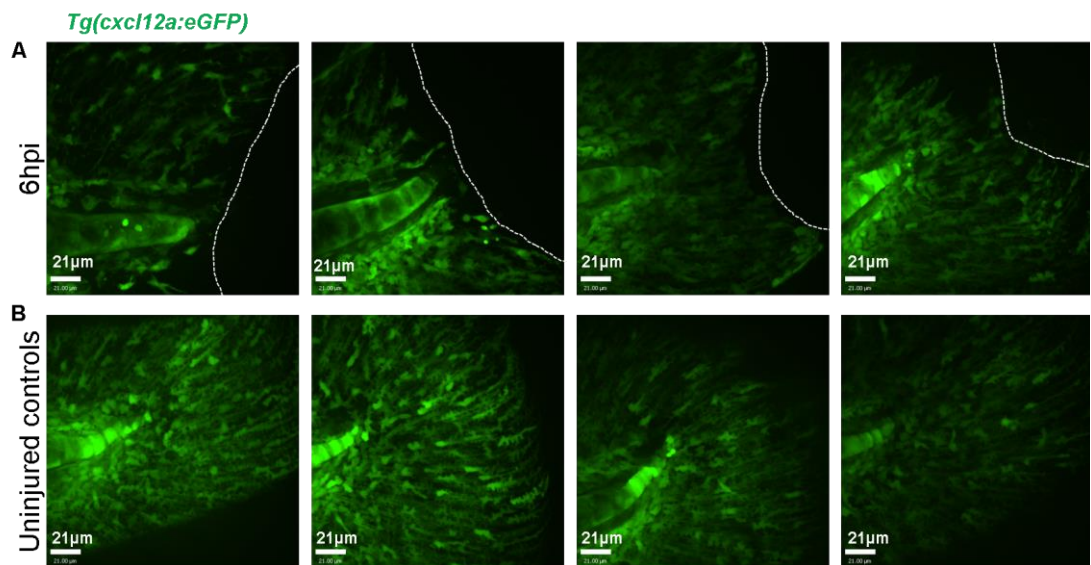
Figure 4.6: Investigating Cxcl12a expression in injured larvae

Tail fin transection of *cxcl12a*:eGFP larvae was performed at 3dpf. Expression of the Cxcl12a transgene at the wound site was visualised at 6hpi. Figure shows 4 the injured tail fins of 4 example larvae where the wound edge is indicated by a dotted white line (A). Imaging of injured larvae was performed alongside uninjured age-matched control larvae (B) where expression of the transgene in the tail fin was also observed.
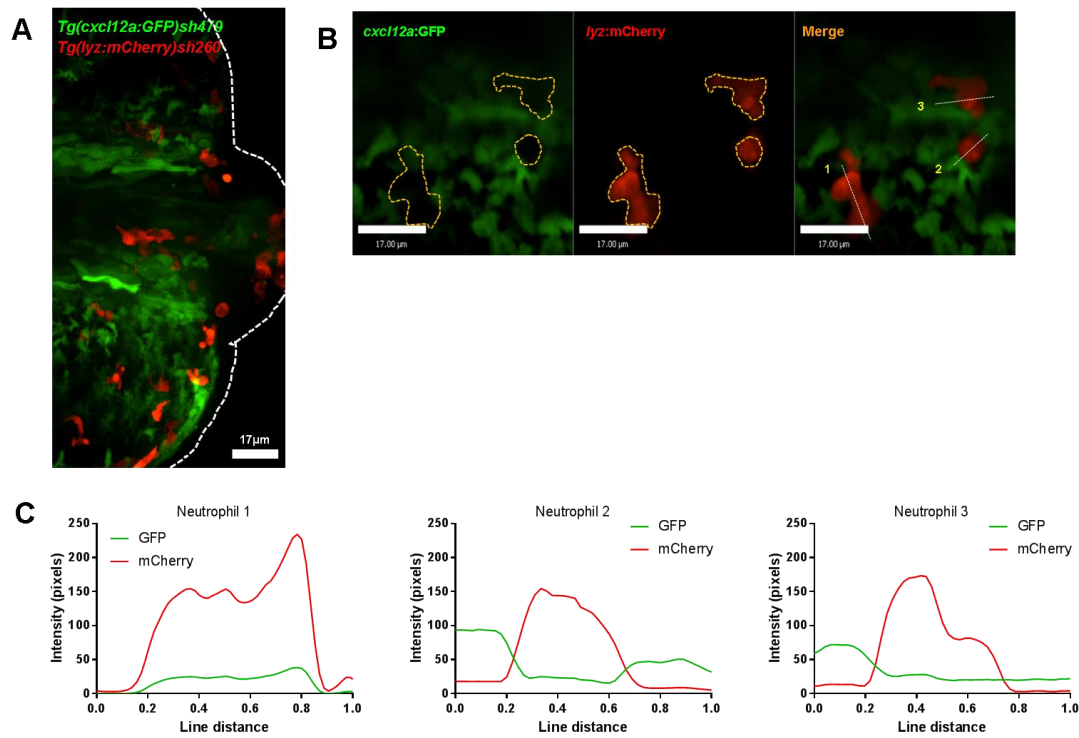
Figure 4.7: Cxcl12a:eGFP is not expressed by neutrophils

3dpf double transgenic *Tg(cxcl12a:eGFP);Tg(lyz:mCherry)* larvae were injured at 3dpf and neutrophils at the wound site were imaged at 5hpi. A representative maximum intensity projection (A) shows neutrophils recruited to the wound site at 5hpi. By studying each z-slice of images it was apparent that neutrophils did not express the Cxcl12a:eGFP transgene at detectable levels (B). Intensity profiles were plotted for 3 neutrophils at the wound site as indicated by yellow dashed lines (B). Representative intensity plots of mCherry eGFP expression further illustrate that no co-localisation is observed between the two transgenes (C).

4.2.5 CXCL12a mRNA is detected at the wound site in injured larvae

It was difficult to draw conclusions about *cxcl12a* expression from experiments performed using the *cxcl12a*:GFP reporter line. I next decided to use whole mount *in situ* hybridisation as a more sensitive method to visualise *cxcl12a* mRNA at the wound site.

WISH was performed as described in methods using an antisense RNA probe made from a plasmid vector containing the zebrafish *cxcl12a* coding sequence. The antisense RNA probe was prepared from linearised plasmid DNA which I received as a kind gift from Dr. Anne Robertson (University of Sheffield) as described in methods. Figure 4.8 shows representative examples of *cxcl12a* mRNA expression in larvae at 4, 8 and 24 hpi. The left panel shows mRNA expression in non-injured age matched control larvae, whilst the middle and right panels show whole body expression and tail-fin expression of injured larvae respectively. Expression of *cxcl12a* mRNA was found in anatomical locations reported in the literature at similar developmental stages such as the disk-shaped somite external cells along the horizontal myoseptum (Svetic et al., 2007), head region (Astin et al., 2014) and lateral mesoderm (Torregroza et al., 2012). Expression in injured larvae at 4hpi was not markedly different to that observed in uninjured control larvae. At 8 and 24hpi the expression of *cxcl12a* was visually higher in injured larvae compared to uninjured controls.

Taken together these experiments suggest that *cxcl12a* is expressed by cells at the wound site and is therefore a good candidate for retention signalling.

4.2.6 Generation of a Cxcr4b transgenic reporter line using the GAL4 UAS system

Measuring Cxcr4 receptor turnover at the cell surface has been used as a tool to calculate Cxcl12 concentration outside of cells in zebrafish larvae (Donà et al., 2013). I next aimed to visualise the spatial distribution of the Cxcr4b receptor in neutrophils to investigate Cxcl12a concentration at the wound site during the inflammatory response. Using the Gal4:UAS system (Scheer and Campos-Ortega, 1999) I drove the expression of a UAS conjugated Cxcr4b GFP fusion protein (Cxcr4b-GFP) in neutrophils expressing Gal4 under the myeloperoxidase promoter.
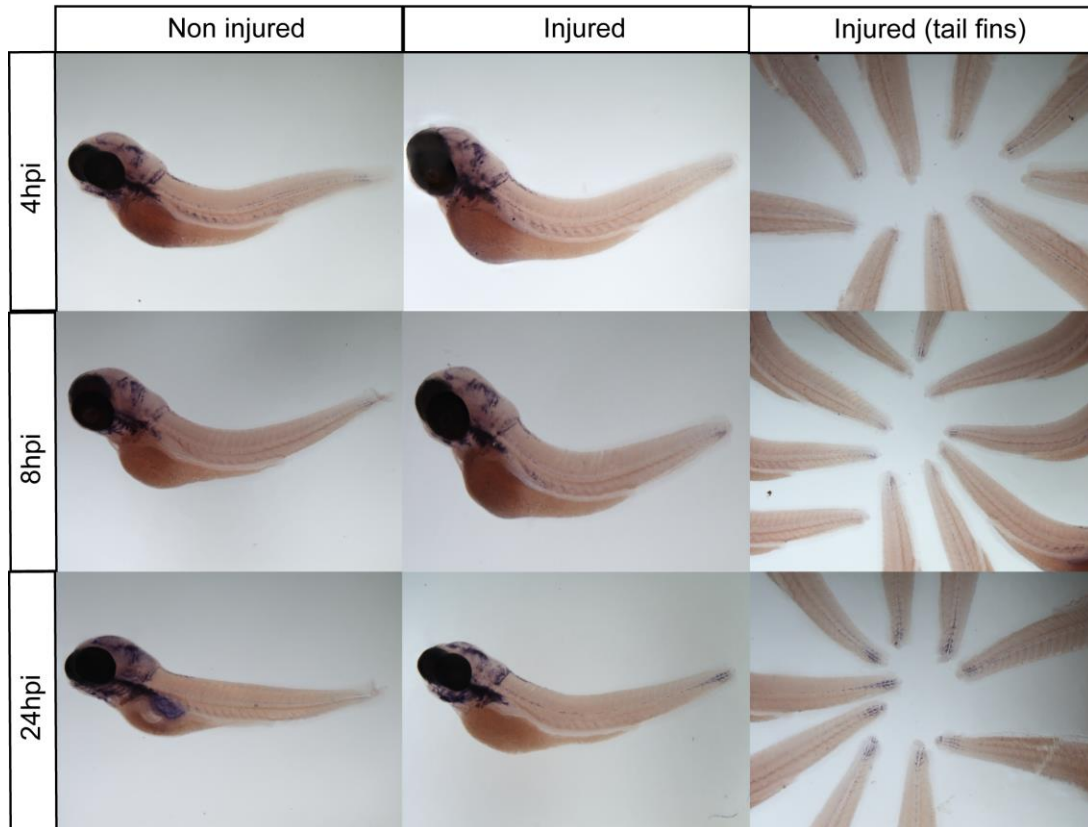
Figure 4.8: Whole mount in situ hybridisation to assess cxcl12a expression at the wound site

Tail fin transection of 3dpf nacre larvae was performed and larvae were fixed in paraformaldehyde at 4, 8 and 24hpi along with non-injured age matched controls. Whole mount *in situ* hybridisation was performed using an antisense probe for Cxcl12a. The expression of Cxcl12a in uninjured larvae is shown in the left panel, injured larvae in the centre panel and a higher magnification of the tail fin region of injured larvae in the right panel. Images are representative of experiments performed over 3 representative repeats.

A construct consisting of a GFP tagged Cxcr4b conjugated to UAS (UAS:Cxcr4b-GFP) flanked by *Tol2* arms was received as a kind gift from Professor Darren Gilmour (University of Zurich). The construct was prepared by transformation from plasmid DNA followed by DNA purification steps as described in methods prior to injection into larvae. The construct was injected into the *Tg(mpx:GAL4)i222* zebrafish reporter line expressing the GAL4 transcriptional activator in neutrophils specifically. Embryos in the *mpx:*GAL4 background were injected with the construct at the one cell stage. Larvae expressing the construct were selected for raising and a stable line of F1 generation larvae was produced as described in methods. Experiments were performed on F2 generation larvae.

Expression of UAS:*cxcr4b*-GFP was observed in the caudal hematopoietic tissue of 3dpf *Tg(mpx:GAL4)i222x(UAS:cxcr4b-GFP)sh503* larvae, which will be referred to as *cxcr4b*:GFP for simplicity (Figure 4.9). I aimed to confirm that the expression of the construct in the stable line was neutrophil specific. To do this I outcrossed *cxcr4b*:GFP zebrafish adults to *Tg(lyz:mCherry)sh260* in which the neutrophil specific lyz promoter drives mCherry. Larvae were screened at 3dpf for double positive expression of GFP and mCherry in the CHT and mounted for imaging as described in methods.

Figure 4.10 shows a representative example of *cxcr4b*:GFP expression in mCherry expressing neutrophils which was observed in at least 20 larvae from 3 experimental repeats. The c*xcr4b*:GFP transgene was only observed in a proportion of neutrophils in the CHT. I next aimed to study Cxcr4b in neutrophils at the inflammatory site throughout the recruitment and resolution of inflammation. I hypothesised that a difference in Cxcr4b dynamics would be observed in neutrophils in the resolution phase compared to the recruitment phase.

Initially I aimed to determine the dynamics of the neutrophilic inflammatory response in the *cxcr4b*:GFP line. F1 *cxcr4b*:GFP adults were crossed to produce offspring and offspring with the brightest neutrophil expression were selected for experiments at 3dpf. Tail-fin transection was performed as described in methods prior to mounting and imaging which began at 1 hour post injury for 10 hours. Interestingly recruitment of neutrophils expressing the *cxcr4b*:GFP transgene to the wound site was not observed in these 10 hour time courses. Representative images of the wound site from three larvae at 6hpi are illustrated in Figure 4.11.

I hypothesised that the impaired recruitment of neutrophils to the wound site was due to the over-expression of Cxcr4b in neutrophils by the GAL4 transcriptional activator, similar to the phenotype observed in WHIM zebrafish with over-active Cxcr4b signalling (Walters et al., 2010).
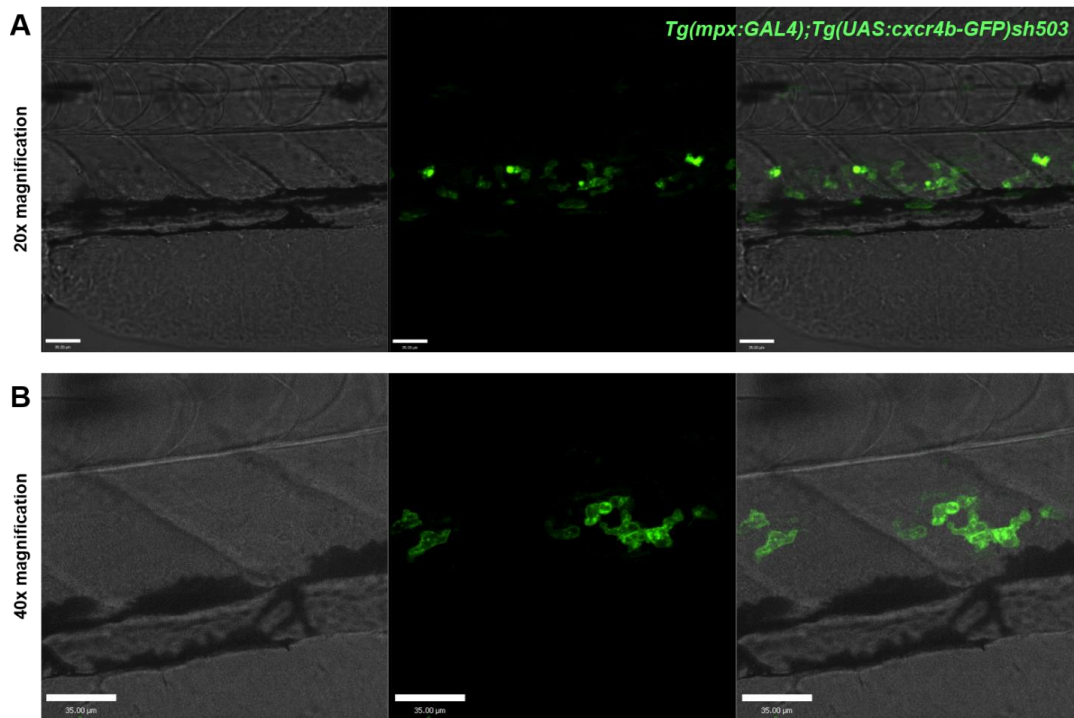
Figure 4.9: Expression of the Cxcr4b.GFP construct in the CHT of larvae

Tg(mpx:GAL4)i222;Tg(,UAS:cxcr4b-GFP)sh503 larvae were mounted for imaging at 3dpf. Images of the CHT of larvae were taken at 20x magnification (A) and 40x magnification (B). Figure shows a representative example of expression of the *cxcr4b-*GFP transgene in the CHT of larvae.
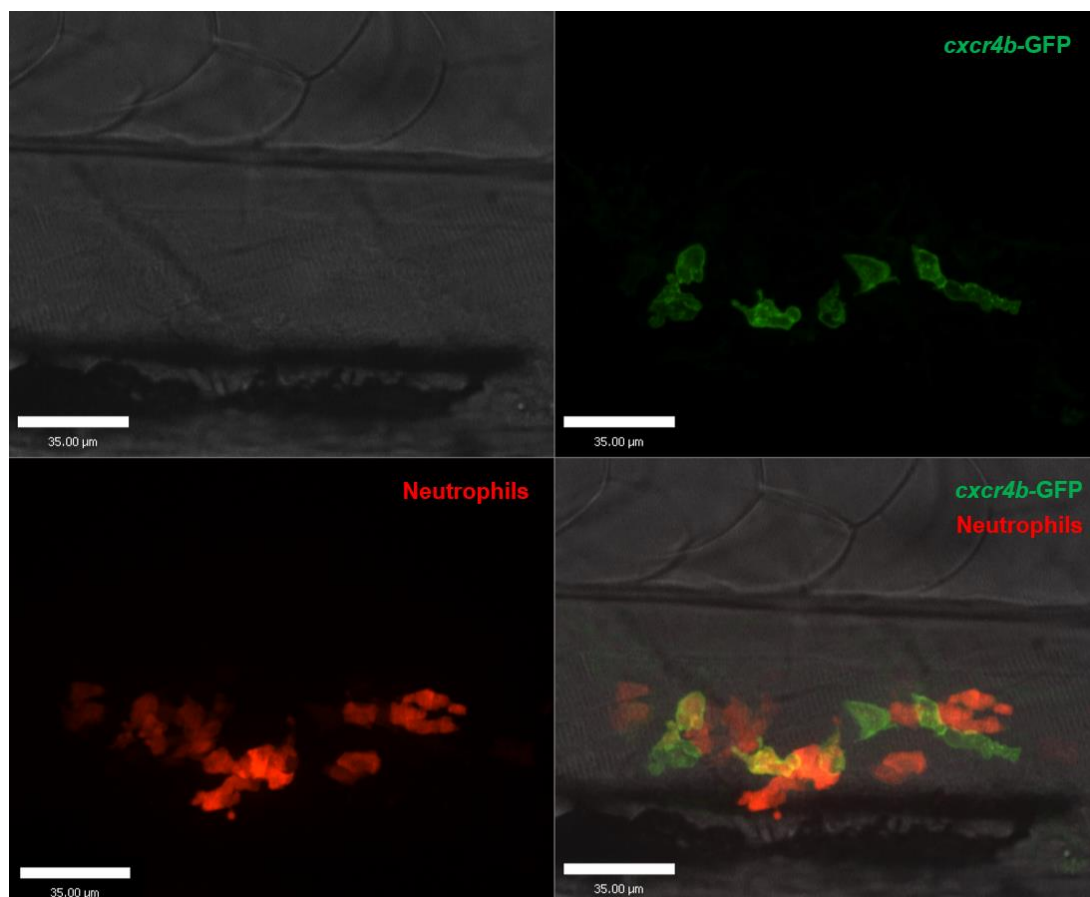
Figure 4.10: Expression of the *cxcr4b*-GFP transgene is neutrophil specific

Tg(mpx:GAL4)i222;Tg(UAS:cxcr4b.GFP)sh503 adults were out crossed to *Tg(lyz:mCherry)sh260* adults and double positive offspring were mounted for imaging at 3dpf. Images of the CHT region of larvae were taken at 40x magnification. Figure shows a representative example of expression of the *cxcr4b*-GFP transgene (green) by neutrophils (red) in the caudal hematopoietic tissue of larvae.

Tg(mpx:GAL4)i222;Tg(UAS:cxcr4b-GFP)sh503
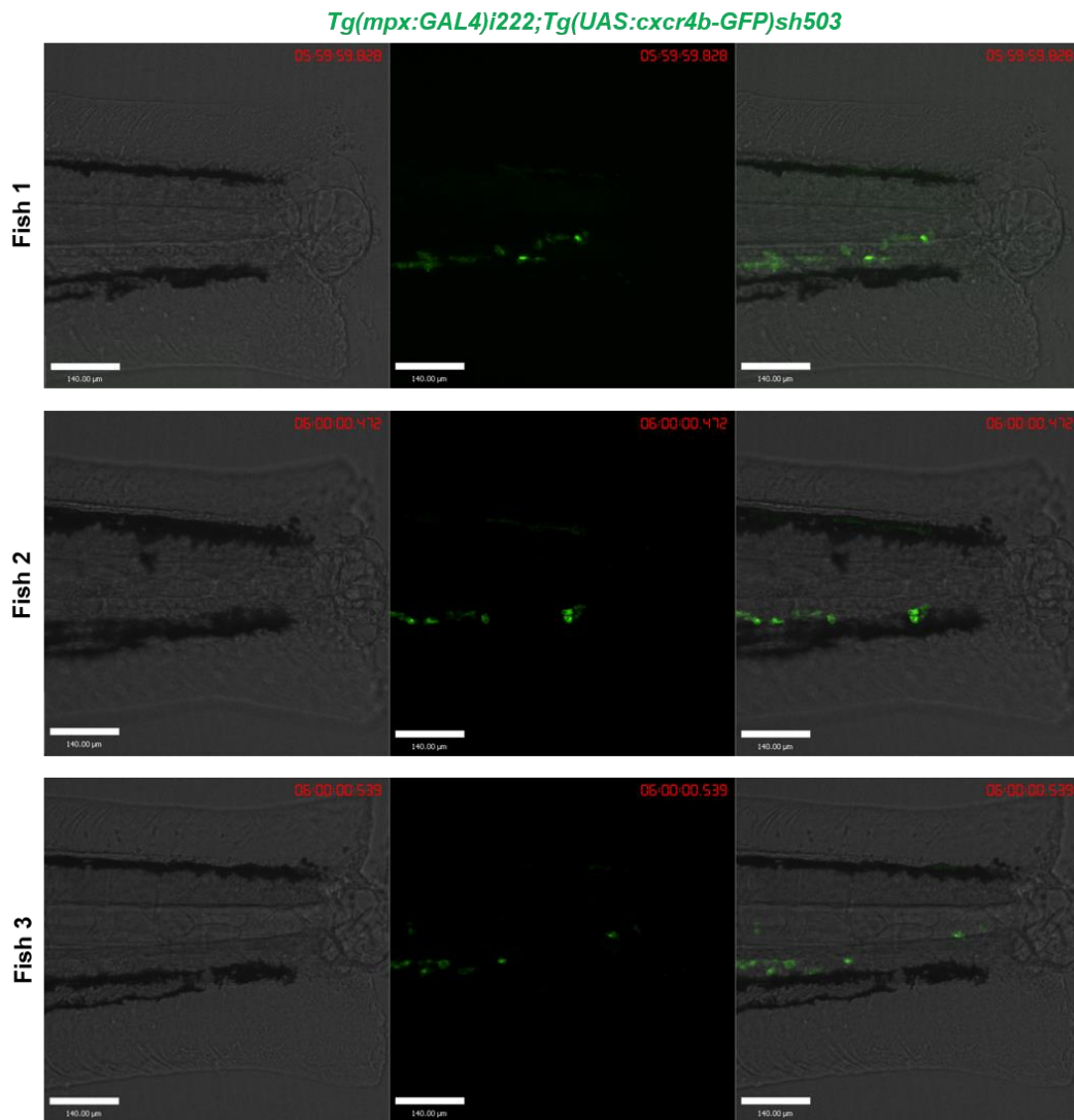
Figure 4.11: A WHIM phenotype is recapitulated in neutrophils expressing the *cxcr4b*-GFP transgene

Tg(mpx:GAL4)i222;Tg(UAS:cxcr4b.GFP)sh503 larvae were injured at 3dpf and time lapse imaging of neutrophil recruitment to the wound site was performed from 1hpi for 5 hours. No neutrophil recruitment to the wound site was observed in larvae during the first 6 hours following injury. Figure shows 3 representative wound sites at 6hpi where no recruitment of neutrophils expressing the Cxcr4b.GFP was observed (n=3 experimental repeats).

To test this hypothesis I studied the recruitment capacity of transgenic neutrophils to wildtype neutrophils in the same larvae. Adult fish from the *cxcr4b:*GFP background were outcrossed to *lyz*:mCherry adults and tail-fins of the double-positive offspring from this cross were transected at 3dpf. The number of neutrophils at the wound site was counted at 5hpi (Figure 4.12). Interestingly, these experiments identified that mCherry expressing neutrophils recruited to the wound site, whilst a significant reduction in neutrophils expressing *cxcr4b*-GFP was observed, despite the CHT of every larvae in the experiment containing *cxcr4b*-GFP labelled neutrophils (n=19 larvae from 2 experimental repeats). These data suggest that in neutrophils over expressing Cxcr4b, recruitment to the wound site is impaired whilst neutrophils not expressing the construct can recruit to the wound site.

These experiments highlight that over expression of CXCR4b in neutrophils caused the same phenotype observed in other zebrafish models of enhanced Cxcr4b signalling such as WHIM syndrome. Therefore, I was unable to use this line using these experiments to study Cxcr4b behaviour at the wound site due to the lack of recruitment of Cxcr4b-GFP expressing neutrophils.
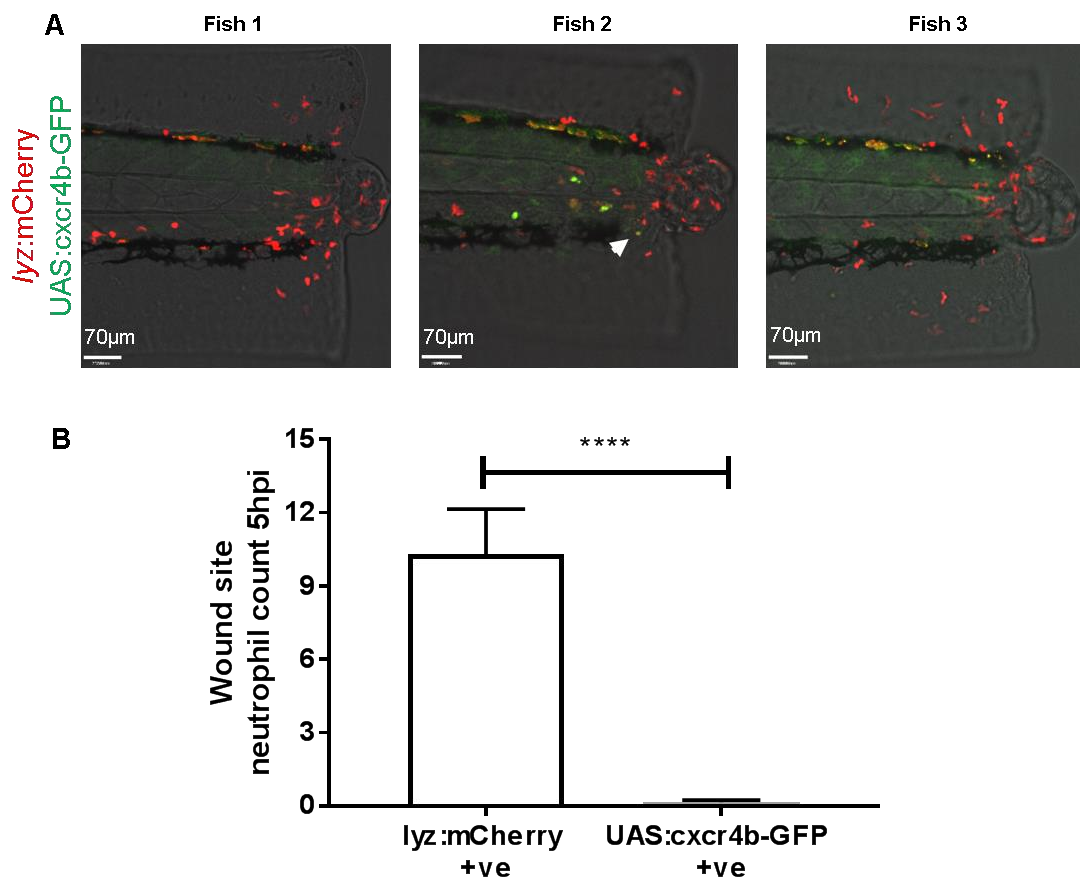
Figure 4.12: Neutrophils which don't express the _cxcr4b_-GFP transgene are recruited to the wound site

Tg(mpx:GAL4)i222;Tg(UAS:cxcr4b.GFP)sh503 adults were out crossed to _Tg(lyz:mCherry)sh260_ adults and tail fin transection was performed on double positive offspring. Imaging of neutrophils recruited to the wound site was performed at 5hpi. Figure shows neutrophils at the wound site in three representative larvae where neutrophils expressing both transgenes are highlighted by white arrows (A). The number of mCherry positive and Cxcr4b.GFP positive neutrophils at the wound site was counted, identifying that single positive lyz:mCherry expressing neutrophils were recruited to the wound site whilst neutrophils expressing the Cxcr4b.GFP transgene were not (B). (_n=20 larvae from 2 experimental repeats. Unpaired t-test where **** p<0.001 Data are shown as mean +/- sem_).

4.3 Using the compound AMD3100 to inhibit the CXCR4/CXCL12 signalling axis

4.3.1 Inhibition of CXCR4/CXCL12 signalling does not affect haematopoiesis during early development

Before using AMD3100 to investigate the role of CXCR4/CXCL12 signalling in neutrophil retention at wound sites, I first aimed to determine that the inhibition of CXCR4/CXCL12 signalling did not affect whole body neutrophil counts in larvae. AMD3100 was administered to larvae via incubation or injection as described in methods, and whole body counts were performed 5 and 24 hours post administration (Figure 4.13).

Inhibition of CXCR4/CXCL12 signalling caused no significant difference in the whole body counts of larvae either injected or incubated with AMD3100 at 2 or 3 dpf, at both 5 and 24 hours post administration. These data demonstrate that AMD3100 does not change the number of neutrophils in the larvae such that any change in neutrophil number observed when investigating neutrophil recruitment to or removal from the wound site should not be attributed to a difference in whole body neutrophil number.

4.3.2 Inhibition of CXCR4/CXCL12 signalling does not affect neutrophil colonisation of the caudal hematopoietic tissue

Neutrophil colonisation of the caudal hematopoietic tissue of zebrafish occurs between 48 and 72hpf. This process is CXCR4/CXCL12 dependent and it has been shown in zebrafish that AMD3100 treatment can reduce the amount of HSPC markers *runx1 and cmyb* in the CHT following treatment during this window (Tamplin et al., 2015).

To determine if inhibition of CXCR4/CXCL12 signalling affected the colonisation of neutrophils specifically in the CHT, *mpx:GFP* larvae were incubated in AMD3100 at concentrations indicated in Figure legend from 48-72hpf.

Neutrophils were counted in the CHT region illustrated in Figure 4.14A**.** In these experiments AMD3100 did not significantly affect neutrophil numbers in the CHT region following incubation (Figure 4.14B) or injection (Figure 4.14C) of the compound (n=27 larvae per experimental group from 3 experimental repeats).
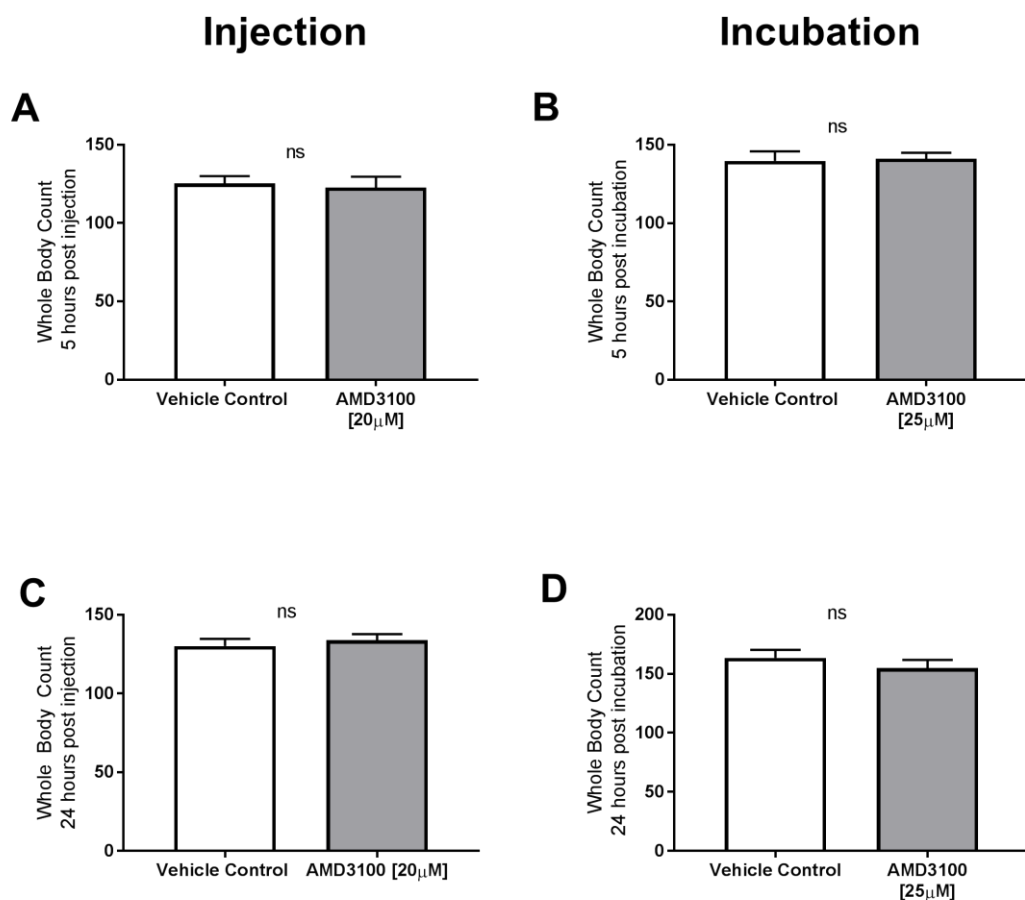
Figure 4.13: Inhibition of CXCR4/CXCL12 signalling does not affect haematopoiesis during early development

AMD3100 was administered to larvae at 48 or 72 hours post fertilisation by microinjection into the Duct of Cuvier or by incubation in E3 media respectively. Assessment of whole body neutrophil counts was performed at 5 and 24 hours post administration. Injection of AMD3100 into 2dpf larvae had no effect on whole body neutrophil counts at 5 and 24 hours post administration (A,C). Similarly incubation of AMD3100 in the media of 3dpf larvae did not change whole body neutrophil counts (B,D). (*n=27 larvae from 3 experimental repeats. Unpaired t-test where p>0.05 Data are shown as mean +/- SEM*).
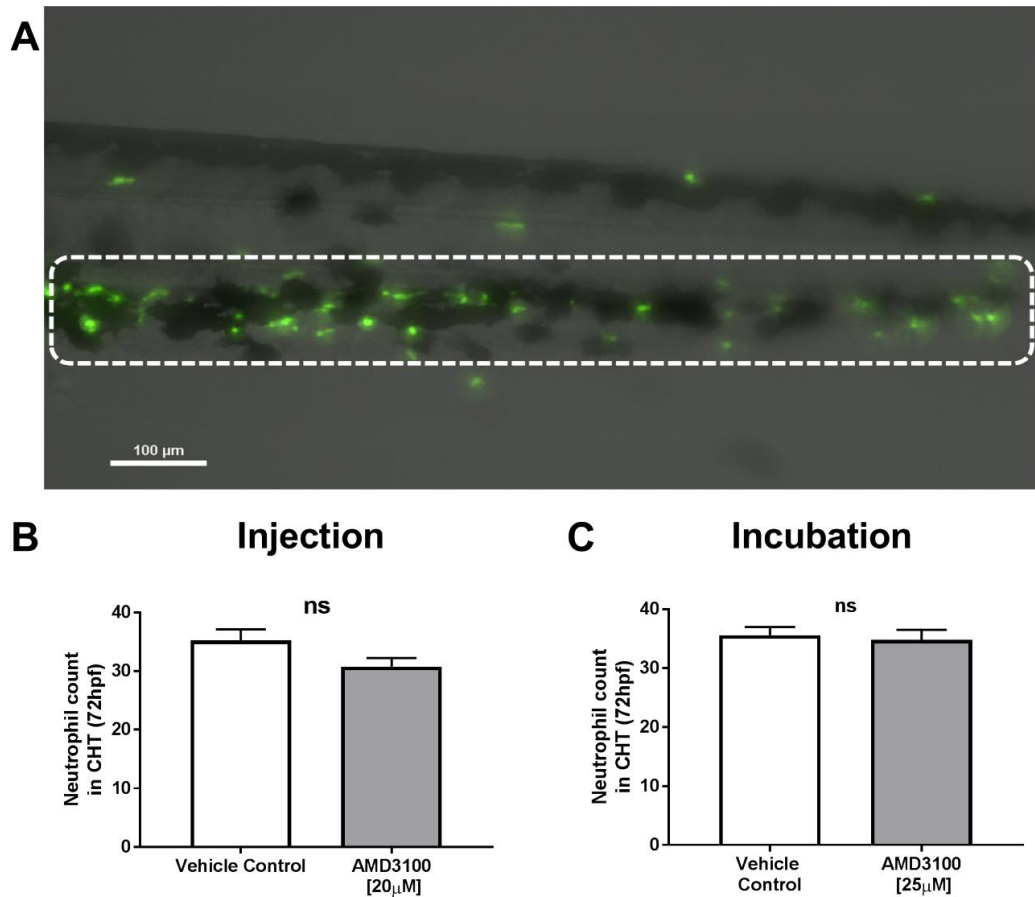
Figure 4.14: Inhibition of CXCR4/CXCL12 signalling does not affect neutrophil colonisation to the CHT

AMD3100 was administered to larvae at 48hpf by microinjection into the Duct of Cuvier or by incubation in E3 media and the CHT of larvae was imaged at 72hpf (A). No significant difference in neutrophil counts in the CHT was observed following AMD3100 injection (B) or incubation in E3 media (C). (*n=25-30 larvae per group from 3 experimental repeats. Unpaired t-test was performed where p>0.05 (B). Data are shown as mean +/- sem*).

4.3.3 Inhibition of CXCR4/CXCL12 signalling does not affect neutrophil retention in the CHT

Following colonisation of the CHT neutrophils are retained in this tissue, a process which is modulated by CXCR4/CXCL12 signalling. It has been shown in a zebrafish model for WHIM syndrome in which C-terminal truncating mutations prevent the internalisation of the CXCR4b receptor from the surface, that neutrophils are inappropriately retained in the CHT.

To test the hypothesis that CXCR4 inhibition using AMD3100 could release neutrophils from the CHT following their colonisation, 3dpf *mpx*:GFP larvae were treated with AMD3100 by incubation in the E3 media. The CHT region was imaged 5 hours post administration as described in methods. To quantify neutrophil retention in the CHT, neutrophil numbers inside and outside of the CHT were counted (Figure 4.15A). In these experiments, AMD3100 administration by incubation (Figure 4.15B), did not alter the number of neutrophils inside nor outside of the CHT (n=26-29 larvae per experimental group from 3 experimental repeats).
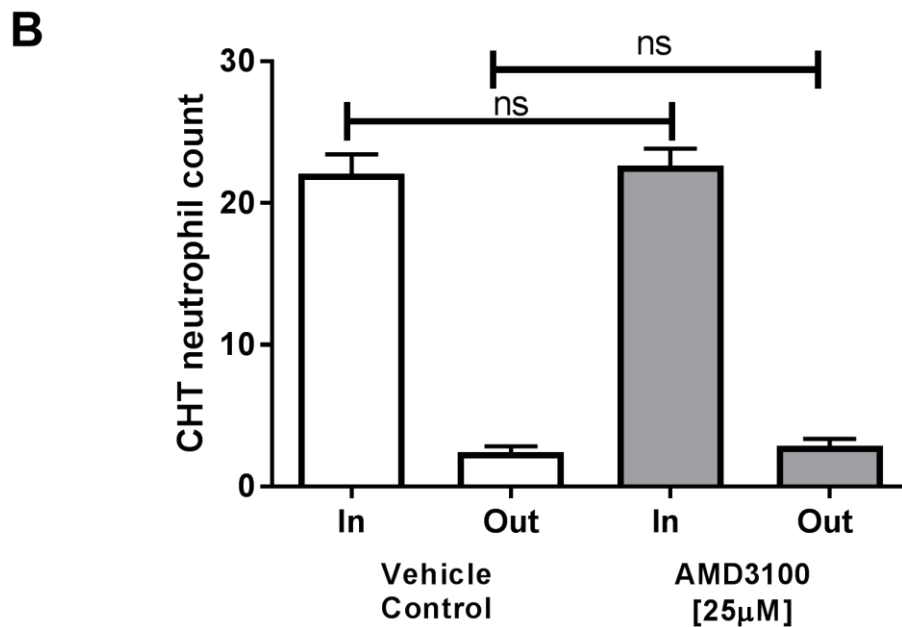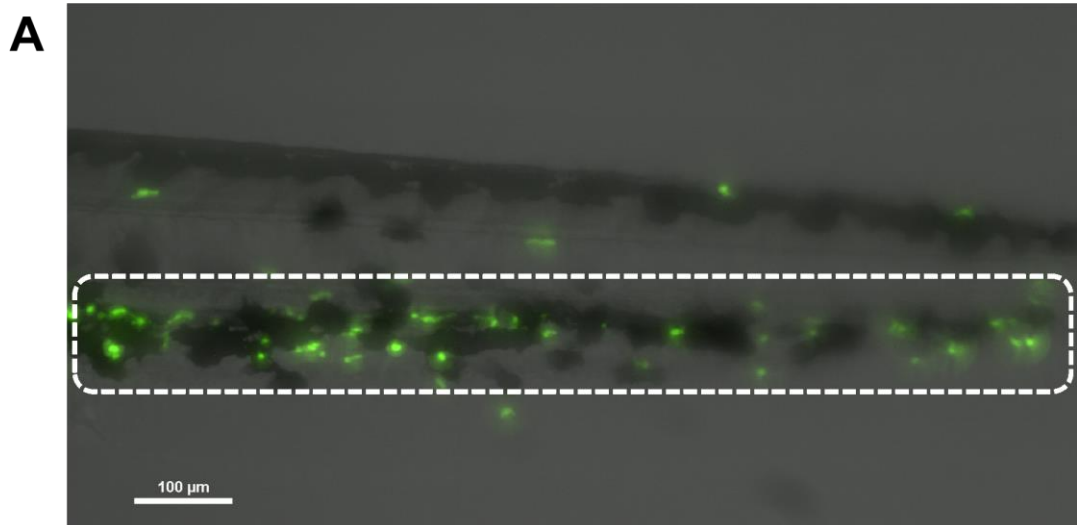
Figure 4.15: Inhibition of CXCR4/CXCL12 signalling does not affect neutrophil retention in the CHT

AMD3100 was administered to 3dpf *mpx*:GFP larvae by incubation in the E3 media. The CHT of larvae was imaged at 5 hours post incubation and the number of neutrophils inside the CHT as indicated by the white region of interest (A) and outside of the CHT were counted (B). No difference in the number of neutrophils inside or outside of the CHT was observed between treatment groups (*n=29 larvae from 3 experimental repeats. Chi squared contingency test with Fishers test where p=0.4376. Data are shown as mean +/- sem).*

4.3.4 Inhibition of CXCR4/CXCL12 signalling increases neutrophil recruitment to the wound site

The recruitment of neutrophils to inflammatory sites is increased in Cxcr4b mutant zebrafish larvae, where it is proposed that loss-of-function Cxcr4b mutations reduce neutrophil retention signalling in the CHT and thus increase neutrophil responsiveness to chemotactic cues released at the wound site (Paredes-Zúñiga et al., 2017).

I therefore hypothesised that inhibition of CXCR4/CXCL12 signalling using AMD3100 would increase the number of neutrophils recruited to the wound. To test this hypothesis AMD3100 was administered by injection or incubation to 2 or 3dpf *mpx*:GFP larvae respectively prior to tail-fin transection as described in methods section.

Injection of AMD3100 significantly increased the number of neutrophils recruited to the wound site (Figure 4.16A, n=36-40 larvae per group from 4 experimental repeats). Incubation of AMD3100 however, had no effect on neutrophil recruitment to the wound site in these experiments (Figure 4.16B, n=29-30 larvae per experimental group from 3 experimental repeats). These data suggest that neutrophils may be able to respond to directional cues released at the wound site more effectively when the CXCR4/CXCL12 signalling axis is inhibited, and that administration of AMD3100 by injection into the circulation may be a more effective way to administer the compound.

4.3.5 Inhibition of CXCR4/CXCL12 signalling accelerates inflammation resolution

To test the hypothesis that CXCR4/CXCL12 signalling generates a neutrophil retention signal, I performed inflammation resolution assays similar to those previously published by our group (Elks et al., 2011; Robertson et al., 2014). I hypothesised that administration of AMD3100 would reduce neutrophil counts at the wound site during the resolution phase of inflammation.

Initial experiments were performed by administration of AMD3100 via injection into the duct of Cuvier at 4hpi at a final blood concentration of 20µM, as described in methods. Neutrophils at the wound site were counted at the peak of recruitment at 6hpi, and during the resolution phase at 8 and 24hpi (Figure 4.17). Neutrophil counts at the wound site at the peak of recruitment were not affected in these experiments (Figure 4.17A), whereas the number of neutrophils at the wound site in AMD3100 treated larvae was significantly lower than the control group at 8hpi (Figure 4.17B).
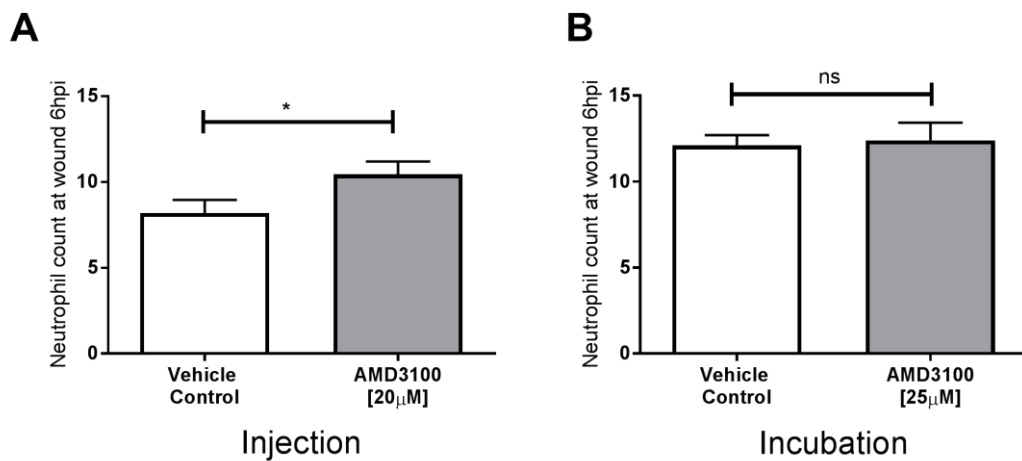
Figure 4.16: Inhibition of CXCR4/CXCL12 signalling increases neutrophil recruitment to the wound site

AMD3100 was administered by microinjection into the Duct of Cuvier for 2dpf larvae, or incubation into the E3 media for 3dpf larvae. 2 and 3dpf *mpx*:GFP larvae were injured 1 hour prior to AMD3100 administration and neutrophils recruited to the wound site at 6hpi were counted. Injection of AMD3100 into 2dpf larvae significantly increased neutrophil counts at the wound site (A) (*n=36-40 larvae from 4 experimental repeats. Unpaired t-test where * represents p<0.05).* There was no difference observed in neutrophil counts in larvae at the wound site following AMD3100 incubation at 3dpf (B) (*n=28-30 larvae from 3 experimental repeats. Unpaired t-test where p>0.05. Data are shown as mean +/- sem).*
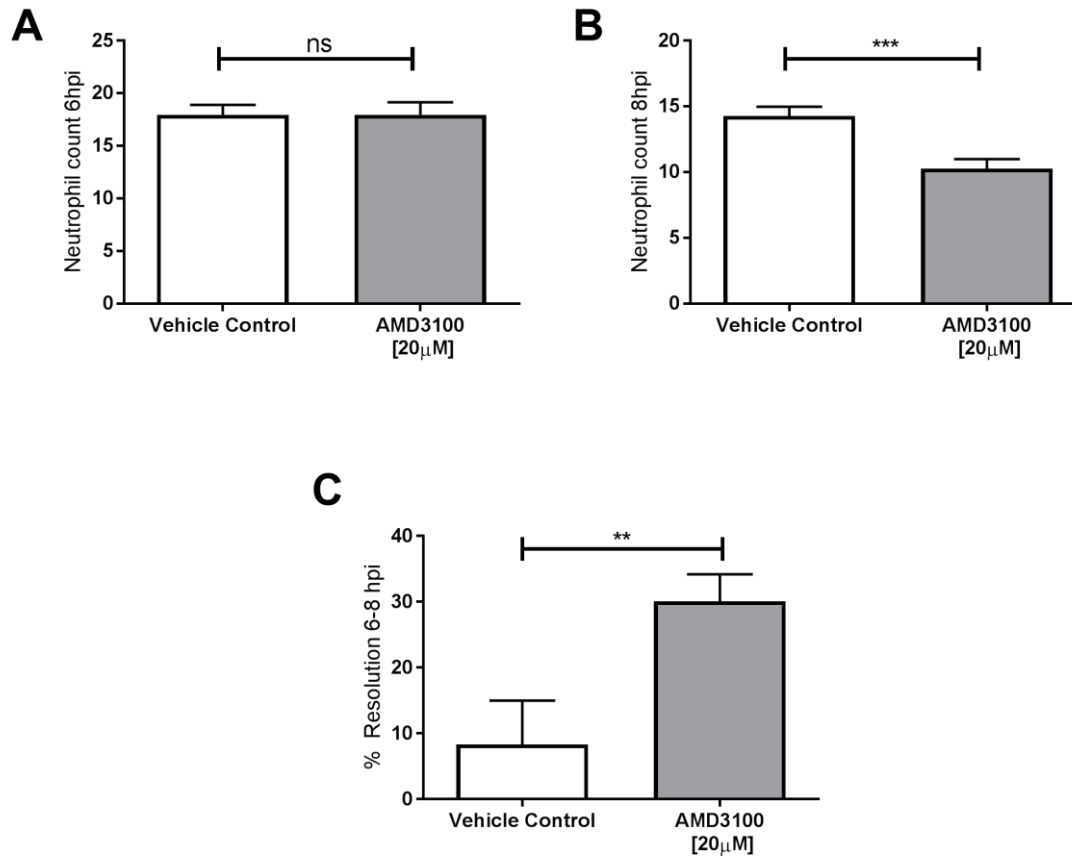
Figure 4.17: Inhibition of CXCR4 signalling by injection of AMD3100 accelerates inflammation resolution

Tail fin transection of 2dpf *mpx*:GFP larvae was performed and larvae with a good neutrophil response were selected for experiments. AMD3100 was injected into the Duct of Cuvier at 5hpi and neutrophils at the wound site were counted at 6 and 8 hpi. There was no difference in neutrophils recruited to the wound site at 6hpi between treatment groups (A), however AMD3100 injected larvae had significantly fewer neutrophils at the wound site at 8hpi (B). The percentage resolution measured between 6 and 8 hours was calculated for vehicle control and AMD3100 injected larvae. Percentage resolution was significantly higher in AMD3100 injected larvae (C) (*n=55 larvae from 5 experimental repeats. Unpaired t-test where **p<0.01 and ***p<0.001. Data are shown as mean +/- sem*)

The percentage resolution was calculated from these data as described in methods, and shows that AMD3100 significantly increases percentage inflammation resolution (Figure 4.17E). These data illustrate that AMD3100 treatment causes the more rapid removal of neutrophils from the wound site in a higher proportion of larvae than in controls.

I next investigated whether incubation of AMD3100 in the E3 media of 3dpf *mpx*:GFP larvae could also accelerate inflammation resolution. AMD3100 was administered to larvae at 4hpi as described in methods. Neutrophils present at the wound site were counted at the peak of recruitment at 6hpi, and during the resolution period at 8, 12 and 24 hours post injury.

These experiments show that AMD3100 incubation causes no change in the number of neutrophils present at the wound site at the peak of recruitment however a significant decrease in the number of neutrophils present at the wound site during the resolution phase of inflammation was seen at 8 and 12hpi (Figure 4.18A). The rate of inflammation resolution was measured by calculating the percentage inflammation resolution of neutrophils from 6-8 hours and 6-12 hours post injury as described in methods (Figure 4.18B and 4.18C respectively). There was no significant difference in percentage resolution between the two groups in these experiments, however there was a trend to increased % resolution in AMD3100 treated larvae.

Together these data demonstrate that AMD3100 is able to accelerate the removal of neutrophils from the wound site in zebrafish larvae, supporting the hypothesis that the CXCR4/CXCL12 signalling axis generates a neutrophil retention signal at the wound site and further provide evidence to suggest that injection of the compound shows a greater effect on CXCR4/CXCL12 signalling than incubation of the compound.
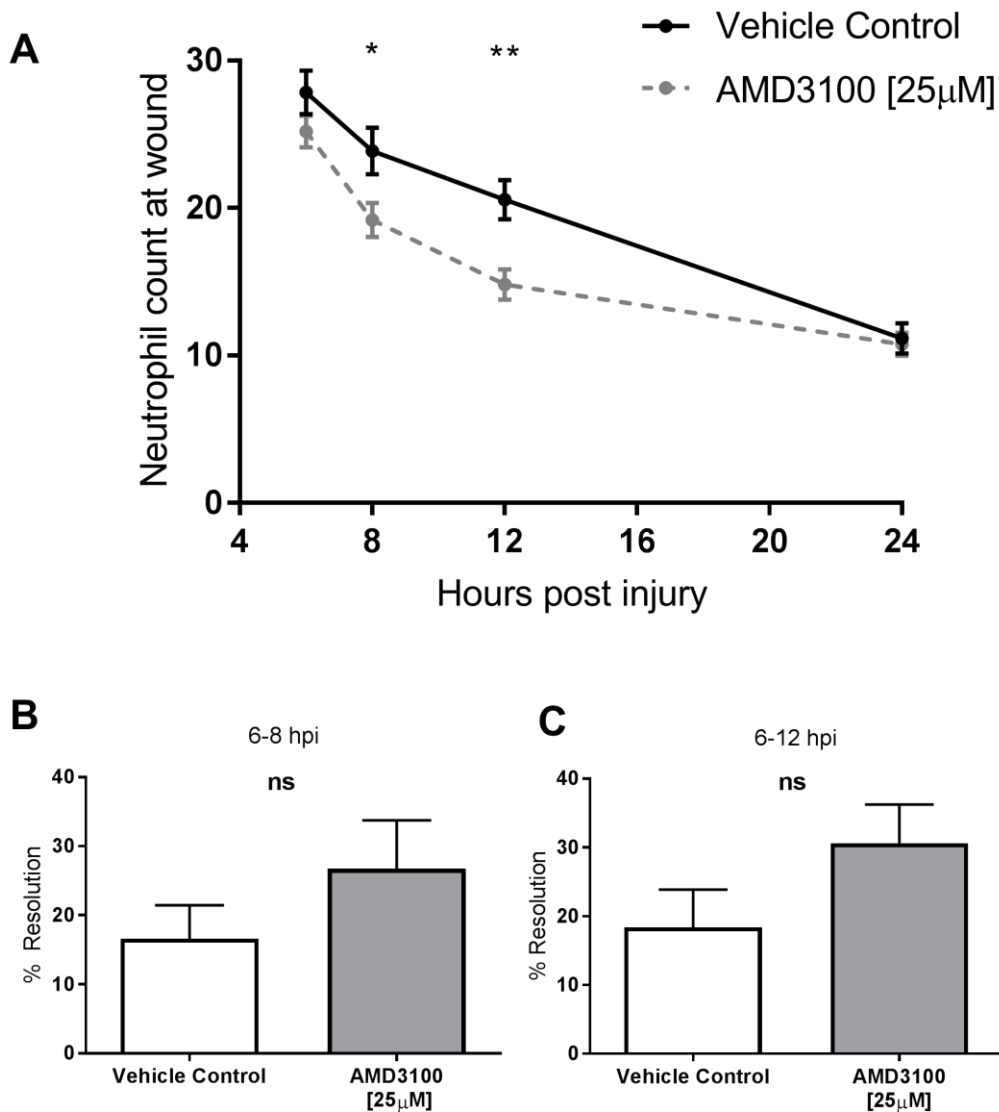
Figure 4.18: Inhibition of CXCR4 signalling by incubation of AMD3100 increases inflammation resolution

3dpf *mpx*:GFP larvae were injured and larvae with a good neutrophil response at the wound site were selected for experiments. AMD3100 or vehicle control was administered by incubation in the E3 media at 4 hours post injury. Neutrophils present at the wound site were counted at 6, 8, 12 and 24 hours post injury. Neutrophil counts were not significantly different at 6hpi between groups, however AMD3100 incubation significantly reduced neutrophil counts at the wound site at 8 and 12 hours post injury (A). The percentage resolution was calculated for both groups between 6-8 hours and 6-12 hours post injury. (*n=29-30 larvae per group from 3 experimental repeats. Unpaired t-test where *p<0.05 and **p<0.01. Data are shown as mean +/- sem*).

4.3.6 Inhibition of CXCR4/CXCL12 signalling accelerates neutrophil reverse migration

I have shown that inhibition of Cxcr4 using AMD3100 is able to accelerate inflammation resolution without reducing the ability of neutrophils to recruit the wound site or altering neutrophil counts in the zebrafish. Inflammation resolution can be achieved in part by the apoptosis of neutrophils and their efferocytosis by macrophages, or by the reverse migration of neutrophils away from the inflammatory site. I hypothesised that the acceleration in inflammation resolution I observed was due to an increase in neutrophil reverse migration.

To investigate this hypothesis reverse migration assays were performed using *Tg(mpx:kaede)i222* larvae at 2 or 3dpf for injection or incubation of AMD3100 respectively, as described in methods.

I first performed these assays by injecting the compound into the duct of Cuvier at 5hpi. In these experiments, I observed more neutrophils migrating away from the wound site in the AMD3100 injected larvae compared to the vehicle control group (Figure 4.19A). Linear regression analysis indicated that this difference was highly significant (n=16-18 larvae per treatment group from 3 experimental repeats, $p < 0.005$). The number of photoconverted neutrophils in the whole tail region of larvae at the first frame of the time lapse was counted and I found that there was no significant difference in the number of photoconverted neutrophils between the two groups (Figure 4.19B). This demonstrates that the increased number of neutrophils detected away from the wound site was not due to a difference in the number of photoconverted neutrophils.

I next repeated these experiments by administering the AMD3100 by incubating the compound in the agarose of larvae throughout the duration of the experiment. AMD3100 was administered to larvae at 5hpi prior to photoconversion at 6hpi, as described in methods. The number of neutrophils which moved away from the wound site was significantly higher in larvae treated with AMD3100 (Figure 4.20A) (n=32-35 larvae from 6 experimental repeats). Linear regression analysis indicated that this difference was highly significant ($p < 0.001$). This difference was not due to a difference in the number of photoconverted neutrophils (Figure 4.20B).

This data suggests that the acceleration of inflammation resolution observed in AMD3100 treated larvae can be attributed at least in part, to the increased reverse migration of neutrophils away from the wound site.

A

AMD3100
[20µM]

Injure 2dpf larvae — Inject compound 4hpi — Mount in agarose + compound and photoconvert 5-6hpi — Image immediately

B

C
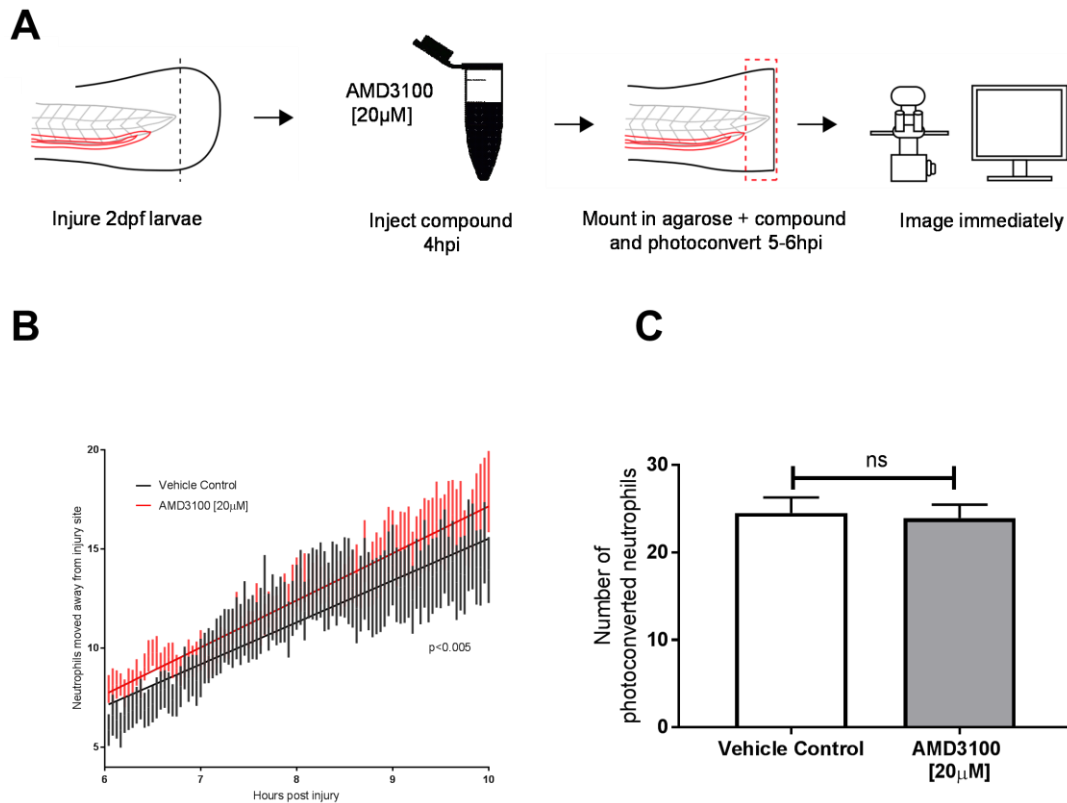
Figure 4.19: Inhibition of CXCR4 by AMD3100 injection accelerates neutrophil reverse migration at 2dpf

Tail fin transection was performed on 2dpf *mpx*:kaede larvae. Those which mounted a good neutrophil response at 3.5hpi were selected for microinjection with AMD3100 or vehicle control at 4hpi. Larvae were mounted in 1% agarose and neutrophils at the wound site were photoconverted at 5hpi from green to red fluorescence. Time lapse imaging was performed from 6-10hpi. Experimental schematic adapted from Ellett et al., 2015 is illustrated in (A). The number of neutrophils which moved away from the wound site into a defined region of interest was quantified throughout the time course. AMD3100 significantly increased the number of neutrophils which moved away from the wound site (B). This increase was not due to a difference in the number of photoconverted neutrophils between treatment groups which were quantified in the first frame of time courses (C). (*n=16-18 larvae from 3 experimental repeats. Linear regression analysis where p<0.001 (A). Unpaired t-test where p>0.05 (B). Data are shown as mean +/- sem*).
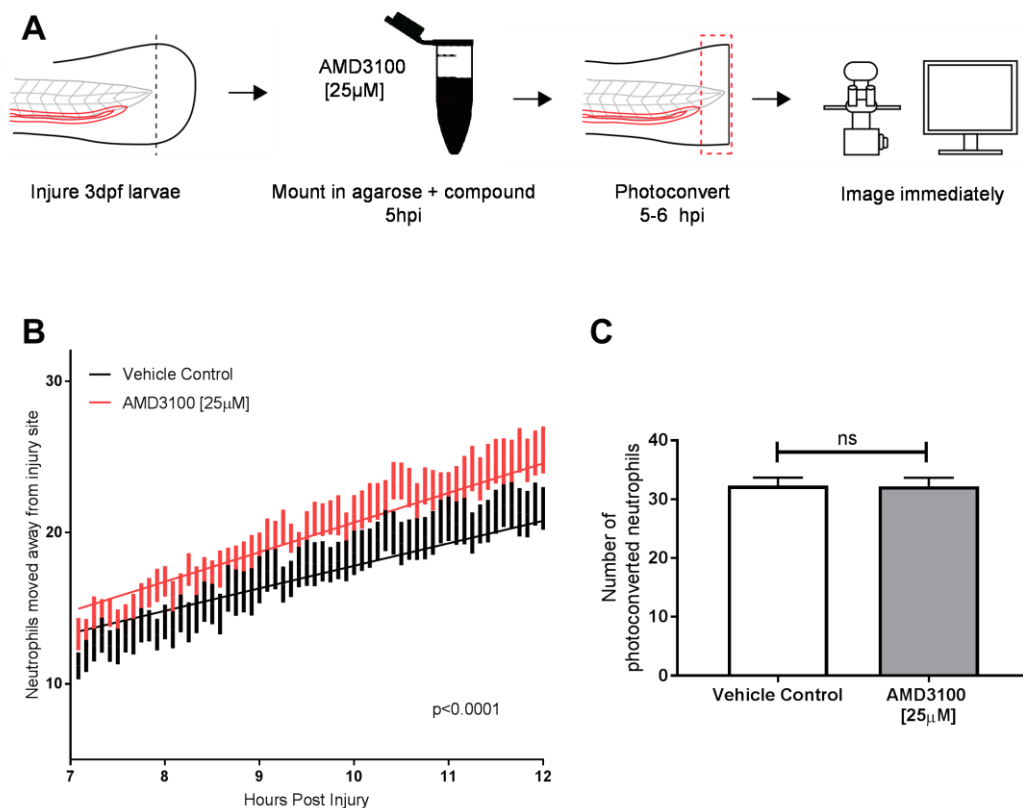
Figure 4.20: Inhibition of CXCR4 by AMD3100 incubation accelerates neutrophil reverse migration at 3dpf

Tail fin transection was performed on 3dpf *mpx*:kaede larvae. Those which mounted a good neutrophil response at 4hpi were selected for experiments and mounted in a 1% agarose containing AMD3100 or vehicle control at 5hpi. Neutrophils at the wound site were photoconverted at 5hpi from green to red fluorescence. Time lapse imaging was performed from 7-12hpi. Experimental schematic adapted from Ellett et al., 2015 is illustrated in (A). The number of neutrophils which moved away from the wound site into a defined region of interest was quantified throughout the time course. AMD3100 significantly increased the number of neutrophils which moved away from the wound site (B). This increase was not due to a difference in the number of photoconverted neutrophils between treatment groups which were quantified in the first frame of time courses (C). (*n=35 larvae from 6 experimental repeats. Linear regression analysis where p<0.001 (A). Unpaired t-test where p>0.05 (B). Data are shown as mean +/- sem*).

4.4 Chapter discussion

In this chapter I have investigated the role of the CXCR4/CXCL12 signalling axis in modulating neutrophil retention at inflammatory sites in zebrafish larvae. I have generated evidence that the components required for a retention signal through CXCR4/CXCL12 are present at the wound site, with the receptor being expressed on zebrafish neutrophils and mRNA for the ligand expressed at the tail-fin in injured larvae. I attempted to disrupt known CXCR4/CXCL12 dependent processes in zebrafish and recapitulated the phenotype observed in Cxcr4b/Cxcl12a mutant larvae where neutrophil recruitment to the wound site is increased (Paredes-Zúñiga et al., 2017). Finally, I have begun to address the hypothesis that CXCR4 generates a neutrophil retention signal by demonstrating that inhibition of the CXCR4 receptor using AMD3100 can accelerate inflammation resolution by driving neutrophil reverse migration.

These experiments provide evidence that the CXCR4/CXCL12 signalling axis exists at the wound site in zebrafish larvae, where neutrophil reverse migration is accelerated in larvae following CXCR4 receptor inhibition. This is the first evidence that CXCR4/CXCL12 signalling is important in neutrophil retention at inflammatory sites and suggests a novel signalling pathway is involved in neutrophil retention at sites of inflammation, however the downstream components of this pathway have yet to be elucidated.

4.4.1 Cxcr4b and Cxcl12a are strong candidates for retention signalling at the wound site

Computational modelling data suggest that neutrophil reverse migration is the stochastic redistribution of neutrophils back into the tissue rather than their active migration away from the wound site (Holmes et al., 2012). These data imply that neutrophil desensitisation to gradients at the wound site rather their active migration away from chemorepulsive gradients (fugetaxis) is more likely to modulate reverse migration. Cellular desensitisation to external gradients is a characteristic feature of signalling through G protein coupled receptors, many of which are expressed on the surface of neutrophils (Magalhaes et al., 2012).

The CXCR4/CXCL12 signalling axis modulates many processes in zebrafish (Donà et al., 2013; Itou et al., 2012; Tamplin et al., 2015), and in terms of neutrophil function, has been shown to regulate the retention of neutrophils in the CHT (Paredes-Zúñiga et al., 2017; Walters et al., 2010). Before investigating the CXCR4/CXCl12 signalling axis in modulating neutrophil retention at inflammatory sites, I first determined that cellular components required for signalling were present at the wound site in zebrafish larvae.

I compared the protein sequences for human and both zebrafish paralogues of CXCR4 and CXCL12 and identified that there is a degree of conservation between the two species, which is useful to determine that the proteins may function similarly. The zebrafish has been used to study Cxcr4 function in many developmental processes so this investigation supports the notion that Cxcr4 is functionally similar to its mammalian counterpart (Donà et al., 2013; Valentin et al., 2007). RNA sequencing data from our collaborator Professor Annemarie Meijer (University of Leiden, NL) identified that *cxcr4b* is the predominantly expressed isoform in neutrophils during early development at 5dpf. This data provides information about Cxcr4b expression at 5dpf, however experiments in this study were performed on zebrafish at 2 and 3dpf. There exists evidence that *cxcr4b* is expressed in a population of hematopoietic cells at 3dpf including neutrophils, which migrate towards tissues expressing *cxcl12a* (Walters et al., 2010). It is reported that the cognate ligand for Cxcr4b is Cxcl12a, so this evidence along with the RNA sequencing data suggests that these are the two isoforms which should be investigated during this study. Cxcr4b/12a in zebrafish neutrophils may function similarly to its human counterpart as CXCR4/CXCL12 signalling acts to retain neutrophils in their niche in both organisms (Day and Link, 2012; Paredes-Zúñiga et al., 2017).

4.4.2 Cxcl12a is produced at the wound site in zebrafish larvae

CXCL12 produced by stromal cells generates a neutrophil retention signal in human bone marrow niches as well as in zebrafish caudal hematopoietic tissue during development (Broxmeyer et al., 2005; Paredes-Zúñiga et al., 2017). Expression of *cxcl12a* has been observed in zebrafish by WISH in the head region (Hess and Boehm, 2012), lateral mesoderm (Torregroza et al., 2012), trunk (Venero Galanternik et al., 2016) and posterior lateral line primordium (Venkiteswaran et al., 2013). Of the reports of *cxcl12a* expression at 3dpf, mRNA is detected by WISH in the ventral side of the head region, caudal hematopoietic tissue and pronephric duct (Walters et al., 2010). There currently exists no evidence of *cxcl12a* expression in the caudal tail-fin 3dpf, although at 2dpf reports show expression in a population of cells at the end of the notochord protrusion which likely correlate with the cells of the posterior lateral line primordium (Walters et al., 2010). From my experiments using a *cxcl12a*:eGFP reporter line and whole mount *in situ* hybridisation, expression of Cxcl12a using both a transgenic reporter and WISH was observed in similar anatomical regions in the head, fins and trunk of larvae. Caudal tail-fin expression of *cxcl12a* appeared higher in the transgenic reporter, although this is likely due to differences in the sensitivity of the imaging performed between the experiments, where high power confocal microscopy was used to visualise the transgenic line whilst low power wide field light microscopy was used to visualise mRNA

following WISH experiments. Taken together I propose that the *cxcl12a*:eGFP reporter recapitulates *cxcl12a* mRNA expression seen by *in situ* hybridisation.

Experiments using a *cxcl12a*:eGFP transgenic reporter line were inconclusive due to the high constitutive levels of Cxcl12a expressed in the zebrafish tail-fin, which made distinguishing between constitutive and upregulated gene expression in injured larvae difficult**.** To improve assays to image the *cxcl12a*:eGFP transgenic line in the future, tail-fin transection could be performed in an anatomical region of the tail-fin away from the intensely bright notochord protrusion. I hypothesise that expression of *cxcl12a* by cells at the wound site in a region where basal levels of GFP intensity are lower would enable the detection of the transgene when driven by weaker promoters. Recent advances in *in vivo* imaging microfluidics devices for zebrafish larvae will enable the tracking of *cxcl12a* expressing cells in individual larvae prior to injury and rapidly following tail-fin transection (Ellett and Irimia, 2017). These new imaging devices hold the head and trunk of larvae in silicon moulds with their caudal tail-fins extruding from the edge. Using these moulds a pre-injury image can be taken and tail-fins can be transected whilst the larvae remain anaesthetised. Imaging of larvae can then continue almost immediately with larvae maintained in the same position. Currently these experiments are not possible to perform due to the requirement to mount larvae in agarose for imaging. In future I hope these new moulds will enable the detection of cells at a wound edge further away from the notochord protrusion and comparisons of individual larvae can be made pre and post injury, so that conclusions can be made with regards to *cxcl12a*:eGFP expression using the transgenic reporter line.

Evidence from WISH experiments illustrate that in uninjured larvae *cxcl12a* expression is detected at low levels at the end of the notochord protrusion, in correlation with the expression observed in the reporter line. The expression observed in uninjured larvae was comparable to that observed by other groups earlier in zebrafish development at 2dpf (Walters et al., 2010)**.** Staining for *cxcl12a* mRNA appeared to increase over time, in keeping with a significant body of evidence that illustrates a role for CXCL12 in tissue repair and regeneration (Bouzaffour et al., 2009; Itou et al., 2012). (Dufourcq and Vriz, 2006; Itou et al., 2012)(Itou et al., 2012). Following tail-fin amputation expression of CXCL12a is observed by WISH from 1 day post amputation and persists during fin regeneration until 5 days post amputation when a rapid downregulation is observed (Dufourcq and Vriz, 2006). It is proposed that CXCL12a is important in providing directional guidance cues to regulate endothelial cell migration during arterial morphogenesis in the regenerating fin (Xu et al., 2014). My data may support a

regenerative capacity for Cxcl12a following tail-fin amputation, as it looks like CXCL12a mRNA increases in expression in the tail-fin of larvae throughout the time course, although quantification of this observation by qPCR is required.

These experiments provide information about the spatial expression of *cxcl12a* mRNA within zebrafish larvae, where it looks like *cxcl12a* mRNA is expressed at the wound site. The limitations of using WISH to observe gene expression are the tissue resolution achieved imaging fixed stained tissue is limited such that the precise cell types expressing the gene could not be identified. WISH provides spatial information about gene expression but quantification is subjective and there exist more robust methods to quantify mRNA levels such as qPCR which could be employed in future. Furthermore, it should be considered that RNA expression is a useful but certainly far from perfect predictor of protein expression, where multiple processes contribute to the synthesis of a protein from its RNA transcript (Liu et al., 2016).

4.4.3   Production of Cxcl12a:eGFP by neutrophils

Neutrophils are the main producers of local CXCL12 in the trachea of influenza infected mice although the release of soluble CXCL12 from neutrophils was not detected (Lim et al., 2015). It was identified in mice that neutrophils migrating in infected lung tissue deposit CXCL12 enriched membrane particles (Lim et al., 2015). It has been proposed that this method of chemokine release provides a membrane tethered source of chemokine to act as a slow-release depot to induce T-cell migration, as opposed to the release of soluble CXCL12 which diffuses into the tissue or is degraded (Lim et al., 2015). There is relatively little known about the release means of CXCL12 by neutrophils, therefore the non-traditional CXCL12 deposition by neutrophils may be experimentally more complicated than anticipated (Lim et al., 2015). The RNA sequencing data suggests that zebrafish neutrophils at 5dpf express both *cxcl12a* and *cxcl12b* although the fpmk values for both genes are much lower than that of *cxcr4b*. The *cxcl12a*:eGFP transgene was not detectable in neutrophils in these experiments, which may be due to *cxcl12a* being switched on in neutrophils later than 3dpf. Potentially there are issues with detection of the transgene driven by the *cxcl12a* promoter, where the microscope settings used to visualise *cxcl12a*:eGFP expression in cells at the wound site may not enable the detection the transgene driven in cells weakly expressing the promoter. More conclusive data could be generated using FACS sorting to separate the *lyz*:mCherry neutrophil population from the rest of the cells in the zebrafish larvae (Rougeot et al., 2014). Quantitative PCR could then be performed on these cells to provide quantitative information about the expression of *cxcl12a* in injured and non-injured larvae at multiple time points throughout the inflammatory response. There is a body of evidence to

suggest that tissue epithelial cells are the predominant producers of CXCL12 in some inflammatory disease settings (Dotan et al., 2010; Petty et al., 2007). Perhaps damaged stromal cells at the wound site are the main producers of Cxcl12, as reported in injured lungs (Petty et al., 2007). In future it would be interesting to determine the cell types which produce CXCL12 in zebrafish, as the development of CRISPRi technology could enable inhibition of Cxcl12 production in these cells specifically.

4.4.4 Generation of a Cxcr4b transgenic reporter line using the Gal4 UAS system

The lack of tools available to study endogenous guidance signals *in vivo* has prevented the visualisation of physiological chemokine gradients. To circumvent these limitations, a novel system has been developed to provide a read out of chemokine activity by measuring receptor turnover at the cell surface. Cxcr4b receptor internalisation in response to Cxcl12a binding is a well characterised cellular response in zebrafish (Minina et al., 2007). A fluorescent timer approach has been used in zebrafish larvae to measure ligand-triggered Cxcr4b receptor turnover in the context of self-generated Cxcl12a gradients by cells of the posterior lateral line primordium (Donà et al., 2013). We proposed that adapting this system for visualisation of Cxcr4b in neutrophils would enable the visualisation of Cxcl12a gradients at the wound site in injured zebrafish larvae. A commonly used method of subcellular fluorescence labelling is using the Gal4-UAS two-component gene expression system (Brand and Perrimon, 1993). Gal4 is a yeast transcriptional activator which binds to and activates its specific effector upstream activating sequences (UAS). When expressed under the control of a tissue-specific promoter, Gal4 activates the transcription of UAS located in an expression cassette close to a minimal promoter upstream of the target gene of interest, such that expression of UAS is largely silent in the absence of Gal4. This results in the transcriptional activation of target genes found downstream of the UAS in specific tissues (del Valle Rodríguez et al., 2011).

I developed a stable transgenic zebrafish line driving the expression of a UAS coupled CXCR4b.GFP fusion construct in neutrophils expressing the Gal4 transcriptional activator under the *mpx* promoter. However, when I out crossed this line to a neutrophil reporter, I found that there was relatively little overlap between expression of the transgenes. The mCherry and Cxcr4b.GFP transgenes in the neutrophils are driven by two separate promoters in this system, suggesting that promoter competition whereby the transcription of one transgene is preferential over the other, is unlikely. The hematopoietic cells in the CHT are immature progenitors to mature cells and could be precursors for different lineages (Tamplin et al., 2015). The CHT cells could be at different developmental stages where in some instances the lyz promoter is switched on

before the Gal4, and vice versa. A second explanation is that perhaps the transcriptional machinery required to drive the expression of the transgenes is utilised by the strong Gal4 promoter, such that in cells where the one of the promoters is switched on before the other, the expression of one of the transgenes occurs at the expense of the other. Regardless of the explanation, it is clear that not every cell in larvae is labelled with the Cxcr4b.GFP transgene.

Initial experiments were performed using the tail-fin transection assay to visualise Cxcr4b.GFP localisation in neutrophils recruited to the wound site. Unfortunately, these experiments were not successful, as neutrophil recruitment to the wound site was severely impaired in the reporter line. Interestingly this phenotype is observed in a zebrafish model for WHIM syndrome in which neutrophils are inappropriately retained in the CHT due to over active CXCR4/CXCL12 signalling (Walters et al., 2010). WHIM zebrafish express a mutant allele of CXCR4b with a c-terminal truncation which renders the receptor unable to be internalised resulting in increased surface expression. Furthermore, Cxcr4b loss of function mutant zebrafish larvae exhibit increased neutrophil recruitment to tail-fin injury, where it is proposed that inhibition of neutrophil retention infers increased sensitivity to chemokine gradients released at the wound site (Paredes-Zúñiga et al., 2017). I hypothesised that the expression of both endogenous CXCR4b and Gal4 driven CXCR4b.GFP in this reporter line could over activate the CXCR4/CXCL12 signalling axis, resulting in the inappropriate retention of neutrophils in the CHT and decreased sensitivity to chemoattractant gradients at the wound site. I tested this hypothesis by crossing the Cxcr4b.GFP reporter zebrafish line to the *lyz*:mCherry transgenic reporter line. I have demonstrated that these larvae have a population of neutrophils which express the Cxcr4b.GFP transgene in addition to endogenous *cxcr4b*, as well as a neutrophil population unlabelled with the transgene which express only endogenous Cxcr4b. I utilised these larvae containing both wildtype and transgenic neutrophils and demonstrated that wildtype neutrophils were recruited to tail-fin injury whilst neutrophils expressing the Cxcr4b.GFP transgene were not seen at the wound site. This illustrates that the Cxcr4b.GFP reporter line is functional, however renders this zebrafish line useless for the experiments I wished to perform. In future it would be interesting to determine if preventing signalling through the Cxcr4b.GFP receptor could rescue the defect in neutrophil recruitment. Similarly interruption of endogenous CXCR4/CXCL12 signalling axis using chemical inhibitors or CRISPR may also rescue the recruitment defect of neutrophils over-expressing Cxcr4b.

4.5 Using AMD3100 to inhibit the CXCR4/CXCL12 signalling axis in zebrafish

The role for the CXCR4/CXCL12 signalling axis in zebrafish developmental processes has been elucidated largely using genetic studies to knock down the genes encoding the CXCR4 and CXCL12 proteins (Donà et al., 2013; Haas and Gilmour, 2006; Valentin et al., 2007). One of the advantages of using the zebrafish as a model to study inflammation is that chemical compounds can be used to manipulate signalling pathways, where several compounds which target neutrophils have been identified using this approach (Robertson et al., 2016, 2014). There are a broad range of chemical compounds used to inhibit CXCR4/CXCL12 signalling in humans, however few reports of the use of these inhibitors exist in zebrafish. AMD3100 has been used to inhibit the CXCR4/CXCL12 signalling axis in a limited number of studies in zebrafish larvae, where concentrations ranging from 10-30µM have been administered to larvae through incubation in fish water for up to 24 hours (Tamplin et al., 2015). Experimental results using chemical inhibitors should be interpreted with care as compounds can target multiple receptors on different cell types. In particular AMD3100 can target Cxcr4a and b, as well as the scavenger receptor Cxcr7, all of which are expressed on multiple cell type in zebrafish (Donà et al., 2013).

4.5.1 Transient inhibition of CXCR4/CXCL12 signalling does not affect haematopoiesis during early development

When inhibiting signalling pathways which are important in developmental processes in a broad number of cell types, it is important to determine any off target or toxic side effects. The CXCR4/CXCL12 signalling axis regulates neutrophil mobilisation from the bone marrow to the circulation (Broxmeyer et al., 2005). Mice with a myeloid lineage CXCR4 deletion have increased numbers of circulating neutrophils (Eash et al., 2009). Zebrafish mutants lacking a functional Cxcl12a or Cxcr4b receptor show increased numbers of circulating neutrophils and disrupted granulopoiesis in the kidney at later stages of development, although this phenotype is not observed at 3dpf (Paredes-Zúñiga et al., 2017). Before performing experiments using AMD3100 to elucidate the role of the CXCR4/CXCL12 signalling axis in the regulation of inflammation resolution, I demonstrated that inhibition of CXCR4/CXCL12 signalling does not affect whole body neutrophil counts. No signs of toxicity were observed in larvae following administration of AMD3100 by either incubation or injection for up to 24 hours post administration. These data support similar findings that the number of neutrophils in the CHT and kidney at 3dpf are not changed in Cxcr4b or Cxcl12a mutant zebrafish larvae (Paredes-Zúñiga et al., 2017). These data demonstrate that early haematopoiesis is not affected by AMD3100

in these experiments, such that any phenotype observed in larvae following treatment with AMD3100 should not be attributed to a difference in whole body neutrophil counts.

4.5.2 Inhibition of CXCR4/CXCL12 signalling does not affect CHT colonisation by neutrophils

I next aimed to demonstrate that AMD3100 could affect neutrophils specifically by attempting to interrupt CXCR4/CXCL12 processes involved in regulating neutrophils in larvae. In zebrafish, definitive hematopoietic stem and progenitor cells (HSPCs) give rise to all blood cells in the dorsal aorta where they are released into the circulation (Bertrand et al., 2010). HSPCs colonise the caudal hematopoietic tissue, an intermediate niche enriched in Cxcl12a where they differentiate into terminally differentiated blood cells including neutrophils, before colonising the adult marrow which in zebrafish is the kidney (Tamplin et al., 2015). A dose dependent reduction in HSPC markers *rux1* and *cmyb* assessed by WISH was observed in larvae treated with AMD3100 from 48-72hpf (Tamplin et al., 2015). Based on this evidence, I hypothesised that AMD3100 may reduce the colonisation of neutrophils arising from HSPCs in the CHT, which would be useful to provide evidence of a neutrophil specific effect of AMD3100. The data from these experiments illustrates that CXCR4/CXCL12 inhibition using AMD3100 does not affect the neutrophil population in the CHT. Perhaps the *cmyb runx1* positive progenitors which are reduced following AMD3100 treatment (Tamplin et al., 2015) may give rise to other blood cell populations. This could explain why CHT colonisation by neutrophils specifically was not effected in my experiments. I could not draw conclusions about the cell autonomous effects of AMD3100 from these experiments so I next aimed to study the retention of neutrophils in the CHT to demonstrate a cell autonomous effect of CXCR4/CXCL12 inhibition using AMD3100.

4.5.3 Inhibition of CXCR4/CXCL12 does not affect neutrophil retention in the CHT

As previously described, over-active CXCR4/CXCL12 signalling results in WHIM syndrome (Kawai and Malech, 2009). The retention of neutrophils in bone marrow niche is proposed to be a tug of war between neutrophil retention signalling through CXCR4/CXCL12 and chemoattractant gradients such as CXCL8 and G-CSF which mobilise neutrophils in to the bloodstream (Eash et al., 2010). AMD3100 is used clinically in combination with G-CSF as a mobiliser of stem cells from bone marrow into the circulation for use in transplantation in multiple melanoma patients (Liles et al., 2003). In zebrafish, neutrophil retention in the CHT is disrupted in Cxcr4b and Cxcl12a mutant larvae where the number of circulating neutrophils is increased in larvae between 5-13 days post fertilisation (Paredes-Zúñiga et al., 2017). I hypothesised that inhibition of

CXCR4/CXCL12 signalling could mobilise neutrophils from the CHT to demonstrate a cell-autonomous effect of CXCR4 inhibition using AMD3100. These experiments identified that CXCR4 inhibition using AMD3100 did not release neutrophils from the CHT. Perhaps inhibition of the neutrophil retention signal alone without the presence of a mobilisation signal is insufficient to drive neutrophils out of the CHT. In future, inhibition of the CXCR4/CXCL12 signalling axis in combination with mobilisers of neutrophils such as exogenous CXCR2 or G-CSF, could be useful to determine if CXCR4 inhibition augments neutrophil release from the CHT. Similarly, performing tail-fin injury in combination with AMD3100 could provide endogenous mobilisation signals for neutrophils to determine if AMD3100 can augment the release of neutrophils from the CHT. It is possible that the dose of AMD3100 used to inhibit the CXCR4 receptor may not be sufficient to recapitulate findings observed in zebrafish mutants. This could be due to the surface expression of CXCR4 on neutrophils being too high for AMD3100 to prevent signalling at the concentration used, or due to problems with bioavailability of the compound associated with administration of compounds via incubation. In future it would be interesting to determine whether genetic manipulation of the CXCR4/CXCL12 axis using CRISPR and CRISPRi technology could release neutrophils from the CHT.

4.5.4   Inhibition of CXCR4/CXCL12 signalling increases neutrophil recruitment to the wound site

The recruitment of neutrophils to the wound site has been shown to increase in CXCR4b mutant larvae where it is suggested that this is due to loss of neutrophil retention signalling in the CHT, resulting in neutrophils being more able to respond to other chemotactic gradients (Paredes-Zúñiga et al., 2017). My data demonstrates that this effect can be recapitulated by chemically inhibiting CXCR4/CXCL12 signalling, although only when AMD3100 is administered by injection into the circulation. Experiments performed to administer AMD3100 by injection and incubation were performed at different developmental stages and are therefore not comparable. I propose that differential expression of Cxcr4b on neutrophils at 2 and 3dpf could confer the difference in neutrophil recruitment to the wound site observed between experiments. Furthermore, neutrophils could be more sensitive to CXCR4 inhibition at 2dpf due to differences in Cxcr4b receptor expression or Cxcl12a ligand production by stromal cells in the CHT. Alternatively, the differences in neutrophil recruitment observed between the two assays could be due to the bioavailability of the compound being higher in injected larvae compared to those incubated in the compound. These questions can be answered by administering AMD3100 by injection and incubation to larvae at 2dpf, to determine if the developmental stage of administration method is important. A further

consideration is that AMD3100 binds to the scavenger receptor Cxcr7 which modulates Cxcl12a concentration by acting as a sink receptor, the expression of which could be expressed differentially at these different stages of development (Donà et al., 2013).

4.5.5 Inhibition of CXCR4/CXCL12 signalling accelerates inflammation resolution by promoting reverse migration

A large body of evidence now exists to suggest a role for the CXCR4/CXCL12 signalling axis in modulating neutrophil retention at inflammatory sites. Aside from this signalling axis generating a neutrophil retention signal in multiple physiological settings (Eash et al., 2010; Suratt et al., 2004), neutrophils taken from patients with chronic inflammatory disease have increased CXCR4 expression, and CXCL12 is produced at sites of lung injury (Hartl et al., 2008; Yamada et al., 2011). A specific role for the CXCR4/CXCL12 signalling axis in modulating inflammation resolution has recently been suggested following the study of neutrophil behaviour at wound sites in zebrafish Cxcr4b and Cxcl12a mutant larvae (Paredes-Zúñiga et al., 2017). To begin to address the key questions of this work, I assessed the effects of CXCR4/CXCL12 inhibition using AMD3100 on the resolution of neutrophilic inflammation using a transgenic reporter lines (Elks et al., 2011; Renshaw and Loynes, 2006). Inflammation resolution assays using pharmacological compounds have been performed in zebrafish larvae where it has been shown that compounds can regulate inflammation resolution by both delaying and accelerating neutrophil removal from the wound site (Elks et al., 2011; Robertson et al., 2014). I hypothesised that if a neutrophil retention signal generated through CXCR4/CXCL12 signalling exists at the wound site, interruption of this signal using AMD3100 to inhibit the CXCR4 receptor would accelerate neutrophil removal from the wound site.

Inhibition of CXCR4/CXCL12 signalling in these assays did not affect neutrophil recruitment to the wound site. AMD3100 was administered to larvae at 4hpi when the majority of neutrophil recruitment had occurred, such that the increased recruitment seen previously was not recapitulated in these experiments. Screening for good responders at 4hpi prior to AMD3100 administration reduced the noise produced by fish-to-fish variation within the assay such that only larvae with similar number of neutrophils at the wound site were selected for experiments. Inhibition of CXCR4/CXCL12 signalling by administration of AMD3100 via injection and incubation reduced the number of neutrophils at the wound site during the resolution phase of inflammation.

The resolution of inflammation in zebrafish is the result of the contribution of neutrophil apoptosis and removal by macrophages, and the reverse migration of neutrophils away from the wound site. I next aimed to assess the contribution of neutrophil reverse migration to driving the resolution of inflammation in this system, a phenomenon which

has been observed by multiple research groups in zebrafish, as well as in mammalian systems (Buckley et al., 2006; Elks et al., 2011; Robertson et al., 2014; Wang et al., 2017). Transendothelial migration of neutrophils has recently been observed in mice, providing some of the first *in vivo* evidence that neutrophils are able to re-enter the circulation following their role at an inflammatory site (Wang et al., 2017). Neutrophils in zebrafish tissue appear to migrate preferentially back through the tissue of the tail-fin rather than back into the vasculature (Holmes et al., 2012). We propose that targeting neutrophil reverse migration will be of therapeutic benefit to drive neutrophils away from inflammatory sites in a chronic inflammatory disease setting. Using zebrafish larvae expressing the photoconvertible protein Kaede in neutrophils, I demonstrated that inhibition of CXCR4/CXCL12 signalling by administration of AMD3100 via injection or incubation drives the reverse migration of neutrophils. I confirmed that this effect was not due to an increased number of photoconverted neutrophils in the AMD3100 treatment group.

It is likely that of the two Cxcr4 isoforms expressed on zebrafish neutrophils, the effects seen using AMD3100 are due to inhibition of Cxcr4b, which my data suggests are expressed at significantly higher levels than Cxcr4a. AMD3100 can also act as an allosteric agonist of CXCR7 (Kalatskaya et al., 2009), which functions as a decoy receptor for CXCL12, with a role in cell generation of self-gradients which is crucial for proper migration of primordial germ cells toward their targets in zebrafish (Boldajipour et al., 2008). Activation of CXCR7 fails to couple to G-proteins and to induce chemokine receptor mediated cellular responses, so AMD3100 is unlikely to activate downstream signalling pathways (Naumann et al., 2010). Cxcr7 may modulate neutrophil sensitivity to Cxcl12 concentration, through its scavenging of the chemokine which reduces the level of the Cxcl12 in the local tissue environment (Bussmann and Raz, 2015). The function of Cxcr7 in this context could be investigated in future using CRISPR/Cas9.

Taken together these data demonstrate that inhibition of the CXCR4/CXCL12 signalling axis drives the resolution of inflammation by increasing neutrophil reverse migration, and support the hypothesis that neutrophil desensitisation to gradients at the wound site results in their passive migration away from the wound site (Holmes et al., 2012). These data add to the existing evidence that neutrophil reverse migration can be targeted pharmacologically to drive the resolution of inflammation. A similar effect to that reported in larvae treated with Tanshinone IIA in a similar assay is seen in larvae treated with AMD3100 (Robertson et al., 2014). The target of Tanshinone IIA is unknown but perhaps interferes with signalling pathways associated with CXCR4 signalling. Inhibition of CXCR4 signalling using AMD3100 is sufficient to promote neutrophil reverse migration

190

away from the wound site, but not to mobilise them from the CHT. I propose that the bioavailability of AMD3100 in these assays is sufficient to compete with the tissue concentration of Cxcl12a at the wound site, whereas Cxcl12a in the CHT might be markedly higher, reducing the ability of the compound to bind to receptors. Furthermore, Cxcr4 expression on the neutrophil surface may be different in activated neutrophils at the wound site compared to resting neutrophils in the CHT, which could further explain why interruption of neutrophil retention through CXCR4/CXCL12 signalling causes an effect in one assay and not another.

A recent role for neutrophil chemokinesis at the wound site has been implicated in modulating neutrophil reverse migration from the wound site (Powell et al., 2017). Reverse migration is impaired in Cxcr2 deficient zebrafish larvae where neutrophils are inappropriately retained at the wound site. It has been proposed that altered susceptibility of neutrophils to gradients at the wound site in Cxcr2 deficient larvae drives their passive migration away from the wound site (Powell et al., 2017). As the CXCR4 and CXCR2 signalling axis is known to antagonistically regulate neutrophil retention in other models (Eash et al., 2010), I propose that the combined outcome of CXCR4 and CXCR2 signalling could modulate the migration of neutrophils during inflammation resolution. It would be interesting to combine CXCR4 and CXCR2 inhibition using both chemical and genetic approaches to determine the outcome on reverse migration. Furthermore, it would be interesting to determine the difference observed in a whole-embryo knock down of Cxcr4b compared to knocking out the receptor specifically in neutrophils. This work is now possible due to the generation of a zebrafish line expressing a dead Cas9 under the neutrophil specific *mpx* promoter (Renshaw group, unpublished).

In future, I would like to investigate the role of AMD3100 in driving neutrophil apoptosis to determine the relative contribution of reverse migration compared to apoptosis in driving inflammation resolution when the CXCR4/CXCL12 signalling axis is inhibited.

These data are exciting as they provide the first evidence that CXCR4 signalling directly regulates neutrophil retention at inflammatory sites. Before drawing firm conclusions about the role for CXCR4 signalling in neutrophil retention it is important that these findings can be recapitulated. Using a second CXCR4 inhibitor as well as genetically manipulating *cxcr4b* and *cxcl12a* would consolidate these findings. For now, these data provide the first evidence that that CXCR4/CXCL12 signalling axis may regulate inflammation resolution.

5 Final discussion and future work

Tissue cues derived from injured cells, recruited blood cells, tissue resident cells and potential pathogens direct neutrophil responses in inflamed tissue. With the relatively recent identification of neutrophil swarming and neutrophil reverse migration, the layers of regulation involved in neutrophil migration in inflamed tissues are becoming increasingly more complex. Understanding the mechanisms which modulate the migration of neutrophils throughout the entirety of the inflammatory response may help to identify novel pathways which may serve as targets for therapeutic intervention in chronic inflammatory diseases. Here I investigated the migratory behaviours of neutrophils during the inflammatory response using a well characterised tail-fin transection model to induce inflammation in zebrafish. The tail-fin transection model is suitable for observing neutrophil behaviour throughout the entirety of the inflammatory response, as transgenic zebrafish reporter lines enable the visualisation of both neutrophil recruitment to and removal from the wound site. To this end I studied neutrophil swarming behaviour of neutrophils which arises following the coordinated migration of neutrophils during their recruitment to the wound site, and the reverse migration of neutrophils away from the wound site during the resolution phase of inflammation. This approach utilised the high resolution achieved by imaging zebrafish tissue and the ability to study neutrophil migration at the single-cell level.

5.1 Characterisation of the neutrophil swarming response in zebrafish

Using *in vivo* imaging to visualise neutrophil migration towards wound sites in transgenic zebrafish larvae, I identified that neutrophil swarming occurs at sites of tissue injury in zebrafish. This study provides the first report of an endogenous neutrophil swarming response in a physiologically relevant *in vivo* tissue injury model. I have performed in depth characterisation of the swarming response and identified similarities between swarming of zebrafish neutrophils with mammalian neutrophils. I have identified a multi stage series of events leading to swarm formation. These experiments illustrate that tissue wounding induces the migration of neutrophils proximal to the wound site (scouting). I have described that a swarm-initiating pioneer neutrophil changes its behaviour at the wound site to adopt a phenotype markedly different to neutrophils in the same tissue context. The migration of neutrophils towards the pioneer neutrophil is then observed, resulting in the swarming of neutrophils in large aggregates at the wound site. The stages described have overlap with those identified in mouse models of swarming, and suggest that the swarming response is likely to occur with similar

dynamics between species. The variation in models used to study swarming makes this difficult to determine for certain.

Many of the inflammatory mediators which promote the swarming response and maintain neutrophil aggregation in clusters are likely to overlap with the signals produced by damaged cells at the wound site, which are a prerequisite for neutrophil recruitment to the wound site (Lämmermann et al., 2013; Reátegui et al., 2017). Limitations in inducing an endogenous swarming response in the zebrafish model include the difficulties associated with the loss-of-function studies required to determine the precise role of signaling in modulating swarming at each stage. Here depleting key signaling pathways required for neutrophil extravasation or initial recruitment to wound sites may inhibit the neutrophilic response. The protocol used to study neutrophil swarming in mice bypasses the extravasation step, enabling the role for these signaling pathways in modulating tissue migration to be established. The zebrafish provides an experimental advantage when studying neutrophil swarm initiation. The neutrophil transplant models used to study swarming in mice circumvent a large proportion of the neutrophil recruitment cascade, making swarm initiation difficult to study. Here the zebrafish has been identified as a strong model to study the initiation of the swarming response, and the tools available to study mechanisms of swarm initiation are promising.

Finally, I identified that the spatiotemporal aspects of neutrophil swarming highlight a role for a tissue context in swarm initiation. From my own observations and evidence in the literature, I hypothesise that pioneer neutrophils encounter a tissue context at the wound site which induces their programmed cell death and subsequent neutrophil swarming. Here I utilised the tools available in our group to begin to study hydrogen peroxide signaling at the wound site. I developed an assay to measure hydrogen peroxide concentration in pioneer neutrophils prior to the swarming response, which in future will be used to determine whether hydrogen peroxide plays a role in swarm initiation.

5.2   Investigating cell death signalling in the context of swarm initiation

I have identified the advantages of using the zebrafish to study the initiation of neutrophil swarming and developed assays to investigate cell death signalling in the context of neutrophil swarm induction. Using a combination of transgenic reporter lines and cell viability stains I have begun to investigate the role of cell death signalling in swarm initiation.

Here I have identified that pioneer neutrophils do not become propidium iodide positive prior to swarm formation. This is contrary to the evidence from mouse studies which

correlates the appearance of propidium iodide positive neutrophils at the wound site with the amplification of neutrophil recruitment to the wound site (Lämmermann et al., 2013). As discussed previously, the neutrophil transfer model to study swarming in mice circumvents the extravasation stage of neutrophil recruitment to the wound. I propose that studying the initiation of the swarming response in a model which bypasses a large part of this stage is sub-optimal. The zebrafish is a more appropriate model to observe the initiation of neutrophil swarming as the behaviour of endogenous neutrophil recruitment can be tracked within minutes following initiation of the inflammatory response. Using this model, I observed the recruitment of swarm-initiating pioneer neutrophils prior to the initiation of the swarming response. Here propidium iodide stained a population of cells at the wound site and often staining was observed deeper into the tissue at the wound edge than the pioneer neutrophil, eradicating any issues associated with the tissue penetration depth of propidium iodide. Propidium iodide labels cells which have lost their membrane integrity, so cell death by primary or secondary necrosis are ruled out to some extent as initiators of neutrophil swarm formation, although further non-related assays to study this type of cell death should be employed before drawing this conclusion. Furthermore the release of nuclear material from the cell, for example during NETosis, would be labelled with propidium iodide, although I propose that a higher dose of PI would be required to visualise these fragments of nuclear material in comparison to the rupture of a cell and release of the entire contents of the nucleus. In future it would be good to confirm these findings using another cell viability assay.

After observing that pioneer neutrophils did not become propidium iodide positive prior to swarm formation I hypothesised that pioneer neutrophils were apoptotic. My data illustrates that the initiation phase of swarming can persist for up to an hour, so I proposed that a programmed cell death may be relevant. Furthermore, apoptotic cells may release 'find me' cues to recruit macrophages to ensure the rapid removal of apoptotic corpses, so I proposed that 'find me' cues could be involved in the chemoattraction of neutrophils towards the pioneer. However, here I demonstrated that pioneer neutrophils do not undergo caspase-3 mediated apoptosis prior to neutrophil swarming. Moreover, cell death by apoptosis does not induce neutrophil swarms. It would be useful to recapitulate these findings using secondary assays as discussed previously. The limitations with using the FRET reporter line to study apoptosis in these assays is that only a read out for caspase-3 mediated apoptosis is provided. Apoptosis can occur independently of caspases; the release of apoptosis-inducing factor from mitochondria also drives cells down the apoptotic pathway (Candé et al., n.d.). This form

of cell death cannot be ruled out from these experiments. The main limitation associated with these assays to study cell death is that multiple methods to confirm one cell death mechanism should be employed before conclusions are made. Furthermore, imaging of transgenic zebrafish lines is relatively low throughput. Imaging of larvae is time consuming which limits the number of larvae, and thus the number of examples of neutrophil swarming, observed per experiment. Currently there is no alternative approach to study swarming, hence assays should be repeated in future to generate ample evidence.

In future, the study of alternative cell death mechanisms including NETosis, pyroptosis, necroptosis and caspase-3 independent apoptosis should be investigated. Once the behaviour of pioneer neutrophils has been identified, the signalling molecules which mediate the initiation of neutrophil swarming could begin to be investigated.

5.3 Elucidating the mechanisms governing neutrophil reverse migration

I next investigated neutrophil migration in the context of inflammation resolution. I investigated the hypothesis that neutrophils are held at inflammatory sites by retention signals, the interruption of which results in their stochastic redistribution into the tissue by reverse migration. I have investigated the expression of candidate G protein coupled receptor Cxcr4b and its ligand Cxcl12a at the wound site in zebrafish larvae.

5.3.1 Cxcr4b and Cxcl12a are strong candidates for retention signaling in zebrafish

I sought to determine whether the molecular components required to generate a retention signal were expressed in the context of inflammation in zebrafish larvae. The molecular candidates investigated were the CXCR4 receptor and its ligand CXCL12. Here I identified that during early development neutrophils predominantly express the Cxcr4b isoform, in keeping with evidence in the literature (Walters et al., 2010). Together with existing evidence the data illustrated here suggest that the components required for retention signaling between neutrophils and the wound site are present. There exists mounting evidence to implicate the CXCR4/CXCL12 signaling axis in modulating neutrophil retention at inflammatory sites (Paredes-Zúñiga et al., 2017; Yamada et al., 2011), so it is likely that a degree of conservation exists between species. Aside from the CXCR4/CXCL12 signaling axis being present at the wound site in zebrafish larvae, is not clear from these studies how retention signaling works. The previously described stochastic redistribution of neutrophils into the tissue during reverse migration in zebrafish (Holmes et al., 2012) could be attributed to changes in neutrophil sensitivity to

local gradients. Neutrophil sensitivity could be altered by a change in Cxcl12a concentration at the wound site, reduced Cxcr4b expression on the neutrophil surface, or a combination of the two. As Cxcl12a expression seems to increase throughout the time course, it could be that ligand-induced receptor internalisation characteristic of GPCR signaling, modulates neutrophil sensitivity to Cxcl12a through reducing Cxcr4b expression on the neutrophil surface. The temporal expression of Cxcl12a at the wound site remains to be quantified and the development of a functional Cxcr4b.GFP reporter line may provide insight into how retention signals are generated. From these experiments I can conclude that the CXCR4/CXCL12 signaling axis is expressed at the wound site during inflammation, and could therefore play a role in its modulation.

5.3.2 Inhibition of the CXCR4/CXCL12 signaling axis accelerates inflammation resolution

In this section of work I used a pharmacological approach to inhibit the CXCR4/CXCL12 signaling axis using AMD3100 to antagonize the CXCR4 receptor. I aimed to determine the effect of CXCR4 on inflammation using our well characterized *mpx*:GFP reporter line (Renshaw and Loynes, 2006), and to look specifically at neutrophil reverse migration using a photoconvertible system where neutrophils at the wound site can be tracked following photoconversion (Elks et al., 2011; Ellett et al., 2015; Robertson et al., 2014). Using AMD3100 I recapitulated the phenotype observed in Cxcr4b and Cxcl12a mutant zebrafish larvae, where neutrophil recruitment to the wound site is increased. Perhaps the most significant finding was the identification that inhibition of the CXCR4/CXCL12 signaling axis accelerates inflammation resolution. Here I found that reverse migration of neutrophils was increased in larvae where the CXCR4 signaling axis was inhibited. This is exciting as it provides the first evidence to directly implicate the CXCR4/CXCL12 signaling axis in modulating neutrophil retention at wound sites.

These findings could fit into the current paradigm that CXCR2 signaling drives neutrophil reverse migration through modulating neutrophil sensitivity to other gradients (Powell et al., 2017). Here Cxcr2 could modulate neutrophil sensitivity to Cxcl12 gradients, resulting in their desensitization subsequent reverse migration by passively redistributing into the tissue. Much work is required to investigate the dual role for CXCR4 and CXCR2 signaling, although antagonistic regulation by these two receptors in combination modulates neutrophil retention in other systems, so this could be the case here. The limitations associated with using pharmacological compounds to inhibit signaling pathways can be overcome by using a genetic approach to study the CXCR4/CXCL12 signaling axis. To investigate the role of Cxcr4b specifically in retention

signalling, CRISPRi will be used to achieve a neutrophil specific knock down of the Cxcr4b receptor.

5.3.3 Final conclusions and closing remarks

To summarise, I have described the migratory behaviour of neutrophils during the swarming response which has not yet been characterised in zebrafish and have begun to investigate cell death signalling in the context of neutrophil swarm initiation. The in depth characterisation of neutrophil swarming in this study has identified that the zebrafish model can be used to study the neutrophil swarming response at all of its stages. I have identified that the Cxcr4b receptor is expressed on zebrafish neutrophils and its ligand Cxcl12a is expressed at wound sites. Finally this study implicates the CXCR4/CXCL12 signalling axis in modulating neutrophil retention at inflammatory sites, as inhibition of the CXCR4 receptor accelerates inflammation resolution by promoting reverse migration. Together these findings have demonstrate that neutrophil migratory behaviours during the inflammatory response can be targeted at multiple points to produce a favourable outcome in terms of inflammation.

The identification of novel neutrophil migration patterns including neutrophil swarming and reverse migration add complexity to the modulation of neutrophil migration and retention within inflamed tissue. The precise physiological role for neutrophil swarming has not yet been determined, and thus the outcome of the swarming response in tissue is unknown. The recent identification that neutrophil swarms may modulate their own resolution through the release of lipids and proteins, suggests that swarm resolution may be important an important driver of inflammation resolution (Reátegui et al., 2017). A role for neutrophil retention signalling within neutrophil clusters is reasonable to suggest. Perhaps neutrophil swarming is modulated by retention signals generated through CXCR4/CXCL12, where AMD3100 could interrupt the clustering of neutrophils and drive their reverse migration. Future studies should combine the study of neutrophil swarm resolution with dissecting the drivers of neutrophil removal from the wound site.

Expanding our knowledge on the precise modulators of neutrophil migration both to and from sites of inflammation is essential, and may help to identify novel targets to drive the resolution of inflammation in the context of chronic inflammation. Much work is required to further confirm the role for the CXCR4/CXCL12 signalling axis in modulating neutrophil retention at inflammatory sites, although this study provides evidence that this is important.

References

Afonso, P. V, Janka-Junttila, M., Lee, Y.J., McCann, C.P., Oliver, C.M., Aamer, K.A., Losert, W., Cicerone, M.T., Parent, C.A., 2012. LTB(4) IS A SIGNAL RELAY MOLECULE DURING NEUTROPHIL CHEMOTAXIS. Dev. Cell 22, 1079–1091.

Aiuti, A., Webb, I.J., Bleul, C., Springer, T., Gutierrez-Ramos, J.C., 1997. The chemokine SDF-1 is a chemoattractant for human CD34+ hematopoietic progenitor cells and provides a new mechanism to explain the mobilization of CD34+ progenitors to peripheral blood. J. Exp. Med. 185, 111–20.

Alessandri, A.L., Sousa, L.P., Lucas, C.D., Rossi, A.G., Pinho, V., Teixeira, M.M., 2013. Resolution of inflammation: Mechanisms and opportunity for drug development. Pharmacol. Ther. 139, 189–212.

Baetu, T.M., 2016. The "Big Picture": The Problem of Extrapolation in Basic Research. Br. J. Philos. Sci. 67, 941–964.

Barton, G.M., 2008. A calculated response: Control of inflammation by the innate immune system. J. Clin. Invest. 118, 413–420.

Beiter, K., Wartha, F., Albiger, B., Normark, S., Zychlinsky, A., Henriques-Normark, B., 2006. An Endonuclease Allows Streptococcus pneumoniae to Escape from Neutrophil Extracellular Traps. Curr. Biol. 16, 401–407.

Bennett, C.M., Kanki, J.P., Rhodes, J., Liu, T.X., Paw, B.H., Kieran, M.W., Langenau, D.M., Delahaye-Brown, A., Zon, L.I., Fleming, M.D., Look, A.T., 2001. Myelopoiesis in the zebrafish, Danio rerio. Blood 98, 643–51.

Bertrand, J.Y., Chi, N.C., Santoso, B., Teng, S., Stainier, D.Y.R., Traver, D., 2010. Haematopoietic stem cells derive directly from aortic endothelium during development. Nature 464, 108–111.

Boldajipour, B., Mahabaleshwar, H., Kardash, E., Reichman-Fried, M., Blaser, H., Minina, S., Wilson, D., Xu, Q., Raz, E., 2008. Control of Chemokine-Guided Cell Migration by Ligand Sequestration. Cell 132, 463–473.

Bolotin, A., Quinquis, B., Sorokin, A., Ehrlich, S.D., 2005. Clustered regularly interspaced short palindrome repeats (CRISPRs) have spacers of extrachromosomal origin. Microbiology 151, 2551–2561.

Borregaard, N., Cowland, J.B., 1997. Granules of the human neutrophilic polymorphonuclear leukocyte. Blood 89, 3503–21.

Bournazou, I., Pound, J.D., Duffin, R., Bournazos, S., Melville, L.A., Brown, S.B., Rossi, A.G., Gregory, C.D., 2008. Apoptotic human cells inhibit migration of granulocytes via release of lactoferrin. J. Clin. Invest. 119, 20–32.

Bouzaffour, M., Dufourcq, P., Lecaudey, V., Haas, P., Vriz, S., 2009. Fgf and Sdf-1 Pathways Interact during Zebrafish Fin Regeneration. PLoS One 4, e5824.

Brand, A.H., Perrimon, N., 1993. Targeted gene expression as a means of altering cell fates and generating dominant phenotypes. Development 118, 401–15.

Brinkmann, V., Reichard, U., Goosmann, C., Fauler, B., Uhlemann, Y., Weiss, D.S., Weinrauch, Y., Zychlinsky, A., 2004. Neutrophil Extracellular Traps Kill Bacteria. Science (80-.). 303, 1532–1535.

Brinkmann, V., Zychlinsky, A., 2012. Neutrophil extracellular traps: Is immunity the second function of chromatin? J. Cell Biol. 198, 773–783.

Broxmeyer, H.E., Orschell, C.M., Clapp, D.W., Hangoc, G., Cooper, S., Plett, P.A., Liles, W.C., Li, X., Graham-Evans, B., Campbell, T.B., Calandra, G., Bridger, G., Dale, D.C., Srour, E.F., 2005. Rapid mobilization of murine and human hematopoietic stem and progenitor cells with AMD3100, a CXCR4 antagonist. J. Exp. Med. 201, 1307–1318.

Buckley, C.D., Ross, E. a, McGettrick, H.M., Osborne, C.E., Haworth, O., Schmutz, C., Stone, P.C.W., Salmon, M., Matharu, N.M., Vohra, R.K., Nash, G.B., Rainger, G.E., 2006. Identification of a phenotypically and functionally distinct population of long-lived neutrophils in a model of reverse endothelial migration. J. Leukoc. Biol. 79, 303–311.

Burdon, P.C.E., Martin, C., Rankin, S.M., 2008. Migration across the sinusoidal endothelium regulates neutrophil mobilization in response to ELR + CXC chemokines. Br. J. Haematol. 142, 100–108.

Bussmann, J., Raz, E., 2015. Chemokine-guided cell migration and motility in zebrafish development. EMBO J. 34, 1309–18.

Candé, C., Cohen, I., Daugas, E., Ravagnan, L., Larochette, N., Zamzami, N., Kroemer, G., n.d. Apoptosis-inducing factor (AIF): a novel caspase-independent death effector released from mitochondria. Biochimie 84, 215–22.

Chen, A.T., Zon, L.I., 2009. Zebrafish blood stem cells. J. Cell. Biochem. 108, 35–42.

Chitramuthu, B.P., Bennett, H.P.J., 2013. High resolution whole mount in situ hybridization within zebrafish embryos to study gene expression and function. J. Vis. Exp. e50644.

Cho, H., Hamza, B., Wong, E.A., Irimia, D., 2014. On-demand, competing gradient arrays for neutrophil chemotaxis. Lab Chip 14, 972–8.

Chong, S.W., Emelyanov, A., Gong, Z., Korzh, V., 2001. Expression pattern of two zebrafish genes, cxcr4a and cxcr4b. Mech. Dev. 109, 347–54.

Chow, O.A., von Köckritz-Blickwede, M., Bright, A.T., Hensler, M.E., Zinkernagel, A.S., Cogen, A.L., Gallo, R.L., Monestier, M., Wang, Y., Glass, C.K., Nizet, V., 2010. Statins Enhance Formation of Phagocyte Extracellular Traps. Cell Host Microbe 8, 445–454.

Chtanova, T., Schaeffer, M., Han, S.-J., van Dooren, G.G., Nollmann, M., Herzmark, P., Chan, S.W., Satija, H., Camfield, K., Aaron, H., Striepen, B., Robey, E.A., 2008. Dynamics of Neutrophil Migration in Lymph Nodes during Infection. Immunity 29, 487–496.

Claesson-Welsh, L., 2015. Vascular permeability--the essentials. Ups. J. Med. Sci. 120, 135–43.

Cohen, G.M., 1997. Caspases: the executioners of apoptosis. Biochem. J. 326 (Pt 1), 1–16.

Cong, L., Ran, F.A., Cox, D., Lin, S., Barretto, R., Habib, N., Hsu, P.D., Wu, X., Jiang, W., Marraffini, L.A., Zhang, F., 2013. Multiplex Genome Engineering Using CRISPR/Cas Systems. Science (80-.). 339, 819–823.

Cooper, M.D., Alder, M.N., 2006. The evolution of adaptive immune systems. Cell 124, 815–822.

Crofford, L.J., 1997. COX-1 and COX-2 tissue expression: implications and predictions. J. Rheumatol. Suppl. 49, 15–9.

Dahlgren, C., Karlsson, A., 1999. Respiratory burst in human neutrophils. J. Immunol. Methods 232, 3–14.

Dalli, J., Norling, L. V., Renshaw, D., Cooper, D., Leung, K.-Y., Perretti, M., 2008. Annexin 1 mediates the rapid anti-inflammatory effects of neutrophil-derived microparticles. Blood 112, 2512–2519.

Dancey, J.T., Deubelbeiss, K.A., Harker, L.A., Finch, C.A., 1976. Neutrophil kinetics in man. J. Clin. Invest. 58, 705–715.

Davidson, A.J., Zon, L.I., 2004. The "definitive" (and "primitive") guide to zebrafish hematopoiesis. Oncogene 23, 7233–7246.

Day, R.B., Link, D.C., 2012. Regulation of neutrophil trafficking from the bone marrow. Cell. Mol. Life Sci. 69, 1415–1423.

de Jong, J.L.O., Zon, L.I., 2005. Use of the Zebrafish System to Study Primitive and Definitive Hematopoiesis. Annu. Rev. Genet. 39, 481–501.

de Oliveira, S., Reyes-Aldasoro, C.C., Candel, S., Renshaw, S.A., Mulero, V., Calado, A., 2013. Cxcl8 (IL-8) mediates neutrophil recruitment and behavior in the zebrafish inflammatory response. J. Immunol. 190, 4349–59.

Deininger, M., Buchdunger, E., Druker, B.J., 2005. Review in translational hematology The development of imatinib as a therapeutic agent for chronic myeloid leukemia. Blood 105, 2640–2653.

del Valle Rodríguez, A., Didiano, D., Desplan, C., 2011. Power tools for gene expression and clonal analysis in Drosophila. Nat. Methods 9, 47–55.

Deng, H., Liu, R., Ellmeier, W., Choe, S., Unutmaz, D., Burkhart, M., Marzio, P.D., Marmon, S., Sutton, R.E., Hill, C.M., Davis, C.B., Peiper, S.C., Schall, T.J., Littman, D.R., Landau, N.R., 1996. Identification of a major co-receptor for primary isolates of HIV-1. Nature 381, 661–666.

Deniset, J.F., Kubes, P., 2018. Neutrophil heterogeneity: Bona fide subsets or polarization states? J. Leukoc. Biol.

Dennis, E.A., Norris, P.C., 2015. Eicosanoid storm in infection and inflammation. Nat. Rev. Immunol. 15, 511–523.

Doitsidou, M., Reichman-Fried, M., Stebler, J., Köprunner, M., Dörries, J., Meyer, D., Esguerra, C. V, Leung, T., Raz, E., 2002. Guidance of primordial germ cell migration by the chemokine SDF-1. Cell 111, 647–59.

Dominguez, A.A., Lim, W.A., Qi, L.S., 2015. Beyond editing: repurposing CRISPR–Cas9 for precision genome regulation and interrogation. Nat. Rev. Mol. Cell Biol. 17, 5–15.

Donà, E., Barry, J.D., Valentin, G., Quirin, C., Khmelinskii, A., Kunze, A., Durdu, S., Newton, L.R., Fernandez-Minan, A., Huber, W., Knop, M., Gilmour, D., 2013. Directional tissue migration through a self-generated chemokine gradient. Nature 503, 285–9.

Dotan, I., Werner, L., Vigodman, S., Weiss, S., Brazowski, E., Maharshak, N., Chen, O., Tulchinsky, H., Halpern, Z., Guzner-Gur, H., 2010. CXCL12 Is a constitutive and inflammatory chemokine in the intestinal immune system. Inflamm. Bowel Dis. 16, 583–592.

Druhan, L.J., Ai, J., Massullo, P., Kindwall-Keller, T., Ranalli, M.A., Avalos, B.R., 2005. Novel mechanism of G-CSF refractoriness in patients with severe congenital neutropenia. Blood 105, 584–91.

Dufourcq, P., Vriz, S., 2006. The chemokine SDF-1 regulates blastema formation during zebrafish fin regeneration. Dev. Genes Evol. 216, 635–639.

Eash, K.J., Greenbaum, A.M., Gopalan, P.K., Link, D.C., 2010. CXCR2 and CXCR4 antagonistically regulate neutrophil trafficking from murine bone marrow. J. Clin. Invest. 120, 2423–2431.

Eash, K.J., Means, J.M., White, D.W., Link, D.C., 2009. CXCR4 is a key regulator of neutrophil release from the bone marrow under basal and stress granulopoiesis conditions. Blood 113, 4711–9.

El-Benna, J., Dang, P.M.-C., Gougerot-Pocidalo, M.-A., 2008. Priming of the neutrophil NADPH oxidase activation: role of p47phox phosphorylation and NOX2 mobilization to the plasma membrane. Semin. Immunopathol. 30, 279–289.

Elks, P.M., Van Eeden, F.J., Dixon, G., Wang, X., Reyes-Aldasoro, C.C., Ingham, P.W., Whyte, M.K.B., Walmsley, S.R., Renshaw, S. a., 2011. Activation of hypoxia-inducible factor-1?? (hif-1??) delays inflammation resolution by reducing neutrophil apoptosis and reverse migration in a zebrafish inflammation model. Blood 118, 712–722.

Ellett, F., Elks, P.M., Robertson, a. L., Ogryzko, N. V., Renshaw, S. a., 2015. Defining the phenotype of neutrophils following reverse migration in zebrafish. J. Leukoc. Biol. 98, 1–7.

Ellett, F., Irimia, D., 2017. Microstructured Devices for Optimized Microinjection and Imaging of Zebrafish Larvae. J. Vis. Exp.

Fadeel, B., Ahlin, A., Henter, J.I., Orrenius, S., Hampton, M.B., 1998. Involvement of caspases in neutrophil apoptosis: regulation by reactive oxygen species. Blood 92, 4808–18.

Fadok, V.A., Bratton, D.L., Konowal, A., Freed, P.W., Westcott, J.Y., Henson, P.M., 1998. Macrophages that have ingested apoptotic cells in vitro inhibit proinflammatory cytokine production through autocrine/paracrine mechanisms involving TGF-beta, PGE2, and PAF. J. Clin. Invest. 101, 890–898.

Falloon, J., Gallin, J.I., 1986. Neutrophil granules in health and disease. J. Allergy Clin. Immunol. 77, 653–62.

Faurschou, M., Borregaard, N., 2003. Neutrophil granules and secretory vesicles in inflammation. Microbes Infect. 5, 1317–27.

Förster, T., 1965. Delocalized excitation and excitation transfer. Florida State University, Talahassee Flor.

Fox, S., Leitch, A.E., Duffin, R., Haslett, C., Rossi, A.G., 2010. Neutrophil apoptosis: relevance to the innate immune response and inflammatory disease. J. Innate Immun. 2, 216–27.

Franchi, L., Muñoz-Planillo, R., Reimer, T., Eigenbrod, T., Núñez, G., 2010. Inflammasomes as microbial sensors. Eur. J. Immunol. 40, 611–615.

Franchi, L., Warner, N., Viani, K., Nuñez, G., 2009. Function of Nod-like receptors in microbial recognition and host defense. Immunol. Rev. 227, 106–28.

Fricker, S.P., Anastassov, V., Cox, J., Darkes, M.C., Grujic, O., Idzan, S.R., Labrecque, J., Lau, G., Mosi, R.M., Nelson, K.L., Qin, L., Santucci, Z., Wong, R.S.Y., 2006. Characterization of the molecular pharmacology of AMD3100: A specific antagonist of the G-protein coupled chemokine receptor, CXCR4. Biochem. Pharmacol. 72, 588–596.

Fuchs, T.A., Abed, U., Goosmann, C., Hurwitz, R., Schulze, I., Wahn, V., Weinrauch, Y.,

Brinkmann, V., Zychlinsky, A., 2007. Novel cell death program leads to neutrophil extracellular traps. J. Cell Biol. 176, 231–241.

Furie, M.B., Randolph, G.J., 1995. Chemokines and Tissue Injury. Am. J. ofPathology 146.

Futosi, K., Fodor, S., Mócsai, A., 2013. Neutrophil cell surface receptors and their intracellular signal transduction pathways. Int. Immunopharmacol. 17, 638–650.

Gallin, J., Fletcher, M., Seligmann, B., Hoffstein, S., Cehrs, K., Mounessa, N., 1982. Human neutrophil-specific granule deficiency: a model to assess the role of neutrophil-specific granules in the evolution of the inflammatory response. Blood 59.

Galluzzi, L., Aaronson, S.A., Abrams, J., Alnemri, E.S., Andrews, D.W., Baehrecke, E.H., Bazan, N.G., Blagosklonny, M. V, Blomgren, K., Borner, C., Bredesen, D.E., Brenner, C., Castedo, M., Cidlowski, J.A., Ciechanover, A., Cohen, G.M., De Laurenzi, V., De Maria, R., Deshmukh, M., Dynlacht, B.D., El-Deiry, W.S., Flavell, R.A., Fulda, S., Garrido, C., Golstein, P., Gougeon, M.L., Green, D.R., Gronemeyer, H., Hajnóczky, G., Hardwick, J.M., Hengartner, M.O., Ichijo, H., Jäättelä, M., Kepp, O., Kimchi, A., Klionsky, D.J., Knight, R.A., Kornbluth, S., Kumar, S., Levine, B., Lipton, S.A., Lugli, E., Madeo, F., Malorni, W., Marine, J.-C.C.W., Martin, S.J., Medema, J.P., Mehlen, P., Melino, G., Moll, U.M., Morselli, E., Nagata, S., Nicholson, D.W., Nicotera, P., Nuñez, G., Oren, M., Penninger, J., Pervaiz, S., Peter, M.E., Piacentini, M., Prehn, J.H.M., Puthalakath, H., Rabinovich, G.A., Rizzuto, R., Rodrigues, C.M.P., Rubinsztein, D.C., Rudel, T., Scorrano, L., Simon, H.U., Steller, H., Tschopp, J., Tsujimoto, Y., Vandenabeele, P., Vitale, I., Vousden, K.H., Youle, R.J., Yuan, J., Zhivotovsky, B., Kroemer, G., 2009. Guidelines for the use and interpretation of assays for monitoring cell death in higher eukaryotes. Cell Death Differ.

Galluzzi, L., Maiuri, M.C., Vitale, I., Zischka, H., Castedo, M., Zitvogel, L., Kroemer, G., 2007. Cell death modalities: classification and pathophysiological implications. Cell Death Differ. 14, 1237–1243.

Galluzzi, L., Vitale, I., Aaronson, S.A., Abrams, J.M., Adam, D., Agostinis, P., Alnemri, E.S., Altucci, L., Amelio, I., Andrews, D.W., Annicchiarico-Petruzzelli, M., Antonov, A. V., Arama, E., Baehrecke, E.H., Barlev, N.A., Bazan, N.G., Bernassola, F., Bertrand, M.J.M., Bianchi, K., Blagosklonny, M. V., Blomgren, K., Borner, C., Boya, P., Brenner, C., Campanella, M., Candi, E., Carmona-Gutierrez, D., Cecconi, F., Chan, F.K.-M., Chandel, N.S., Cheng, E.H., Chipuk, J.E., Cidlowski, J.A., Ciechanover, A., Cohen, G.M., Conrad, M., Cubillos-Ruiz, J.R., Czabotar, P.E., D'Angiolella, V., Dawson, T.M., Dawson, V.L., De Laurenzi, V., De Maria, R., Debatin, K.-M., DeBerardinis, R.J., Deshmukh, M., Di Daniele, N., Di Virgilio, F., Dixit, V.M., Dixon, S.J., Duckett, C.S., Dynlacht, B.D., El-Deiry, W.S., Elrod, J.W., Fimia, G.M., Fulda, S., García-Sáez, A.J., Garg, A.D., Garrido, C., Gavathiotis, E., Golstein, P., Gottlieb, E., Green, D.R., Greene, L.A., Gronemeyer, H., Gross, A., Hajnoczky, G., Hardwick, J.M., Harris, I.S., Hengartner, M.O., Hetz, C., Ichijo, H., Jäättelä, M., Joseph, B., Jost, P.J., Juin, P.P., Kaiser, W.J., Karin, M., Kaufmann, T., Kepp, O., Kimchi, A., Kitsis, R.N., Klionsky, D.J., Knight, R.A., Kumar, S., Lee, S.W., Lemasters, J.J., Levine, B., Linkermann, A., Lipton, S.A., Lockshin, R.A., López-Otín, C., Lowe, S.W., Luedde, T., Lugli, E., MacFarlane, M., Madeo, F., Malewicz, M., Malorni, W., Manic, G., Marine, J.-C., Martin, S.J., Martinou, J.-C., Medema, J.P., Mehlen, P., Meier, P., Melino, S., Miao, E.A., Molkentin, J.D., Moll, U.M., Muñoz-Pinedo, C., Nagata, S., Nuñez, G., Oberst, A., Oren, M., Overholtzer, M., Pagano, M., Panaretakis, T., Pasparakis, M., Penninger, J.M., Pereira, D.M., Pervaiz, S., Peter, M.E., Piacentini, M., Pinton, P., Prehn, J.H.M., Puthalakath, H., Rabinovich, G.A., Rehm, M., Rizzuto, R., Rodrigues, C.M.P., Rubinsztein, D.C., Rudel, T., Ryan, K.M., Sayan, E., Scorrano, L., Shao, F., Shi, Y., Silke, J., Simon, H.-U., Sistigu, A., Stockwell, B.R., Strasser, A., Szabadkai, G., Tait, S.W.G., Tang, D., Tavernarakis, N., Thorburn, A., Tsujimoto, Y., Turk, B., Vanden Berghe, T., Vandenabeele, P., Vander

Heiden, M.G., Villunger, A., Virgin, H.W., Vousden, K.H., Vucic, D., Wagner, E.F., Walczak, H., Wallach, D., Wang, Y., Wells, J.A., Wood, W., Yuan, J., Zakeri, Z., Zhivotovsky, B., Zitvogel, L., Melino, G., Kroemer, G., 2018. Molecular mechanisms of cell death: recommendations of the Nomenclature Committee on Cell Death 2018. Cell Death Differ. 25, 486–541.

Geering, B., Stoeckle, C., Conus, S., Simon, H.-U., 2013. Living and dying for inflammation: neutrophils, eosinophils, basophils. Trends Immunol. 34, 398–409.

Gilbert, L.A., Larson, M.H., Morsut, L., Liu, Z., Brar, G.A., Torres, S.E., Stern-Ginossar, N., Brandman, O., Whitehead, E.H., Doudna, J.A., Lim, W.A., Weissman, J.S., Qi, L.S., 2013. CRISPR-Mediated Modular RNA-Guided Regulation of Transcription in Eukaryotes. Cell 154, 442–451.

Gilchrist, A., Stern, P.H., Stern, P.H., 2015. Chemokines and Bone. Clin. Rev. Bone Miner. Metab. 13, 61–82.

Gilmour, D., Knaut, H., Maischein, H.-M., Nüsslein-Volhard, C., 2004. Towing of sensory axons by their migrating target cells in vivo. Nat. Neurosci. Publ. online 18 April 2004; | doi10.1038/nn1235 7, 491.

Goldmann, O., Medina, E., 2012. The expanding world of extracellular traps: not only neutrophils but much more. Front. Immunol. 3, 420.

Golstein, P., Kroemer, G., 2007. Cell death by necrosis: towards a molecular definition. Trends Biochem. Sci. 32, 37–43.

Gratz, S.J., Ukken, F.P., Rubinstein, C.D., Thiede, G., Donohue, L.K., Cummings, A.M., O 'connor-Giles, K.M., 2014. Highly Specific and Efficient CRISPR/Cas9-Catalyzed Homology-Directed Repair in Drosophila.

Greene, E.R., Huang, S., Serhan, C.N., Panigrahy, D., 2011. Regulation of inflammation in cancer by eicosanoids. Prostaglandins Other Lipid Mediat. 96, 27–36.

Gregory, C., 2009. Cell biology: Sent by the scent of death. Nature 461, 181–182.

Griffith, J.W., Sokol, C.L., Luster, A.D., 2014. Chemokines and Chemokine Receptors: Positioning Cells for Host Defense and Immunity. Annu. Rev. Immunol. 32, 659–702.

Guryev, V., Koudijs, M.J., Berezikov, E., Johnson, S.L., Plasterk, R.H.A., van Eeden, F.J.M., Cuppen, E., 2006. Genetic variation in the zebrafish. Genome Res. 16, 491–7.

Guttman, J.A., Finlay, B.B., 2009. Tight junctions as targets of infectious agents. Biochim. Biophys. Acta - Biomembr. 1788, 832–841.

Haas, P., Gilmour, D., 2006. Chemokine Signaling Mediates Self-Organizing Tissue Migration in the Zebrafish Lateral Line. Dev. Cell 10, 673–680.

Häger, M., Cowland, J.B., Borregaard, N., 2010. Neutrophil granules in health and disease. J. Intern. Med. 268, no-no.

Hallett, M.B., Lloyds, D., 1995. Neutrophil priming: the cellular signals that say "amber" but not "green." Immunol. Today 16, 264–268.

Hampton, M.B., Stamenkovic, I., Winterbourn, C.C., 2002. Interaction with substrate sensitises caspase-3 to inactivation by hydrogen peroxide. FEBS Lett. 517, 229–32.

Hanlon, C.D., Andrew, D.J., 2015. Outside-in signaling - a brief review of GPCR signaling with a focus on the Drosophila GPCR family. J. Cell Sci. 3533–3542.

Harizi, H., Corcuff, J.-B., Gualde, N., 2008. Arachidonic-acid-derived eicosanoids: roles in

biology and immunopathology. Trends Mol. Med. 14, 461–469.

Hartl, D., Krauss-Etschmann, S., Koller, B., Hordijk, P.L., Kuijpers, T.W., Hoffmann, F., Hector, A., Eber, E., Marcos, V., Bittmann, I., Eickelberg, O., Griese, M., Roos, D., 2008. Infiltrated neutrophils acquire novel chemokine receptor expression and chemokine responsiveness in chronic inflammatory lung diseases. J. Immunol. 181, 8053–67.

Headland, S.E., Norling, L. V., 2015. The resolution of inflammation: Principles and challenges. Semin. Immunol.

Heit, B., Robbins, S.M., Downey, C.M., Guan, Z., Colarusso, P., Miller, B.J., Jirik, F.R., Kubes, P., 2008. PTEN functions to "prioritize" chemotactic cues and prevent "distraction" in migrating neutrophils. Nat. Immunol. 9, 743–752.

Heit, B., Tavener, S., Raharjo, E., Kubes, P., 2002a. An intracellular signaling hierarchy determines direction of migration in opposing chemotactic gradients. J. Cell Biol. 159, 91–102.

Heit, B., Tavener, S., Raharjo, E., Kubes, P., 2002b. An intracellular signaling hierarchy determines direction of migration in opposing chemotactic gradients. J. Cell Biol. 159, 91–102.

Hengartner, M.O., 2000. The biochemistry of apoptosis. Nature 407, 770–776.

Henry, K.M., Loynes, C. a, Whyte, M.K.B., Renshaw, S. a, 2013. Zebrafish as a model for the study of neutrophil biology. J. Leukoc. Biol. 94, 633–42.

Hess, I., Boehm, T., 2012. Intravital Imaging of Thymopoiesis Reveals Dynamic Lympho-Epithelial Interactions. Immunity 36, 298–309.

Hind, L.E., Vincent, W.J.B., Huttenlocher, A., 2016. Leading from the Back: The Role of the Uropod in Neutrophil Polarization and Migration. Dev. Cell 38, 161–9.

Holmes, G.R., Anderson, S.R., Dixon, G., Robertson, A.L., Reyes-Aldasoro, C.C., Billings, S.A., Renshaw, S.A., Kadirkamanathan, V., 2012. Repelled from the wound, or randomly dispersed? Reverse migration behaviour of neutrophils characterized by dynamic modelling. J. R. Soc. Interface 9, 3229–39.

Holmes, W.E., Lee, J., Kuang, W.J., Rice, G.C., Wood, W.I., 1991. Structure and functional expression of a human interleukin-8 receptor. Science 253, 1278–80.

Hugot, J.-P., Chamaillard, M., Zouali, H., Lesage, S., Cézard, J.-P., Belaiche, J., Almer, S., Tysk, C., O'Morain, C.A., Gassull, M., Binder, V., Finkel, Y., Cortot, A., Modigliani, R., Laurent-Puig, P., Gower-Rousseau, C., Macry, J., Colombel, J.-F., Sahbatou, M., Thomas, G., 2001. Association of NOD2 leucine-rich repeat variants with susceptibility to Crohn's disease. Nature 411, 599–603.

Insall, R.H., 2010. Understanding eukaryotic chemotaxis: a pseudopod-centred view. Nat. Rev. Mol. Cell Biol. 11, 453–458.

Itou, J., Oishi, I., Kawakami, H., Glass, T.J., Richter, J., Johnson, A., Lund, T.C., Kawakami, Y., 2012. Migration of cardiomyocytes is essential for heart regeneration in zebrafish. Development 139, 4133–4142.

Jones, K., Won Kim, D., Park, J.S., Hyun Khang, C., 2016. Live-cell fluorescence imaging to investigate the dynamics of plant cell death during infection by the rice blast fungus Magnaporthe oryzae. BMC Plant Biol. 16.

Kalatskaya, I., Berchiche, Y.A., Gravel, S., Limberg, B.J., Rosenbaum, J.S., Heveker, N., 2009. AMD3100 Is a CXCR7 Ligand with Allosteric Agonist Properties. Mol.

Pharmacol. 75, 1240–1247.

Kawai, T., Malech, H.L., 2009. WHIM syndrome: congenital immune deficiency disease. Curr. Opin. Hematol. 16, 20–6.

Kay, A.B., 2016. Paul Ehrlich and the Early History of Granulocytes. Microbiol. Spectr. 4.

Kelly, M., Hwang, J.M., Kubes, P., 2007. Modulating leukocyte recruitment in inflammation. J Allergy Clin Immunol 120, 3–10.

Kienle, K., Lämmermann, T., 2016. Neutrophil swarming: an essential process of the neutrophil tissue response. Immunol. Rev. 273, 76–93.

KILE, B.T., 2009. The role of the intrinsic apoptosis pathway in platelet life and death. J. Thromb. Haemost. 7, 214–217.

Kim, D., Haynes, C.L., 2012. Neutrophil chemotaxis within a competing gradient of chemoattractants. Anal. Chem. 84, 6070–8.

Kim, H.K., De La Luz Sierra, M., Williams, C.K., Gulino, A.V., Tosato, G., 2006. G-CSF down-regulation of CXCR4 expression identified as a mechanism for mobilization of myeloid cells. Blood 108, 812–820.

Kim, M.H., Chung, J., Yang, J. wook, Chung, S.M., Kwag, N.H., Yoo, J.S., 2003. Hydrogen Peroxide-Induced Cell Death in a Human Retinal Pigment Epithelial Cell Line, ARPE-19. Korean J. Ophthalmol. 17, 19.

Klebanoff, S.J., 2005. Myeloperoxidase: friend and foe. J. Leukoc. Biol. 77, 598–625.

Kolaczkowska, E., Kubes, P., 2013. Neutrophil recruitment and function in health and inflammation. Nat. Rev. Immunol. 13, 159–75.

Korotkova, M., Jakobsson, P.-J., 2014. Persisting eicosanoid pathways in rheumatic diseases. Nat. Rev. Rheumatol. 10, 229–241.

Kreisel, D., Nava, R.G., Li, W., Zinselmeyer, B.H., Wang, B., Lai, J., Pless, R., Gelman, A.E., Krupnick, A.S., Miller, M.J., 2010. In vivo two-photon imaging reveals monocyte-dependent neutrophil extravasation during pulmonary inflammation. Proc. Natl. Acad. Sci. 107, 18073–18078.

Kumar, H., Kawai, T., Akira, S., 2011. Pathogen Recognition by the Innate Immune System. Int. Rev. Immunol. 30, 16–34.

Kumar, S., Hedges, S.B., 1998. A molecular timescale for vertebrate evolution. Nature 392, 917–920.

Lahiri, K., Vallone, D., Gondi, S.B., Santoriello, C., Dickmeis, T., Foulkes, N.S., 2005. Temperature regulates transcription in the zebrafish circadian clock. PLoS Biol. 3, e351.

Lämmermann, T., 2015. In the eye of the neutrophil swarm--navigation signals that bring neutrophils together in inflamed and infected tissues. J. Leukoc. Biol. 100.

Lämmermann, T., Afonso, P. V, Angermann, B.R., Wang, J.M., Kastenmüller, W., Parent, C.A., Germain, R.N., 2013. Neutrophil swarms require LTB4 and integrins at sites of cell death in vivo.

Larson, M.H., Gilbert, L.A., Wang, X., Lim, W.A., Weissman, J.S., Qi, L.S., 2013. CRISPR interference (CRISPRi) for sequence-specific control of gene expression. Nat. Protoc. 8, 2180–2196.

Lawson, N.D., Wolfe, S.A., 2011. Forward and Reverse Genetic Approaches for the

Analysis of Vertebrate Development in the Zebrafish. Dev. Cell 21, 48–64.

Lee, E.K.S., Gillrie, M.R., Li, L., Arnason, J.W., Kim, J.H., Babes, L., Lou, Y., Sanati-Nezhad, A., Kyei, S.K., Kelly, M.M., Mody, C.H., Ho, M., Yipp, B.G., 2018. Leukotriene B4-Mediated Neutrophil Recruitment Causes Pulmonary Capillaritis during Lethal Fungal Sepsis. Cell Host Microbe 23, 121–133.e4.

Lee, H.C., 1997. Mechanisms of calcium signaling by cyclic ADP-ribose and NAADP. Physiol. Rev. 77, 1133–1164.

Lee, W.L., Harrison, R.E., Grinstein, S., 2003. Phagocytosis by neutrophils. Microbes Infect. 5, 1299–1306.

Ley, K., Laudanna, C., Cybulsky, M.I., Nourshargh, S., 2007. Getting to the site of inflammation: the leukocyte adhesion cascade updated. Nat. Rev. Immunol. 7, 678–689.

Lieschke, G.J., Currie, P.D., 2007. Animal models of human disease: zebrafish swim into view. Nat. Rev. Genet. 8, 353–367.

Lieschke, G.J., Grail, D., Hodgson, G., Metcalf, D., Stanley, E., Cheers, C., Fowler, K.J., Basu, S., Zhan, Y.F., Dunn, A.R., 1994. Mice lacking granulocyte colony-stimulating factor have chronic neutropenia, granulocyte and macrophage progenitor cell deficiency, and impaired neutrophil mobilization. Blood 84, 1737–46.

Lieschke, G.J., Oates, A.C., Crowhurst, M.O., Ward, A.C., Layton, J.E., 2001. Morphologic and functional characterization of granulocytes and macrophages in embryonic and adult zebrafish.

Lieschke, G.J., Oates, A.C., Paw, B.H., Thompson, M.A., Hall, N.E., Ward, A.C., Ho, R.K., Zon, L.I., Layton, J.E., 2002. Zebrafish SPI-1 (PU.1) Marks a Site of Myeloid Development Independent of Primitive Erythropoiesis: Implications for Axial Patterning. Dev. Biol. 246, 274–295.

Liles, W.C., Broxmeyer, H.E., Rodger, E., Wood, B., Hübel, K., Cooper, S., Hangoc, G., Bridger, G.J., Henson, G.W., Calandra, G., Dale, D.C., 2003. Mobilization of hematopoietic progenitor cells in healthy volunteers by AMD3100, a CXCR4 antagonist. Blood 102, 2728–2730.

Lim, K., Hyun, Y.-M., Lambert-Emo, K., Capece, T., Bae, S., Miller, R., Topham, D.J., Kim, M., 2015. Neutrophil trails guide influenza-specific CD8+ T cells in the airways. Science (80-.). 349, aaa4352-aaa4352.

Liu, Y., Beyer, A., Aebersold, R., 2016. On the Dependency of Cellular Protein Levels on mRNA Abundance. Cell 165, 535–550.

Lorenzon, P., Vecile, E., Nardon, E., Ferrero, E., Harlan, J.M., Tedesco, F., Dobrina, A., 1998. Endothelial cell E- and P-selectin and vascular cell adhesion molecule-1 function as signaling receptors. J. Cell Biol. 142, 1381–91.

Lotze, M.T., Tracey, K.J., 2005. High-mobility group box 1 protein (HMGB1): nuclear weapon in the immune arsenal. Nat. Rev. Immunol. 5, 331–342.

Magalhaes, A.C., Dunn, H., Ferguson, S.S.G., 2012. Regulation of GPCR activity, trafficking and localization by GPCR-interacting proteins. Br. J. Pharmacol. 165, 1717–1736.

Majmundar, A.J., Wong, W.J., Simon, M.C., 2010. Hypoxia-Inducible Factors and the Response to Hypoxic Stress. Mol. Cell 40, 294–309.

Marie Moresco, E.Y., LaVine, D., Beutler, B., 2011. Toll-like receptors. CURBIO 21, R488–R493.

Marnett, L.J., Rowlinson, S.W., Goodwin, D.C., Kalgutkar, A.S., Lanzo, C.A., 1999. Arachidonic acid oxygenation by COX-1 and COX-2. Mechanisms of catalysis and inhibition. J. Biol. Chem. 274, 22903–6.

Marraffini, L.A., 2016. The CRISPR-Cas system of Streptococcus pyogenes: function and applications, Streptococcus pyogenes : Basic Biology to Clinical Manifestations. University of Oklahoma Health Sciences Center.

Mathias, J.R., Perrin, B.J., Liu, T.-X., Kanki, J., Look, A.T., Huttenlocher, A., 2006. Resolution of inflammation by retrograde chemotaxis of neutrophils in transgenic zebrafish. J. Leukoc. Biol. 80, 1281–1288.

McCudden, C.R., Hains, M.D., Kimple, R.J., Siderovski, D.P., Willard, F.S., 2005. G-protein signaling: back to the future. Cell. Mol. Life Sci. 62, 551–77.

McFall-Ngai, M., 2007. Adaptive Immunity: Care for the community. Nature 445, 153–153.

McGinn, O.J., Marinov, G., Sawan, S., Stern, P.L., 2013. CXCL12 receptor preference, signal transduction, biological response and the expression of 5T4 oncofoetal glycoprotein. J. Cell Sci. 125.

McIlwain, D.R., Berger, T., Mak, T.W., 2013. Caspase functions in cell death and disease. Cold Spring Harb. Perspect. Biol. 5, a008656.

McKeown, S.R., 2014. Defining normoxia, physoxia and hypoxia in tumours-implications for treatment response. Br. J. Radiol. 87, 20130676.

Mečnikov, I.I. (1845-1916), 1892. Leçons sur la pathologie comparée de l'inflammation : faites à l'Institut Pasteur en avril et mai 1891 / par Élie Metchnikoff,...

Medzhitov, R., 2007. Recognition of microorganisms and activation of the immune response. Nature 449, 819–826.

Medzhitov, R., 2008. Origin and physiological roles of inflammation. Nature 454, 428–435.

Medzhitov, R., 2010. Inflammation 2010: New Adventures of an Old Flame. Cell 140, 771–776.

Medzhitov, R., Horng, T., 2009. Transcriptional control of the inflammatory response. Nat. Rev. Immunol. 9, 692–703.

Medzhitov, R., Janeway, C.A., 2002. Decoding the Patterns of Self and Nonself by the Innate Immune System. Science (80-.). 296.

Meng, X., Noyes, M.B., Zhu, L.J., Lawson, N.D., Wolfe, S.A., 2008. Targeted gene inactivation in zebrafish using engineered zinc-finger nucleases. Nat. Biotechnol. 26, 695–701.

Metzler, K.D., Fuchs, T.A., Nauseef, W.M., Reumaux, D., Roesler, J., Schulze, I., Wahn, V., Papayannopoulos, V., Zychlinsky, A., 2011. Myeloperoxidase is required for neutrophil extracellular trap formation: implications for innate immunity. Blood 117, 953–959.

Miceli-Richard, C., Lesage, S., Rybojad, M., Prieur, A.-M., Manouvrier-Hanu, S., Häfner, R., Chamaillard, M., Zouali, H., Thomas, G., Hugot, J.-P., 2001. CARD15 mutations in Blau syndrome. Nat. Genet. 29, 19–20.

Minina, S., Reichman-Fried, M., Raz, E., 2007. Control of Receptor Internalization, Signaling Level, and Precise Arrival at the Target in Guided Cell Migration. Curr. Biol. 17, 1164–1172.

Moens, C.B., Donn, T.M., Wolf-Saxon, E.R., Ma, T.P., 2008. Reverse genetics in zebrafish by TILLING. Briefings Funct. Genomics Proteomics 7, 454–459.

Mogensen, T.H., 2009. Pathogen Recognition and Inflammatory Signaling in Innate Immune Defenses. Clin. Microbiol. Rev. 22, 240–273.

Mojica, F.J.M., Díez-Villaseñor, C., García-Martínez, J., Soria, E., 2005. Intervening sequences of regularly spaced prokaryotic repeats derive from foreign genetic elements. J. Mol. Evol. 60, 174–182.

Mori, K., Yanagita, M., Hasegawa, S., Kubota, M., Yamashita, M., Yamada, S., Kitamura, M., Murakami, S., 2015. Necrosis-induced TLR3 Activation Promotes TLR2 Expression in Gingival Cells. J. Dent. Res. 94, 1149–1157.

Muller, W.A., 2013. Getting leukocytes to the site of inflammation. Vet. Pathol. 50, 7–22.

Murphy, P.M., Tiffany, H.L., 1991. Cloning of complementary DNA encoding a functional human interleukin-8 receptor. Science 253, 1280–3.

Nair, S., Schilling, T.F., 2008. Chemokine Signaling Controls Endodermal Migration During Zebrafish Gastrulation. Science (80-.). 322.

Nasevicius, a, Ekker, S.C., 2000. Effective targeted gene "knockdown" in zebrafish. Nat. Genet. 26, 216–20.

Nathan, C., 2002a. Points of control in inflammation. Nature 420, 846–852.

Nathan, C., 2002b. Points of control in inflammation. Nature 420, 846–852.

Naumann, U., Cameroni, E., Pruenster, M., Mahabaleshwar, H., Raz, E., Zerwes, H.-G., Rot, A., Thelen, M., 2010. CXCR7 Functions as a Scavenger for CXCL12 and CXCL11. PLoS One 5, e9175.

Newton, K., Dixit, V.M., 2012. Signaling in innate immunity and inflammation. Cold Spring Harb. Perspect. Biol. 4.

Ng, L.G., Qin, J.S., Roediger, B., Wang, Y., Jain, R., Cavanagh, L.L., Smith, A.L., Jones, C.A., de Veer, M., Grimbaldeston, M.A., Meeusen, E.N., Weninger, W., 2011. Visualizing the neutrophil response to sterile tissue injury in mouse dermis reveals a three-phase cascade of events. J. Invest. Dermatol. 131, 2058–2068.

Nie, Y., Waite, J., Brewer, F., Sunshine, M.-J., Littman, D.R., Zou, Y.-R., 2004. The role of CXCR4 in maintaining peripheral B cell compartments and humoral immunity. J. Exp. Med. 200, 1145–56.

Niethammer, P., Grabher, C., Look, A.T., Mitchison, T.J., 2009a. A tissue-scale gradient of hydrogen peroxide mediates rapid wound detection in zebrafish. Nature 459, 996–999.

Niethammer, P., Grabher, C., Look, A.T., Mitchison, T.J., 2009b. A tissue-scale gradient of hydrogen peroxide mediates rapid wound detection in zebrafish. Nature 459, 996–9.

Nourshargh, S., Renshaw, S.A., Imhof, B.A., 2016. Series: Neutrophils in Action Reverse Migration of Neutrophils: Where, When, How, and Why?

Nüsslein-Volhard, C. (Christiane), Dahm, R., 2002. Zebrafish : a practical approach. Oxford University Press.

Ogawa, Y., Calhoun, W.J., 2006. The role of leukotrienes in airway inflammation. J. Allergy Clin. Immunol.

Okuthe, G.E., 2013. DNA and RNA pattern of staining during oogenesis in zebrafish (Danio rerio): A confocal microscopy study. Acta Histochem. 115, 178–184.

Ortega-Gómez, A., Perretti, M., Soehnlein, O., 2013. Resolution of inflammation: an integrated view. EMBO Mol. Med. 5, 661–74.

Ortiz-Barahona, A., Villar, D., Pescador, N., Amigo, J., del Peso, L., 2010. Genome-wide identification of hypoxia-inducible factor binding sites and target genes by a probabilistic model integrating transcription-profiling data and in silico binding site prediction. Nucleic Acids Res. 38, 2332–45.

Paredes-Zúñiga, S., Morales, R.A., Muñoz-Sánchez, S., Muñoz-Montecinos, C., Parada, M., Tapia, K., Rubilar, C., Allende, M.L., Peña, O.A., 2017. CXCL12a/CXCR4b acts to retain neutrophils in caudal hematopoietic tissue and to antagonize recruitment to an injury site in the zebrafish larva. Immunogenetics 69, 341–349.

Pase, L., Nowell, C.J., Lieschke, G.J., 2012. In Vivo Real-Time Visualization of Leukocytes and Intracellular Hydrogen Peroxide Levels During a Zebrafish Acute Inflammation Assay. Methods Enzymol. 506, 135–156.

Peskar, B.M., Sawka, N., Ehrlich, K., Peskar, B.A., 2003. Role of Cyclooxygenase-1 and -2, Phospholipase C, and Protein Kinase C in Prostaglandin-Mediated Gastroprotection. J. Pharmacol. Exp. Ther. 305, 1233–1238.

Peters, N.C., Egen, J.G., Secundino, N., Debrabant, A., Kimblin, N., Kamhawi, S., Lawyer, P., Fay, M.P., Germain, R.N., Sacks, D., 2008. In vivo imaging reveals an essential role for neutrophils in leishmaniasis transmitted by sand flies. Science 321, 970–4.

Petty, J.M., Lenox, C.C., Weiss, D.J., Poynter, M.E., Suratt, B.T., 2009. Crosstalk between CXCR4/Stromal Derived Factor-1 and VLA-4/VCAM-1 Pathways Regulates Neutrophil Retention in the Bone Marrow. J. Immunol. 182, 604–612.

Petty, J.M., Sueblinvong, V., Lenox, C.C., Jones, C.C., Cosgrove, G.P., Cool, C.D., Rai, P.R., Brown, K.K., Weiss, D.J., Poynter, M.E., Suratt, B.T., 2007. Pulmonary stromal-derived factor-1 expression and effect on neutrophil recruitment during acute lung injury. J. Immunol. 178, 8148–57.

Pfeffer, W., 1884. Locomotorische Richtngsbewegungenu durch chemische Reize. Untersuchungen aus d. Bot. Inst. Tübingen 1, 363–482.

Piccinini, A.M., Midwood, K.S., 2010. DAMPening inflammation by modulating TLR signalling. Mediators Inflamm. 2010.

Pillay, J., den Braber, I., Vrisekoop, N., Kwast, L.M., de Boer, R.J., Borghans, J.A.M., Tesselaar, K., Koenderman, L., 2010. In vivo labeling with 2H2O reveals a human neutrophil lifespan of 5.4 days. Blood 116, 625–627.

Poltorak, A., He, X., Smirnova, I., Liu, M.Y., Van Huffel, C., Du, X., Birdwell, D., Alejos, E., Silva, M., Galanos, C., Freudenberg, M., Ricciardi-Castagnoli, P., Layton, B., Beutler, B., 1998. Defective LPS signaling in C3H/HeJ and C57BL/10ScCr mice: mutations in Tlr4 gene. Science 282, 2085–8.

Powell, D., Tauzin, S., Hind, L.E., Deng, Q., Beebe, D.J., Huttenlocher, A., 2017. Chemokine Signaling and the Regulation of Bidirectional Leukocyte Migration in Interstitial Tissues. Cell Rep. 19, 1572–1585.

Qi, L.S., Larson, M.H., Gilbert, L.A., Doudna, J.A., Weissman, J.S., Arkin, A.P., Lim, W.A., 2013. Repurposing CRISPR as an RNA-guided platform for sequence-specific control of gene expression. Cell 152, 1173–83.

Ran, F.A., Hsu, P.D., Lin, C.-Y., Gootenberg, J.S., Konermann, S., Trevino, A.E., Scott, D.A., Inoue, A., Matoba, S., Zhang, Y., Zhang, F., 2013. Double nicking by RNA-guided CRISPR Cas9 for enhanced genome editing specificity. Cell 154, 1380–9.

Ransohoff, R.M., 2009. Chemokines and chemokine receptors: standing at the crossroads of immunobiology and neurobiology. Immunity 31, 711–21.

Ravichandran, K.S., 2010. Find-me and eat-me signals in apoptotic cell clearance: progress and conundrums. J. Exp. Med. 207, 1807–17.

Reátegui, E., Jalali, F., Khankhel, A.H., Wong, E., Cho, H., Lee, J., Serhan, C.N., Dalli, J., Elliott, H., Irimia, D., 2017. Microscale arrays for the profiling of start and stop signals coordinating human-neutrophil swarming. Nat. Biomed. Eng. 1, 94.

Reis, A.C., Alessandri, A.L., Athayde, R.M., Perez, D.A., Vago, J.P., Ávila, T. V, Ferreira, T.P.T., de Arantes, A.C., de Sá Coutinho, D., Rachid, M.A., Sousa, L.P., Martins, M.A., Menezes, G.B., Rossi, A.G., Teixeira, M.M., Pinho, V., 2015. Induction of eosinophil apoptosis by hydrogen peroxide promotes the resolution of allergic inflammation. Cell Death Dis. 6, e1632.

Remijsen, T.V.Q., Kuijpers, T.W., Wirawan, E., Lippens, S., Vandenabeele, P., Vanden Berghe, T., 2011a. Dying for a cause: NETosis, mechanisms behind an antimicrobial cell death modality. Cell Death Differ.

Remijsen, T.V.Q., Wirawan, E., Asselbergh, B., Parthoens, E., De Rycke, R., Noppen, S., Delforge, M., Willems, J., Vandenabeele, P., 2011b. Neutrophil extracellular trap cell death requires both autophagy and superoxide generation. Cell Res. 21, 290–304.

Renshaw, S.A., Parmar, J.S., Singleton, V., Rowe, S.J., Dockrell, D.H., Dower, S.K., Bingle, C.D., Chilvers, E.R., Whyte, M.K.B., 2003. Acceleration of human neutrophil apoptosis by TRAIL. J. Immunol. 170, 1027–33.

Renshaw, S., Loynes, C., 2006. A transgenic zebrafish model of neutrophilic inflammation. Blood… 108, 3976–3978.

Ricciotti, E., FitzGerald, G.A., 2011. Prostaglandins and inflammation. Arterioscler. Thromb. Vasc. Biol. 31, 986–1000.

Ridley, A.J., Schwartz, M. a, Burridge, K., Firtel, R. a, Ginsberg, M.H., Borisy, G., Parsons, J.T., Horwitz, A.R., 2003. Cell migration: integrating signals from front to back. Science 302, 1704–1709.

Riedel, S., 2005. Edward Jenner and the history of smallpox and vaccination. Proc. (Bayl. Univ. Med. Cent). 18, 21–5.

Robertson, A.L., Holmes, G.R., Bojarczuk, A.N., Burgon, J., Loynes, C. a, Chimen, M., Sawtell, A.K., Hamza, B., Willson, J., Walmsley, S.R., Anderson, S.R., Coles, M.C., Farrow, S.N., Solari, R., Jones, S., Prince, L.R., Irimia, D., Rainger, G.E., Kadirkamanathan, V., Whyte, M.K.B., Renshaw, S. a, 2014. A zebrafish compound screen reveals modulation of neutrophil reverse migration as an anti-inflammatory mechanism. Sci. Transl. Med. 6, 225ra29.

Robertson, A.L., Ogryzko, N. V, Henry, K.M., Loynes, C.A., Foulkes, M.J., Meloni, M.M., Wang, X., Ford, C., Jackson, M., Ingham, P.W., Wilson, H.L., Farrow, S.N., Solari, R., Flower, R.J., Jones, S., Whyte, M.K.B., Renshaw, S.A., 2016. Identification of benzopyrone as a common structural feature in compounds with anti-inflammatory activity in a zebrafish phenotypic screen. Dis. Model. Mech. 9, 621–32.

Rougeot, J., Zakrzewska, A., Kanwal, Z., Jansen, H.J., Spaink, H.P., Meijer, A.H., 2014. RNA Sequencing of FACS-Sorted Immune Cell Populations from Zebrafish Infection

Models to Identify Cell Specific Responses to Intracellular Pathogens. Humana Press, New York, NY, pp. 261–274.

Sadik, C.D., Kim, N.D., Luster, A.D., 2011. Neutrophils cascading their way to inflammation. Trends Immunol. 32, 452–460.

Sánchez-Martín, L., Sánchez-Mateos, P., Cabañas, C., 2013. CXCR7 impact on CXCL12 biology and disease. Trends Mol. Med. 19, 12–22.

Sander, J.D., Cade, L., Khayter, C., Reyon, D., Peterson, R.T., Joung, J.K., Yeh, J.-R.J., 2011. Targeted gene disruption in somatic zebrafish cells using engineered TALENs. Nat. Biotechnol. 29, 697–698.

Scheer, N., Campos-Ortega, J.A., 1999. Use of the Gal4-UAS technique for targeted gene expression in the zebrafish. Mech. Dev. 80, 153–158.

Schenkel, A.R., Mamdouh, Z., Muller, W.A., 2004. Locomotion of monocytes on endothelium is a critical step during extravasation. Nat. Immunol. 5, 393–400.

Schioppa, T., Uranchimeg, B., Saccani, A., Biswas, S.K., Doni, A., Rapisarda, A., Bernasconi, S., Saccani, S., Nebuloni, M., Vago, L., Mantovani, A., Melillo, G., Sica, A., 2003. Regulation of the chemokine receptor CXCR4 by hypoxia. J. Exp. Med. 198, 1391–1402.

Schwab, J.M., Schluesener, H.J., Meyermann, R., Serhan, C.N., 2003. COX-3 the enzyme and the concept: steps towards highly specialized pathways and precision therapeutics? Prostaglandins. Leukot. Essent. Fatty Acids 69, 339–43.

Semerad, C.L., Liu, F., Gregory, A.D., Stumpf, K., Link, D.C., 2002. G-CSF is an essential regulator of neutrophil trafficking from the bone marrow to the blood. Immunity 17, 413–23.

Serhan, C.N., 2007. Resolution phase of inflammation: novel endogenous anti-inflammatory and proresolving lipid mediators and pathways. Annu. Rev. Immunol. 25, 101–137.

Serhan, C.N., Sheppard, K.A., 1990. Lipoxin formation during human neutrophil-platelet interactions: Evidence for the transformation of leukotriene A4 by platelet 12-lipoxygenase in vitro. J. Clin. Invest. 85, 772–780.

Servant, G., Weiner, O.D., Herzmark, P., Balla, T., Sedat, J.W., Bourne, H.R., 2000. Polarization of chemoattractant receptor signaling during neutrophil chemotaxis. Science 287, 1037–40.

Sharma, J.N., Mohammed, L.A., 2006. The role of leukotrienes in the pathophysiology of inflammatory disorders: Is there a case for revisiting leukotrienes as therapeutic targets? Inflammopharmacology 14, 10–16.

Simmons, D.L., 2004. Cyclooxygenase Isozymes: The Biology of Prostaglandin Synthesis and Inhibition. Pharmacol. Rev. 56, 387–437.

Stables, M.J., Shah, S., Camon, E.B., Lovering, R.C., Newson, J., Bystrom, J., Farrow, S., Gilroy, D.W., 2011. Transcriptomic analyses of murine resolution-phase macrophages. Blood 118, e192–e208.

Staudt, N., Müller-Sienerth, N., Fane-Dremucheva, A., Yusaf, S.P., Millrine, D., Wright, G.J., 2015. A panel of recombinant monoclonal antibodies against zebrafish neural receptors and secreted proteins suitable for wholemount immunostaining. Biochem. Biophys. Res. Commun. 456, 527–33.

Stephen, J., Scales, H.E., Benson, R.A., Erben, D., Garside, P., Brewer, J.M., 2017.

Neutrophil swarming and extracellular trap formation play a significant role in Alum adjuvant activity. npj Vaccines 2, 1.

Streisinger, G., Walker, C., Dower, N., Knauber, D., Singer, F., 1981. Production of clones of homozygous diploid zebra fish (Brachydanio rerio). Nature 291, 293–296.

Su, T., Liu, F., Gu, P., Jin, H., Chang, Y., Wang, Q., Liang, Q., Qi, Q., 2016. A CRISPR-Cas9 Assisted Non-Homologous End-Joining Strategy for One-step Engineering of Bacterial Genome 6, 37895.

Su, Y., Richmond, A., 2015. Chemokine Regulation of Neutrophil Infiltration of Skin Wounds. Adv. wound care 4, 631–640.

Summers, C., Rankin, S.M., Condliffe, A.M., Singh, N., Peters, a. M., Chilvers, E.R., 2010. Neutrophil kinetics in health and disease. Trends Immunol. 31, 318–324.

Suratt, B.T., Petty, J.M., Young, S.K., Malcolm, K.C., Lieber, J.G., Nick, J.A., Gonzalo, J.A., Henson, P.M., Worthen, G.S., 2004. Role of the CXCR4/SDF-1 chemokine axis in circulating neutrophil homeostasis. Blood 104, 565–571.

Tamplin, O.J., Durand, E.M., Carr, L.A., Childs, S.J., Hagedorn, E.J., Li, P., Yzaguirre, A.D., Speck, N.A., Zon, L.I., 2015. Hematopoietic Stem Cell Arrival Triggers Dynamic Remodeling of the Perivascular Niche. Cell 160, 241–252.

Tauzin, S., Starnes, T.W., Becker, F.B., Lam, P. -y., Huttenlocher, a., 2014. Redox and Src family kinase signaling control leukocyte wound attraction and neutrophil reverse migration. J. Cell Biol. 207, 589–598.

Taylor, J.S., Braasch, I., Frickey, T., Meyer, A., Van de Peer, Y., 2003. Genome duplication, a trait shared by 22000 species of ray-finned fish. Genome Res. 13, 382–90.

Tofts, P.S., Chevassut, T., Cutajar, M., Dowell, N.G., Peters, A.M., 2011. Doubts concerning the recently reported human neutrophil lifespan of 5.4 days. Blood 117, 6050-2-4.

Torregroza, I., Holtzinger, A., Mendelson, K., Liu, T.-C., Hla, T., Evans, T., 2012. Regulation of a Vascular Plexus by gata4 Is Mediated in Zebrafish through the Chemokine sdf1a. PLoS One 7, e46844.

Tulotta, C., Stefanescu, C., Beletkaia, E., Bussmann, J., Tarbashevich, K., Schmidt, T., Snaar-Jagalska, B.E., 2016. Inhibition of cross-species CXCR4 signaling by the small molecule IT1t impairs triple negative breast cancer early metastases in zebrafish. Dis. Model. Mech.

Valentin, G., Haas, P., Gilmour, D., 2007. The chemokine SDF1a coordinates tissue migration through the spatially restricted activation of Cxcr7 and Cxcr4b. Curr. Biol. 17, 1026–1031.

van Ham, T.J., Mapes, J., Kokel, D., Peterson, R.T., 2010. Live imaging of apoptotic cells in zebrafish. FASEB J. 24, 4336–4342.

van Kessel, K.P.M., Bestebroer, J., van Strijp, J.A.G., 2014. Neutrophil-Mediated Phagocytosis of Staphylococcus aureus. Front. Immunol. 5, 467.

Venero Galanternik, M., Lush, M.E., Piotrowski, T., 2016. Glypican4 modulates lateral line collective cell migration non cell-autonomously. Dev. Biol. 419, 321–335.

Venkiteswaran, G., Lewellis, S.W., Wang, J., Reynolds, E., Nicholson, C., Knaut, H., 2013. XGeneration and dynamics of an endogenous, self-generated signaling gradient across a migrating tissue. Cell 155, 674–87.

Volpp, B.D., Nauseef, W.M., Clark, R.A., 1988. Two cytosolic neutrophil oxidase

components absent in autosomal chronic granulomatous disease. Science 242, 1295–7.

von Kockritz-Blickwede, M., Goldmann, O., Thulin, P., Heinemann, K., Norrby-Teglund, A., Rohde, M., Medina, E., 2008. Phagocytosis-independent antimicrobial activity of mast cells by means of extracellular trap formation. Blood 111, 3070–3080.

Walters, K.B., Green, J.M., Surfus, J.C., Yoo, S.K., Huttenlocher, A., 2010. Live imaging of neutrophil motility in a zebrafish model of WHIM syndrome. Blood 116, 2803–2811.

Wan, K.S., Wu, W.F., 2007. Eicosanoids in asthma.

Wang, J., Hossain, M., Thanabalasuriar, A., Gunzer, M., Meininger, C., Kubes, P., 2017. Visualizing the function and fate of neutrophils in sterile injury and repair. Science (80-.). 358, 111–116.

Wang, X., Li, C., Chen, Y., Hao, Y., Zhou, W., Chen, C., Yu, Z., 2008. Hypoxia enhances CXCR4 expression favoring microglia migration via HIF-1alpha activation. Biochem. Biophys. Res. Commun. 371, 283–8.

Wareing, M.D., Shea, A.L., Inglis, C.A., Dias, P.B., Sarawar, S.R., 2007. CXCR2 Is Required for Neutrophil Recruitment to the Lung during Influenza Virus Infection, But Is Not Essential for Viral Clearance. Viral Immunol. 20, 369–378.

Wartha, F., Beiter, K., Albiger, B., Fernebro, J., Zychlinsky, A., Normark, S., Henriques-Normark, B., 2007. Capsule and d-alanylated lipoteichoic acids protect Streptococcus pneumoniae against neutrophil extracellular traps. Cell. Microbiol. 9, 1162–1171.

Wartha, F., Henriques-Normark, B., 2008. ETosis: a novel cell death pathway. Sci. Signal. 1, pe25.

Weiner, O.D., Servant, G., Welch, M.D., Mitchison, T.J., Sedat, J.W., Bourne, H.R., 1999. Spatial control of actin polymerization during neutrophil chemotaxis. Nat. Cell Biol. 1, 75–81.

Wenger, R.H., Stiehl, D.P., Camenisch, G., 2005. Integration of Oxygen Signaling at the Consensus HRE. Sci. Signal. 2005, re12-re12.

WHO, 2011. Global Vaccine Action Plan Global Vaccine Action Plan. WHO 4–7.

WHO | The top 10 causes of death, 2017. . WHO.

Witko-Sarsat, V., Pederzoli-Ribeil, M., Hirsh, E., Sozzani, S., Cassatella, M. a., 2011. Regulating neutrophil apoptosis: New players enter the game. Trends Immunol. 32, 117–124.

Wlodkowic, D., Skommer, J., Faley, S., Darzynkiewicz, Z., Cooper, J.M., 2009. Dynamic analysis of apoptosis using cyanine SYTO probes: From classical to microfluidic cytometry. Exp. Cell Res. 315, 1706–1714.

Woodfin, A., Voisin, M.-B., Beyrau, M., Colom, B., Caille, D., Diapouli, F.-M., Nash, G.B., Chavakis, T., Albelda, S.M., Rainger, G.E., Meda, P., Imhof, B.A., Nourshargh, S., 2011. The junctional adhesion molecule JAM-C regulates polarized transendothelial migration of neutrophils in vivo. Nat. Immunol. 12, 761–769.

Wright, H.L., Moots, R.J., Bucknall, R.C., Edwards, S.W., 2010. Neutrophil function in inflammation and inflammatory diseases. Rheumatology 49, 1618–1631.

Xia, Z., Liu, Y., 2001. Reliable and global measurement of fluorescence resonance energy transfer using fluorescence microscopes. Biophys. J. 81, 2395–402.

Xu, C., Hasan, S.S., Schmidt, I., Rocha, S.F., Pitulescu, M.E., Bussmann, J., Meyen, D., Raz, E., Adams, R.H., Siekmann, A.F., 2014. Arteries are formed by vein-derived endothelial tip cells. Nat. Commun. 5, 5758.

Yamada, M., Kubo, H., Kobayashi, S., Ishizawa, K., He, M., Suzuki, T., Fujino, N., Kunishima, H., Hatta, M., Nishimaki, K., Aoyagi, T., Tokuda, K., Kitagawa, M., Yano, H., Tamamura, H., Fujii, N., Kaku, M., 2011. The increase in surface CXCR4 expression on lung extravascular neutrophils and its effects on neutrophils during endotoxin-induced lung injury. Cell. Mol. Immunol. 8, 305–14.

Yousefi, S., Gold, J.A., Andina, N., Lee, J.J., Kelly, A.M., Kozlowski, E., Schmid, I., Straumann, A., Reichenbach, J., Gleich, G.J., Simon, H.-U., 2008. Catapult-like release of mitochondrial DNA by eosinophils contributes to antibacterial defense. Nat. Med. 14, 949–953.

Zampolla, T., Zhang, T., Rawson, D.M., 2008. Evaluation of zebrafish (Danio rerio) ovarian follicle viability by simultaneous staining with fluorescein diacetate and propidium iodide. Cryo-Letters 29, 463–475.

Zhang, J.-P., Li, X.-L., Li, G.-H., Chen, W., Arakaki, C., Botimer, G.D., Baylink, D., Zhang, L., Wen, W., Fu, Y.-W., Xu, J., Chun, N., Yuan, W., Cheng, T., Zhang, X.-B., 2017. Efficient precise knockin with a double cut HDR donor after CRISPR/Cas9-mediated double-stranded DNA cleavage.

Zhong, X.-Y., von Muhlenen, I., Li, Y., Kang, A., Gupta, A.K., Tyndall, A., Holzgreve, W., Hahn, S., Hasler, P., 2007. Increased Concentrations of Antibody-Bound Circulatory Cell-Free DNA in Rheumatoid Arthritis. Clin. Chem. 53, 1609–1614.

Zou, Y.-R., Kottmann, A.H., Kuroda, M., Taniuchi, I., Littman, D.R., 1998. Function of the chemokine receptor CXCR4 in haematopoiesis and in cerebellar development. Nature 393, 595–599.